2025 Vol. 78 No. 1
eISSN 2080-4873 Quarterly

Impact Factor: 1.4
CiteScore 2.3 (SCOPUS)
CiteScore rank in Urology: 68/120

Central European Journal of Urology

CEJU

PubMed • Index Copernicus • Web of Science

Central European Journal of Urology

MEDLINE/PubMed

Polish Ministry of Science and Higher Education (70 pts)

Index Copernicus (121.95 pts)

2023 Journal Citation Reports® (Clarivate):
Journal Impact Factor 1.4; 5-year Impact Factor 1.4

2023 Scopus:
CiteScore 2.3; CiteScore rank in Urology: 68/120

SNIP 0.688; SJR 0.39

CENTRAL EUROPEAN JOURNAL OF UROLOGY

Formerly the Polish Journal of Urology

Central European Journal of Urology (CEJU) is indexed in: PubMed, Emerging Sources Citation Index (Clarivate), Chemical Abstracts CAS, CAB Abstracts, CrossRef, EBSCO, Google Scholar, Index Copernicus (121.95 pts), Global Health Databases, SCOPUS and the Polish Medical Library (GBL), Polish Ministry of Science and Higher Education (70 pts)

www.ceju.online

PUBLISHER'S & EDITOR'S OFFICE: Polish Urological Association, 19, Łowicka Street, 02–574 Warsaw, Poland
phone: +48 22 845 69 17, fax: +48 22 845 69 10

Graphic Designer and Photo Editor: wyrazista.com.pl

CZŁONKOWIE WSPIERAJĄCY 2025

astellas

IPSEN

W MIEJSCOWO ZAAWANSOWANYM LUB PRZERZUTOWYM RAKU UROTELIALNYM

WYBIERZ KURS NA **DŁUŻSZE ŻYCIE**

Z LEKIEM PADCEV W PORÓWNANIU ZE STANDARDOWĄ CHEMIOTERAPIĄ WYBRANĄ ZGODNIE Z DECYZJĄ BADACZA

PADCEV to innowacyjne leczenie ukierunkowane na nektynę-4, wydłużające mOS do 12,9 miesięcy u pacjentów, którzy otrzymali wcześniej chemioterapię zawierającą platynę i inhibitor PD-1 lub PD-L1 w porównaniu ze standardową chemioterapią wybraną przez badacza (mOS, 12,9 vs 9 miesięcy; HR = 0,70, 95% CI: 0,56–0,89; p = 0,001)[1,2].

PADCEV™

enfortumab wedotyny

Proszek do sporządzania koncentratu roztworu do infuzji
20 mg i 30 mg

WSKAZANIA

Produkt leczniczy PADCEV w skojarzeniu z pembrolizumabem jest wskazany w pierwszej linii leczenia raka urotelialnego nieresekcyjnego lub z przerzutami u dorosłych pacjentów, którzy kwalifikują się do chemioterapii opartej na pochodnych platyny[1]. Produkt leczniczy PADCEV jest wskazany w monoterapii raka urotelialnego miejscowo zaawansowanego lub z przerzutami u dorosłych pacjentów, którzy otrzymali wcześniej chemioterapię opartą na pochodnych platyny i inhibitor receptora programowanej śmierci komórki 1 lub inhibitor ligandu programowanej śmierci komórki 1[1].

CI – przedział ufności; HR – współczynnik ryzyka; mOS – mediana przeżycia całkowitego; PD-1 – inhibitor receptora programowanej śmierci komórki 1; PD-L1 – inhibitor ligandu programowanej śmierci komórki 1.

Referencje: 1. Charakterystyka Produktu Leczniczego PADCEV. 2. Powles T et al. Enfortumab vedotin in previously treated advanced urothelial carcinoma. N Engl J Med 2021; 384(12): 1125-1135.

astellas

MAT-PL-PAD-2025-00007 | Styczeń 2025

Informacja o leku

▼ Niniejszy produkt leczniczy będzie dodatkowo monitorowany. Umożliwi to szybkie zidentyfikowanie nowych informacji o bezpieczeństwie. Osoby należące do fachowego personelu medycznego powinny zgłaszać wszelkie podejrzewane działania niepożądane. Aby dowiedzieć się, jak zgłaszać działania niepożądane – patrz punkt 4.8. Charakterystyki Produktu Leczniczego (ChPL).

Nazwa produktu leczniczego: Padcev 20 mg proszek do sporządzania koncentratu roztworu do infuzji, Padcev 30 mg proszek do sporządzania koncentratu roztworu do infuzji. **Skład jakościowy i ilościowy:** Jedna fiolka proszku do sporządzania koncentratu roztworu do infuzji zawiera 20 mg enfortumabu wedotyny (Padcev 20 mg) albo 30 mg enfortumabu wedotyny (Padcev 30 mg). Po rekonstytucji każdy ml roztworu zawiera 10 mg enfortumabu wedotyny. Enfortumab wedotyny składa się z w pełni ludzkiego przeciwciała IgG1 kappa, sprzężonego ze środkiem niszczącym mikrotubule, monometylo aurystatyną E (ang. *Monomethyl Auristatin E*, MMAE) za pośrednictwem maleimidokaproilo walino-cytrulinowego łacznika rozszczepianego przez proteazę. Pełny wykaz substancji pomocniczych, patrz punkt 6.1 ChPL. **Postać farmaceutyczna:** Proszek do sporządzania koncentratu roztworu do infuzji. **Wskazania do stosowania:** Produkt leczniczy Padcev w skojarzeniu z pembrolizumabem jest wskazany w pierwszej linii leczenia raka urotelialnego nieresekcyjnego lub z przerzutami u dorosłych pacjentów, którzy kwalifikują się do chemioterapii opartej na pochodnych platyny. Produkt leczniczy Padcev jest wskazany w monoterapii raka urotelialnego miejscowo zaawansowanego lub z przerzutami u dorosłych pacjentów, którzy otrzymali wcześniej chemioterapię opartą na pochodnych platyny i inhibitor receptora programowanej śmierci komórki 1 lub inhibitor ligandu programowanej śmierci komórki 1 (patrz punkt 5.1 ChPL). **Dawkowanie i sposób podawania:** Leczenie produktem leczniczym Padcev powinien rozpocząć i nadzorować lekarz mający doświadczenie w stosowaniu terapii przeciwnowotworowych. Przed rozpoczęciem leczenia należy zapewnić dobry dostęp żylny (patrz punkt 4.4 ChPL). *Dawkowani*e: Zalecana dawka enfortumabu wedotyny w monoterapii wynosi 1,25 mg/kg mc. (maksymalnie do 125 mg u pacjentów o masie ciała ≥ 100 kg) i podaje się ją we wlewie dożylnym przez 30 minut w 1., 8. i 15. dniu 28-dniowego cyklu do czasu progresji choroby lub wystąpienia niemożliwych do zaakceptowania objawów toksyczności. Zalecana dawka enfortumabu wedotyny w skojarzeniu z pembrolizumabem wynosi 1,25 mg/kg mc. (maksymalnie do 125 mg u pacjentów o masie ciała ≥ 100 kg) i podaje się ją we wlewie dożylnym przez 30 minut w 1. i 8. dniu każdego trzytygodniowego (21-dniowego) cyklu do czasu progresji choroby lub wystąpienia niemożliwych do zaakceptowania objawów toksyczności. Zalecana dawka pembrolizumabu to 200 mg co 3 tygodnie albo 400 mg co 6 tygodni podawana we wlewie dożylnym przez 30 minut. Jeżeli oba leki są podawane tego samego dnia, pacjenci powinni otrzymać pembrolizumab po enfortumabie wedotyny. Dodatkowe informacje na temat dawkowania pembrolizumabu, patrz ChPL pembrolizumabu. Zalecane zmniejszenie dawki enfortumabu wedotyny w przypadku działań niepożądanych znajduje się w poniższej tabeli (Tabela 1):

	Stopień zmniejszenia dawki
Dawka początkowa	1,25 mg/kg mc. do 125 mg
Pierwsze zmniejszenie dawki	1,0 mg/kg mc. do 100 mg
Drugie zmniejszenie dawki	0,75 mg/kg mc. do 75 mg
Trzecie zmniejszenie dawki	0,5 mg/kg mc. do 50 mg

Modyfikacje dawki: Informacja o przerwaniu, zmniejszeniu i odstawieniu dawki enfortumabu wedotyny u pacjentów z rakiem urotelialnym miejscowo zaawansowanym lub z przerzutami znajduje się w poniższej tabeli (Tabela 2):

Działanie niepożądane	**Nasilenie***	**Modyfikacja dawki***
Reakcje skórne	Podejrzewany zespół Stevensa-Johnsona (ang. *Stevens-Johnson Syndrome*, SJS) lub martwica toksyczno-rozpływna naskórka (ang. *Toxic Epidermal Necrolysis*, TEN), lub zmiany pęcherzowe	Natychmiast wstrzymać podawanie i objąć pacjenta opieką specjalistyczną
	Potwierdzony SJS lub TEN; stopień 4. lub nawracający stopień 3.	Zakończyć leczenie
	Pogorszenie stopnia 2. Stopień 2. z gorączką Stopień 3.	• Wstrzymać podawanie do uzyskania stopnia ≤ 1. • Rozważyć objęcie pacjenta opieką specjalistyczną • Wznowić podawanie w tej samej dawce lub rozważyć zmniejszenie dawki o jeden stopień (patrz Tabela 1)
Hiperglikemia	Glikemia > 13,9 mmol/l (> 250 mg/dl)	• Wstrzymać podawanie, dopóki zwiększone stężenie glukozy nie zmniejszy się do wartości ≤ 13,9 mmol/l (≤ 250 mg/dl) • Wznowić leczenie w tej samej dawce
Nieinfekcyjne zapalenie płuc/śródmiąższowa choroba płuc (ang. *interstitial lung disease*, ILD)	Stopień 2.	Wstrzymać podawanie do uzyskania stopnia ≤ 1., następnie wznowić podawanie w tej samej dawce lub rozważyć zmniejszenie dawki o jeden stopień (patrz Tabela 1)
	Stopień ≥ 3.	Zakończyć leczenie
Neuropatia obwodowa	Stopień 2.	• Wstrzymać podawanie do uzyskania stopnia ≤ 1. • W przypadku pierwszego wystąpienia wznowić leczenie w tej samej dawce • W przypadku nawrotu wstrzymać podawanie do uzyskania stopnia ≤ 1., a następnie wznowić leczenie w dawce zmniejszonej o jeden stopień (patrz Tabela 1)
	Stopień ≥ 3.	Zakończyć leczenie

* Toksyczności oceniano według Wspólnych Kryteriów Terminologii Zdarzeń Niepożądanych National Cancer Institute (ang. *National Cancer Institute Common Terminology Criteria for Adverse Events*; NCI-CTCA), wersja 5,0, zgodnie z którymi stopień 1. oznacza nasilenie łagodne, stopień 2. umiarkowane, stopień 3. ciężkie, a stopień 4. zagrażające życiu. Specjalne grupy pacjentów: *Pacjenci w podeszłym wieku*: Nie ma konieczności dostosowania dawki u pacjentów w wieku ≥ 65 lat (patrz punkt 5.2 ChPL). *Zaburzenia czynności nerek:* Nie ma konieczności dostosowania dawki u pacjentów z łagodnymi [klirens kreatyniny (ang. *Creatinine Clearance*, CrCL) > 60-90 ml/min], umiarkowanymi (CrCL 30-60 ml/min) ani ciężkimi (CrCL 15- < 30 ml/min) zaburzeniami czynności nerek. Enfortumabu wedotyny nie oceniano u pacjentów ze schyłkową niewydolnością nerek (CrCL < 15 ml/min) (patrz punkt 5.2 ChPL). *Zaburzenia czynności wątroby:* Nie ma konieczności dostosowania dawki u pacjentów z łagodnymi zaburzeniami czynności wątroby [bilirubina całkowita od 1 do 1,5 × górnej granicy normy (GGN) i dowolna aktywność aminotransferazy asparaginianowej (AST) lub bilirubina całkowita ≤ GGN i AST > GGN]. Enfortumab wedotyny oceniano tylko w ograniczonej grupie pacjentów z umiarkowanymi i ciężkimi zaburzeniami czynności wątroby. Należy spodziewać się, że zaburzenia czynności wątroby zwiększają ogólnoustrojową ekspozycję na MMAE (lek cytotoksyczny); dlatego też należy ściśle monitorować pacjentów w kierunku potencjalnych działań niepożądanych. Ze względu na niewielką liczbę danych dotyczących pacjentów z umiarkowanymi i ciężkimi zaburzeniami czynności wątroby nie można podać konkretnych zaleceń dotyczących dawkowania (patrz punkt 5.2 ChPL). *Dzieci i młodzież:* Stosowanie enfortumabu wedotyny u dzieci i młodzieży nie jest właściwe we wskazaniu leczenie raka urotelialnego miejscowo zaawansowanego lub z przerzutami. Sposób podawania: Produkt leczniczy Padcev podaje się dożylnie. Zalecana dawka musi być podawana we wlewie dożylnym przez 30 minut. Enfortumabu wedotyny nie można podawać we wstrzyknięciu dożylnym ani w szybkim wstrzyknięciu dożylnym (bolus). Instrukcja dotycząca rekonstytucji i rozcieńczenia produktu leczniczego przed podaniem, patrz punkt 6.6 ChPL. **Przeciwwskazania:** Nadwrażliwość na substancję czynną lub na którąkolwiek substancję pomocniczą wymienioną w punkcie 6.1 ChPL. **Specjalne ostrzeżenia i środki ostrożności dotyczące stosowania:** Identyfikowalność: W celu poprawienia identyfikowalności biologicznych produktów leczniczych należy dokładnie odnotować nazwę i numer serii podawanego produktu. Reakcje skórne: Reakcje skórne związane z podawaniem enfortumabu wedotyny są wynikiem jego wiązania do nektyny-4 ulegającej ekspresji w skórze. W przypadku wystąpienia gorączki lub objawów grypopodobnych, które mogą być pierwszymi objawami ciężkiej reakcji skórnej, należy obserwować pacjentów. Donoszono o występowaniu reakcji skórnych o nasileniu łagodnym do umiarkowanego w związku ze stosowaniem enfortumabu wedotyny, głównie w postaci wysypki plamisto-grudkowej. Częstość występowania reakcji skórnych była większa, gdy enfortumab wedotyny podawano w skojarzeniu z pembrolizumabem w porównaniu do enfortumabu wedotyny podawanego w monoterapii (patrz punkt 4.8 ChPL). U pacjentów leczonych enfortumabem wedotyny występowały również skórne działania niepożądane o ciężkim nasileniu, w tym SJS i TEN, ze skutkiem śmiertelnym, głównie w trakcie pierwszego cyklu leczenia. Należy monitorować pacjentów w kierunku reakcji skórnych, począwszy od pierwszego cyklu i przez cały czas leczenia. W przypadku wystąpienia reakcji skórnych o nasileniu łagodnym do umiarkowanego można rozważyć odpowiednie leczenie, takie jak miejscowe podawanie kortykosteroidów i podawanie leków przeciwhistaminowych. W razie podejrzenia SJS lub TEN, lub w przypadku wystąpienia zmian pęcherzowych należy natychmiast wstrzymać leczenie i objąć pacjentów opieką specjalistyczną; potwierdzenie histologiczne, w tym rozważenie wykonania kilku biopsji, ma kluczowe znaczenie dla wczesnego rozpoznania, ponieważ diagnoza i interwencja mogą poprawić rokowanie. Należy trwale odstawić produkt leczniczy Padcev w przypadku potwierdzenia SJS lub TEN, reakcji stopnia 4. lub nawracających reakcji skórnych stopnia 3. W przypadku pogorszenia reakcji stopnia 2., wystąpienia reakcji stopnia 2. z gorączką lub wystąpienia reakcji skórnych stopnia 3. należy wstrzymać leczenie do uzyskania stopnia ≤ 1. i rozważyć objęcie pacjentów opieką specjalistyczną. Wznowić leczenie w tej samej dawce lub rozważyć zmniejszenie dawki o jeden stopień (patrz punkt 4.2 ChPL). Nieinfekcyjne zapalenie płuc/ILD: U pacjentów leczonych enfortumabem wedotyny występowało nieinfekcyjne zapalenie płuc/ILD o ciężkim nasileniu, zagrażające życiu lub prowadzące do zgonu. Częstość występowania nieinfekcyjnego zapalenia płuc/ILD, w tym zdarzeń o ciężkim nasileniu, była większa podczas podawania enfortumabu wedotyny w skojarzeniu z pembrolizumabem w porównaniu do enfortumabu wedotyny podawanego w monoterapii (patrz punkt 4.8 ChPL). Pacjentów należy monitorować w kierunku przedmiotowych i podmiotowych objawów nieinfekcyjnego zapalenia płuc/ILD, takich jak niedotlenienie, kaszel, duszność lub nacieki śródmiąższowe w badaniach radiologicznych. W przypadku zdarzeń stopnia ≥ 2. należy podać kortykosteroidy (np. prednizon lub jego odpowiednik w dawce początkowej 1-2 mg/kg mc./dobę, którą następnie należy stopniowo zmniejszać). Należy wstrzymać leczenie produktem leczniczym Padcev w przypadku nieinfekcyjnego zapalenia płuc/ILD stopnia 2. i rozważyć zmniejszenie dawki. Należy zakończyć leczenie produktem leczniczym Padcev w przypadku nieinfekcyjnego zapalenia płuc/ILD stopnia ≥ 3. (patrz punkt 4.2 ChPL). Hiperglikemia: Hiperglikemia i kwasica ketonowa cukrzycowa (ang. *Diabetic Ketoacidosis*, DKA), w tym przypadki zgonów, występowały u pacjentów z cukrzycą w wywiadzie lub bez niej, leczonych enfortumabem wedotyny (patrz punkt 4.8 ChPL). Hiperglikemia występowała częściej u pacjentów z wcześniej istniejącą hiperglikemią lub wysokim wskaźnikiem masy ciała (BMI ≥ 30 kg/m^2). Pacjentów ze stężeniem HbA1c ≥ 8% w punkcie wyjściowym wykluczono z badań klinicznych. Przed podaniem dawki i okresowo przez cały czas trwania leczenia zgodnie ze wskazaniami klinicznymi należy monitorować stężenie glukozy u pacjentów z cukrzycą lub narażonych na ryzyko cukrzycy bądź hiperglikemii. Jeżeli stężenie glukozy jest podwyższone, tj. ma wartość > 13,9 mmol/l (> 250 mg/dl), należy odstawić produkt leczniczy Padcev do czasu aż stężenie glukozy nie zmniejszy się do wartości ≤ 13,9 mmol/l (≤ 250 mg/dl) i wdrożyć odpowiednie leczenie (patrz punkt 4.2 ChPL). Ciężkie zakażenia: Donoszono o występowaniu ciężkich zakażeń, takich jak posocznica (w tym przypadków śmiertelnych) u pacjentów leczonych enfortumabem wedotyny. Podczas leczenia należy ściśle monitorować pacjentów w kierunku pojawienia się ewentualnych ciężkich zakażeń. Neuropatia obwodowa: Podczas podawania enfortumabu wedotyny występowała neuropatia obwodowa, głównie neuropatia obwodowa czuciowa, w tym reakcje stopnia ≥ 3. (patrz punkt 4.8 ChPL). Pacjentów z wcześniej istniejącą neuropatią obwodową stopnia ≥ 2. wykluczono z badań klinicznych. Pacjentów należy monitorować w kierunku wystąpienia objawów lub nasilenia istniejącej neuropatii obwodowej, ponieważ tacy pacjenci mogą wymagać opóźnienia w podawaniu, zmniejszenia dawki lub odstawienia enfortumabu wedotyny (patrz Tabela 1). Produkt leczniczy Padcev należy trwale odstawić w przypadku neuropatii obwodowej stopnia ≥ 3. (patrz punkt 4.2 ChPL). Zaburzenia oka: U pacjentów leczonych enfortumabem wedotyny występowały zaburzenia oka, głównie zespół suchego oka (patrz punkt 4.8 ChPL). Należy monitorować pacjentów w kierunku zaburzenia oka. W ramach profilaktyki zespołu suchego oka należy rozważyć podawanie sztucznych łez i skierowanie na badanie okulistyczne, jeżeli objawy oczne nie ustąpiły lub uległy pogorszeniu. Wynaczynienie w miejscu podania wlewu: W przypadku wynaczynienia obserwowano uszkodzenie skóry i tkanek miękkich po podaniu enfortumabu wedotyny (patrz punkt 4.8 ChPL). Przed rozpoczęciem podawania produktu leczniczego Padcev należy zapewnić dobry dostęp żylny i w trakcie podawania monitorować możliwe wynaczynienia w miejscu podania wlewu. Jeżeli nastąpi wynaczynienie, należy przerwać wlew i monitorować pacjenta w kierunku wystąpienia działań niepożądanych. Toksyczność dla zarodka lub płodu i antykoncepcja: Kobiety w ciąży należy poinformować o potencjalnym ryzyku dla płodu (patrz punkty 4.6 i 5.3 ChPL). Kobietom w wieku rozrodczym należy zalecić wykonanie testu ciążowego w ciągu 7 dni przed rozpoczęciem leczenia enfortumabem wedotyny, stosowanie skutecznej metody antykoncepcji w trakcie leczenia i przez co najmniej 6 miesięcy od zakończenia leczenia. Zaleca się, aby mężczyźni leczeni enfortumabem wedotyny nie spłodzili dziecka w czasie trwania leczenia i przez co najmniej 4 miesiące od podania ostatniej dawki produktu leczniczego Padcev. Informacja dla pacjenta: Lekarz przepisujący Padcev ma obowiązek omówić z pacjentem ryzyka związane z leczeniem tym produktem leczniczym, w tym z leczeniem skojarzonym z pembrolizumabem. Każdorazowo po przepisaniu leku pacjent powinien otrzymać ulotkę dla pacjenta oraz kartę dla pacjenta. **Działania niepożądane:** Podsumowanie profilu bezpieczeństwa: *Enfortumab wedotyny w monoterapii:* Bezpieczeństwo stosowania enfortumabu wedotyny w monoterapii oceniano u 793 pacjentów, którzy otrzymali co najmniej jedną dawkę enfortumabu wedotyny w dawce 1,25 mg/kg mc. w dwóch badaniach fazy I (EV-101 i EV-102), trzech badaniach fazy II (EV-103, EV-201 i EV-203) oraz jednym badaniu fazy III (EV-301) (patrz punkt **Działania niepożądane u pacjentów leczonych enfortumabem wedotyny w monoterapii** poniżej). Mediana czasu ekspozycji pacjentów na enfortumab wedotyny wynosiła 4,7 miesiąca (zakres: od 0,3 do 55,7 miesiąca). Najczęstszymi działaniami niepożądanymi enfortumabu wedotyny były: łysienie (47,7%), zmniejszony apetyt (47,2%), zmęczenie (46,8%), biegunka (39,1%), neuropatia obwodowa czuciowa (38,5%), nudności (37,8%), świąd (33,4%), zaburzenia smaku (30,4%), niedokrwistość (29,1%), zmniejszenie masy ciała (25,2%), wysypka plamisto-grudkowa (23,6%), suchość skóry (21,8%), wymioty (18,7%), zwiększona aktywność aminotransferazy asparaginianowej (17%), hiperglikemia (14,9%), zespół suchego oka (12,7%), zwiększona aktywność aminotransferazy alaninowej (12,7%) i wysypka (11,6%). Najczęstszymi ciężkimi działaniami niepożądanymi (≥ 2%) były biegunka (2,1%) i hiperglikemia (2,1%). Dwadzieścia jeden procent pacjentów trwale odstawiło enfortumab wedotyny z powodu działań niepożądanych; najczęstszym działaniem niepożądanym (≥ 2%) prowadzącym do odstawienia dawki była neuropatia obwodowa czuciowa (4,8%). Działania niepożądane prowadzące do przerwania podawania dawki wystąpiły u 62% pacjentów; najczęstszymi działaniami niepożądanymi (≥ 2%) prowadzącymi do przerwania podawania dawki były: neuropatia obwodowa czuciowa (14,8%), zmęczenie (7,4%), wysypka plamisto-grudkowa (4%), zwiększenie aktywności aminotransferazy asparaginianowej (3,4%), zwiększenie aktywności aminotransferazy alaninowej (3,2%), niedokrwistość (3,2%) i hiperglikemia (3,2%), zmniejszona liczba neutrofilów (3%), biegunka (2,8%), wysypka (2,4%) i neuropatia obwodowa ruchowa (2,1%). Trzydzieści osiem procent pacjentów wymagało zmniejszenia dawki z powodu wystąpienia działań niepożądanych; najczęstszymi działaniami niepożądanymi (≥ 2%) prowadzącymi do zmniejszenia dawki były: neuropatia obwodowa czuciowa (10,3%), zmęczenie (5,3%), wysypka plamisto-grudkowa (4,2%) i zmniejszony apetyt (2,1%). *Enfortumab wedotyny w skojarzeniu z pembrolizumabem:* Jeżeli enfortumab wedotyny jest podawany w skojarzeniu z pembrolizumabem, przed rozpoczęciem leczenia należy zapoznać się z ChPL pembrolizumabu. Bezpieczeństwo stosowania enfortumabu wedotyny w skojarzeniu z pembrolizumabem oceniano u 564 pacjentów, którzy otrzymali co najmniej jedną dawkę enfortumabu wedotyny wynoszącą 1,25 mg/kg mc. w skojarzeniu z pembrolizumabem w jednym badaniu fazy II (EV-103) oraz jednym badaniu fazy III (EV-302) (patrz punkt **Działania niepożądane u pacjentów leczonych enfortumabem wedotyny w skojarzeniu z pembrolizumabem** poniżej). Mediana czasu ekspozycji pacjentów na enfortumab wedotyny w skojarzeniu z pembrolizumabem wynosiła 9,4 miesiąca (zakres: od 0,3 do 34,4 miesiąca). Najczęstszymi działaniami niepożądanymi enfortumabu wedotyny w skojarzeniu z pembrolizumabem były: neuropatia obwodowa czuciowa (53,4%), świąd (41,1%), zmęczenie (40,4%), biegunka (39,2%), łysienie (38,5%), wysypka plamisto-grudkowa (36%), zmniejszona masa ciała (36%), zmniejszony apetyt (33,9%), nudności (28,4%), niedokrwistość (25,7%), zaburzenia smaku (24,3%), suchość skóry (18,1%), zwiększona aktywność aminotransferazy alaninowej (16,8%), hiperglikemia (16,7%), zwiększona aktywność aminotransferazy asparaginianowej (15,4%), zespół suchego oka (14,4%), wymioty (13,3%), wysypka plamista (11,3%), niedoczynność tarczycy (10,5%) i neutropenia (10,1%). Najczęstszymi ciężkimi działaniami niepożądanymi (≥ 2%) były biegunka (3%) i nieinfekcyjne zapalenie płuc (2,3%). Trzydzieści sześć procent pacjentów trwale odstawiło enfortumab wedotyny z powodu działań niepożądanych, najczęstszymi działaniami niepożądanymi (≥ 2%) prowadzącymi do odstawienia były neuropatia obwodowa czuciowa (12,2%) i wysypka plamisto-grudkowa (2%). Działania niepożądane prowadzące do przerwania podawania dawki enfortumabu wedotyny wystąpiły u 72% pacjentów. Najczęstszymi działaniami niepożądanymi (≥ 2%) prowadzącymi do przerwania podawania dawki były neuropatia obwodowa czuciowa (17%), wysypka plamisto-grudkowa (6,9%), biegunka (4,8%), zmęczenie (3,7%), nieinfekcyjne zapalenie płuc (3,7%), hiperglikemia (3,4%), neutropenia (3,2%), zwiększona aktywność aminotransferazy alaninowej (3%), świąd (2,3%) i niedokrwistość (2%). Działania niepożądane prowadzące do zmniejszenia dawki enfortumabu wedotyny wystąpiły u 42,4% pacjentów. Najczęstszymi działaniami niepożądanymi (≥ 2%) prowadzącymi do zmniejszenia dawki były neuropatia obwodowa czuciowa (9,9%), wysypka plamisto-grudkowa (6,4%), zmęczenie (3,2%), biegunka (2,3%) i neutropenia (2,1%). Działania niepożądane obserwowane podczas badań klinicznych enfortumabu wedotyny w monoterapii lub w skojarzeniu z pembrolizumabem lub zgłaszane po wprowadzeniu enfortumabu wedotyny do obrotu wymieniono w tym punkcie według częstości występowania. Częstość określono w następujący sposób: bardzo często (≥ 1/10); często (≥ 1/100 do < 1/10); niezbyt często (≥ 1/1000 do < 1/100); rzadko (≥ 1/10 000 do < 1/1000); bardzo rzadko (< 1/10 000); częstość nieznana (częstość nie może być określona na podstawie dostępnych danych). W obrębie każdej grupy o określonej częstości występowania objawy niepożądane są wymienione zgodnie ze zmniejszającą się ciężkością. **Działania niepożądane u pacjentów leczonych enfortumabem wedotyny w monoterapii: Zakażenia i zarażenia pasożytnicze:** Często: posocznica. **Zaburzenia krwi i układu chłonnego:** Bardzo często: niedokrwistość. Nieznana[1]: neutropenia, gorączka neutropeniczna, zmniejszona liczba neutrofili. **Zaburzenia metabolizmu i odżywiania:** Bardzo często: hiperglikemia, zmniejszony apetyt. Nieznana[1]: cukrzycowa kwasica ketonowa. **Zaburzenia układu nerwowego:** Bardzo często: neuropatia obwodowa czuciowa, zaburzenia smaku. Często: neuropatia obwodowa, neuropatia obwodowa ruchowa, neuropatia obwodowa czuciowo-ruchowa, parestezja, niedoczulica, zaburzenia chodu, osłabienie mięśni. Niezbyt często: Polineuropatia demielinizacyjna, polineuropatia, neurotoksyczność, dysfunkcja ruchowa, zaburzenia czucia, atrofia mięśni, neuralgia, porażenie nerwu strzałkowego, utrata czucia, uczucie pieczenia skóry, uczucie pieczenia. **Zaburzenia oka:** Bardzo często: zespół suchego oka. **Zaburzenia układu oddechowego, klatki piersiowej i śródpiersia:** Często: nieinfekcyjne zapalenie płuc/ILD[2]. **Zaburzenia żołądka i jelit:** Bardzo często: biegunka, wymioty, nudności. **Zaburzenia skóry i tkanki podskórnej:** Bardzo często: łysienie, świąd, wysypka, wysypka plamisto-grudkowa, suchość skóry. Często: wykwit polekowy, złuszczanie skóry, zapalenie spojówek, dermatoza pęcherzowa, powstawanie pęcherzy, zapalenie jamy ustnej, zespół erytrodystezji dłoniowo-podeszwowej, wyprysk, rumień, wysypka rumieniowata, wysypka plamista, wysypka grudkowa, wysypka świądowa, wysypka pęcherzykowa. Niezbyt często: uogólnione złuszczające zapalenie skóry, rumień wielopostaciowy, wysypka złuszczająca, pemfigoid, wysypka plamisto-pęcherzykowa, zapalenie skóry, alergiczne zapalenie skóry, kontaktowe zapalenie skóry, wyprzenie, podrażnienie skóry, wyprysk zastoinowy, pęcherz z krwią. Nieznana[1]: Martwica toksyczno-rozpływna naskórka, przebarwienia skóry, odbarwienie skóry, zaburzenia pigmentacji, zespół Stevensa-Johnsona, martwica naskórka, związane z lekiem symetryczne wyprzenie i wykwity zgięciowe. **Zaburzenia ogólne i stany w miejscu podania:** Bardzo często: zmęczenie. Często: wynaczynienie w miejscu wlewu. **Badania diagnostyczne:** Bardzo często: zwiększona aktywność aminotransferazy alaninowej, zwiększona aktywność aminotransferazy asparaginianowej, zmniejszona masa ciała. **Urazy, zatrucia i powikłania po zabiegach:** Często: reakcje związane z wlewem**. Działania niepożądane u pacjentów leczonych enfortumabem wedotyny w skojarzeniu z pembrolizumabem: Zakażenia i zarażenia pasożytnicze:** Często: posocznica. **Zaburzenia krwi i układu chłonnego:** Bardzo często: niedokrwistość. Nieznana[1]: neutropenia, gorączka neutropeniczna, zmniejszona liczba neutrofili. **Zaburzenia endokrynologiczne:** Bardzo często: niedoczynność tarczycy. **Zaburzenia metabolizmu i odżywiania:** Bardzo często: hiperglikemia, zmniejszony apetyt. Nieznana[1]: cukrzycowa kwasica ketonowa. **Zaburzenia układu nerwowego:** Bardzo często: neuropatia obwodowa czuciowa, zaburzenia smaku. Często: neuropatia obwodowa ruchowa, neuropatia obwodowa czuciowo-ruchowa, parestezja, niedoczulica, zaburzenia chodu, osłabienie mięśni. Niezbyt często: neurotoksyczność, zaburzenia czucia, miastenia rzekomoporaźna, neuralgia, porażenie nerwu strzałkowego, uczucie pieczenia skóry. **Zaburzenia oka:** Bardzo często: zespół suchego oka. **Zaburzenia układu oddechowego, klatki piersiowej i śródpiersia:** Bardzo często: nieinfekcyjne zapalenie płuc/ILD[2]. **Zaburzenia żołądka i jelit:** Bardzo często: biegunka, wymioty, nudności. **Zaburzenia skóry i tkanki podskórnej:** Bardzo często: łysienie, świąd, wysypka, wysypka plamisto-grudkowa, suchość skóry, wysypka plamista. Często: wysypka, złuszczanie skóry, zapalenie spojówek, dermatoza pęcherzowa, powstawanie pęcherzy, zapalenie jamy ustnej, zespół erytrodystezji dłoniowo-podeszwowej, wyprysk, rumień, wysypka rumieniowata, wysypka plamista, wysypka grudkowa, wysypka świądowa, wysypka pęcherzykowa, rumień wielopostaciowy, zapalenie skóry. Niezbyt często: wykwit polekowy, uogólnione złuszczające zapalenie skóry, wysypka złuszczająca, pemfigoid, kontaktowe zapalenie skóry, wyprzenie, podrażnienie skóry, wyprysk zastoinowy. Nieznana[1]: martwica toksyczno-rozpływna naskórka, przebarwienia skóry, odbarwienie skóry, zaburzenia pigmentacji, zespół Stevensa-Johnsona, martwica naskórka, związane z lekiem symetryczne wyprzenie i wykwity zgięciowe. **Zaburzenia mięśniowo-szkieletowe i tkanki łącznej:** Często: zapalenie mięśni. **Zaburzenia ogólne i stany w miejscu podania:** Bardzo często: zmęczenie. Często: wynaczynienie w miejscu wlewu. **Badania diagnostyczne:** Bardzo często: zwiększona aktywność aminotransferazy alaninowej, zwiększona aktywność aminotransferazy asparaginianowej, zmniejszona masa ciała. Często: lipaza podwyższona. **Urazy, zatrucia i powikłania po zabiegach:** Często: reakcje związane z wlewem. [1] Na podstawie danych zgromadzonych na całym świecie po wprowadzeniu produktu do obrotu. [2] Obejmuje: zespół ostrej niewydolności oddechowej, autoimmunologiczną chorobę płuc, chorobę płuc o podłożu immunologicznym, śródmiąższową chorobę płuc, zmętnienie płuc, organizujące się zapalenie płuc, zapalenie płuc, zwłóknienie płuc, toksyczność płucną i sarkoidozę. Opis wybranych działań niepożądanych: *Immunogenność:* Łącznie 697 pacjentów zbadano w kierunku immunogenności enfortumabu wedotyny podanego w dawce 1,25 mg/kg mc. w monoterapii; 16 pacjentów potwierdzono jako dodatnich pod względem obecności przeciwciał przeciwlekowych (ang. *Anti-Drug Antibodies*, ADA) w punkcie wyjściowym, a spośród pacjentów ujemnych w punkcie wyjściowym (N = 681), łącznie 24 (3,5%) było później dodatnich. Łącznie 490 pacjentów zbadano w kierunku immunogenności enfortumabu wedotyny po podawaniu enfortumabu wedotyny w skojarzeniu z pembrolizumabem; 24 pacjentów potwierdzono jako dodatnich pod względem obecności ADA w punkcie wyjściowym, a spośród pacjentów ujemnych w punkcie wyjściowym (N = 466), łącznie 14 (3%) było później dodatnich. Częstość występowania przeciwciał przeciwko enfortumabowi wedotyny wywołanych leczeniem była spójna z oceną po podawaniu enfortumabu wedotyny w monoterapii oraz w skojarzeniu z pembrolizumabem. Ze względu na ograniczoną liczbę pacjentów, u których potwierdzono obecność przeciwciał przeciwko produktowi leczniczemu Padcev, nie można wyciągnąć wniosków dotyczących możliwego wpływu immunogenności na skuteczność, bezpieczeństwo stosowania i farmakokinetykę produktu. *Reakcje skórne:* W badaniach klinicznych enfortumabu wedotyny w monoterapii reakcje skórne wystąpiły u 57% (452) spośród 793 pacjentów leczonych enfortumabem wedotyny w dawce 1,25 mg/kg mc. Reakcje skórne o ciężkim nasileniu (stopień 3. lub 4.) wystąpiły u 14% (108) pacjentów i większość z tych reakcji obejmowała wysypkę plamisto-grudkową, zapalenie jamy ustnej, wysypkę rumieniowatą, wysypkę lub wykwit polekowy. Mediana czasu do wystąpienia reakcji skórnych o ciężkim nasileniu wynosiła 0,7 miesiąca (zakres od 0,1 do 8,2 miesiąca). Ciężkie reakcje skórne wystąpiły u 4,3% (34) pacjentów. Wśród pacjentów, u których wystąpiły reakcje skórne i dla których były dostępne dane dotyczące ustąpienia (N = 366), u 61% objawy ustąpiły całkowicie, u 24% uzyskano częściową poprawę, a u 15% nie wystąpiła poprawa w momencie ostatniej oceny. Spośród 39% pacjentów z resztkowymi reakcjami skórnymi podczas ostatniej oceny 38% miało zdarzenia stopnia ≥ 2. W badaniach klinicznych enfortumabu wedotyny w skojarzeniu z pembrolizumabem reakcje skórne wystąpiły u 70% (392) spośród 564 pacjentów, a większość tych reakcji skórnych obejmowała wysypkę plamisto-grudkową, wysypkę plamistą oraz wysypkę grudkową. Ciężkie (stopnia 3. lub 4.) reakcje skórne wystąpiły u 17% (97) pacjentów (stopnia 3.: 16%, stopnia 4.: 1%). Mediana czasu do wystąpienia ciężkich reakcji skórnych wynosiła 1,7 miesiąca (zakres: od 0,1 do 17,2 miesiąca). Wśród pacjentów, u których wystąpiły reakcje skórne i którzy mieli dane dotyczące ustąpienia (N = 391), u 59% objawy ustąpiły całkowicie, u 30% uzyskano częściową poprawę, a u 10% nie wystąpiła poprawa w momencie ostatniej oceny. Spośród 41% pacjentów z resztkowymi reakcjami skórnymi w momencie ostatniej oceny 27% miało zdarzenia stopnia ≥ 2. *Nieinfekcyjne zapalenie płuc/ILD:* W badaniach klinicznych enfortumabu wedotyny w monoterapii nieinfekcyjne zapalenie płuc/ILD wystąpiło u 26 (3,3%) spośród 793 pacjentów leczonych enfortumabem wedotyny w dawce 1,25 mg/kg mc. Mniej niż 1% pacjentów doświadczyło ciężkiego (stopień 3. lub 4.) nieinfekcyjnego zapalenia płuc/ILD (stopień 3.: 0,5%, stopień 4.: 0,3%). Nieinfekcyjne zapalenie płuc/ILD doprowadziło do przerwania leczenia enfortumabem wedotyny u 0,5% pacjentów. Nie było zgonów z powodu nieinfekcyjnego zapalenia płuc/ILD. Mediana czasu do wystąpienia nieinfekcyjnego zapalenia płuc/ILD dowolnego stopnia wynosiła 2,7 miesiąca (zakres od 0,6 do 6,0 miesięcy), a mediana czasu trwania nieinfekcyjnego zapalenia płuc/ILD wynosiła 1,6 miesiąca (zakres od 0,1 do 43,0 miesięcy). Spośród 26 pacjentów, u których wystąpiło nieinfekcyjne zapalenie płuc/ILD, u 18 (30,8%) objawy ustąpiły. W badaniach klinicznych enfortumabu wedotyny w skojarzeniu z pembrolizumabem nieinfekcyjne zapalenie płuc/ILD wystąpiło u 58 (10,3%), spośród 564 pacjentów. Ciężkie (stopnia 3. lub 4.) nieinfekcyjne zapalenie płuc/ILD wystąpiło u 20 pacjentów (stopnia 3.: 3,0 %, stopnia 4.: 0,5%). Nieinfekcyjne zapalenie płuc/ILD doprowadziło do przerwania leczenia enfortumabem wedotyny u 2,1% pacjentów. U dwóch pacjentów nieinfekcyjne zapalenie płuc/ILD zakończyło się zgonem. Mediana czasu do wystąpienia jakiegokolwiek stopnia nieinfekcyjnego zapalenia płuc/ILD wynosiła 4 miesiące (zakres: od 0,3 do 26,2 miesiąca). *Hiperglikemia:* W badaniach klinicznych enfortumabu wedotyny w monoterapii hiperglikemia (stężenie glukozy we krwi > 13,9 mmol/l) wystąpiła u 17% (133) spośród 793 pacjentów leczonych enfortumabem wedotyny w dawce 1,25 mg/kg mc. Ciężkie zdarzenia hiperglikemii wystąpiły u 2,5% pacjentów, u 7% pacjentów wystąpiła ciężka (stopnia 3. lub 4.) hiperglikemia, a u 0,3% pacjentów nastąpił zgon, u jednego pacjenta hiperglikemia a u drugiego kwasica ketonowa cukrzycowa. Częstość występowania hiperglikemii stopnia 3.-4. systematycznie rosła u pacjentów z wyższym wskaźnikiem masy ciała i u pacjentów z większym stężeniem hemoglobiny A1C (HbA1c) w punkcie wyjściowym. Mediana czasu do wystąpienia hiperglikemii wynosiła 0,5 miesiąca (zakres od 0 do 20,3). Wśród pacjentów, u których wystąpiła hiperglikemia i dla których były dostępne dane dotyczące ustąpienia (N = 106), u 66% objawy ustąpiły całkowicie, u 19% nastąpiła częściowa poprawa, a u 15% nie wystąpiła poprawa w momencie ostatniej oceny. Spośród 34% pacjentów z resztkową hiperglikemią podczas ostatniej oceny 64% miało zdarzenia stopnia ≥ 2. *Neuropatia obwodowa:* W badaniach klinicznych enfortumabu wedotyny w monoterapii neuropatia obwodowa wystąpiła u 53% (422) spośród 793 pacjentów leczonych enfortumabem wedotyny w dawce 1,25 mg/kg mc. Pięć procent pacjentów doświadczyło ciężkiej (stopień 3. lub 4.) neuropatii obwodowej, w tym zdarzeń czuciowych i ruchowych. Mediana czasu do wystąpienia neuropatii obwodowej stopnia ≥ 2. wynosiła 4,6 miesiąca (zakres od 0,1 do 20,2). Wśród pacjentów, u których wystąpiła neuropatia i dla których były dostępne dane dotyczące ustąpienia (N = 340), u 14% objawy ustąpiły całkowicie, u 46% nastąpiła częściowa poprawa, a u 41% nie wystąpiła poprawa w momencie ostatniej oceny. Spośród 86% pacjentów z resztkową neuropatią podczas ostatniej oceny 51% miało zdarzenia stopnia ≥ 2. *Zaburzenia oka:* W badaniach klinicznych enfortumabu wedotyny w monoterapii 30% pacjentów miało zespół suchego oka w trakcie leczenia enfortumabem wedotyny w dawce 1,25 mg/kg mc. Leczenie przerwało 1,3% pacjentów, a 0,1% trwale przerwało leczenie z powodu zespołu suchego oka. Ciężki (stopnia 3.) zespół suchego oka wystąpił jedynie u 3 pacjentów (0,4%). Mediana czasu do wystąpienia zespołu suchego oka wynosiła 1,7 miesiąca (zakres od 0 do 30,6 miesiąca). Specjalne grupy pacjentów: *Pacjenci w podeszłym wieku:* Enfortumab wedotyny w skojarzeniu z pembrolizumabem oceniano u 173 pacjentów < 65 roku życia i 391 pacjentów ≥ 65 roku życia. Ogólnie częstość występowania zdarzeń niepożądanych była wyższa u pacjentów w wieku ≥ 65 lat w porównaniu z pacjentami w wieku < 65 lat, szczególnie w przypadku ciężkich zdarzeń niepożądanych (odpowiednio 56,3% i 35,3%) oraz zdarzeń ≥ stopnia 3. (odpowiednio 80,3% i 64,2%), podobnie jak w grupie kontrolnej otrzymującej chemioterapię. **Zgłaszanie podejrzewanych działań niepożądanych:** Po dopuszczeniu produktu leczniczego do obrotu istotne jest zgłaszanie podejrzewanych działań niepożądanych. Umożliwia to nieprzerwane monitorowanie stosunku korzyści do ryzyka stosowania produktu leczniczego. Osoby należące do fachowego personelu medycznego powinny zgłaszać wszelkie podejrzewane działania niepożądane za pośrednictwem Departamentu Monitorowania Niepożądanych Działań Produktów Leczniczych Urzędu Rejestracji Produktów Leczniczych, Wyrobów Medycznych i Produktów Biobójczych, Al. Jerozolimskie 181C, PL-02 222 Warszawa, tel.: +48 22 4921 301, faks: +48 22 4921 309, Strona internetowa: https://smz.ezdrowie.gov.pl. **Podmiot odpowiedzialny:** Astellas Pharma Europe B.V., Sylviusweg 62, 2333 BE Leiden, Holandia. **Numery pozwoleń na dopuszczenie do obrotu:** EU/1/21/1615/001-002 – wydane przez Komisję Europejską. **Kategoria dostępności:** Produkt leczniczy wydawany na receptę do zastrzeżonego stosowania – Rpz.

Charakterystyka Produktu Leczniczego dostępna na stronie internetowej Europejskiej Agencji Leków http://www.ema.europa.eu lub na stronie www.astellas.com/pl/product-introductions/charakterystyki-produktow-leczniczych.

Betmiga™
mirabegron

ZWRÓĆ SWOIM PACJENTOM WOLNOŚĆ

ROZWAŻ MIRABEGRON U PACJENTÓW Z OAB, ABY ZWIĘKSZYĆ ZADOWOLENIE Z LECZENIA[1]

OAB – zespół pęcherza nadreaktywnego (ang. *overactive bladder*)

1. Charakterystyka Produktu Leczniczego Betmiga.

MAT-PL-BET-2024-00001 | Kwiecień 2024

astellas

Informacja o leku

Nazwa produktu leczniczego: Betmiga 25 mg, Betmiga 50 mg; tabletki o przedłużonym uwalnianiu. **Skład jakościowy i ilościowy:** Każda tabletka zawiera 25 mg lub 50 mg mirabegronu. Pełny wykaz substancji pomocniczych, patrz punkt 6.1 Charakterystyki Produktu Leczniczego (ChPL). **Postać farmaceutyczna:** Tabletka o przedłużonym uwalnianiu. **Wskazania do stosowania:** Objawowe leczenie naglącego parcia na mocz, częstomoczu i (lub) nietrzymania moczu spowodowanego naglącymi parciami, które mogą wystąpić u dorosłych pacjentów z zespołem pęcherza nadreaktywnego (ang. *overactive bladder*, OAB). **Dawkowanie i sposób podawania:** Dawkowanie: *Dorośli (w tym pacjenci w podeszłym wieku):* Zalecana dawka to 50 mg raz na dobę. *Szczególne grupy pacjentów: Zaburzenia czynności nerek i wątroby:* Produktu leczniczego Betmiga nie badano u pacjentów z krańcowym stadium niewydolności nerek (GFR < 15 ml/min/1,73 m^2 pc. lub pacjenci wymagający hemodializy) czy u pacjentów z ciężkimi zaburzeniami czynności wątroby (klasa C wg skali Child-Pugh), z tego względu nie zaleca się jego stosowania w tej grupie pacjentów (patrz punkt 4.4 i 5.2 ChPL). Zalecenia dotyczące dawki dobowej u pacjentów z zaburzeniami czynności nerek lub wątroby, gdy stosuje się silne inhibitory CYP3A i gdy się ich nie stosuje. Gdy nie stosuje się silnych inhibitorów CYP3A: Łagodne i umiarkowane zaburzenia czynności nerek* oraz łagodne zaburzenia czynności wątroby**: 50 mg. Ciężkie zaburzenia czynności nerek* oraz umiarkowane zaburzenia czynności wątroby**: 25 mg. Gdy stosuje się silne inhibitory CYP3A: Łagodne i umiarkowane zaburzenia czynności nerek* oraz łagodne zaburzenia czynności wątroby**: 25 mg. Ciężkie zaburzenia czynności nerek* oraz umiarkowane zaburzenia czynności wątroby**: nie zaleca się stosowania produktu. *(* Zaburzenia czynności nerek: łagodne: GFR od 60 ml/min/1,73 m^2 pc. do 89 ml/min/1,73 m^2 pc.; umiarkowane: GFR od 30 ml/min/1,73 m^2 pc. do 59 ml/min/1,73 m^2 pc.; ciężkie: GFR od 15 ml/min/1,73 m^2 pc. do 29 ml/min/1,73 m^2 pc. ** Zaburzenia czynności wątroby: łagodne: klasa A wg skali Child-Pugh; umiarkowane: klasa B wg skali Child-Pugh. Silne inhibitory CYP3A: patrz pkt 4.5 ChPL).* Płeć: Nie ma konieczności dostosowania dawki w zależności od płci. Dzieci i młodzież: Nie określono dotychczas bezpieczeństwa stosowania i skuteczności mirabegronu u dzieci w wieku do 18 lat. Dane nie są dostępne. Sposób podawania: Tabletkę należy połknąć w całości, popijając płynami, nie należy jej żuć, dzielić ani kruszyć. Można ją przyjąć z posiłkiem lub bez posiłku. **Przeciwwskazania:** Nadwrażliwość na substancję czynną lub na którąkolwiek substancję pomocniczą wymienioną w punkcie 6.1 ChPL. Ciężkie niekontrolowane nadciśnienie tętnicze [ciśnienie skurczowe ≥ 180 mmHg i (lub) ciśnienie rozkurczowe ≥ 110 mmHg]. **Specjalne ostrzeżenia i środki ostrożności dotyczące stosowania:** Zaburzenia czynności nerek: Nie przeprowadzono badań produktu Betmiga u pacjentów z krańcowym stadium niewydolności nerek (GFR < 15 ml/min/1,73 m^2 pc. lub pacjenci wymagający hemodializy), z tego względu nie zaleca się jego stosowania w tej grupie pacjentów. Dane dotyczące pacjentów z ciężkimi zaburzeniami czynności nerek (GFR od 15 ml/min/1,73 m^2 pc. do 29 ml/min/1,73 m^2 pc.) są ograniczone; na podstawie badań farmakokinetycznych (patrz punkt 5.2 ChPL) zaleca się zmniejszenie dawki do 25 mg w tej grupie pacjentów. Nie zaleca się stosowania tego produktu leczniczego u pacjentów z ciężką niewydolnością nerek (GFR od 15 ml/min/1,73 m^2 pc. do 29 ml/min/1,73 m^2 pc.), przyjmujących jednocześnie silne inhibitory CYP3A (patrz punkt 4.5 ChPL). Zaburzenia czynności wątroby: Nie przeprowadzono badań produktu Betmiga u pacjentów z ciężkimi zaburzeniami czynności wątroby (klasa C wg skali Child-Pugh), z tego względu nie zaleca się jego stosowania w tej grupie pacjentów. Nie zaleca się stosowania tego produktu leczniczego u pacjentów z umiarkowanymi zaburzeniami czynności wątroby (klasa B wg skali Child-Pugh) przyjmujących jednocześnie silne inhibitory CYP3A (patrz punkt 4.5 ChPL). Nadciśnienie tętnicze: Mirabegron może zwiększać ciśnienie tętnicze krwi. Należy zmierzyć ciśnienie krwi przed rozpoczęciem stosowania mirabegronu i monitorować je okresowo w trakcie leczenia, szczególnie u pacjentów z nadciśnieniem tętniczym. Istnieją ograniczone dane dotyczące pacjentów z nadciśnieniem 2. stopnia [ciśnienie skurczowe ≥ 160 mmHg i (lub) ciśnienie rozkurczowe ≥ 100 mmHg]. Pacjenci z wrodzonym lub nabytym wydłużeniem odstępu QT: W badaniach klinicznych produkt leczniczy Betmiga, w dawkach terapeutycznych, nie powodował znaczącego klinicznie wydłużenia odstępu QT (patrz punkt 5.1 ChPL). Jednakże, ze względu na to, że pacjenci z wydłużeniem odstępu QT w wywiadzie lub pacjenci przyjmujący produkty lecznicze, o których wiadomo, że wydłużają odstęp QT, nie byli włączeni do tych badań, działanie mirabegronu u tych pacjentów nie jest znane. Należy zachować ostrożność, stosując mirabegron u tych pacjentów. Pacjenci ze zwężeniem drogi odpływu moczu z pęcherza moczowego i pacjenci przyjmujący antymuskarynowe produkty lecznicze w leczeniu OAB: Po wprowadzeniu produktu leczniczego do obrotu, u pacjentów przyjmujących mirabegron, w grupie pacjentów ze zwężeniem drogi odpływu moczu z pęcherza moczowego (ang. *bladder outlet obstruction*, BOO) i u pacjentów przyjmujących antymuskarynowe produkty lecznicze w leczeniu OAB, zgłaszano zatrzymanie moczu. Kontrolowane badanie kliniczne dotyczące bezpieczeństwa stosowania przeprowadzone u pacjentów z BOO nie wykazało zwiększenia występowania zatrzymania moczu u pacjentów przyjmujących produkt leczniczy Betmiga. Tym niemniej należy zachować ostrożność, stosując produkt leczniczy Betmiga u pacjentów z istotnym klinicznie BOO. Należy również zachować ostrożność, stosując produkt leczniczy Betmiga u pacjentów przyjmujących antymuskarynowe produkty lecznicze w leczeniu OAB. **Działania niepożądane:** Podsumowanie profilu bezpieczeństwa: Bezpieczeństwo stosowania produktu leczniczego Betmiga oceniano u 8433 pacjentów z OAB, z których 5648 otrzymało co najmniej jedną dawkę mirabegronu w ramach programu klinicznego II/III fazy, a 622 pacjentów otrzymywało produkt leczniczy Betmiga przez co najmniej 1 rok (365 dni). W trzech, trwających 12 tygodni, badaniach klinicznych III fazy, przeprowadzonych metodą podwójnie ślepej próby, kontrolowanych placebo, 88% pacjentów ukończyło leczenie tym produktem leczniczym, a 4% pacjentów przerwało leczenie ze względu na zdarzenia niepożądane. Większość działań niepożądanych wykazywało nasilenie łagodne do umiarkowanego. Najczęstszymi działaniami niepożądanymi zgłaszanymi przez pacjentów, którym podawano produkt leczniczy Betmiga w dawce 50 mg, w trzech, trwających 12 tygodni, badaniach klinicznych III fazy, przeprowadzonych metodą podwójnie ślepej próby, kontrolowanych placebo, były tachykardia i zakażenia układu moczowego. Tachykardia występowała z częstością 1,2% u pacjentów otrzymujących produkt leczniczy Betmiga w dawce 50 mg. Tachykardia prowadziła do zaprzestania leczenia u 0,1% pacjentów otrzymujących produkt leczniczy Betmiga w dawce 50 mg. Zakażenia układu moczowego występowały z częstością 2,9% u pacjentów otrzymujących produkt leczniczy Betmiga w dawce 50 mg. Zakażenia układu moczowego nie prowadziły do zaprzestania leczenia u żadnego z pacjentów otrzymujących produkt leczniczy Betmiga w dawce 50 mg. Ciężkie działania niepożądane obejmowały migotanie przedsionków (0,2%). Działania niepożądane obserwowane w trakcie trwającego rok (długotrwałego) badania klinicznego kontrolowanego substancją czynną (antagonista receptorów muskarynowych) były podobnego rodzaju i o podobnym nasileniu, jak działania niepożądane zgłaszane w trzech, trwających 12 tygodni, badaniach klinicznych III fazy, przeprowadzonych metodą podwójnie ślepej próby, kontrolowanych placebo. Poniżej przedstawiono działania niepożądane obserwowane w trakcie stosowania mirabegronu w trzech, trwających 12 tygodni, badaniach klinicznych III fazy, przeprowadzonych metodą podwójnie ślepej próby, kontrolowanych placebo. Częstość działań niepożądanych zdefiniowano w następujący sposób: bardzo często (≥ 1/10); często (≥ 1/100 do < 1/10); niezbyt często (≥ 1/1000 do < 1/100); rzadko (≥ 1/10 000 do < 1/1000); bardzo rzadko (< 1/10 000) i częstość nieznana (nie może być określona na podstawie dostępnych danych). W obrębie każdej grupy o określonej częstości występowania działania niepożądane wymieniono zgodnie ze zmniejszającym się nasileniem. Zakażenia i zarażenia pasożytnicze: często: zakażenie układu moczowego; niezbyt często: zakażenie pochwy, zapalenie pęcherza moczowego. Zaburzenia psychiczne: częstość nieznana: bezsenność*, stan splątania*. Zaburzenia układu nerwowego: często: ból głowy*, zawroty głowy*. Zaburzenia oka: rzadko: obrzęk powiek. Zaburzenia serca: często: tachykardia; niezbyt często: kołatanie serca, migotanie przedsionków. Zaburzenia naczyniowe: bardzo rzadko: przełom nadciśnieniowy*. Zaburzenia żołądka i jelit: często: nudności*, zaparcia*, biegunka*; niezbyt często: niestrawność, zapalenie żołądka; rzadko: obrzęk warg. Zaburzenia skóry i tkanki podskórnej: niezbyt często: pokrzywka, wysypka; wysypka plamista, wysypka grudkowa, świąd; rzadko: alergiczne zapalenie naczyń, plamica, obrzęk naczynioruchowy*. Zaburzenia mięśniowo-szkieletowe i tkanki łącznej: niezbyt często: obrzęk stawów. Zaburzenia nerek i dróg moczowych: rzadko: zatrzymanie moczu*. Zaburzenia układu rozrodczego i piersi: niezbyt często: świąd pochwy i sromu. Badania diagnostyczne: niezbyt często: wzrost ciśnienia tętniczego, wzrost GGT, wzrost AspAT, wzrost AlAT. (*) Obserwowane po wprowadzeniu produktu leczniczego do obrotu. Zgłaszanie podejrzewanych działań niepożądanych: Po dopuszczeniu produktu leczniczego do obrotu istotne jest zgłaszanie podejrzewanych działań niepożądanych. Umożliwia to nieprzerwane monitorowanie stosunku korzyści do ryzyka stosowania produktu leczniczego. Osoby należące do fachowego personelu medycznego powinny zgłaszać wszelkie podejrzewane działania niepożądane za pośrednictwem Departamentu Monitorowania Niepożądanych Działań Produktów Leczniczych Urzędu Rejestracji Produktów Leczniczych, Wyrobów Medycznych i Produktów Biobójczych: Al. Jerozolimskie 181C, PL-02 222 Warszawa, tel.: +48 22 49 21 301, faks: +48 22 49 21 309, strona internetowa: https://smz.ezdrowie.gov.pl. **Podmiot odpowiedzialny:** Astellas Pharma Europe B.V., Sylviusweg 62, 2333 BE Leiden, Holandia. **Numery pozwoleń na dopuszczenie do obrotu:** EU/1/12/809/001-006, EU/1/12/809/008-013, EU/1/12/809/015-018 wydane przez Komisję Europejską. **Kategoria dostępności:** Produkty lecznicze wydawane z przepisu lekarza – Rp.

Charakterystyka Produktu Leczniczego dostępna na stronie internetowej Europejskiej Agencji Leków http://www.ema.europa.eu/ lub na stronie www.astellas.com/pl/product-introductions/charakterystyki-produktow-leczniczych.

MAT-PL-BET-2024-00001 | Kwiecień 2024

Xtandi™
enzalutamid

Korzyści dla przeżycia

we wszystkich wskazaniach w zaawansowanym raku gruczołu krokowego[1]

Xtandi enzalutamid
REFUNDACJA
W PL B.56.

mHSPC

ARCHES[2,3]: p < 0,0001
XTANDI + ADT: n = 574
Placebo + ADT: n = 576; HR: 0,66 (95% CI: 0,53-0,81)
Mediana OS przy kontroli:
Nie osiągnięto, szacunkowo 44,6 miesięcy dla wszystkich grup*

Redukcja ryzyka zgonu o 34%

nmCRPC

PROSPER[4,5]: p = 0,0011
XTANDI + ADT: n = 933
Placebo + ADT: n = 468
HR: 0,734 (95% CI: 0,608-0,885)
Mediana OS przy kontroli: 67,0 miesiąca w porównaniu do 56,3 (placebo)

Redukcja ryzyka zgonu o 27%

mCRPC

AFFIRM[6]: p < 0,0001
XTANDI + ADT: n = 800
Placebo + ADT: n = 399
HR: 0,63 (95% CI: 0,53-0,75)
Mediana OS: 18,4 miesiąca w porównaniu do 13,6 (placebo)

Redukcja ryzyka zgonu o 37%

PREVAIL[7,8]: p = 0,0008
XTANDI + ADT: n = 872
Placebo + ADT: n = 845
HR: 0,835 (95% CI: 0,75-0,93)
Mediana OS: 35,5 miesiąca w porównaniu do 31,4 (placebo)

Redukcja ryzyka zgonu o 17%

Szczegółowy zakres wskazań w informacji o leku.

mHSPC – hormonowrażliwy rak gruczołu krokowego z przerzutami (ang. *metastatic hormone-sensitive prostate cancer*); nmCRPC – oporny na kastrację rak gruczołu krokowego bez przerzutów (ang. *non-metastatic castration-resistant prostate cancer*); mCRPC – oporny na kastrację rak gruczołu krokowego z przerzutami (ang. *metastatic castration-resistant prostate cancer*); ADT – terapia antyandrogenowa (ang. *androgen deprivation therapy*); CI – przedział ufności (ang. *confidence interval*); HR – współczynnik ryzyka (ang. *hazard ratio*); OS – całkowity czas przeżycia (ang. *overall survival*).

astellas

Xtandi™ enzalutamid

Nazwa produktu leczniczego: Xtandi 40 mg, kapsułki miękkie. Xtandi 40 mg, tabletki powlekane. **Skład jakościowy i ilościowy:** Każda kapsułka miękka zawiera 40 mg enzalutamidu. Każda tabletka powlekana zawiera 40 mg enzalutamidu. Substancja pomocnicza o znanym działaniu: Każda kapsułka miękka zawiera 57,8 mg sorbitolu. Pełny wykaz substancji pomocniczych, patrz punkt 6.1 Charakterystyki Produktu Leczniczego (ChPL). **Postać farmaceutyczna:** Kapsułka, miękka. Białe lub prawie białe podłużne kapsułki miękkie (około 20 mm × 9 mm) z nadrukiem „ENZ" po jednej stronie, wykonanym czarnym tuszem. Tabletka powlekana. Żółte okrągłe tabletki powlekane, z wytłoczeniem „E 40". **Wskazania do stosowania:** Produkt leczniczy Xtandi jest wskazany: w monoterapii lub w połączeniu z leczeniem deprywacją androgenów w leczeniu biochemicznie nawracającego (ang. *biochemical recurrent*, BCR) hormonowrażliwego raka gruczołu krokowego wysokiego ryzyka (ang. *non-metastatic hormone-sensitive prostate cancer*, nmHSPC) bez przerzutów u dorosłych mężczyzn, którzy nie klasyfikują się do radioterapii ratunkowej (patrz punkt 5.1 ChPL); w połączeniu z leczeniem deprywacją androgenów w leczeniu hormonowrażliwego raka gruczołu krokowego z przerzutami (ang. *metastatic hormone-sensitive prostate cancer*, mHSPC) u dorosłych mężczyzn (patrz punkt 5.1 ChPL); w leczeniu opornego na kastrację raka gruczołu krokowego wysokiego ryzyka (ang. *castration-resistant prostate cancer*, CRPC) bez przerzutów u dorosłych mężczyzn (patrz punkt 5.1 ChPL); w leczeniu CRPC z przerzutami u dorosłych mężczyzn, u których nie występują objawy lub występują łagodne objawy po niepowodzeniu leczenia deprywacją androgenów i u których chemioterapia nie jest jeszcze klinicznie wskazana (patrz punkt 5.1 ChPL); w leczeniu CRPC z przerzutami u dorosłych mężczyzn, u których podczas lub po zakończeniu leczenia docetakselem nastąpiła progresja choroby. **Dawkowanie i sposób podawania:** Leczenie enzalutamidem powinien rozpocząć i nadzorować lekarz mający doświadczenie w leczeniu raka gruczołu krokowego. Dawkowanie: Zalecana dawka enzalutamidu to 160 mg (cztery kapsułki miękkie po 40 mg lub cztery tabletki powlekane po 40 mg) w jednorazowej dawce dobowej. U pacjentów z CRPC lub mHSPC niekastrowanych chirurgicznie należy w trakcie leczenia kontynuować farmakologiczną kastrację analogami hormonu uwalniającego hormon luteinizujący (LHRH). Pacjenci z BCR nmHSPC wysokiego ryzyka mogą być leczeni produktem leczniczym Xtandi z analogiem LRHR lub bez analogu LRHR. W przypadku pacjentów otrzymujących produkt leczniczy Xtandi z lub bez analogu LRHR leczenie można wstrzymać, jeżeli stężenie PSA jest niewykrywalne (< 0,2 ng/ml) po 36 tygodniach terapii. Leczenie należy wznowić, gdy stężenie PSA wzrosło do ≥ 2,0 ng/ml u pacjentów mających wcześniej prostatektomię radykalną lub ≥ 5,0 ng/ml u pacjentów, którzy mieli wcześniej pierwotną radioterapię. Leczenie należy kontynuować, jeżeli stężenie PSA jest wykrywalne (≥ 0,2 ng/ml) po 36 tygodniach terapii (patrz punkt 5.1 ChPL). W przypadku pominięcia przyjęcia produktu Xtandi o zwykłej porze przepisaną dawkę należy przyjąć tak szybko jak to możliwe. W przypadku pominięcia dawki w danym dniu leczenie należy wznowić następnego dnia, przyjmując zazwyczaj stosowaną dawkę dobową. Jeśli u pacjenta wystąpią objawy toksyczności stopnia ≥ 3. lub trudne do tolerowania działania niepożądane, należy przerwać stosowanie produktu na tydzień lub do czasu zmniejszenia objawów do stopnia ≤ 2. Następnie należy wznowić stosowanie produktu w tej samej lub, jeżeli jest to uzasadnione, zmniejszonej dawce (120 mg lub 80 mg). *Jednoczesne stosowanie z silnymi inhibitorami CYP2C8:* Jeśli jest to możliwe, należy unikać jednoczesnego stosowania silnych inhibitorów CYP2C8. Jeśli konieczne jest jednoczesne stosowanie silnych inhibitorów CYP2C8, należy zmniejszyć dawkę enzalutamidu do 80 mg raz na dobę. W przypadku przerwania jednoczesnego stosowania silnych inhibitorów CYP2C8 należy wznowić stosowanie enzalutamidu w dawce stosowanej przed rozpoczęciem leczenia silnymi inhibitorami CYP2C8 (patrz punkt 4.5 ChPL). *Pacjenci w podeszłym wieku:* Nie ma konieczności dostosowania dawki u pacjentów w podeszłym wieku (patrz punkty 5.1 i 5.2 ChPL). *Zaburzenia czynności wątroby:* Nie ma konieczności dostosowania dawki u pacjentów z lekkimi, umiarkowanymi lub ciężkimi zaburzeniami czynności wątroby (odpowiednio klasa A, B lub C wg skali Child-Pugh). Jednak u pacjentów z ciężkimi zaburzeniami czynności wątroby obserwowano wydłużenie okresu półtrwania enzalutamidu (patrz punkty 4.4 i 5.2 ChPL). *Zaburzenia czynności nerek:* Nie ma konieczności dostosowania dawki u pacjentów z lekkimi lub umiarkowanymi zaburzeniami czynności nerek (patrz punkt 5.2 ChPL). Należy zachować ostrożność u pacjentów z ciężkimi zaburzeniami czynności nerek lub w krańcowym stadium choroby nerek (patrz punkt 4.4 ChPL). *Dzieci i młodzież:* Stosowanie enzalutamidu u dzieci i młodzieży nie jest właściwe we wskazaniu leczenia CRPC, mHSPC lub BCR nmHSPC wysokiego ryzyka u dorosłych mężczyzn. Sposób podawania: Produkt leczniczy Xtandi stosuje się doustnie. Kapsułek miękkich nie należy żuć, rozpuszczać ani otwierać, lecz należy połknąć w całości, popijając wodą, z posiłkiem lub bez posiłku. Tabletek powlekanych nie należy przecinać, rozkruszać ani żuć, lecz należy połknąć w całości, popijając wodą, z posiłkiem lub bez posiłku. **Przeciwwskazania:** Nadwrażliwość na substancję czynną lub na którąkolwiek substancję pomocniczą wymienioną w punkcie 6.1 ChPL. Kobiety, które są w ciąży lub mogą zajść w ciążę (patrz punkty 4.6 i 6.6 ChPL). **Specjalne ostrzeżenia i środki ostrożności dotyczące stosowania:** Ryzyko napadu drgawkowego: Stosowanie enzalutamidu powiązano z występowaniem napadów drgawkowych (patrz punkt 4.8 ChPL). Decyzję o kontynuowaniu leczenia pacjentów, u których wystąpiły napady drgawkowe, należy podejmować w każdym przypadku indywidualnie. Zespół tylnej odwracalnej encefalopatii: U pacjentów otrzymujących Xtandi rzadko zgłaszano zespół tylnej odwracalnej encefalopatii (ang. *posterior reversible encephalopathy syndrome*, PRES). PRES jest rzadko występującym, odwracalnym zaburzeniem neurologicznym, w którym objawy takie jak: drgawki, ból głowy, splątanie, ślepota oraz inne zaburzenia widzenia i zaburzenia neurologiczne mogą się szybko nasilać i któremu towarzyszy lub nie – nadciśnienie tętnicze. Rozpoznanie PRES wymaga potwierdzenia radiologicznym badaniem obrazowym mózgu, najlepiej rezonansem magnetycznym. U pacjentów, u których potwierdzono PRES, zaleca się przerwanie stosowania Xtandi. Drugie pierwotne nowotwory: W badaniach klinicznych zgłaszano przypadki występowania drugiego pierwotnego nowotworu złośliwego u pacjentów leczonych enzalutamidem. W badaniach klinicznych 3. fazy najczęściej zgłaszanymi zdarzeniami u pacjentów leczonych enzalutamidem oraz częściej niż w przypadku placebo były rak pęcherza moczowego (0,3%), gruczolakorak okrężnicy (0,2%), rak przejściowokomórkowy (0,2%) i czerniak złośliwy (0,2%). Należy zalecić pacjentom, aby niezwłocznie zgłosili się do lekarza, jeśli podczas leczenia enzalutamidem zauważą objawy krwawienia z przewodu pokarmowego, krwiomocz makroskopowy lub inne objawy, takie jak trudności w oddawaniu moczu lub nagłe parcie na mocz. Jednoczesne stosowanie z innymi produktami leczniczymi: Enzalutamid jest silnym induktorem enzymów i może powodować brak skuteczności wielu powszechnie stosowanych produktów leczniczych (patrz przykłady w punkcie 4.5 ChPL). Wprowadzając leczenie enzalutamidem, należy dokonać przeglądu jednocześnie stosowanych produktów. Na ogół należy unikać stosowania enzalutamidu jednocześnie z produktami leczniczymi, które są wrażliwymi substratami wielu enzymów metabolizujących lub nośników (patrz punkt 4.5 ChPL), jeżeli ich działanie terapeutyczne ma duże znaczenie dla pacjenta i jeżeli dostosowanie dawkowania nie jest łatwo osiągalne poprzez monitorowanie skuteczności lub stężenia tych produktów w osoczu. Należy unikać jednoczesnego stosowania z warfaryną i przeciwzakrzepowymi produktami leczniczymi, pochodnymi kumaryny. Jeżeli produkt Xtandi jest stosowany jednocześnie z przeciwzakrzepowymi produktami leczniczymi metabolizowanymi przez CYP2C9 (takimi jak warfaryna lub acenokumarol), należy wprowadzić dodatkowe monitorowanie czasu protrombinowego (ang. *International Normalized Ratio*, INR) (patrz punkt 4.5 ChPL). Zaburzenia czynności nerek: Należy zachować ostrożność u pacjentów z ciężkimi zaburzeniami czynności nerek, ponieważ enzalutamid nie był badany w tej grupie pacjentów. Ciężkie zaburzenia czynności wątroby: U pacjentów z ciężkimi zaburzeniami czynności wątroby obserwowano wydłużenie okresu półtrwania enzalutamidu, co może wiązać się ze zwiększoną dystrybucją tkankową. Znaczenie kliniczne tej obserwacji jest nieznane. Można jednak przewidzieć, że czas do osiągnięcia stężenia w stanie stacjonarnym wydłuży się, a czas do osiągnięcia maksymalnego działania farmakologicznego, jak również czas wystąpienia i zmniejszenia indukcji enzymów (patrz punkt 4.5 ChPL) może się zwiększyć. Istniejące choroby układu krążenia: Z badań klinicznych 3. fazy wyłączono pacjentów z niedawno przebytym zawałem mięśnia sercowego (w ostatnich 6 miesiącach) lub niestabilną dusznicą (w ostatnich 3 miesiącach), pacjentów z niewydolnością serca klasy III lub IV według NYHA (ang. *New York Heart Association*), z wyjątkiem przypadków, gdy frakcja wyrzutowa lewej komory (ang. *Left Ventricular Ejection Fraction*, LVEF) wynosiła ≥ 45%, pacjentów z bradykardią lub nieleczonym lub niepoddającym się leczeniu nadciśnieniem tętniczym. Należy wziąć to pod uwagę, przepisując produkt leczniczy Xtandi tym pacjentom. Leczenie deprywacją androgenów może wydłużać odstęp QT: U pacjentów, u których w wywiadzie stwierdzono czynniki ryzyka wydłużenia odstępu QT oraz u pacjentów przyjmujących jednocześnie leki, które mogą wydłużać odstęp QT (patrz punkt 4.5 ChPL), przed rozpoczęciem stosowania produktu Xtandi należy ocenić stosunek korzyści do ryzyka, uwzględniając możliwość wystąpienia częstoskurczu komorowego typu *torsade de pointes*. Stosowanie w czasie chemioterapii: Nie określono bezpieczeństwa stosowania i skuteczności produktu Xtandi w czasie chemioterapii. Jednoczesne podawanie enzalutamidu nie ma klinicznie istotnego wpływu na farmakokinetykę podawanego dożylnie docetakselu (patrz punkt 4.5 ChPL), jednak nie można wykluczyć zwiększenia częstości występowania neutropenii indukowanej docetakselem. Ciężkie reakcje skórne: Podczas stosowania enzalutamidu zgłaszano ciężkie skórne działania niepożądane (SCAR), w tym zespół Stevensa-Johnsona, które mogą zagrażać życiu lub być śmiertelne. W momencie przepisywania, pacjentów należy poinformować o objawach przedmiotowych i podmiotowych oraz starannie monitorować pacjenta w celu wykrycia reakcji skórnych. W przypadku wystąpienia objawów przedmiotowych i podmiotowych sugerujących taką reakcję, enzalutamid należy natychmiast odstawić i (w razie potrzeby) rozważyć odpowiednie leczenie alternatywne. Reakcje nadwrażliwości: Po zastosowaniu enzalutamidu obserwowano reakcje nadwrażliwości, objawiające się m.in. wysypką lub obrzękiem twarzy, języka, warg lub gardła (patrz punkt 4.8 ChPL). Xtandi w monoterapii u pacjentów z BCR nmHSPC wysokiego ryzyka: Wyniki badania EMBARK sugerują, że Xtandi w monoterapii i w połączeniu z leczeniem deprywacją androgenów nie są równoważnymi opcjami terapeutycznymi u pacjentów z BCR nmHSP wysokiego ryzyka (patrz punkt 4.8 i 5.1 ChPL). Xtandi w połączeniu z leczeniem deprywacją androgenów należy rozważyć jako preferowaną opcję leczenia, z wyjątkiem sytuacji gdy dodanie leczenia deprywacją androgenów może skutkować nieakceptowalną toksycznością albo ryzykiem. Substancje pomocnicze: Produkt leczniczy Xtandi zawiera 57,8 mg sorbitolu (E420) w kapsułce miękkiej i mniej niż 1 mmol sodu (mniej niż 23 mg) w tablecie powlekanej, to znaczy lek uznaje się za „wolny od sodu". **Działania niepożądane:** Podsumowanie profilu bezpieczeństwa: Najczęstszymi działaniami niepożądanymi są astenia/zmęczenie, uderzenia gorąca, nadciśnienie tętnicze, złamania i przewracanie się. Inne ważne działania niepożądane obejmują zaburzenia, chorobę niedokrwienną serca i napady drgawkowe. Napad drgawkowy wystąpił u 0,6% pacjentów leczonych enzalutamidem, u 0,1% pacjentów otrzymujących placebo i u 0,3% pacjentów leczonych bikalutamidem. U pacjentów leczonych enzalutamidem rzadko obserwowano zespół tylnej odwracalnej encefalopatii (patrz punkt 4.4 ChPL). W związku z leczeniem enzalutamidem zgłaszano zespół Stevensa-Johnsona (patrz punkt 4.4 ChPL). Poniżej zamieszczono działania niepożądane obserwowane podczas badań klinicznych wg częstości występowania. Częstość określono w następujący sposób: bardzo często (≥ 1/10), często (≥ 1/100 do < 1/10), niezbyt często (≥ 1/1000 do < 1/100), rzadko (≥ 1/10 000 do < 1/1000), bardzo rzadko (< 1/10 000), częstość nieznana (częstość nie może być określona na podstawie dostępnych danych). W obrębie każdej grupy o określonej częstości występowania objawy niepożądane są wymienione zgodnie ze zmniejszającym się nasileniem. Działania niepożądane zidentyfikowane w kontrolowanych badaniach klinicznych i po wprowadzeniu produktu do obrotu: *Zaburzenia krwi i układu chłonnego:* Niezbyt często: leukopenia, neutropenia. Częstość nieznana*: trombocytopenia. *Zaburzenia układu immunologicznego:* Częstość nieznana*: obrzęk twarzy, obrzęk języka, obrzęk warg, obrzęk gardła. *Zaburzenia psychiczne:* Często: lęk. Niezbyt często: omamy wzrokowe. *Zaburzenia układu nerwowego:* Często: ból głowy, zaburzenia pamięci, utrata pamięci, zaburzenia uwagi, zaburzenia smaku, zespół niespokojnych nóg, zaburzenia funkcji poznawczych. Niezbyt często: napady drgawkowe[¥]. Częstość nieznana*: zespół tylnej odwracalnej encefalopatii. *Zaburzenia serca:* Często: choroba niedokrwienna serca[†]. Częstość nieznana*: wydłużenie odstępu QT (patrz punkty 4.4 i 4.5 ChPL). *Zaburzenia naczyniowe:* Bardzo często: uderzenia gorąca, nadciśnienie. *Zaburzenia żołądka i jelit:* Częstość nieznana*: nudności, wymioty, biegunka. *Zaburzenia wątroby i dróg żółciowych:* Niezbyt często: zwiększona aktywność enzymów wątrobowych. *Zaburzenia skóry i tkanki podskórnej:* Często: suchość skóry, świąd. Częstość nieznana*: rumień wielopostaciowy, zespół Stevensa-Johnsona, wysypka. *Zaburzenia mięśniowo-szkieletowe i tkanki łącznej:* Bardzo często: złamania[‡]. Częstość nieznana*: ból mięśni, skurcze mięśni, osłabienie mięśni, ból pleców. *Zaburzenia układu rozrodczego i piersi:* Często: ginekomastia, ból brodawki sutkowej[#], tkliwość piersi[#]. *Zaburzenia ogólne i stany w miejscu podania:* Bardzo często: astenia, zmęczenie. *Urazy, zatrucia i powikłania po zabiegach:* Bardzo często: upadek. * Zgłoszenia spontaniczne po wprowadzeniu produktu do obrotu. [¥] Na podstawie oceny wąskiego zapytania SMQ „Drgawki", obejmującego napad padaczkowy, napad typu *grand mal*, złożone napady częściowe, napady częściowe i stan padaczkowy. Obejmuje to rzadkie przypadki napadów padaczkowych z powikłaniami prowadzącymi do zgonu. [†] Na podstawie oceny wąskiego zapytania SMQ „Zawał mięśnia sercowego" i „Inna niedokrwienna choroba serca", w tym następujących terminów preferowanych zaobserwowanych u co najmniej dwóch pacjentów w randomizowanych, kontrolowanych placebo badaniach 3. fazy: dławica piersiowa, choroba wieńcowa, zawał mięśnia sercowego, ostry zawał mięśnia sercowego, ostry zespół wieńcowy, niestabilna dławica piersiowa, niedokrwienie mięśnia sercowego i miażdżyca tętnic wieńcowych. [‡] Obejmuje wszystkie terminy preferowane ze słowem „złamanie" w odniesieniu do kości. [#] Działania niepożądane enzalutamidu w monoterapii. Opis wybranych działań niepożądanych: *Napad drgawkowy:* W kontrolowanych badaniach klinicznych napad drgawkowy wystąpił u 31 pacjentów (0,6%) spośród 5110 pacjentów leczonych dawką dobową 160 mg enzalutamidu, u czterech pacjentów (0,1%) otrzymujących placebo i u jednego pacjenta (0,3%), któremu podawano bikalutamid. W oparciu o dane niekliniczne oraz dane z badań ze schematem zwiększających się dawek wydaje się, że wielkość dawki jest ważnym prognostykiem ryzyka wystąpienia napadu drgawkowego. Z kontrolowanych badań klinicznych wykluczono pacjentów, u których wcześniej wystąpił napad drgawkowy lub istnieją czynniki ryzyka wystąpienia napadu drgawkowego. W jednoramiennym badaniu 9785-CL-0403 (UPWARD) oceniającym częstości występowania napadów drgawkowych u pacjentów z czynnikami predysponującymi do ich wystąpienia (u 1,6% napad drgawkowy w wywiadzie) u 8 z 366 (2,2%) pacjentów leczonych enzalutamidem wystąpił napad drgawkowy. Mediana czasu leczenia wynosiła 9,3 miesiąca. Nie jest znany mechanizm obniżania progu drgawkowego przez enzalutamid, ale może on wynikać z tego, że jak pokazują dane z badań *in vitro*, enzalutamid oraz jego aktywny metabolit wiążą się z kanałem chlorkowym bramkowanym GABA i mogą hamować jego aktywność. *Choroba niedokrwienna serca:* W randomizowanych badaniach klinicznych kontrolowanych placebo choroba niedokrwienna serca wystąpiła u 3,5% pacjentów leczonych enzalutamidem w połączeniu z ADT w porównaniu z 1,2% pacjentów otrzymujących placebo w połączeniu z ADT. U czternastu (0,4%) pacjentów leczonych enzalutamidem w połączeniu z ADT i 3 (0,1%) pacjentów leczonych placebo w połączeniu z ADT wystąpiło zdarzenie w postaci choroby niedokrwiennej serca, które doprowadziła do zgonu. W badaniu EMBARK choroba niedokrwienna serca wystąpiła u 5,4% pacjentów leczonych enzalutamidem w połączeniu z leuproreliną i 9% pacjentów leczonych enzalutamidem w ramach monoterapii. U żadnego pacjenta leczonego enzalutamidem w połączeniu z leuproreliną i u jednego (0,3%) pacjenta leczonego enzalutamidem w monoterapii wystąpiło zdarzenie w postaci choroby niedokrwiennej serca, która doprowadziła do zgonu. *Ginekomastia:* W badaniu EMBARK ginekomastię (wszystkich stopni) zaobserwowano u 29 spośród 353 (8,2%) pacjentów leczonych enzalutamidem w połączeniu z leuproreliną i u 159 spośród 354 (44,9%) pacjentów leczonych enzalutamidem w monoterapii. Ginekomastii stopnia 3. lub wyższego nie zaobserwowano u żadnego pacjenta leczonego enzalutamidem w połączeniu z leuproreliną i zaobserwowano u 3 pacjentów (0,8%) leczonych enzalutamidem w monoterapii. *Ból brodawki sutkowej:* W badaniu EMBARK ból brodawki sutkowej (wszystkich stopni) zaobserwowano u 11 spośród 353 (3,1%) pacjentów leczonych enzalutamidem w połączeniu z leuproreliną i u 54 spośród 354 (15,3%) pacjentów leczonych enzalutamidem w monoterapii. Bólu brodawki sutkowej stopnia 3. lub wyższego nie zaobserwowano u żadnego pacjenta leczonego enzalutamidem w połączeniu z leuproreliną lub enzalutamidem w monoterapii. *Tkliwość piersi:* W badaniu EMBARK tkliwość piersi (wszystkich stopni) zaobserwowano u 5 spośród 353 (1,4%) pacjentów leczonych enzalutamidem w połączeniu z leuproreliną i u 51 spośród 354 (14,4%) pacjentów leczonych enzalutamidem w monoterapii. Tkliwości piersi stopnia 3. lub wyższego nie zaobserwowano u żadnego pacjenta leczonego enzalutamidem w połączeniu z leuproreliną lub enzalutamidem w monoterapii. Zgłaszanie podejrzewanych działań niepożądanych: Po dopuszczeniu produktu leczniczego do obrotu istotne jest zgłaszanie podejrzewanych działań niepożądanych. Umożliwia to nieprzerwane monitorowanie stosunku korzyści do ryzyka stosowania produktu leczniczego. Osoby należące do fachowego personelu medycznego powinny zgłaszać wszelkie podejrzewane działania niepożądane za pośrednictwem Departamentu Monitorowania Niepożądanych Działań Produktów Leczniczych Urzędu Rejestracji Produktów Leczniczych, Wyrobów Medycznych i Produktów Biobójczych, Al. Jerozolimskie 181C, PL-02 222 Warszawa, tel.: +48 22 49 21 301, faks: +48 22 49 21 309, strona internetowa: https://smz.ezdrowie.gov.pl. **Podmiot odpowiedzialny:** Astellas Pharma Europe B.V., Sylviusweg 62, 2333 BE Leiden, Holandia. **Numery pozwoleń na dopuszczenie do obrotu:** Xtandi 40 mg, kapsułki miękkie: EU/1/13/846/001; Xtandi 40 mg, tabletki powlekane: EU/1/13/846/002; wydane przez Komisję Europejską. **Kategoria dostępności:** Produkt leczniczy wydawany z przepisu lekarza – Rp. Informacja na podstawie ChPL z 25.04.2024 r.

Charakterystyka Produktu Leczniczego dostępna na stronie internetowej Europejskiej Agencji Leków http://www.ema.europa.eu lub na stronie www.astellas.com/pl/product-introductions/charakterystyki-produktow-leczniczych.

MAT-PL-XTD-2024-00034

* Mediany czasu całkowitego przeżycia nie osiągnięto w żadnej z leczonych grup[1].

1. ChPL XTANDI. 2. Armstrong AJ i wsp. J Clin Oncol 2019; 37(32): 2974-2986. 3. Armstrong AJ i wsp. J Clin Oncol 2022; 40(15): 1616-1622. 4. Hussain M i wsp. N Engl J Med 2018; 378(26): 2465-2474. 5. Sternberg CN i wsp. N Engl J Med 2020; 382(23): 2197-2206. 6. Scher HI i wsp. N Engl J Med 2012; 367(13): 1187-1197. 7. Beer TM i wsp. Eur Urol 2017; 71: 151-154. 8. Armstrong AJ et al. Eur Urol 2020; 78(3): 347-357.

MAT-PL-XTD-2024-00051 | Czerwiec 2024

astellas

Diphereline® to temat rozpoczynający rozmowę

Diphereline®
triptorelin

MUTE
Wycisz jego raka prostaty

TALK
Porozmawiaj o tym, co ma dla niego znaczenie

Postaw na ULTRA-niskie stężenia T i wydłużaj OS

99% pacjentów osiągnęło ultra-niskie stężenia T po zastosowaniu Diphereline SR 11,25 mg*[1]

Diphereline® to jedyny analog GnRH z udowodnioną korelacją pomiędzy poziomem T a czasem przeżycia całkowitego (OS)**[1]

T – testosteron; OS – czas całkowitego przeżycia
* W retrospektywnej analizie zbiorczej danych z trzech prospektywnych badań fazy III udowodniono, że nadir stężenia testosteronu <10 ng/dl osiągnięty podczas leczenia tryptoreliną wpływa na poprawę OS i DSS u pacjentów z zaawansowanym rakiem gruczołu krokowego[1]
Odsetek liczby pacjentów leczonych tryptorelinią 11,25 mg, u których nadir stężenia testosteronu wynosił <10 ng/dl[1]
Ultra-niskie stężenia T - znacznie poniżej rekomendowanego poziomu kastracyjnego; dolna granica oznaczalności stężenia testosteronu w badaniu klinicznym wynosiła 0,2 nmol/l (6 ng/dl)[1]
** Badanie przeprowadzone na tryptorelinie, brak szczegółowych danych dla pozostałych substancji czynnych z grupy analogów GnRH

1. Klotz L et al. 2023, BJUI Compass, 1-11

IPSEN

DIP-PL-000726

Diphereline® SR 11,25 mg (Triptorelinum); Skład jakościowy i ilościowy: 1 fiolka zawiera 11,25 mg tryptoreliny (Triptorelinum) w postaci tryptoreliny pamoinianu. **Postać farmaceutyczna:** Proszek i rozpuszczalnik do sporządzania zawiesiny o przedłużonym uwalnianiu do wstrzykiwań (*im.* lub *sc.*) **Wskazania do stosowania:** Rak gruczołu krokowego Leczenie raka gruczołu krokowego kiedy wymagane jest obniżenie stężenia testosteronu do stężenia charakterystycznego dla braku czynności gruczołów płciowych (stężenia kastracyjnego). Pacjenci, którzy uprzednio nie byli poddawani terapii hormonalnej, lepiej reagują na leczenie tryptoreliną. **Dawkowanie i sposób podawania:** Jedno wstrzyknięcie domięśniowe lub podskórne preparatu o przedłużonym uwalnianiu co 3 miesiące. U pacjentów z rakiem gruczołu krokowego z przerzutami opornym na kastrację, niepoddającym się leczeniu operacyjnemu, otrzymujących tryptorelinę oraz kwalifikujących się do leczenia inhibitorami biosyntezy androgenów, leczenie tryptoreliną powinno być kontynuowane. **Przeciwwskazania:** Nadwrażliwość na GnRH, jej analogi lub na którąkolwiek substancję pomocniczą. Stosowanie tryptoreliny jest przeciwwskazane w okresie ciąży i karmienia piersią. **Specjalne ostrzeżenia i środki ostrożności dotyczące stosowania:** Stosowanie analogów GnRH może zmniejszać gęstość mineralną kości. U mężczyzn wstępne dane wskazują, że stosowanie bisfosfonianów w skojarzeniu z analogami GnRH może zmniejszyć utratę gęstości kości. Zachowanie szczególnej ostrożności jest konieczne u pacjentów z dodatkowymi czynnikami ryzyka osteoporozy (np. przewlekłe nadużywanie alkoholu, palenie papierosów, długoterminowa terapia lekami zmniejszającymi gęstość mineralną kości, np. leki przeciwdrgawkowe lub kortykosteroidy, dodatni wywiad rodzinny w kierunku osteoporozy, niedożywienie). W rzadkich przypadkach stosowanie analogów GnRH może ujawnić obecność wcześniej nierozpoznanego gruczolaka wywodzącego się z komórek gonadotropowych przysadki. U pacjentów tych może wystąpić udar przysadki, objawiający się nagłym bólem głowy, wymiotami, zaburzeniami widzenia i porażeniem mięśni oka. Istnieje zwiększone ryzyko wystąpienia epizodu depresyjnego (z możliwymi przypadkami ciężkiej depresji) u pacjentów będących w trakcie leczenia agonistami hormonu uwalniającego gonadotropinę, takich jak tryptorelina. Pacjentów należy odpowiednio poinformować i leczyć w zależności od występujących objawów. Pacjenci z depresją powinni być ściśle kontrolowani podczas terapii. Na początku leczenia tryptorelina, podobnie jak inne analogi GnRH, powoduje przemijający wzrost stężenia testosteronu w surowicy. W rezultacie, sporadycznie, w pierwszych tygodniach leczenia w pojedynczych przypadkach rozwijało się przemijające nasilenie przedmiotowych i podmiotowych objawów raka gruczołu krokowego. W początkowej fazie leczenia należy rozważyć dodatkowe podanie odpowiedniego antyandrogenu, aby przełamać początkowy wzrost stężenia testosteronu w surowicy i nasilenie objawów klinicznych. U niewielkiej liczby pacjentów może dojść do przejściowego nasilenia podmiotowych i przedmiotowych objawów raka gruczołu krokowego (przejściowe zaostrzenie objawów nowotworu) i przejściowego nasilenia bólu związanego z chorobą nowotworową (ból związany z przerzutami), które można leczyć objawowo. Podobnie jak w przypadku innych analogów GnRH obserwowano izolowane przypadki ucisku (kompresji) rdzenia kręgowego lub niedrożności cewki moczowej. Jeżeli rozwinie się ucisk (kompresja) rdzenia kręgowego lub niewydolność nerek, należy wdrożyć standardowe leczenie, a w ekstremalnych przypadkach należy rozważyć wykonanie pilnej orchidektomii (usunięcie jądra). W pierwszych tygodniach leczenia wskazane jest staranne monitorowanie terapii, szczególnie u pacjentów z przerzutami do kręgosłupa, narażonych na ryzyko ucisku rdzenia kręgowego oraz u pacjentów z niedrożnością układu moczowego. Po kastracji chirurgicznej tryptorelina nie indukuje dalszego zmniejszenia stężenia testosteronu w surowicy. Długotrwała deprywacja androgenu, zarówno po obustronnej orchidektomii (usunięcie jądra), jak i po podaniu analogów GnRH, związana jest ze zwiększonym ryzykiem utraty masy kostnej i może prowadzić do osteoporozy oraz wzrostu ryzyka złamań kości. Deprywacja androgenowa może wydłużać odstęp QT. U pacjentów z występującym w wywiadzie wydłużeniem odstępu QT lub z czynnikami ryzyka jego wystąpienia, jak również u pacjentów otrzymujących leczenie towarzyszące, które może powodować wydłużenie odstępu QT lekarz powinien oszacować stosunek korzyści do ryzyka, w tym możliwość wystąpienia zaburzeń rytmu serca typu torsade de pointes, przed włączeniem produktu leczniczego Diphereline SR 11,25 mg. Ponadto, w badaniach epidemiologicznych obserwowano, że u pacjentów może dojść do zmian metabolicznych (np. nietolerancja glukozy, stłuszczenie wątroby) lub może zwiększać się ryzyko choroby układu krążenia w czasie terapii z deprywacją androgenu. Jednakże prospektywne dane nie potwierdziły związku pomiędzy analogami GnRH i wzrostem śmiertelności z przyczyn sercowych. Pacjentów z dużym ryzykiem chorób metabolicznych i chorób układu krążenia należy starannie ocenić przed włączeniem leczenia i w odpowiedni sposób kontrolować w czasie terapii z deprywacją androgenu. Podawanie tryptoreliny w dawkach terapeutycznych powoduje supresję osi przysadkowo-gonadalnej. Normalna funkcja powraca zwykle po zaprzestaniu leczenia. Dlatego testy diagnostyczne gonadalnej funkcji przysadki w czasie leczenia i po zaprzestaniu terapii za pomocą analogów mogą być mylące. Na początku leczenia stwierdza się przemijające zwiększenie aktywności fosfatazy kwaśnej. W czasie leczenia zaleca się przeprowadzać ocenę reakcji układu kostnego za pomocą scyntygrafii i (lub) tomografii komputerowej, natomiast ocenę reakcji gruczołu krokowego na leczenie przeprowadza się za pomocą USG i (lub) tomografii komputerowej oraz badania klinicznego i *per rectum*. Skuteczność leczenia może być monitorowana poprzez oznaczanie stężenia testosteronu i antygenu specyficznego dla prostaty w surowicy krwi. Ten produkt leczniczy zawiera mniej niż 1 mmol (23 mg) sodu na dawkę, to znaczy produkt leczniczy uznaje się za „wolny od sodu". **Działania niepożądane:** Ponieważ pacjenci z miejscowo zaawansowanym lub przerzutowym zależnym od hormonów rakiem gruczołu krokowego są zazwyczaj osobami w starszym wieku i występują u nich inne choroby typowe dla wieku podeszłego, działania niepożądane leku zgłosiło ponad 90% pacjentów uczestniczących w badaniach klinicznych, ocena istnienia związku przyczynowego między stosowanym lekiem a występującym objawem jest trudna. Podobnie jak w przypadku leczenia z udziałem innych agonistów GnRH lub po kastracji chirurgicznej, najczęściej obserwowane działania niepożądane związane z leczeniem tryptoreliną spowodowane były przewidywanym działaniem farmakologicznym. Działania te obejmowały uderzenia gorąca i spadek libido. Wszystkie zdarzenia niepożądane z wyjątkiem reakcji immuno-alergicznych (rzadko) oraz odczynów w miejscu podania wstrzyknięcia (<5%), są związane ze zmianą stężenia testosteronu. Uznano, że zgłoszone następujące działania niepożądane były prawdopodobnie związane ze stosowaniem tryptoreliny. O większości z nich wiadomo, że są związane z biochemiczną lub chirurgiczną kastracją. Częstość występowania działań niepożądanych została sklasyfikowana w następujący sposób: bardzo często (≥ 1/10); często (≥ 1/100 do < 1/10); niezbyt często (≥ 1/1000 do < 1/100.); rzadko (≥ 1/10 000 do < 1/1000).*Bardzo często:* osłabienie, ból pleców, parestezje w kończynach dolnych, zmniejszenie libido, zaburzenia erekcji (w tym brak wytrysku, zaburzenia wytrysku), nadmierna potliwość, uderzenia gorąca; *Często:* uczucie suchości w jamie ustnej, nudności, odczyn w miejscu wstrzyknięcia (w tym rumień, zapalenie i ból), obrzęk, nadwrażliwość, zwiększenie masy ciała, ból mięśniowo-szkieletowy, ból kończyn, zawroty głowy, ból głowy, depresja*, utrata libido, zaburzenia nastroju*, ból miednicy, nadciśnienie tętnicze; *Niezbyt często:* trombocytoza, kołatanie serca, szum w uszach, zawroty głowy, upośledzenie widzenia, ból brzucha, zaparcie, biegunka, wymioty, letarg, obrzęki obwodowe, ból, dreszcze, senność, zwiększona aktywność aminotransferazy alaninowej, zwiększona aktywność aminotransferazy asparginowej, zwiększone stężenie kreatyniny we krwi, wzrost ciśnienia tętniczego krwi, zwiększone stężenie mocznika we krwi, zwiększona aktywność gamma-glutamylotransferazy, spadek masy ciała, jadłowstręt, cukrzyca, dna moczanowa, hiperlipidemia, zwiększenie apetytu, ból stawów, ból kości, skurcze mięśni, osłabienie mięśniowe, ból mięśniowy, parestezje, bezsenność, drażliwość, nokturia, zatrzymanie moczu, ginekomastia, ból sutków (gruczołów piersiowych), atrofia jąder, ból jąder, duszność, krwawienie z nosa, trądzik, łysienie, rumień, świąd, wysypka, pokrzywka; *Rzadko:* nieprawidłowe uczucie w obrębie oczu, zaburzenia widzenia, wzdęcia, zaburzenia smaku, wzdęcia z oddawaniem wiatrów, ból w klatce piersiowej, trudność w utrzymaniu pozycji stojącej, objawy grypopodobne, gorączka, reakcja anafilaktyczna, zapalenie jamy nosowej i gardła, zwiększona aktywność fosfatazy alkalicznej we krwi, sztywność stawów, obrzęk stawów, sztywność układu mięśniowo-szkieletowego, zapalenie kości i stawów, zaburzenia pamięci, stan splątania, zmniejszenie aktywności, euforyczny nastrój, duszność w pozycji leżącej, powstawanie pęcherzy, plamica, spadek ciśnienia; *Dodatkowe działania niepożądane stwierdzone w okresie po wprowadzeniu do obrotu - częstość występowania nieznana:* wydłużenie odstępu QT *(Częstość występowania podano na podstawie częstości występowania wspólnej dla całej klasy agonistów GnRH)*, udar przysadki *(Działanie niepożądane zgłaszane po pierwszym podaniu u pacjentów z gruczolakiem przysadki)*, złe samopoczucie, wstrząs anafilaktyczny, niepokój, nietrzymanie moczu, obrzęk naczynioruchowy. Tryptorelina powoduje przemijający wzrost stężenia krążącego testosteronu w ciągu pierwszego tygodnia po pierwszej iniekcji postaci o przedłużonym uwalnianiu. Przy takim początkowym wzroście stężenia krążącego testosteronu u niewielkiego odsetka pacjentów (≤ 5%) może dojść do przemijającego nasilenia podmiotowych i przedmiotowych objawów raka gruczołu krokowego (przejściowe zaostrzenie objawów nowotworu), które zwykle objawia się nasileniem objawów ze strony układu moczowego (< 2%) oraz bólu związanego z obecnością przerzutów (5%), które można leczyć objawowo. Objawy te są przemijające i zwykle ustępują w ciągu jednego do dwóch tygodni. W pojedynczych przypadkach wystąpiło zaostrzenie objawów choroby, objawiające się niedrożnością cewki moczowej lub uciskiem (kompresją) rdzenia kręgowego, związaną z obecnością przerzutów. Dlatego pacjentów z przerzutami do kręgosłupa i (lub) niedrożnością górnego lub dolnego odcinka dróg moczowych należy ściśle obserwować w pierwszych tygodniach terapii. Stosowanie analogów GnRH w terapii raka gruczołu krokowego może wiązać się ze zwiększoną utratą masy kostnej i może prowadzić do osteoporozy oraz zwiększonego ryzyka złamań kości. U pacjentów otrzymujących długotrwałe leczenie analogiem GnRH w połączeniu z radioterapią może wystąpić więcej działań niepożądanych, głównie żołądkowo-jelitowych i związanych z radioterapią. **Podmiot odpowiedzialny:** Ipsen Pharma, 65 Quai Georges Gorse, 92100, Boulogne Billancourt, Francja. **Informacji o leku udziela:** Ipsen Poland Sp. z o.o., ul. Chmielna 73, 00-801 Warszawa, tel.: (22) 653 68 00, fax: (22) 653 68 22. **Numer pozwolenia na dopuszczenie do obrotu wydanego przez MZ:** 8944. Kategoria dostępności: Produkt leczniczy wydawany z przepisu lekarza - Rp. Produkt leczniczy umieszczony na wykazie leków refundowanych w chorobach przewlekłych; cena detaliczna 620,09 PLN; wysokość dopłaty świadczeniobiorcy w raku prostaty - dawka 11,25 mg – 63,81 PLN zgodnie z Obwieszczeniem Ministra Zdrowia w sprawie wykazu refundowanych leków, środków spożywczych specjalnego przeznaczenia żywieniowego oraz wyrobów medycznych. *Przed zastosowaniem należy zapoznać się z zatwierdzoną Charakterystyką Produktu Leczniczego. Data ostatniej aktualizacji ChPL: 20.06.2024 r.*

Acknowledgement to Reviewers

I wish to thank all the reviewers for their generous assistance in evaluating manuscripts submitted to the "Central European Journal of Urology" during the past year. I fully appreciate the effort required to read, analyze, and evaluate a scientific manuscript. Thoughtful and unbiased reviews are essential to maintaining the high quality of each scientific journal, and without your expert contributions, the "Central European Journal of Urology" would not be the outstanding journal that it is. The list below comprises all of them.

Reviewers active in 2024

Faris Abushamma
Eugenio Alessandria
Eleni Anastasiadis
Maria Giovanna Asmundo
Krzysztof Balawender
Włodzimierz Baranowski
Dimitri Barski
Ali Baseskioglu
Kensuke Bekku
Łukasz Białek
Alberto Bianchi
Gabriele Bignante
Matthias Boeykens
Eugenio Bologna
Edyta Borkowska
Ewa Bres-Niewada
Piotr Bryniarski
Omer Cakir
Abdullah Canda
Marco Capece
Paolo Capogrosso
Filippo Carletti
Daniele Castellani
Francesco Chierigo
Cecilia Cracco
Vincent de Coninck
Fotios Dimitriadis
Francesco Ditonno
Laurian Dragos
Jacopo Durante
Bartosz Dybowski
Kemal Ener
Karina Felberg
Nicolò Fiorello
Jerzy Gajewski
Vineet Gauhar
Enrique Gomez Gomez
Nikolaos Grivas
Nico Grossmann
Mudhar Hasan
Milosz Jasinski
Mindaugas Jievaltas
Patrick Jones
Tomasz Jurys
Krystian Kaczmarek
Odunayo Kalejaiye
Hubert Kamecki
Parizi Mehdi Kardoust
Jakub Karwacki
Sławomir Kata
Michał Kępiński
Anna Kołodziej
Nikolaos Kostakopoulos
Filip Kowalski
Mieszko Kozikowski
Wojciech Krajewski
Andras Kubik
Jakub Kufel
Błażej Kuffel
Francesco Lasorsa
Angus Luk
Stefano Mancon
Guglielmo Mantica
Marcin Matuszewski
Łukasz Mielczarek
Jeremy Nettleton
Angelo Orsini
Rafał Osiecki
Maciej Oszczudłowski
Matteo Pacini
Maximilian Pallauf
Gianpaolo Perletti
Cristian Persu
Amelia Pietropaolo
Sławomir Poletajew
Silvia Proietti
Mauro Ragonese
Grzegorz Rempega
Daniele Robesti
Artur Rogowski
Vasileios Sakalis
Laila Schneidewind
Michał Skrzypczyk
Jolanta Słowikowska-Hilczer
Marta Sochaj
Mohammad A. Soebadi
Bhaskar Somani
Theodoros Spinos
Theodora Stasinou
Raimund Stein
Evangelos N. Symeonidis
Łukasz Szylberg
Aleksander Ślusarczyk
Arman Tsaturyan
Nick Watkin
Łukasz Zapała
Piotr Zapała
Przemysław Zugaj

I am delighted to present ten reviewers who provided the highest number of most valuable reviews. Their contributions to evaluating submitted manuscripts are invaluable, and their dedication and time form the foundation of the high standards of our journal. These exceptional individuals deserve special recognition – their insight, thoroughness, and scientific rigor are exemplary.

Jerzy Gajewski

Miłosz Jasiński

Marcin Matuszewski

Łukasz Zapała

Cristian Persu

Gabriele Bignante

Daniele Castellani

Filip Kowaski

Maciej Oszczudłowski

Matteo Pacini

I regret that an ideal way to fully appreciate such tremendous effort has yet to be devised. Nevertheless, on behalf of the Editorial Office and the Executive Board of the Polish Urological Association I express our profound gratitude and hope that your work for CEJU will continue.

Bartosz Dybowski
Editor in Chief

Contents

Contents

SUBMISSIONS

The Central European Journal of Urology accepts submissions in the following categories: Original basic and clinical articles, Review articles, Short communications (preliminary results and mini-reviews), Commentaries on medical innovations, new technologies, and clinical trials, Letters to the Editor, Case reports, Editorial comments, Video presentations on surgical skills.

Authors Guidelines are available at **www.ceju.online**

Online Submission System is available at **www.ceju.online**

ORIGINAL PAPER

UROLOGICAL ONCOLOGY

Discrepancies in volume: impact of Artemis segmented magnetic resonance imaging, ultrasound, and ExactVu measurements on prostate specific antigen density and National Comprehensive Cancer Network risk stratification

Maximilian J. Rabil[1], Lindsey T. Webb[1], Gabriela M. Diaz[1], Soum D. Lokeshwar[1], Ankur U. Choksi[1], Preston C. Sprenkle[1,2]

[1]*Yale University School of Medicine, New Haven, Connecticut, United States of America*
[2]*Veterans Affairs Connecticut Healthcare System, West Haven, Connecticut, United States of America*

Citation: Rabil MJ, Webb LT, Diaz GM, et al. Discrepancies in volume: impact of Artemis segmented magnetic resonance imaging, ultrasound, and ExactVu measurements on prostate specific antigen density and National Comprehensive Cancer Network risk stratification. Cent European J Urol. 2025; 78: 1-4.

Article history
Submitted: Nov. 18, 2024
Accepted: Dec. 2, 2024
Published online: Mar. 18, 2025

Corresponding author
Maximilian J. Rabil
Yale University School of Medicine, Yale Urology, 789 Howard Avenue, FMP 300, New Haven, Connecticut 06519, USA
maximilian.rabil@yale.edu

Introduction The combination of magnetic resonance imaging (MRI) and ultrasound (US) allows for better lesion targeting and diagnostic probability compared to random prostate biopsies. The Artemis Fusion Biopsy system and ExactVu micro-US technology capitalize on this advantage and provide higher-resolution imaging of the prostate during biopsy. Their accuracy in measuring prostate volume and resulting implications on prostate specific antigen (PSA) density and risk stratification, however, has not been evaluated. We hypothesized that PSA densities as measured by these modalities will demonstrate clinically insignificant differences compared to standard measurement.

Material and methods We retrospectively reviewed all prostate fusion biopsy cases performed at our health system with Artemis or ExactVu systems from April 2021 to July 2023 and compared the PSA density calculated from the volume obtained with these systems to standard measurement with ellipsoid calculation from MRI. Change in National Comprehensive Cancer Network (NCCN) prostate cancer risk stratification was analyzed for each system.

Results Artemis MRI segmentation (0.179 ng/ml, p = 0.04) and US (0.181 ng/ml, p = 0.067) underestimated and ExactVu micro-US (0.247 ng/ml, p <0.001) overestimated PSA density. Risk stratification changed in 1.2% of Artemis MRI segmentation cases, 1.6% of Artemis US cases, and 1.2% of ExactVu micro-US cases.

Conclusions Despite differences in PSA density, choice of fusion biopsy system has minimal clinical impact on risk stratification and any of these studied systems may be used without fear of misrepresenting a patient's disease state.

Key Words: prostate biopsy ‹› prostate cancer ‹› prostate cancer risk stratification ‹› prostate MRI ‹› prostate ultrasound ‹› PSA density

INTRODUCTION

Fusion of multi-parametric magnetic resonance imaging (mpMRI) and ultrasound (US) allows for better lesion targeting and diagnostic probability of clinically significant prostate cancer compared to template prostate biopsies using US alone [1]. Numerous fusion systems are currently FDA approved, and, in addition to their utility in targeting prostatic lesions, aid in clinical decision making through prostate volume measurement.

The Artemis™ (Eigen, Grass Valley, CA, USA) fusion system provides two prostate volume measurements: standard US manual measurement and

proprietary segmentation software which permits fine tuning of the volume measurement to the gland's morphology on MRI using 3D reconstruction [2]. Once automated segmentation is complete, the reading radiologist contours the measurement to obtain a prostate volume.

The ExactVu™ (Exact Imaging, Inc, Markham, ON, CA) micro-ultrasound system provides high spatial resolution images for volume measurement and cancer detection, which can be further leveraged through fusion [3, 4]. Using an ellipsoid or bullet-shaped measurement paradigm to calculate prostate volume from an mpMRI has been shown to provide significantly different results in PSA density, making it imperative providers understand the modality used to measure prostate volume and hence the resulting PSA density [5].

Accuracy of MRI fusion and micro-US in measuring prostate volume and the resultant implications for PSA density-based decision making, however, have not been evaluated. We hypothesized that PSA density as calculated by volume measurements using either Artemis MRI segmentation, Artemis US, or ExactVu micro-ultrasound will demonstrate clinically insignificant differences compared to MRI ellipsoid calculation.

MATERIAL AND METHODS

We retrospectively reviewed all cases of prostate fusion biopsy performed with either Artemis™ or ExactVu™ at our academic health system from April 2021 to July 2023. Patients without a pre-biopsy MRI were excluded.

Prostate volumes as measured by Artemis MRI segmentation, Artemis US measurement, and ExactVu micro-US measurement were used to calculate PSA density. These were compared to PSA density calculated from standard MRI ellipsoid measurement as the gold standard using a paired t-test with statistical significance set at $p < 0.05$ in Microsoft Excel (Microsoft Corporation, Redmond, WA).

Change in National Comprehensive Cancer Network (NCCN) risk stratification on the basis of the PSA density criterion for very low risk prostate cancer (PSA density <0.15 ng/ml/g) was analyzed for all comparisons to assess the clinical impact of the discrepancies in measured volume.

RESULTS

In total, prostate volumes were available for 172 patients with Artemis MRI 3D segmentation, 189 with Artemis US 3D segmentation, and 340 with ExactVu micro-US prostate measurement and ellipsoid volume calculation. 3D-segmented prostate volumes of both Artemis system MRI and US are generally larger than the ellipsoid calculation – resulting in lower average PSA density. The converse was true for the ExactVu micro-ultrasound resulting in, on average, an overestimation of PSA density. Mean PSA density differed significantly from MRI ellipsoid-based calculation when volume was measured with Artemis MRI with segmentation and ExactVu micro-US but did not reach significance for Artemis US (Table 1).

NCCN risk stratification changed in 2/172 (1.2%) Artemis 3D-MRI cases (1 risk progression, 1 regres-

Table 1. *PSA density as calculated by different modalities*

Artemis MRI segmentation vs ellipsoid MRI							
n = 172	Artemis MRI [ng/ml]	Ellipsoid MRI [ng/ml]	p-value	Mean difference (abs. value)	% Error	Changes to NCCN risk stratification (N)	
Mean	0.179	0.196	0.04	0.044	18.15	Stage progression	1
Variance	0.032	0.046	–	–	–	Stage regression	1
Artemis US vs ellipsoid MRI							
n = 189	Artemis US [ng/ml]	Ellipsoid MRI [ng/ml]	p-value	Mean difference (abs. value)	% Error	Changes to NCCN risk stratification (N)	
Mean	0.181	0.193	0.067	0.046	21.44	Stage progression	1
Variance	0.027	0.037	–	–	–	Stage regression	2
ExactVu US vs ellipsoid MRI							
n = 340	ExactVu US [ng/ml]	Ellipsoid MRI [ng/ml]	p-value	Mean difference (abs. value)	% Error	Changes to NCCN risk stratification (N)	
Mean	0.247	0.180	<0.001	0.079	24.69	Stage progression	4
Variance	0.083	0.032	–	–	–	Stage regression	0

MRI – magnetic resonance imaging; NCCN – National Comprehensive Cancer Network; US – ultrasound

sion); 3/189 (1.6%) Artemis US cases (1 risk progression, 2 regression); and 4/340 (1.2%) ExactVu cases (all risk progression).

DISCUSSION

Although our modalities for measuring prostate volume provide statistically significant differences in PSA density, these discrepancies do not result in clinically significant differences in NCCN risk stratification, allowing clinical decision making to proceed confidently. Stated differently, while prostate volumes as measured with different modalities may vary, this study suggests that direct comparisons of risk assessment can be made with PSA density measurements from any of the studied imaging systems without compromising accuracy and clinical relevance.

A study from over a decade ago investigated variation in PSA density measurement between trans-rectal-US, trans-abdominal US, computed tomography (CT) scans finding only CT produced statistically significant differences in PSA density [6], but the dearth of literature comparing the imaging advancements in the interim decade persists.

To our knowledge, this is the first study to investigate variation in PSA density and its impact on prostate cancer risk stratification, and we hope that our findings inform others' practice and encourage discourse and further investigation.

In light of our findings, the question remains whether current a prostate-specific antigen density (PSAd) thresholds, established in the era of earlier imaging, remain accurate with the myriad new imaging systems used for fusion prostate biopsy which offer new techniques to measure prostate volume. A PSAd threshold to distinguish clinically significant and insignificant prostate cancer of 0.10 ng/ml/cc was first established in 1994 on retrospective review of prostate volumes calculated with direct measurement of prostatectomy pathology specimens and TRUS ellipsoid measurement [7].

The practice patterns of prostate cancer and the tools we use have naturally changed significantly in the intervening 30 years. The need for re-evaluation of PSAd thresholds with new imaging techniques is well established: the currently used 0.15 ng/ml/cc was deemed too high and not sensitive enough when prostate volume was measured by a spherical formula for dimensions measured by US [8].

As mpMRI became more prevalently used in prostate cancer care in the late 2000s and early 2010s, the improved visualization offered made measurement by the ellipsoid formula and early semi-automated segmentation programs more precise, bringing a threshold of 0.15 ng/ml/cc to favor especially when combined with Prostate Imaging-Reporting and Data System (PI-RADS) scores to make clinical decisions [9, 10].

With quality of MRI improved and more robust segmentation schemes developed, Pellegrino et al. [11] suggests, instead, a PSAd threshold of 0.20 ng/ml/cc for patients with a negative MRI to undergo prostate biopsy as the current threshold of 0.15 ng/ml/cc is too non-specific except in the case of low quality MRI imaging. If this higher threshold was used in our analysis, all Artemis 3D-MRI and US risk changes two of the four ExactVue risk discrepancies would no longer have occurred.

In contrast, increasing the PSAd threshold is not fully supported by the literature base; despite the more accurate contouring of segmentation software, PSAd cannot be relied on in isolation of other patient factors. Use of PSAd alone to make decisions on whether or not to biopsy risks missing clinically significant cancer, with 15% of clinically significant cancers would be missed in patients with PI-RADS score of 3 and PSAd below 0.15 ng/ml/cc [12].

Finally, if there is one situation where new methods of prostate volume measurement differ most from the ellipsoid formula and thus PSAd would be most affected, it would be in cases of abnormal prostate anatomy such as post-transurethral resection of the prostate [13].

Altogether, further investigation is needed to decide if PSAd thresholds need to be changed as the landscape of peri-biopsy prostate imaging evolves. To aid in this, clear documentation of prostate volume methods should be included in studies of PSAd and its uses in dictating clinical decisions. With our findings and the existing literature base in mind, it is the authors' assertion that PSAd thresholds likely should be reconsidered given the diversity of methods used across practices, the greater granularity provided by modern imaging systems and their accompanying software-based enhancement and measurement capabilities, and the rich store of other risk-stratifying data points (PI-RADS score, genomic classifiers, etc.) for which PSAd can serve as an adjunct.

This study is limited by its single-institution retrospective design, inclusion of only two of the many available fusion biopsy imaging systems, inability to make direct comparisons between imaging modalities as measurement by one fusion system was mutually exclusive of measurement with the other, and the small role PSA density plays in NCCN risk stratification as it only separates very low risk and low risk disease. Nevertheless, the distinction

between very low risk and low risk prostate cancer in the context of the broader clinical picture may still dictate a patient's decision and a Urologist's recommendation.
Future studies validating these findings outside of our health system and including other fusion biopsy imaging systems in comparisons would broaden the implications of these findings and be valuable in supporting that confidence in decision-making.

CONCLUSIONS

The measured volumes across the studied fusion biopsy systems differ considerably, but PSA density values as calculated by Artemis MRI segmentation, Artemis US, or ExactVu micro-ultrasound do not demonstrate significant differences in NCCN risk stratification when compared to measurement by MRI ellipsoid calculation. They can therefore be safely used to make clinical decisions without fear of misrepresenting the patient's medical condition.

CONFLICTS OF INTEREST
The authors declare no conflict of interest.

FUNDING
This research received no external funding.

ETHICS APPROVAL STATEMENT
The ethical approval was not required.

References

1. Kaneko M, Sugano D, Lebastchi AH, et al. Techniques and Outcomes of MRI-TRUS Fusion Prostate Biopsy. Curr Urol Rep. 2021; 22: 27.
2. Angileri SA, Di Meglio L, Petrillo M, et al. Software-assisted US/MRI fusion-targeted biopsy for prostate cancer. Acta Biomed. 2020; 91(10-S): e2020006.
3. Vassallo R, Aleef TA, Zeng Q, Wodlinger B, Black PC, Salcudean SE. Robotically controlled three-dimensional micro-ultrasound for prostate biopsy guidance. Int J Comput Assist Radiol Surg. 2023; 18: 1093-1099.
4. Wang B, Broomfield S, Martin AM, Albers P, Fung C, Kinnaird A. Detection of clinically significant prostate cancer by micro-ultrasound-informed systematic biopsy during MRI/micro-ultrasound fusion biopsy. Can Urol Assoc J. 2023; 17: 117-120.
5. Stanzione A, Ponsiglione A, Di Fiore GA, et al. Prostate Volume Estimation on MRI: Accuracy and Effects of Ellipsoid and Bullet-Shaped Measurements on PSA Density. Acad Radiol. 2021; 28: e219-e226.
6. Varkarakis I, Zarkadoulias A, Bourdoumis A, Chatzidarellis E, Antoniou N, Deliveliotis C. Measurement of PSA density by 3 imaging modalities and its correlation with the PSA density of radical prostatectomy specimen. Urol Oncol. 2013; 31: 1038-1042.
7. Epstein JI, Walsh PC, Carmichael M, Brendler CB. Pathologic and clinical findings to predict tumor extent of nonpalpable (stage T1c) prostate cancer. JAMA. 1994; 271: 368-374.
8. Boulos MTB, Rifkin MD, Ross J. Should prostate-specific antigen or prostate-specific antigen density be used as the determining factor when deciding which prostates should undergo biopsy during prostate ultrasound. Ultrasound Q. 2001; 17: 177-180.
9. Dianat SS, Rancier Ruiz RM, Bonekamp D, Carter HB, Macura KJ. Prostate volumetric assessment by magnetic resonance imaging and transrectal ultrasound: impact of variation in calculated prostate-specific antigen density on patient eligibility for active surveillance program. J Comput Assist Tomogr. 2013; 37: 589-595.
10. Stevens E, Truong M, Bullen JA, Ward RD, Purysko AS, Klein EA. Clinical utility of PSAD combined with PI-RADS category for the detection of clinically significant prostate cancer. Urol Oncol. 2020; 38: 846.e9-846.e16.
11. Pellegrino F, Tin AL, Martini A, et al. Prostate-specific Antigen Density Cutoff of 0.15 ng/ml/cc to Propose Prostate Biopsies to Patients with Negative Magnetic Resonance Imaging: Efficient Threshold or Legacy of the Past? Eur Urol Focus. 2023; 9: 291-297.
12. Nguyen TA, Fourcade A, Zambon A, et al. Optimal PSA density threshold and predictive factors for the detection of clinically significant prostate cancer in patient with a PI-RADS 3 lesion on MRI. Urol Oncol. 2023; 41: 354.e11-354.e18.
13. Lin YT, Hung SW, Chiu KY, Chai JW, Lin JC. Assessment of Prostate Volume and Prostate-specific Antigen Density With the Segmentation Method on Magnetic Resonance Imaging. In Vivo. 2023; 37: 786-793.

ORIGINAL PAPER

UROLOGICAL ONCOLOGY

Postoperative complications, emergency department utilisation, and readmission after radical cystectomy

Maxwell Sandberg[1], Claudia Marie-Costa[2], Rachel Vancavage[3], Emily Ye[2], Gavin Underwood[2], Rainer Rodriguez[2], Emily Roebuck[2], Sean Catley[2], Jorge Seoane[2], Arjun Choudhary[4], Stephen Tranchina[1], Ashok Hemal[1], Alejandro R. Rodriguez[1]

[1]*Department of Urology, Atrium Health Wake Forest Baptist Medical Center, United States of America*
[2]*Wake Forest University School of Medicine, Winston Salem, United States of America*
[3]*Albany Medical College, United States of America*
[4]*Tufts University School of Medicine, Boston, United States of America*

Citation: Sandberg M, Marie-Costa C, Vancavage R, et al. Postoperative complications, emergency department utilisation, and readmission after radical cystectomy. Cent European J Urol. 2025; 78: 5-13.

Article history
Submitted: Aug. 5, 2024
Accepted: Nov. 3, 2024
Published online: Nov. 30, 2024

Corresponding author
Maxwell Sandberg
Medical Center Boulevard
Winston Salem, NC, 27187,
United States of America
maxwellsandberg@msn.com

Introduction There is minimal research on the types of complications patients experience after radical cystectomy (RC). Moreover, the impact of these complications is not well qualified. The primary purpose of this study is to qualify complications after RC and quantify rates of emergency department (ED) utilisation and readmissions to the hospital. The secondary purpose is to associate risk factors for ED visits and hospital readmission.

Material and methods Patients were retrospectively analysed, who underwent RC for bladder cancer. ED visits within 90 days of discharge from RC and readmission at both 30 and 31–90 days of discharge were collected. Complications were graded using the Clavien-Dindo system and classified using the Memorial Sloan-Kettering Cancer Center complication system.

Results Three hundred and eighty-six patients were included. The in-house complication rate before discharge was 36%, and the 90-day complication rate after discharge was 54.8%. 33.7% of patients had ≥1 ED visit postoperatively, 18.7% were readmitted within 30 days, and 17.3% within 31–90 days of discharge. The primary reason for ED presentation, readmission at 30 and 31–90 days was infection. Cutaneous ureterostomy (CU) was associated with greater likelihood of presentation to the ED and readmission 31–90 days postoperatively ($p < 0.01$). Overall survival (OS) was worse in patients who presented to the ED and/or were readmitted at both the 30- and 31–90-day marks ($p < 0.01$).

Conclusions ED utilisation and readmission rates after RC are high. The most common complication is infection. Patients with a CU are at higher risk for healthcare utilisation. OS is worse in patients with an ED visit or readmission to the hospital, and these patients may require closer monitoring.

Key Words: radical cystectomy ‹› emergency department ‹› readmission ‹› bladder cancer

INTRODUCTION

Radical cystectomy (RC) for bladder cancer is a procedure urologists perform with high morbidity and mortality. Outcomes for RC are well reported in the literature. Estimates are around 50% for postoperative complications within 3 months of surgery [1]. Further, oncologic outcomes have been extensively published, with disease-free survival at 5 years ranging from 53 to 74%, cancer-specific survival 66 to 80%, and overall survival (OS) 61 to 80% [2]. Most current research focuses on how to minimise immediate postoperative complications and/or maximise patient survival. This is critical information that warrants considerable time studying. However, there is a paucity of research on the types of complications patients experience after RC. Moreover, the impact of these complications is not well quali-

fied, namely emergency department (ED) utilisation and readmission rates after RC.

Because RC has such high postoperative morbidity, it is surprising that more papers do not qualify the specific types of complications patients experience, but rather the grade of complication alone. Shabsigh et al. attempted to qualify complication type after RC into 11 categories, in what has become known as the Memorial Sloan-Kettering Cancer Center (MSKCC) complication system [3]. Using this framework, some have noted that either urinary tract infections (UTIs) or gastrointestinal (GI) complications are the most common postoperative complications, but there is no consensus on this [4, 5]. ED visits after RC are also difficult to quantify, with some estimates around 7–14% up to 90-days after surgery [4, 6]. Readmission rates are slightly better understood: around 23–28% at 30 days postoperatively and about 39% within 90 days of surgery, but additional study is still lacking [6–8]. Moreover, models that can predict risk factors for patients who are most likely to visit the ED after surgery and/or be readmitted are needed.

The primary purpose of this study is to qualify complications after RC and quantify rates of ED utilisation and readmissions to the hospital. The secondary purpose of this paper is to associate risk factors for ED visits and readmission to the hospital.

MATERIAL AND METHODS

After obtaining Atrium Health Wake Forest Baptist Medical Center institutional review board approval (IRB00100649), a retrospective analysis of all patients who underwent RC at our institution from 2012 to 2023 was conducted. All operations were performed for a diagnosis of bladder cancer, and any patients who had a cystectomy performed for non-oncologic purposes were excluded. A total of 8 operating surgeons were included, all of whom had either completed a urologic oncology fellowship and/or had been in practice as an attending urologist for at least 10 years,

A variety of preoperative and perioperative variables including patient age, gender, race, body mass index (BMI), Charlson Comorbidity Index (CCI), comorbidities (diabetes, hypertension, chronic obstructive pulmonary disease [COPD], and coronary artery disease [CAD]), urinary diversion type, operative approach, operative time (OT), length of stay (LOS), and tumour pathology were collected. Neoadjuvant and adjuvant chemotherapy was inconsistently documented in the medical record and so was not included. ED visits were tracked within the first 90 days of discharge from the hospital for RC, as well as the reason for ED visit based on MSKCC standardised complications [3]. All reasons for ED visits or readmission were counted for each patient such that some patients had multiple causes for an ED visit or readmission. Readmissions to the hospital were charted at both 30 and 31–90 days from discharge after RC along with the reason for readmission using MSKCC criteria. Most recent-follow up, OS, and cancer-specific survival were also collected on each patient. All patients received a phone call from clinic staff approximately 3 days after discharge from RC to assess how they were doing postoperatively and were seen in clinic within one month of RC by the operating surgeon. Postoperative follow-up after this was based on provider discretion.

The independent samples t-test was used to compare continuous variables for analysis involving 2 groups. The chi-squared test was used to compare categorical variables for analysis involving 2 or more groups. Because only 2 patients in the study received an Indiana pouch, they were excluded from any analysis on urinary diversion type. Based on univariable analysis showing a significant difference in ED visitation and readmission 31–90 days after discharge by diversion type, binary logistic regression was also run with 2 separate outcomes: ED visitation, and readmission 31–90 days after discharge from RC. Variables with $p < 0.01$ and/or clinical relevance were selected for inclusion in the binary logistic regression model ensuring no collinearity between variables. Kaplan-Meier survival curves with log-rank test were created to compare OS between patients who did and did not present to the ED after discharge as well as patients who were and were not readmitted 30 days and 31–90 days after discharge from RC. All statistical analysis was performed using SPSS Statistics Version 28 (Armonk, NY). Clinical significance was set at $p < 0.05$.

Bioethical standards

The study was approved by Atrium Health Wake Forest Baptist Medical Center institutional review board approval (approval No. IRB00100649).

RESULTS

A total of 386 patients met the inclusion criteria for analysis in the study. The full complement of patient demographics can be found in Table 1. Of these, 78 (20.2%) were women. The median age at surgery was 68 years, and the median CCI was 5. In total, 219 (56.7%) patients had an open RC and 167 (43.3) had robotic RC. Most patients had an ileal conduit diversion (n = 317, 82.3%), followed by cutaneous ureterostomy (CU; n = 50, 13%), percutaneous nephrostomy tube (PCN; n = 9, 2.3%), neobladder (n = 8,

2.1%), and Indiana pouch (n = 2, 0.52%). The median length of stay (LOS) was 5 days, and the median OT was 348 minutes. One hundred and thirty-seven (35.5%) patients had a complication before ever being discharged from the hospital during initial stay, of which 59 (43%) were Clavien grade I, 45 (32.8%) grade II, 8 (5.8%) grade IIIa, 6 (4.4%) grade IIIb, 3 (2.2%) grade IVa, 12 (8.8%) grade IVb, and 4 (3%) grade V. Mean follow-up was 35 months, and 171 (44.3%) patients had died by the end of the study window with a median OS of 12 months. One hundred and fifteen deaths (67.3%) were due to bladder cancer specifically. Postoperatively, 130 (33.7%) patients had at least one ED visit postoperatively. The primary reason for the first ED visit after RC was infectious aetiologies (n = 47), followed by GI (n = 26), and then GU reasons (n = 23). No significant differences were seen in OT, operative approach, LOS, age at surgery, gender, race, CCI, or medical comorbidities aside from hypertension between patients who did and did not present to the ED within 90 days after discharge from RC ($p > 0.05$). Diversion type differed based on ED visits, with a significantly greater proportion of CU patients visiting the ED after discharge ($p < 0.001$). Postoperative complications prior to discharge from RC, Clavien-Dindo grade, and tumour pathology were not significantly different ($p > 0.05$). OS was significantly longer in patients who did not present to the ED within 90 days of discharge from RC (Figure 1A; $p = 0.001$). On multivariable logistic regression, CU diversion patients were 3 times more likely to visit the ED relative to ileal conduit patients when controlling for gender, operative approach, tumour pathology, and race (Table 5; $p < 0.001$).

Table 1. *Demographics of the study population. The following table lists baseline demographic, surgical, and postoperative characteristics of the study population. Numbers listed are either total with percentages for categorical variables in parentheses, or medians with interquartile ranges for continuous variables*

Variable	Total (%) or Median (IQR)
Patients	386
Age at surgery (years)	68 (60–74)
Female	78 (20.2)
Race	
Caucasian	337 (87.3)
Black	38 (9.8)
Hispanic	3 (0.78)
Asian	3 (0.78)
Other	5 (1.3)
Hypertension	203 (52.6)
Diabetes	94 (24)
Coronary artery disease	70 (18.1)
COPD	49 (12.7)
CCI	5 (4–6)
Approach	
Open	219 (56.7)
Robotic	167 (43.3)
Diversion	
Ileal conduit	317/386 (82.1)
Indiana pouch	2/386 (0.5)
Neobladder	8/386 (2.1)
Cutaneous ureterostomy	50/386 (13)
PCN	9/386 (2.3)
LOS	5 (4–7)
Operative time (minutes)	348 (296–402)
Complication before discharge	139 (36)
Reason for complication	
Infectious	16
Bleeding	10
Surgical	6
Genitourinary	23
Gastrointestinal	25
Wound	12
Thromboembolic	4
Cardiac	23
Pulmonary	6
Neurological	6
Miscellaneous	4
Clavien-Dindo grade	
I	59 (43.1)
II	45 (32.8)
IIIa	8 (5.8)
IIIb	6 (4.4)
IVa	3 (2.2)
IVb	12 (8.8)
V	4 (3)
Tumour pathology	
T0	45/383 (11.7)
Ta	13/383 (3.4)
Tis	28/383 (7.3)
T1	30/383 (7.8)
T2a	63/383 (16.4)
T2b	55/383 (14.4)
T3a	50/383 (13.1)
T3b	32/388 (8.4)
T4a	59/383 (15.4)
T4b	8/383 (2.1)
Follow-up (months)	13 (4–33.8)
ED visit within 90 days of discharge	130 (33.7)
Number of ED visits	1 (1–2)
Readmission within 30 days of discharge	72 (18.7)
Readmission 31–90 days from discharge	67 (17.3)
≥1 readmission ≤90 days from discharge	115 (29.8)
Died	171 (44.4)
Cancer-specific death	115/160 (71.9)
Overall survival (months)	12 (4–25)

CCI – Charlson Comorbidity Index; COPD – chronic obstructive pulmonary disease; LOS – length of stay; PCN – percutaneous nephrostomy

For 30-day readmissions, 72 (18.7%) patients were readmitted (Table 2). The most common reason for readmission was infectious (n = 24), then GI (n = 20), and GU (n = 10) aetiologies. No significant differences were seen in OT, operative approach, urinary diversion type, LOS, age at surgery, gender, race, CCI, or medical comorbidities aside from hypertension between patients who were and were not readmitted within 30 days of discharge from RC (p >0.05). Postoperative complications during initial hospital stay were more common in patients who were not readmitted within 30 days of RC (p = 0.031). Clavien-Dindo grade and tumour pathology were not significantly different (p >0.05). OS was greater in patients not readmitted within 30 days of RC (Figure 1B; p <0.001).

Sixty-seven (17.3%) patients were readmitted between 31 and 90 days of discharge from RC. The most common reason for readmission was infectious (n = 27), then GU (n = 16), and GI (n = 13) aetiologies. No significant differences were seen in OT, operative approach, LOS, age at surgery, gender, race, CCI, or medical comorbidities aside from COPD between patients who were and were not readmitted within 90 days of discharge from RC (p >0.05). Diversion type differed based on 31–90-day readmis-

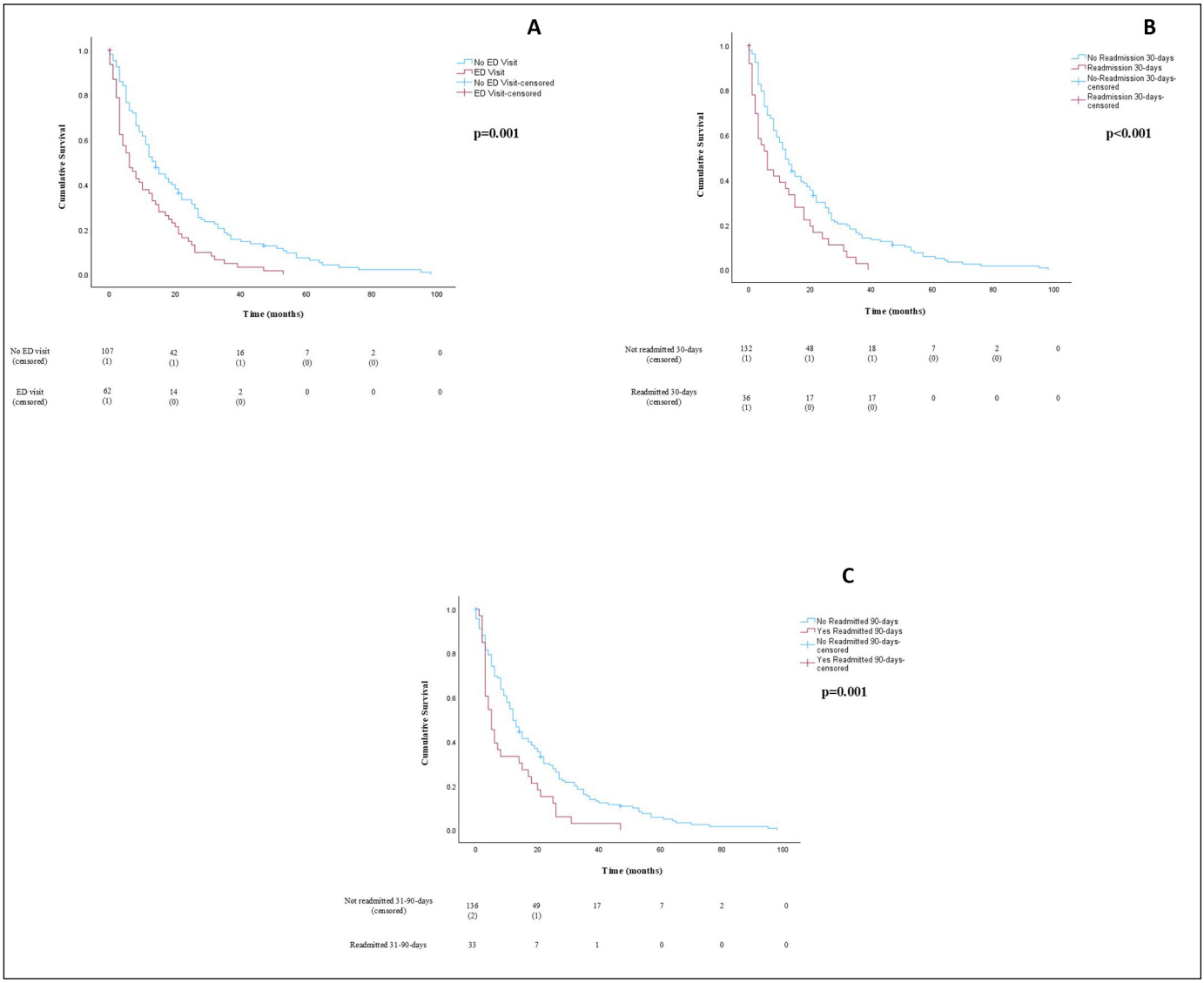

Figure 1. *Kaplan-Meier survival curve. The following figure compares overall survival based on:* **A)** *ED visit versus no ED visit after discharge;* **B)** *Readmission versus no readmission 30 days after discharge;* **C)** *Readmission 31–90 days after discharge. Overall survival is in months on the x-axis, and cumulative survival is displayed on the y-axis. Each death during the study window was recorded as an event for the survival curve. Censored patients are displayed with a hash mark on the graphs. Log-rank values are displayed on each graph. Number at risk table is also provided under each graph.*

sion status, with a significantly greater proportion of CU patients readmitted ($p < 0.001$). Postoperative complications during initial hospital stay and Clavien-Dindo grade were not significantly different ($p > 0.05$). Tumour pathology differed between those who were and were not readmitted between 31 and 90 days of discharge from RC, with a greater proportion of higher-stage tumours in patients readmitted ($p = 0.042$). OS was greater in patients not readmitted within 31–90 days of RC (Figure 1C; $p = 0.001$).

Table 2. *Risk factors for emergency department visits after discharge from radical cystectomy. The following compares patient variables between those who did and did not present to the ED after RC to identify risk factors for ED utilisation. The first row shows the MSKCC reasons for ED visitation. Numbers listed are either totals with percentages for categorical variables in parentheses or means with standard deviations for continuous variables. Indiana pouch patients are not listed because they were excluded from analysis. Associated p-values are also listed for each comparison*

Variable	ED visit (n = 130)	No ED visit (n = 256)	p-value
Reason for first ED visit			
Infectious	47	–	–
Bleeding	4		
Surgical	3		
Genitourinary	23		
Gastrointestinal	26		
Wound	13		
Thromboembolic	4		
Cardiac	4		
Pulmonary	6		
Neurological	0		
Miscellaneous	0		
Operative time (minutes)	355.2 (101.8)	346 (89.2)	0.389
LOS (days)	7.2 (8.8)	17.2 (139)	0.410
Age (years)	67 (9)	66.4 (11.1)	0.588
CCI	5.1 (2)	5.4 (2)	0.147
Female	33 (25.4)	45 (17.6)	0.071
Race	–	–	0.295
Approach			
Open	81 (62.3)	138 (53.9)	0.115
Robotic	49 (37.7)	118 (46.1)	
Diversion			
Ileal conduit	95 (73)	222 (88)	<0.001
Neobladder	5 (3.8)	3 (1.2)	
Cutaneous ureterostomy	29 (22.3)	21 (8.3)	
PCN	1 (0.8)	8 (3.1)	
Postoperative complication prior to discharge	52 (40)	85 (33.2)	0.392
Clavien-Dindo grade	–	–	0.527
Tumour pathology	–	–	0.138
Diabetes	38 (29.2)	54 (21)	0.076
Hypertension	80 (61.5)	123 (48)	0.012
Coronary artery disease	26 (20)	44 (17.1)	0.498
COPD	12 (9.2)	37 (14.5)	0.145
Overall survival (months)	11.3 (12.2)	20.8 (20.4)	0.001

CCI – Charlson Comorbidity Index; COPD – chronic obstructive pulmonary disease; LOS – length of stay; PCN – percutaneous nephrostomy

Table 3. *Risk factors for 30-day readmission after discharge from radical cystectomy. The following compares patient variables between those who were and were not readmitted to the hospital after RC within 30 days of discharge to identify risk factors for 30-day readmission. The first row shows the MSKCC reasons for readmission. Numbers listed are either totals with percentages for categorical variables in parentheses or means with standard deviations for continuous variables. Indiana pouch patients are not listed because they were excluded from analysis. Associated p-values are also listed for each comparison*

Variable	Readmission 30-days (n = 72)	No readmission 30-days (n = 314)	p-value
Reason for readmission			
Infectious	24	–	–
Bleeding	2		
Surgical	2		
Genitourinary	10		
Gastrointestinal	20		
Wound	8		
Thromboembolic	4		
Cardiac	3		
Pulmonary	3		
Neurological	0		
Miscellaneous	2		
Operative time (minutes)	359.6 (97.2)	346.7 (92.6)	0.297
Length of stay (days)	7.4 (10.3)	15.3 (125.4)	0.594
Age (years)	66.4 (11)	66.9 (9.4)	0.749
CCI	4.9 (1.8)	5.4 (2)	0.064
Female	17 (23.6)	61 (19.4)	0.425
Race	–	–	0.347
Approach			
Open	81 (62.3)	138 (53.9)	0.115
Robotic	49 (37.7)	118 (46.1)	
Diversion			
Ileal conduit	55 (76.4)	262 (84.5)	0.288
Neobladder	2 (2.8)	6 (1.9)	
Cutaneous ureterostomy	14 (19.4)	36 (17.1)	
PCN	1 (1.4)	8 (2.6)	
Postoperative complication prior to discharge	18 (25)	121 (38.5)	0.031
Clavien-Dindo grade	–	–	0.104
Tumour pathology	–	–	0.138
Diabetes	38 (29.2)	54 (21)	0.076
Hypertension	80 (61.5)	123 (48)	0.012
Overall survival (months)	10.5 (11.2)	19.3 (19.5)	<0.001

CCI – Charlson Comorbidity Index; COPD – chronic obstructive pulmonary disease; PCN – percutaneous nephrostomy

On multivariable logistic regression, CU diversion patients were 3.47 times more likely to be readmitted 31–90 days after discharge from RC relative to ileal conduit patients when controlling for gender, operative approach, tumour pathology, and race (Table 6; p <0.001).

DISCUSSION

The complication frequency in our cohort after RC was in line with previous publications. Thirty-six per cent of patients had some form of complication after RC before discharge from the hospital, and 75.9% of these were low grade (≤ grade II). Other literature has reported in-house complication rates around 35% [9]. When also including complications after discharge requiring readmission within 90 days of discharge, the complication rate was 54.8%. Current meta-analysis estimates are that ~60% of patients will experience a complication within 90 days of RC, concurring with our findings [1, 9, 10].

We saw that prior to discharge from RC, GI and GU causes were the most likely type of complication, with infectious aetiologies a distant third. However, for both 30- and 90-day readmissions, infection was the most common complication. In their 90-day analysis of morbidity and mortality from RC, Hirobe et al. [4] noted that UTI was the most frequent complication patients experienced, followed by wound infections and then paralytic ileus. Yuh et al. [11] found an overall greater rate of complications in their RC analysis (80%) than our study, but in terms of classifications, infectious was most common after RC. Katsimperis et al. [10] elected to separate UTI and infectious complications in their classification system, but again found that 25% of all postoperative complications could be attributed to either of these issues. A unique strength of our study is the additional inclusion of complications prior to discharge, which appears to differ in classification from those seen after discharge based on our results. Maibom et al. [9] attempted to identify risk factors for specific RC complications in their meta-analysis. They saw mixed results but noted that continent reservoirs over ileal conduits may be a risk factor for postoperative UTI, as is a higher CCI [9]. Looking at GI complications, it appears that increasing age is most likely to contribute to an increased risk of these issues [9]. Further study is needed to properly identify risk factors of each MSKCC complication type after RC.

We found that 33.7% of our RC cohort presented to the ED at least once postoperatively within 90 days of discharge. The most common reason for an ED visit was an infectious aetiology, followed by GI and GU reasons. Baack Kukreja et al. [12] reported an over-

Table 4. *Risk factors for 90-day readmission after discharge from radical cystectomy. The following compares patient variables between those who were and were not readmitted to the hospital after RC within 30 days of discharge to identify risk factors for 90-day readmission. The first row shows the MSKCC reasons for readmission. Numbers listed are either totals with percentages for categorical variables in parentheses or means with standard deviations for continuous variables. Indiana pouch patients are not listed because they were excluded from analysis. Associated p-values are also listed for each comparison*

Variable	Readmission 90-days (n = 67)	No readmission 90-days (n = 319)	p-value
Reason for readmission			
Infectious	27		
Bleeding	1		
Surgical	2		
Genitourinary	16		
Gastrointestinal	13		
Wound	5	–	
Thromboembolic	3		
Cardiac	4		
Pulmonary	4		
Neurological	0		
Miscellaneous	1		
Operative time (minutes)	344.1 (93.3)	350 (93.8)	0.641
Length of stay (days)	7.9 (10.9)	6.4 (5.5)	0.255
Age (years)	65.9 (12.8)	66.8 (8.8)	0.575
CCI	5.3 (2.1)	5.3 (1.9)	0.937
Female	15 (22.4)	63 (19.7)	0.625
Race	–	–	0.208
Approach			
Open	41 (61.2)	178 (55.8)	0.418
Robotic	26 (38.8)	141 (44.2)	
Diversion			
Ileal conduit	45 (67)	272 (86.3)	
Neobladder	0	8 (2.5)	<0.001
Cutaneous ureterostomy	20 (30)	30 (9.5)	
PCN	2 (3)	7 (2.2)	
Postoperative complication prior to discharge	20 (29.8)	119 (37.3)	0.248
Clavien-Dindo grade	–	–	0.590
Tumour pathology			
T0	8/66 (12.1)	37/317 (11.7)	
Ta	1/66 (1.5)	12/317 (3.8)	
Tis	2/66 (3)	26/317 (8.2)	
T1	1/66 (1.5)	29/317 (9.2)	
T2a	6/66 (9.1)	57/317 (9.1)	0.042
T2b	12/66 (18.2)	43/317 (13.6)	
T3a	12/66 (18.2)	38/317 (12)	
T3b	10/66 (15.2)	22/317 (6.9)	
T4a	13/66 (19.7)	46/317 (14.5)	
T4b	1/66 (1.5)	7/317 (2.2)	
Diabetes	19 (28.4)	73 (22.9)	0.339
Hypertension	40 (59.7)	163 (51.1)	0.200
Coronary artery disease	12 (17.9)	58 (18.2)	0.624
COPD	2 (3)	47 (14.7)	0.009
Overall survival (months)	10.4 (11)	19.6 (19.4)	0.001

CCI – Charlson Comorbidity Index; COPD – chronic obstructive pulmonary disease; PCN – percutaneous nephrostomy

Table 5. *Regression model for emergency department visitation after radical cystectomy. The following table is a binary logistic regression model with emergency department visit after radical cystectomy as the outcome. For urinary diversion, ileal conduit is the referent group. Indiana pouch patients are not listed because they were excluded from analysis*

Variable	B	SE	Significance	Exp(B)	95% CI	
					Upper	Lower
Gender	0.48	0.27	0.078	1.6	0.95	2.75
Approach	–0.28	0.23	0.23	0.76	0.48	1.19
Diversion	–	–	0.003	–	–	–
Ileal conduit	Referent	–	–	–	–	–
Neobladder	1.39	0.77	0.070	4.0	0.89	18.0
CU	1.10	0.32	<0.001	3.0	1.59	5.66
PCN	–1.22	1.07	0.25	0.29	0.036	2.41
Tumour pathology	0.015	0.045	0.73	1.02	0.93	1.11
Race	–0.012	0.18	0.95	0.99	0.70	1.40

B – unadjusted odds ratio; CI – confidence intervals; CU – cutaneous ureterostomy; Exp(B) – adjusted odds ratio; PCN – percutaneous nephrostomy; SE – standard error

Table 6. *Regression model readmission 31–90 days after radical cystectomy. The following table is a binary logistic regression model with emergency visit after radical cystectomy as the outcome. For urinary diversion, ileal conduit is the referent group. Indiana pouch patients are not listed because they were excluded from analysis*

Variable	B	SE	Significance	Exp(B)	95% CI	
					Upper	Lower
Gender	0.17	0.34	0.61	1.19	0.61	2.31
Approach	–0.14	0.28	0.63	0.87	0.50	1.53
Diversion	–	–	0.01	–	–	–
Ileal conduit	Referent	–	–	–	–	–
Neobladder	–19.20	14156.22	0.99	0.001	0.001	–
CU	1.24	0.35	<0.001	3.47	1.76	6.83
PCN	0.60	0.83	0.47	1.82	0.36	9.17
Tumour pathology	0.11	0.06	0.063	1.11	0.99	1.25
Race	–0.017	0.23	0.94	0.99	0.62	1.56

B – unadjusted odds ratio; CI – confidence intervals; CU – cutaneous ureterostomy; Exp(B) – adjusted odds ratio; PCN – percutaneous nephrostomy; SE – standard error

all ED visit rate of 38.5% after RC and found that differences in management recovery pathways had no effect on likelihood of an ED visit. Spencer et al. [6] found that 14% of their RC cohort who were not readmitted still required an ED visit after surgery. Hirobe et al. [4] found that 7% of their RC cohort required an ED visit despite not being readmitted to the hospital. Our overall ED visit rate is similar to much of the current body of literature, although studies are too limited to compare. On univariable analysis, history of hypertension was significantly associated with an ED visit after RC. There is almost no current information on risk factors for ED department utilisation after RC, but it has been well established that cardiopulmonary comorbidities are a risk factor for increased ED utilisation after major surgeries in other fields [13]. CU diversions also were a risk factor for ED visitation after RC, and they remained significant on logistic regression. While there is literature on the relationship between diversion and readmission status, little exists on ED utilisation, and more work is needed in this area. OS was also worse in those who presented to the ED. It is not unexpected that patients who required an ED visit fared worse postoperatively, and these may be patients who providers need to follow closer. We also feel our results highlight the need for standard protocol development in patient management after RC to reduce ED utilisation overall.

Readmissions to the hospital were within established ranges in our patient population, but few modifiable risk factors were seen on analysis. Some researchers have identified neobladder as a risk factor for readmission after RC [14–17]. Others

have not found an association between readmission to the hospital and any urinary diversion [18]. CU is not included in many current papers and is a unique risk factor for readmission in the 31–90-day window after discharge we identified in our patient population, which remained significant on logistic regression. While Kim et al. [15] did not study CU, they did find urinary diversion only played a role in the likelihood of readmission in the late period after RC (31–90 days), which we similarly discovered. This finding could be explained in 2 ways: 1) CU is usually done in patients with multiple co-morbidities and who are more fragile. These patients usually require a shorter OT, and for this reason, a CU is selected as the urinary diversion of choice; 2) stents for CU are typically removed during the first month, and the risk of stricture requiring re-stenting and readmission is thus increased. It is due to this second point that some urologists recommend prolonged stenting for CU [19]. Postoperative complications prior to discharge were also associated with a lower rate of readmission in the 30-day window after discharge. Minillo et al. [20] found that LOS ≥15 days predicted lower likelihood of readmission after RC. LOS was not associated with readmission in our study, but patients with postoperative complications may have closer follow-up and monitoring secondary to complex hospital stays leading to less need for readmission long-term after RC. As seen with ED visits, OS was worse in those who were readmitted after RC; providers need to follow these patients closer postoperatively.

We acknowledge that our study is inherently limited by its retrospective nature, most notably due to selection bias in our cohort. Furthermore, we cannot fully account for ED visits and readmissions outside of our healthcare system. Moreover, we elected to limit our analysis to 90 days of discharge from RC and so cannot comment on complications outside of this window. While we did have standardised follow-up criteria in the first month after surgery for the study cohort, it was up to provider discretion after this, which limits the strength of our conclusions. Though the MSKCC criteria for complication after RC are widely employed, other urologists may elect to categorise complications in a different way than we did for our analysis. Lastly, we did not have a full complement of neoadjuvant or adjuvant chemotherapy regimens on all patients, and so no analysis was performed on these potentially confounding variables. Strengths of our study include a large sample size and capturing ED visits, which many studies lack. Furthermore, we identified risk factors for ED visitation and readmission, which can guide practitioners in appropriate management after RC.

CONCLUSIONS

The complication rate after RC is high both during initial hospital stay and within the first 90 days after discharge. Nevertheless, most complications are low grade. ED utilisation after RC remains poorly understood, but our results indicate that around one-third of patients will have at least one ED visit within the first 90 days of discharge from RC. Readmission rates are also high, 30 and 31–90 days after discharge. The most likely reason for ED presentation and readmission is infection, with GI and GU as the next most common. CU diversion appears to be a risk factor for ED visits and readmission 90 days after discharge from RC, which is a novel finding. Postoperative complications may also be associated with lower readmission rates to the hospital within 30 days of discharge, but further research is needed. OS is worse for patients who presented to the ED and who were readmitted at the 30- and 31–90-day intervals, which is not unexpected given that these patients often had more complex postoperative issues.

We feel that our findings have multiple implications for physicians' practice. Preoperatively, patients should be counselled appropriately in terms of both the likelihood and type of complications to expect after RC. Urologists should also fully consider all diversion options for patients in preoperative planning for RC, making note of our analysis showing increased ED use and readmission with CU. Furthermore, ED providers can be better educated on RC patients, specifically the most likely reasons for patient presentation to the ED and how to appropriately triage and manage them. Patient management protocols after RC also remain an area open to further research to better improve care for RC. Ultimately, healthcare utilisation after RC is high, and measures to identify these patients most at risk early on after RC can help prevent excess strain on the system and lead to cost savings in the future.

CONFLICTS OF INTEREST

The authors declare no conflict of interest.

FUNDING

This research received no external funding.

ETHICS APPROVAL STATEMENT

The study was approved by Atrium Health Wake Forest Baptist institutional review board approval (approval No. IRB00100649).

References

1. Novara G, De Marco V, Aragona M, et al. Complications and Mortality After Radical Cystectomy for Bladder Transitional Cell Cancer. J Urol. 2009; 182: 914-921.
2. Yuh B, Wilson T, Bochner B, et al. Systematic review and cumulative analysis of oncologic and functional outcomes after robot-assisted radical cystectomy. Eur Urol. 2015; 67: 402-422.
3. Shabsigh A, Korets R, Vora KC, et al. Defining Early Morbidity of Radical Cystectomy for Patients with Bladder Cancer Using a Standardized Reporting Methodology. Eur Urol. 2009; 55: 164-174.
4. Hirobe M, Tanaka T, Shindo T, et al. Complications within 90 days after radical cystectomy for bladder cancer: results of a multicenter prospective study in Japan. Int J Clin Oncol. 2018; 23: 734-741.
5. Johar RS, Hayn MH, Stegemann AP, et al. Complications after robot-assisted radical cystectomy: Results from the international robotic cystectomy consortium. Eur Urol. 2013; 64: 52-57.
6. Spencer SE, Lyons MD, Greene P, et al. Understanding the Relationship Between 30- and 90-Day Emergency Room Visits, Readmissions, and Complications after Radical Cystectomy. J Am Coll Surg. 2015; 221: S135.
7. Chappidi MR, Escobar D, Meng MV, Washington SL, Porten SP. Readmissions trends following radical cystectomy for bladder cancer unchanged in the era of enhanced recovery after surgery (ERAS) protocols. Urol Oncol. 2023; 41: 355.e19-355.e28.
8. Kirk PS, Skolarus TA, Jacobs BL, et al. Characterising 'bounce-back' readmissions after radical cystectomy. BJU Int. 2019; 124: 955-961.
9. Maibom SL, Joensen UN, Poulsen AM, Kehlet H, Brasso K, Røder MA. Short-term morbidity and mortality following radical cystectomy: A systematic review. BMJ Open. 2021; 11: e043266.
10. Katsimperis S, Tzelves L, Tandogdu Z, et al. Complications After Radical Cystectomy: A Systematic Review and Meta-analysis of Randomized Controlled Trials with a Meta-regression Analysis. Eur Urol Focus. 2023; 9: 920-929.
11. Yuh BE, Nazmy M, Ruel NH, et al. Standardized analysis of frequency and severity of complications after robot-assisted radical cystectomy. Eur Urol. 2012; 62: 806-813.
12. Baack Kukreja JE, Kiernan M, et al. Quality Improvement in Cystectomy Care with Enhanced Recovery (QUICCER) study. BJU Int. 2017; 119: 38-49.
13. Chaves KF, Novoa Y Novoa VA, et al. Prevalence of and Risk Factors for Emergency Department Visits After Outpatient Gynecologic Surgery. J Minim Invasive Gynecol. 2023; 30: 19-24.
14. Nahar B, Koru-Sengul T, Miao F, et al. Comparison of readmission and short-term mortality rates between different types of urinary diversion in patients undergoing radical cystectomy. World J Urol. 2018; 36: 393-399.
15. Kim SH, Yu A, Jung JH, Lee YJ, Lee ES. Incidence and risk factors of 30-day early and 90-day late morbidity and mortality of radical cystectomy during a 13-year follow-up: A comparative propensity-score matched analysis of complications between neobladder and ileal Conduit. Jpn J Clin Oncol. 2014; 44: 677-685.
16. Aydin AM, Reich RR, Cao B, et al. Clinical indications for necessary and discretionary hospital readmissions after radical cystectomy. Urol Oncol. 2022; 40: 164.e1-164.e7.
17. Lee AY, Allen JC, Teoh JYC, et al. Predicting perioperative outcomes of robot-assisted radical cystectomy: Data from the Asian Robot-Assisted Radical Cystectomy Consortium. Int J Urol. 2022; 29: 1002-1009.
18. Gore JL, Lai J, Gilbert SM. Readmissions in the postoperative period following urinary diversion. World J Urol. 2011; 29: 79-84.
19. Rodríguez AR, Lockhart A, King J, et al. Cutaneous ureterostomy technique for adults and effects of ureteral stenting: An alternative to the ileal conduit. J Urol. 2011; 186: 1939-1943.
20. Minnillo BJ, Maurice MJ, Schiltz N, et al. Few modifiable factors predict readmission following radical cystectomy. Can Urol Assoc J. 2015; 9: e439-e446.

REVIEW PAPER

UROLOGICAL ONCOLOGY

Prostate biopsy in patients without rectal access: a systematic review and proportional meta-analysis

Konstantinos Kotrotsios, Konstantinos Douroumis, Panagiotis Katsikatsos, Evangelos Fragkiadis, Dionysios Mitropoulos

First Urologic Clinic of Athens University, Laiko General Hospital, Athens, Greece

Citation: Kotrotsios K, Douroumis K, Katsikatsos P, et al. Prostate biopsy in patients without rectal access: a systematic review and proportional meta-analysis. Cent European J Urol. 2025; 78: 14-22.

Article history
Submitted: Apr. 12, 2024
Accepted: Aug. 19, 2024
Published online: Jan. 24, 2025

Corresponding author
Konstantinos Kotrotsios
First Urologic Clinic of Athens University,
Laiko General Hospital
Agiou Thoma 17,
Athens 115 27, Greece
kotrwtsiosk@gmail.com

Introduction Historically, the anal canal plays a substantial role in both screening and diagnosis of prostate cancer with digital rectal examination (DRE) and transrectal ultrasound (TRUS) guided biopsy, respectively. However, in patients with a prior history of abdominoperineal resection the transrectal route towards the prostate capsule cannot be utilized and thus alternative approaches have to be employed. The aim of this systematic review and proportional meta-analysis is to evaluate the available alternative prostate biopsy techniques in patients without rectal access.

Material and methods The systematic literature review was performed using MEDLINE, Scopus, EMBASE, and the CENTRAL register for randomized controlled trials (RCTs). The following search algorithm was used: "resection of rectum" OR "abdominoperineal resection" OR "without rectal access" AND "prostate biopsy" (PROSPERO 2023 CRD42023459080).

Results A total of 21 studies and 203 patients were included in this systematic review and meta-analysis, while 6 different prostate biopsy techniques were detected in the current literature. The transperineal approach under transperineal US (TPUS) and the transgluteal approach guided by computed tomography (CT) were associated with 0.74 [0.48; 0.94] and 0.70 [0.49; 0.89] pooled diagnostic yield estimates as well as 0.01 [0.00; 0.01] and 0 [0.00; 0.01] pooled complication rate estimates. The performance of multiparametric magnetic resonance imaging (mpMRI) prior to transgluteal CT-guided prostate biopsy seemed to significantly affect the biopsy result (p = 0.0002).

Conclusions Based on current data, the TPUS-guided prostate biopsy has the highest pooled diagnostic yield estimate. However, this conclusion is based on poor evidence and more reliable and well-organized studies are needed to thoroughly explore this problem.

Key Words: prostate ‹› biopsy ‹› prostate cancer ‹› transperineal ‹› ultrasound

INTRODUCTION

Prostate cancer is the second most common malignancy detected in men with virtually one million new cases reported every year. In fact, prostate cancer accounts for 10.0% of new malignancies diagnosed annually in males and is responsible for 300,000 deaths every year [1, 2]. Some well-established risk factors associated with prostate cancer are age, with almost 75.0% of men above 80 years displaying some kind of latent disease, family history, African-American race and certain genetic factors, for instance, *BRCA1* and *BRCA2* mutations [3–7].

The fact that prostate cancer incurs a substantial incidence and mortality burden of that magnitude poses an invincible need for a well-coordinated screening program [8]. Although there are no consensus guidelines for prostate cancer screening most of the experts' recommendations incorporate prostate-specific antigen (PSA) measurement as the initial screening tool [8–11]. In addition to PSA, digital rectal examination (DRE) can be utilized to aid screening and can potentially increase the intrinsically

low specificity of PSA, especially when it is performed by an experienced clinician [12].
After shared-decision making, a reasonable step for a patient with adequate life expectancy and abnormal findings in screening tests is prostate biopsy [13]. Historically, transrectal ultrasound (TRUS) guided biopsy has been the mainstay of obtaining prostate specimens from patients with increased suspicion of prostate cancer [14]. Its cancer detection rates (CDRs) have been reported to be as high as 37.5% in patients with elevated PSA levels, while the introduction of a novel prostate imaging technique, more specifically the multiparametric magnetic resonance imaging (mpMRI), in combination with TRUS has increased the detection of clinically important lesions [15, 16].
From the aforementioned data, it has been demonstrated that the anatomical proximity between the prostate and the rectum is a feature of high significance regarding both the screening and the diagnosis of prostate cancer. The abdominoperineal resection (APR) is the cornerstone of surgical treatment in cases of rectal cancer, ulcerative colitis and familial polyposis [17]. During this procedure, the rectum along with the mesorectum, the anus, perineal soft tissue and pelvic floor musculature are resected [18].
Considering that the detection of synchronous and metachronous prostate and rectal cancers is highly prevalent, the screening and diagnosis of prostate cancer after APR are a common diagnostic challenge for healthcare providers [19].
Taking into account the prevailing occurrence of rectal cancer beyond the age of 50, which is the same age category with men of high risk for prostate cancer, a prostate cancer screening by measuring PSA levels before undergoing APR has been suggested [20, 21]. In case of elevated levels of PSA after APR, several methods have been proposed in order to acquire sufficient prostate tissue to reliably establish a diagnosis [22].
The aim of this study is to perform a systematic review of the current literature with respect to management of a patient without rectal access and elevated conjecture regarding the presence of prostate cancer and to provide through a pooled proportional meta-analysis and insight on the most effective and safe prostate biopsy technique in these untypical patients.

MATERIAL AND METHODS

A literature search was performed (9th of June 2023) using the MEDLINE, the CENTRAL, the EMBASE and the SCOPUS databases (PROSPERO 2023 CRD42023459080). The following terms were used in the search text fields; "resection of rectum" OR "abdominoperineal resection" OR "without rectal access" AND "prostate biopsy".
Published observational and interventional studies describing prostate biopsy techniques in patients without rectal access and evaluating its efficiency were included. Reviews, letters, commentaries and articles whose texts were not available in English were excluded.
The abstracts of all articles were screened and the full texts of all the relevant articles were examined for possible inclusion by 2 separate reviewers. Subsequent to the initial study, selection was the citation searching of the already included studies. Upon the conclusion of the compilation of studies a risk of bias assessment was performed utilizing the 2013 National Heart, Lung and Blood Institute (NHLBI) quality assessment tool and the Risk Of Bias In Non-randomized Studies – of Exposures (ROBINS-E) of the Cochrane group for case series and observational cohort studies, respectively [23, 24].
Efficiency of the prostate biopsy technique used was identified as the primary outcome because it ensures the feasibility of the method, while complications rate was the secondary outcome because it is associated with direct harm to the patients. The sample size and the number of patients with positive prostate biopsy were used to pool the diagnostic yield of each biopsy technique. A random-effects model was assumed using the DerSimonian-Laird approach with Freeman-Tukey double arcsine transformed proportion at 95.0% CI.

RESULTS

A flow diagram of the selection procedure is presented in Figure 1. We initially identified 754 papers and after removal of duplicates, 647 were considered eligible for title-abstract based screening. Subsequently, 33 articles were selected for full text screening, 15 of them were excluded due to the reasons presented in Figure 1, while 17 of them met the inclusion criteria and were finally included. Furthermore, references of the included studies along with articles published by high impact journals were hand-searched and 4 additional articles that were lost from the initial search were also included. A summary of the included studies' characteristics along with some of their most important results is presented in order to provide a brief outlook on the available data before their more thorough review (Table 1).
A total of 203 patients were included in this systematic review and meta-analysis and 6 different pros-

tate biopsy techniques were detected in the current literature; transperineal approach with cognitive guidance by intravenous urogram (IVU) and ultrasound (US), transgluteal approach guided by computed tomography (CT), transperineal approach under concurrent transperineal US (TPUS), transperineal approach under concurrent transurethral US, transperineal approach under fluoroscopy guidance and transperineal approach during mpMRI and transabdominal ultrasound fusion.

The first case of prostate biopsy in a patient without rectal access was described by Schapira [26] in 1982. In this case the prostate was approached transperineally with the patient in lithotomy position, while the lesion was targeted cognitively based on the findings of an IVU and a sonogram that both were previously performed. The histological examination revealed fragments of prostatic adenocarcinoma.

The transperineal route and the advancement of the needle to the prostate capsule under transperineal ultrasound guidance was the procedure of choice in 8 studies [27–34]. In pooled estimates, overall diagnostic yield of this technique was 0.74 [0.48; 0.94] (Figure 2). After moderator analysis, for age, PSA level and pre-biopsy mpMRI performance, it emerged that none of these moderators significantly affected the diagnostic yield of the technique ($p = 0.2997$, $p = 0.9891$, $p = 0.3368$, respectively). Regarding the safety of the technique, the complication rate in pooled estimates is as high as 0.01 [0.00; 0.18].

A novel approach to the prostate, which was introduced by Krauss et al. [35] in 1993, utilizes CT imaging as a guide and the gluteal region as the needle inserting point all the way to the prostatic gland. This technique was described by 7 studies [35–41]. In pooled estimates, its overall diagnostic yield was 0.70 [0.49; 0.89] (Figure 3). The primary pooled proportional analysis was followed by moderator analysis for age, PSA level and pre-biopsy mpMRI performance. It was concluded that pre-biopsy mpMRI was the sole moderator significantly affecting the outcome ($p = 0.0002$). Only 4 complication events were observed throughout these 7 studies leading to a pooled estimate of 0.00 [0.00; 0.01].

Transurethral ultrasound was the imaging technique of choice regarding needle guidance in 6 cases described by Kirby et al. [42] and Seaman et al. [43]. The first author published a case report of a patient with a previous abdominoperineal resection and a significantly elevated PSA level (>30 ng/ml). This patient had undergone two prior prostate biopsies with the third attempt being performed by placing the patient in lithotomy position and under mild sedation inserting an ultrasound transducer into the prostatic urethra with the help of a flexible cystoscope. Perineal prostatic biopsies were then obtained

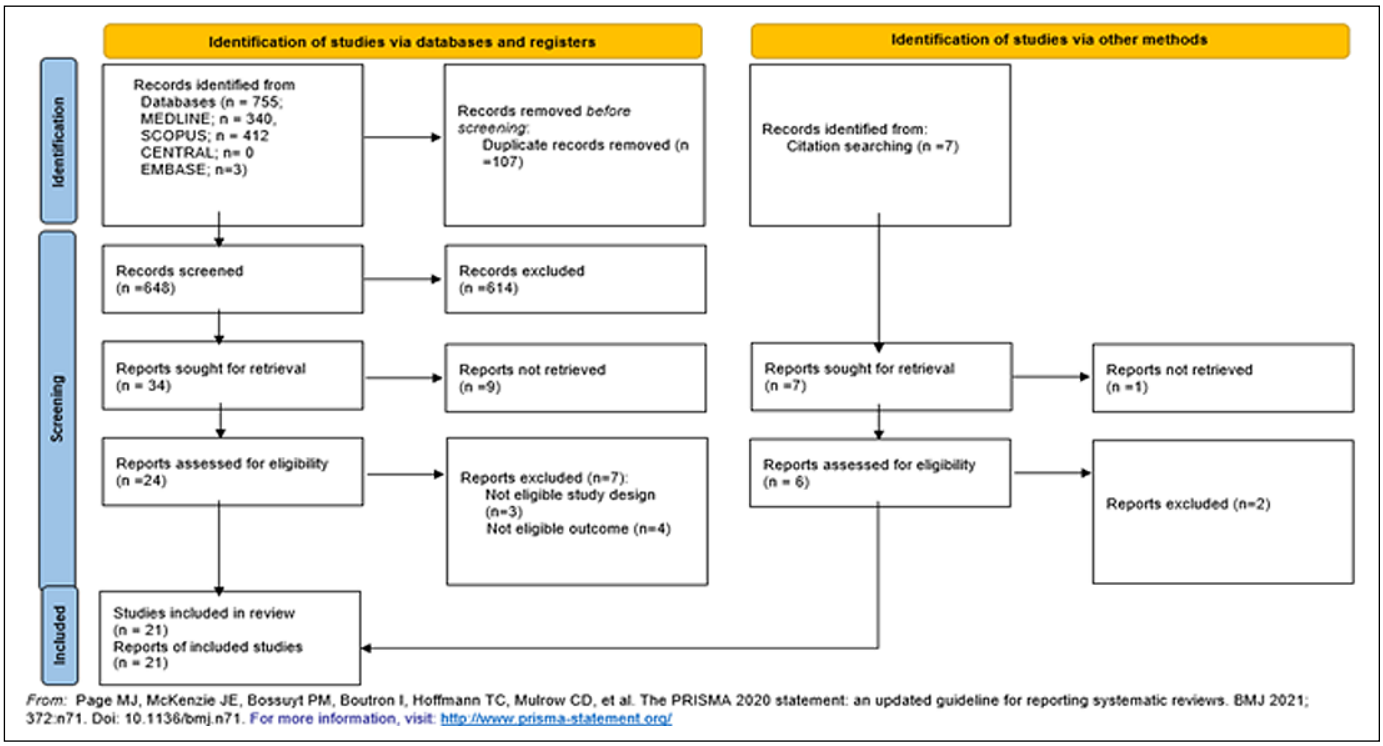

Figure 1. *PRISMA flow diagram summarizes the selection process [25].*

while circumferential real-time ultrasonic images were acquired. The histologic specimens originating mainly from the posterior prostate confirmed the presence of benign prostatic gland tissue. This particular technique was applied by Seaman et al. [43] in 5 patients without rectal access and lead to the diagnosis of prostate cancer in 3 of them.

Instead of cognitively combining prior mpMRI and real-time ultrasound images, De Vulder et al. [44] described the first case of a patient with a history of abdominoperineal resection and rising PSA who underwent mpMRI-US fusion biopsy. MRI images were pre-imported into the ultrasound system and a region of interest, meaning the area suspected of being malignant, was identified. A transabdominal ultrasound approach was necessary in order to begin the fusion with the cranial and caudal most aspects of the pubic symphysis being the primary fusion points. Then, the ultrasound probe was placed to the perineum and prostate biopsies were obtained free hand establishing a Gleason 8 prostatic adenocarcinoma.

Table 1. *Basic characteristics of the studies*

Author	Publication (year)	Study design	Mean PSA (ng/ml)	Prostate approach	Guidance	PCa cases, Mean GS
Schapira [26]	1982	Case report	NA	Transperineal	Cognitive IVU, US guided	n = 1, NA
Krauss et al. [35]	1993	Case report	13.5	Transgluteal	CT	n = 1, NA
Twidwell et al. [27]	1993	Case series	6.5	Transperineal	US	n = 2, NA
Filderman et al. [28]	1994	Case series	16.5	Transperineal	US	n = 2, NA
Fornage et al. [29]	1995	Case report	17.0	Transperineal	US	n = 1, combined 8
Kirby et al. [42]	1995	Case report	>30.0	Intraluminal	Transurethral US	n = 0
Seaman et al. [43]	1996	Case series	13.5	Transperineal	Transurethral US	n = 3, NA
Papanicolaou et al. [36]	1996	Case series	34	Transgluteal	CT	n = 6, NA
D'Amico et al. [45]	2000	Case report	43.5	Transperineal	Cognitive mpMRI MRI guided	n = 1, 6 (3 + 3)
Shinohara et al. [31]	2003	Case series	22	Transperineal	US	n = 23, 6.6
Cantwell et al. [37]	2008	Retrospective study	11.1	Transgluteal	CT	n = 14, 7.4
Goenka et al. [38]	2015	Retrospective study	11.4	Transgluteal	CT	n = 8, combined 8
Caglic et al. [40]	2016	Case report	14.2	Transgluteal	Cognitive mpMRI, CT guided	n = 2, 7.5
Hansen et al. [34]	2016	Case series	14.5	Transperineal	Cognitive mpMRI, US guided	n = 7, 8
Olson et al. [39]	2016	Retrospective study	7.8	Transgluteal	CT	n = 31, 7
Amin et al. [30]	2020	Case report	NA	Transperineal	US	n = 1, 7
Merrick et al. [46]	2020	Case report	8.84	Transperineal	CT planned, fluoroscopy guided	n = 1, 9
Kailavasan et al. [32]	2021	Case series	9.4	Transperineal	Cognitive mpMRI, US guided	n = 3, 7
Patel et al. [41]	2021	Retrospective study	14.1	Transgluteal	Cognitive mpMRI, CT guided	n = 9, 7
De Vulder et al. [44]	2021	Case report	NA	Transperineal	MRI-transperineal US fusion	n = 1, 8
Park et al. [33]	2023	Retrospective study	22.6	Transperineal	Cognitive mpMRI, US guided	n = 7, 7.5

CT – computed tomography; GS – Gleason score; IVU – intravenous urogram; mpMRI – multiparametric magnetic resonance imaging; US – ultrasound; PCa – prostate cancer; PSA – prostate-specific antigen

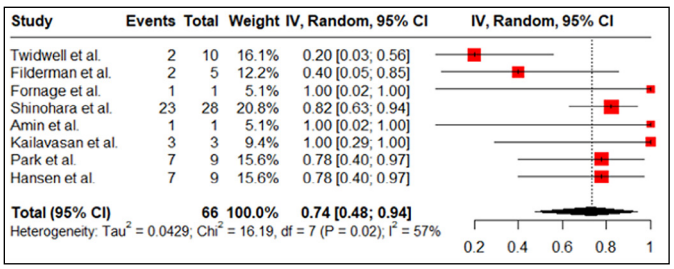

Figure 2. *Forest plot transperineal ultrasound-guided prostate biopsy.*

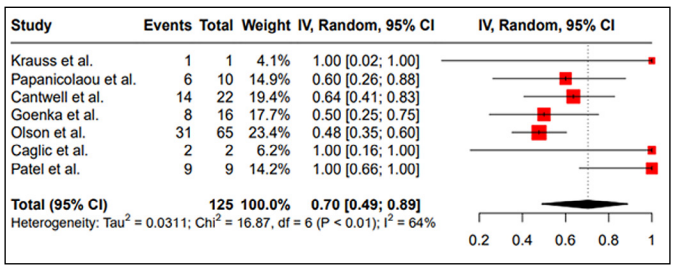

Figure 3. *Forest plot transgluteal computed tomography prostate biopsy.*

The 2 last prostate biopsy protocols have only been described once. The first one refers to a patient with prior proctocolectomy due to ulcerative colitis and increasing values of PSA. Firstly, the patient underwent a prostate MRI in order to identify regions highly suspicious for cancer. Then the patient was placed into the imaging bore of the open intraoperative magnet in the lithotomy position under general anesthesia. Intraoperatively, new MRI images were obtained and according to the correlation of both MRI examinations and using appropriate software, a stereotactic transperineal approach to the lesion was achieved. The histopathologic evaluation revealed a Gleason 6 prostate adenocarcinoma, while no complications were reported [45].
The second case report involves a patient with PSA level of 8.84 ng/ml who underwent total colectomy due to ulcerative colitis. The biopsy locations were pre-planned based on a pre-biopsy CT. Intraoperatively, the patient under intravenous (IV) sedation was placed in dorsal lithotomy position, then saline with dilute contrast were administered into the bladder and into the catheter bulb, while a brachytherapy template was used for needle placement. The needle position was confirmed via anterio-posterior and lateral fluoroscopy. At biopsy 32 cores were obtained and established the diagnosis of a Gleason 9 prostatic adenocarcinoma [46].

DISCUSSION

To our knowledge this is the first systematic review and meta-analysis evaluating prostate biopsy techniques in patients without rectal access. Based on the current data available the majority of the procedures were described in diminutive patient numbers, while only the transperineal approach under US guidance and the transgluteal approach under CT guidance were reported in an adequate number of studies with bearable heterogeneity making it feasible to perform a pooled proportional meta-analysis. The studies' risk of bias was assessed using the NIH quality assessment tool and the ROBINS-E tool for case series and single arm retrospective studies, respectively.
The non-consecutive nature of the cases, the lack of baseline characteristics presentation and the concealment of the follow-up period were features that in some cases undermined the quality of the case series studies (Table 2). Regarding the single arm retrospective studies, during the planning stage of ROBINS-E assessment, age, PSA level, prior unsuccessful biopsies, Gleason score, prostate size, comorbidities, inflammation or prostatic intraepithelial neoplasia and radiation dose were noted as potential confounding factors. After diligent examination of the available single arm retrospective studies it was concluded that there was sufficient potential for confounding that an unadjusted result was not reliable. Thus, these studies were considered of very high risk of bias [33, 37–39, 41].
Prostate cancer and rectosigmoid cancer hold 2 positions among the most frequent diagnosed cancers in men [47]. In fact, it has been observed that these 2 types of cancer tend to co-occur within the same patient in a rate that ranges from 1.9% to 5.0% [48, 49]. In most of the cases the cancers do not occur simultaneously, but they follow a subsequent path, with the rectosigmoid cancer being the first one detected in 41.0% of the cases [50].
Given abdominoperineal resection is required not only in 40.0% of patients with rectal cancer but also occasionally for the management of inflammatory bowel disease, Fournier gangrene and fecal incontinence not amenable to sphincter sparing surgery the need for a standardized protocol regarding the prostate cancer diagnosis in men without rectal access is of paramount importance [51, 52].
One of the major advantages of the transperineal route to the prostatic capsule is the improved sampling of the far lateral peripheral zone. This is attributed to the relatively parallel course of the needle to the long axis of the prostate at the mid portion and the base allowing to obtain more prostatic tissue from the peripheral zone [53].
According to our analysis, the transperineal approach of the prostate under transperineal ultrasound guidance was associated with a diagnostic yield of 0.74 [0.48; 0.94]. This result complies with the pooled detection rate of a previously published meta-analysis, which evaluated the diagnostic effectiveness of free hand transperineal prostate biopsy with the Precision Point Transperineal Access System in patients with rectal access and achieved a prostate cancer detection rate of 68.0% [54]. The slightly higher detection rate in our analysis might be explained by the fact that patients without rectal access might present with larger and more clinically significant cancers due to delayed diagnosis [55].
To our surprise, the visual registration of prior mpMRI did not seem to affect the diagnostic yield of the technique. This does not accord with preceding studies that had proven the superiority of cognitively combining pre-biopsy magnetic resonance imaging with transrectal ultrasound than ultrasound guidance alone [56].
Moreover, in order for an invasive procedure to become the mainstay in diagnosis of a condition it is essential to be accurate as well as safe for the patient. According to our analysis, the pooled compli-

cation rate estimate of transperineal biopsy under TPUS guidance was calculated to be as low as 1.0%. The most recent systematic review comparing the transperineal with the traditional transrectal route stated that the transperineal approach seems to protect patients from rectal bleeding and fever but significantly increases patient pain [57]. These reports come to an agreement with our included studies where no infectious complications were observed and only one patient felt mild perineal discomfort.

One of the major concerns when utilizing the transperineal course to the prostate is the association of the procedure with increased danger for post-biopsy urinary retention. More specifically, in a recent nationwide study where 73,630 patients were included, it was indicated that the patients who underwent a transperineal prostate biopsy were of higher risk for urinary retention and were more likely to have stayed overnight immediately post-operatively [58]. In our analysis, acute urinary retention occurred in 2 patients postoperatively [34]. The higher risk of urinary retention might be related to general anaesthesia use or to the higher number of cores obtained.

Our systematic literature review has proven the feasibility of the transperineal biopsy under local anaesthesia given that local anesthesia was preferred in the majority of the cases [27–30, 33].

The most commonly utilized prostate biopsy technique in patients without rectal access was the transgluteal approach under CT guidance. One of the most important features of this technique is the clear depiction of the pelvis anatomy and the higher quality of the prostate visualization when compared with the ultrasound. These 2 characteristics not only diminish the likelihood of bowel, bladder and surrounding vasculature injury but also help overcome the intrinsic complexity of prostate sampling in patients that had undergone anorectal resection [22].

According to our analysis, the transgluteal approach of the prostate under CT guidance was associated with a pooled diagnostic yield of 0.70 [0.49; 0.89].

Table 2. *Case series quality evaluation using the NIH quality assessment tool*

	Twidwell et al. [27]	Filderman et al. [28]	Seaman et al. [43]	Papanicolaou et al. [36]	Shinohara et al. [31]	Hansen et al. [34]	Kailavasan et al. [32]
1. Was the study question or objective clearly stated?	Yes	Yes	Yes	Yes	Yes	Yes	Yes
2. Was the study population clearly and fully described, including a case definition?	Yes	Yes	Yes	Yes	Yes	Yes	Yes
3. Were the cases consecutive?	No	NR	NR	Yes	Yes	Yes	Yes
4. Were the subjects comparable?	NR	No	Yes	Yes	No	Yes	Yes
5. Was the intervention clearly described?	Yes	Yes	Yes	Yes	Yes	Yes	Yes
6. Were the outcome measures clearly defined, valid, reliable and implemented consistently across all study participants?	Yes	Yes	Yes	Yes	Yes	Yes	Yes
7. Was the length of follow-up adequate?	NA	NA	NA	NA	NR	NA	NA
8. Were the statistical methods well described?	No	No	No	No	No	No	No
9. Were the results well described?	No	Yes	No	No	Yes	Yes	Yes
Quality rating (good, fair, poor)	Poor (non-consecutive nature of cases, no baseline characteristics available, no statistical methods description and no risk classification)	Poor (great differences in baseline PSA and age, the statistical methods and follow-up duration were not reported)	Fair (a description of the statistical methods used and a more adequate interpretation of the results would be desired)	Fair (a description of the statistical methods used and a more adequate interpretation of the results would be desired)	Fair (there were great differences in baseline PSA)	Good	Good

NA – not applicable; NR – not reported

This might be explained by the fact that in most cases biopsies were performed according to a quadrant approach, while an extended peripheral zone biopsy scheme where 12 cores are acquired may increase cancer detection rates with this technique [59].

There are no prior data in respect of the efficacy of CT as a needle guide during prostate biopsy. This might be related to the superiority of other techniques and especially MRI in prostate visualization, which can also improve the initial detection of prostate cancer [60]. In fact our moderator analysis regarding the pooled diagnostic yield of CT-guided transgluteal prostate biopsy demonstrated that prior mpMRI prostate visualization significantly affected the result ($p = 0.0002$). Moreover, it has been described that CT can also be combined with prostate-specific membrane antigen (PSMA) positron emission tomography (PET) and achieve a prostate cancer detection rate of 96.0% [61].

Concerning its safety profile, CT-guided transgluteal biopsy in patients without rectal access has a pooled complication rate estimate of 0% [0%; 1.0%]. In the included studies only 4 minor complication events were recorded, including 1 event of gross spontaneously resolving hematuria and 3 periprostatic hematomas, while no major complications were observed. At this point it is important to underline that in contrast with the conventional transrectal US-guided prostate biopsy where post-biopsy infection is an issue of great concern, when following the transgluteal approach to the prostate as the rectum is not transgressed the risk of infectious complications is diminished [62]. Thus, no antibiotic prophylaxis was routinely administered in virtually all the studies utilizing the transgluteal approach, minimizing the potential burden of antibiotic-resistant bacteria development [63].

Towards the direction of vanishing infectious complications from prostate biopsy favors the transperineal approach as well, which seems to lower the incidence of post-biopsy sepsis in comparison with the traditional transrectal approach (0.1% vs 0.8%, respectively) [64]. Both the transperineal and the transgluteal approach could be considered as alternative choices in patients receiving immunosuppression or transplant recipients who have usually been exposed in extended hospitalizations or complex antibiotic regimens and their colon is colonized by multi-resistant bacteria [65, 66].

This systematic review and proportional meta-analysis has several limitations. First of all, both the lack of head-to-head comparisons between the techniques and the studies' design, that were almost exclusively in case series or single arm retrospective studies format, made pooled proportional meta-analysis the sole feasible choice and inserted great risk of bias in the resulting evidence, respectively. Also, the limited number of patients included in the analysis undermined the certainty of evidence emerging from the analysis. Last but not least, most of the techniques were described once or twice in case reports and as a result a statistical analysis of their results would not be reliable and thus a narrative presentation was preferred in order to achieve historical thoroughness on the subject.

Given that transperineal prostate fusion biopsy constitutes a safe and reliable prostate biopsy technique for selected patients with rectal access, it could be considered the standard of care as well for patients without a rectum [67]. However, this novel approach is not available in all clinical settings due to both limited equipment and technical knowledge.

CONCLUSIONS

Taking into account that prostate cancer and rectosigmoid cancer are 2 malignancies with prevailing occurrence in men aged over 50 and that ano-rectal resection is indicated in a significant proportion of men with rectosigmoid cancer and men suffering from other conditions, such as inflammatory bowel disease (IBD) or Fournier gangrene, a thorough evaluation of the available prostate biopsy techniques that omit the traditional transrectal route was necessary. Several procedures have been reported in the current literature including with the most commonly utilized techniques being the transperineal approach under concurrent TPUS and the transgluteal approach guided by CT which were associated with 0.74 [0.48; 0.94] and 0.70 [0.49; 0.89] pooled diagnostic yield estimates as well as 0.01 [0.00; 0.01] and 0 [0.00; 0.01] pooled complication rate estimates. However, the level of evidence is still suboptimal due to the small retrospective, case series and case report format of the included studies. Thus, well designed multi-institutional prospective studies are required to elucidate the diagnostic efficacy of each different technique in this unique population.

CONFLICTS OF INTEREST

The authors declare no conflict of interest.

FUNDING

This research received no external funding.

ETHICS APPROVAL STATEMENT

The ethical approval was not required.

References

1. Ferlay J, Shin HR, Bray F, Forman D, Mathers C, Parkin DM. Estimates of worldwide burden of cancer in 2008: GLOBOCAN 2008. Int J Cancer. 2020; 127: 2893-2917.

2. Chang ET, Boffetta P, Adami HO, Cole P, Mandel JS. A critical review of the epidemiology of Agent Orange/TCDD and prostate cancer. Eur J Epidemiol. 2014; 29: 667-723.

3. Billis A. Latent carcinoma and atypical lesions of prostate. An autopsy study. Urology. 1986; 28: 324-329.

4. Edwards SM, Rosalind AE. Unravelling the genetics of prostate cancer. Am J Med Genet C Semin Med Genet. 2004; 129 C: 65-73.

5. Virnig BA, Baxter NN, Habermann EB, Feldman RD, Bradley CJ. A matter of race: early-versus late-stage cancer diagnosis. Health Aff (Millwood). 2009; 28: 160-168.

6. Tao ZQ, Shi AM, Wang KX, Zhang WD. Epidemiology of prostate cancer: current status. Eur Rev Med Pharmacol Sci. 2015; 19: 805-812.

7. Kote-Jarai Z, Leongamornlert D, Saunders E, et al. BRCA2 is a moderate penetrance gene contributing to young-onset prostate cancer: implications for genetic testing in prostate cancer patients. Br J Cancer. 2011; 105: 1230-1234.

8. Tenke P, Horti J, Balint P, Kovacs B. Prostate cancer screening. Recent Results Cancer Res. 2007; 175: 65-81.

9. Jean-Pierre G. Advice About Screening for Prostate Cancer With Prostate-Specific Antigen. J Adv Pract Oncol. 2017; 8: 639-645.

10. Wolf AM, Wender RC, Etzioni RB, et al. American Cancer Society guideline for the early detection of prostate cancer: update 2010. CA Cancer J Clin. 2010; 60: 70-98.

11. Carter HB. American Urological Association (AUA) guideline on prostate cancer detection: process and rationale. BJU Int. 2013; 112: 543-547.

12. Naji L, Randhawa H, Sohani Z, et al. Digital Rectal Examination for Prostate Cancer Screening in Primary Care: A Systematic Review and Meta-Analysis. Ann Fam Med. 2018; 16: 149-154.

13. NCCN. Clinical Practice Guidelines in Oncology, Prostate Cancer Early Detection. Version 2.2018. Available at: https://www.urology.wiki/Guidelines/Cancers/NCCN/2018/prostate_detection.pdf.

14. Streicher J, Meyerson BL, Karivedu V, Sidana A. A review of optimal prostate biopsy: indications and techniques. Ther Adv Urol. 2019; 11: 1756287219870074.

15. Eklund M, Jäderling F, Discacciati A, et al. MRI-Targeted or Standard Biopsy in Prostate Cancer Screening. N Engl J Med. 2021; 385: 908-920.

16. Kasivisvanathan V, Emberton M, Moore CM. MRI-Targeted Biopsy for Prostate-Cancer Diagnosis. N Engl J Med. 2018; 379: 589-590.

17. Garcia-Henriquez N, Galante DJ, Monson JRT. Selection and Outcomes in Abdominoperineal Resection. Front Oncol. 2020; 10: 1339.

18. Hawkins AT, Albutt K, Wise PE, et al. Abdominoperineal Resection for Rectal Cancer in the Twenty-First Century: Indications, Techniques, and Outcomes. J Gastrointest Surg. 2018; 22: 1477-1487.

19. Lee TK, Barringer M, Myers RT, Sterchi JM. Multiple primary carcinomas of the colon and associated extracolonic primary malignant tumors. Ann Surg. 1982; 195: 501-507.

20. Duggan MA, Anderson WF, Altekruse S, Penberthy L, Sherman ME. The Surveillance, Epidemiology, and End Results (SEER) Program and Pathology: Toward Strengthening the Critical Relationship. Am J Surg Pathol. 2016; 40: e94-e102.

21. Terris MK, Wren SM. Results of a screening program for prostate cancer in patients scheduled for abdominoperineal resection for colorectal pathologic findings. Urology. 2001; 57: 943-945.

22. Klaassen Z, King RS, Moses KA, Madi R, Terris MK. Abdominoperineal Resection: Consideration and Limitations of Prostate Cancer Screening and Prostate Biopsy [Internet]. Advances in Prostate Cancer. InTech; 2013. Available at: http://dx.doi.org/10.5772/52291

23. Murad MH, Sultan S, Haffar S, Bazerbachi F. Methodological quality and synthesis of case series and case reports. BMJ Evid Based Med. 2018; 23: 60-63.

24. Higgins J, Morgan R, Rooney A, et al. Risk Of Bias In Non-randomized Studies – of Exposure (ROBINS-E). Launch version, 20 June 2023. Available at: https://www.riskofbias.info/welcome/robins-e-tool

25. Page MJ, McKenzie JE, Bossuyt PM, et al. The PRISMA 2020 statement: an updated guideline for reporting systematic reviews. BMJ. 2021; 372: n71.

26. Schapira HE. Prostatic needle biopsy in patients after abdominoperineal resection. Urology. 1982; 20: 76-77.

27. Twidwell JJ, Matthews RD, Huisam TK, Sands JP. Ultrasound evaluation of the prostate after abdominoperineal resection. J Urol. 1993; 150: 902-904.

28. Filderman PS, Jacobs SC. Prostatic ultrasound in the patient without a rectum. Urology. 1994; 43: 722-724.

29. Fornage BD, Dinney CP, Troncoso P. Ultrasound-guided transperineal needle biopsy of the prostate after abdominoperineal resection. J Clin Ultrasound. 1995; 23: 263-265.

30. Amin A, Blazevski A, Scheltema M, Stricker P. Transperineal biopsy of the prostate in a patient post abdominoperineal resection. Urol Case Rep. 2019; 28: 101055.

31. Shinohara K, Gulati M, Koppie T, Terris MK. Transperineal prostate biopsy after abdominoperineal resection. J Urol. 2003; 169: 141-144.

32. Kailavasan M, Khan M. Cognitively targeted transperineal prostate biopsy in patients with previous abdominoperineal excision of the rectum. J Clin Urol. 2023; 16: 86-90.

33. Park BK, Chung JH, Song W, et al. New transperineal ultrasound-guided biopsy for men in whom PSA is increasing after Miles' operation. Insights Imaging. 2023; 14: 42.

34. Hansen NL, Caglic I, Berman LH, Kastner C, Doble A, Barrett T. Multiparametric Prostate Magnetic Resonance Imaging and Cognitively Targeted Transperineal Biopsy in Patients With Previous Abdominoperineal Resection and Suspicion of Prostate Cancer. Urology. 2016; 96: 8-14.

35. Krauss DJ, Clark KG, Nsouli IS, Amin RM, Kelly CM, Mortek MA. Prostate biopsy

in patients after proctectomy. J Urol. 1993; 149: 604-606.

36. Papanicolaou N, Eisenberg PJ, Silverman SG, McNicholas MM, Althausen AF. Prostatic biopsy after proctocolectomy: a transgluteal, CT-guided approach. AJR Am J Roentgenol. 1996; 166: 1332-1334.

37. Cantwell CP, Hahn PF, Gervais DA, Mueller PR. Prostate biopsy after ano-rectal resection: value of CT-guided trans-gluteal biopsy. Eur Radiol. 2008; 18: 738-742.

38. Goenka AH, Remer EM, Veniero JC, Thupili CR, Klein EA. CT-Guided Transgluteal Biopsy for Systematic Random Sampling of the Prostate in Patients Without Rectal Access. AJR Am J Roentgenol. 2015; 205: 578-583.

39. Olson MC, Atwell TD, Mynderse LA, King BF, Welch T, Goenka AH. CT-guided transgluteal biopsy for systematic sampling of the prostate in patients without rectal access: a 13-year single-center experience. Eur Radiol. 2017; 27: 3326-3332.

40. Caglic I, Breznik S, Matela J, Barrett T. Lesion Targeted CT-Guided Transgluteal Prostate Biopsy in Combination With Prebiopsy MRI in Patients Without Rectal Access. Urol Case Rep. 2016; 10: 6-8.

41. Patel N, Coakley FV, Foster BR. Performance of transgluteal CT-guided biopsy of prostate lesions in men without rectal access: A retrospective study. Clin Imaging. 2021; 79: 225-229.

42. Kirby KA, Upson C, Grasso M. Intraluminal ultrasound-guided biopsy of the prostate: case report. J Endourol. 1995; 9: 323-324.

43. Seaman EK, Sawczuk IS, Fatal M, Olsson CA, Shabsigh R. Transperineal prostate needle biopsy guided by transurethral ultrasound in patients without a rectum. Urology. 1996; 47: 353-355.

44. De Vulder N, Geldof K, Baekelandt F, Gieraerts K. Transperineal MRI-US Fusion-Guided Target Biopsy of the Prostate after Abdominoperineal Resection: A Case Report. J Belg Soc Radiol. 2021; 105: 57.

45. D'Amico AV, Tempany CM, Cormack R, et al. Transperineal magnetic resonance image guided prostate biopsy. J Urol. 2000; 164: 385-387.

46. Merrick GS, Kurko B, Scholl W, Butler WM, Adamovich E. CT-PLANNED transperineal prostate BIOPSY IN patients without a rectum. Urol Case Rep. 2020; 33: 101409.

47. Mattiuzzi C, Lippi G. Current Cancer Epidemiology. J Epidemiol Glob Health. 2019; 9: 217-222.

48. Van Hemelrijck M, Drevin L, Holmberg L, Garmo H, Adolfsson J, Stattin P. Primary cancers before and after prostate cancer diagnosis. Cancer. 2012, 118: 6207-6216.

49. Dema S, Bota A, Tăban SM, et al. Multiple Primary Tumors Originating From the Prostate and Colorectum A Clinical-Pathological and Therapeutic Challenge. Am J Mens Health. 2021; 15: 15579883211044881.

50. Jacobs CD, Trotter J, Palta M, et al. Multi-Institutional Analysis of Synchronous Prostate and Rectosigmoid Cancers. Front Oncol. 2020; 10: 345.

51. Holden J, Nayak JG, Botkin C, Helewa RM. Abdominoperineal Resection with Absorbable Mesh Repair of Perineal Defect for Fournier's Gangrene: A Case Report. Int Med Case Rep J. 2021; 14: 133-138.

52. Meima-van Praag EM, Buskens CJ, Hompes R, Bemelman WA. Surgical management of Crohn's disease: a state of the art review. Int J Colorectal Dis. 2021; 36: 1133-1145.

53. Igel TC, Knight MK, Young PR, et al. Systematic transperineal ultrasound guided template biopsy of the prostate in patients at high risk. J Urol. 2001; 165: 1575-1579.

54. Tzeng M, Basourakos SP, Patel HD, Allaway MJ, Hu JC, Gorin MA. Pooled outcomes of performing freehand transperineal prostate biopsy with the PrecisionPoint Transperineal Access System. BJUI Compass. 2022; 3: 434-442.

55. Umbreit EC, Dozois EJ, Crispen PL, Tollefson MK, Karnes RJ, Blute ML. Radical prostatectomy for prostate cancer after ileal pouch-anal anastomosis offers oncologic control and sustains quality of life. J Am Coll Surg. 2010; 210: 232-239.

56. Puech P, Rouvière O, Renard-Penna R, et al. Prostate cancer diagnosis: multiparametric MR-targeted biopsy with cognitive and transrectal US-MR fusion guidance versus systematic biopsy – prospective multicenter study. Radiology. 2013; 268: 461-469.

57. Xiang J, Yan H, Li J, Wang X, Chen H, Zheng X. Transperineal versus transrectal prostate biopsy in the diagnosis of prostate cancer: a systematic review and meta-analysis. World J Surg Oncol. 2019; 17: 31.

58. Berry B, Parry MG, Sujenthiran A, et al. Comparison of complications after transrectal and transperineal prostate biopsy: a national population-based study. BJU Int. 2020; 126: 97-103.

59. Presti JC Jr, O'Dowd GJ, Miller MC, Mattu R, Veltri RW. Extended peripheral zone biopsy schemes increase cancer detection rates and minimize variance in prostate specific antigen and age related cancer rates: results of a community multi-practice study. J Urol. 2003; 169: 125-129.

60. Schlemmer HP, Krause BJ, Schütz V, Bonekamp D, Schwarzenböck SM, Hohenfellner M. Imaging of Prostate Cancer. Dtsch Arztebl Int. 2021; 118: 713-719.

61. Kumar R, Singh SK, Mittal BR, et al. Safety and Diagnostic Yield of 68Ga Prostate-specific Membrane Antigen PET/CT-guided Robotic-assisted Transgluteal Prostatic Biopsy. Radiology. 2022; 303: 392-398.

62. Jones TA, Radtke JP, Hadaschik B, Marks LS. Optimizing safety and accuracy of prostate biopsy. Curr Opin Urol. 2016; 26: 472-480.

63. Nam W, Park MU, Chae HK, et al. Recent Trends in Prostate Biopsy Complication Rates and the Role of Aztreonam in Periprocedural Antimicrobial Prophylaxis – A Nationwide Population-Based Study from Korea. Antibiotics (Basel). 2022; 11: 312.

64. Bennett HY, Roberts MJ, Doi SA, Gardiner RA. The global burden of major infectious complications following prostate biopsy. Epidemiol Infect. 2016; 144: 1784-1791.

65. Sherer BA, Warrior K, Godlewski K, et al. Prostate cancer in renal transplant recipients. Int Braz J Urol. 2017; 43: 1021-1032.

66. Liss MA, Taylor SA, Batura D, et al. Fluoroquinolone resistant rectal colonization predicts risk of infectious complications after transrectal prostate biopsy. J Urol. 2014; 192: 1673-1678.

67. Hu JC, Assel M, Allaf ME, et al. Transperineal Versus Transrectal Magnetic Resonance Imaging-targeted and Systematic Prostate Biopsy to Prevent Infectious Complications: The PREVENT Randomized Trial. Eur Urol. 2024; 86: 61-68. ■

REVIEW PAPER

UROLOGICAL ONCOLOGY

Review of different convolutional neural networks used in segmentation of prostate during fusion biopsy

Maciej Zwolski, Andrzej Kupilas, Przemysław Cnota

Department of Urology and Urooncology, Municipal Hospital No. 4 in Gliwice, Poland

Citation: Zwolski M, Kupilas A, Cnota P. Review of different convolutional neural networks used in segmentation of prostate during fusion biopsy. Cent European J Urol. 2025; 78: 23-39.

Article history
Submitted: Mar. 11, 2024
Accepted: Oct. 16, 2024
Published online: Mar. 21, 2025

Corresponding author
Maciej Zwolski
Department of Urology and Urooncology,
Municipal Hospital No. 4 in Gliwice,
29 Kościuszki St.,
Gliwice, Poland
zwolskimd@gmail.com

Introduction The incidence of prostate cancer is increasing in Poland, particularly due to the aging population. This review explores the potential of deep learning algorithms to accelerate prostate contouring during fusion biopsies, a time-consuming but crucial process for the precise diagnosis and appropriate therapeutic decision-making in prostate cancer. Implementing convolutional neural networks (CNNs) can significantly improve segmentation accuracy in multiparametric magnetic resonance imaging (mpMRI).

Material and methods A comprehensive literature review was conducted using PubMed and IEEE Xplore, focusing on open-access studies from the past five years, and following PRISMA 2020 guidelines. The review evaluates the enhancement of prostate contouring and segmentation in MRI for fusion biopsies using CNNs.

Results The results indicate that CNNs, particularly those utilizing the U-Net architecture, are predominantly selected for advanced medical image analysis. All the reviewed algorithms achieved a Dice similarity coefficient (DSC) above 74%, indicating high precision and effectiveness in automatic prostate segmentation. However, there was significant heterogeneity in the methods used to evaluate segmentation outcomes across different studies.

Conclusions This review underscores the need for developing and optimizing segmentation algorithms tailored to the specific needs of urologists performing fusion biopsies. Future research with larger cohorts is recommended to confirm these findings and further enhance the practical application of CNN-based segmentation tools in clinical settings.

Key Words: fusion biopsy ‹› convolutional neural networks (CNNs) ‹› deep learning ‹› prostate cancer ‹› prostate segmentation

INTRODUCTION

Prostate cancer is the second most common cancer in men of all age ranges, with estimated number of new cases 1,466,718 in 2022 in the world [1]. In Poland, there is an increasing trend in prostate cancer incidence, with forecasts indicating a 55.2% increase in cases compared to the year 2019 [2]. Vital priority in coming years should be to increase the capacity of the healthcare system to diagnose prostate cancer for the early detection of clinically significant prostate cancer (CSPCa) and the implementation of appropriate therapeutic decisions. We posit that optimizing fusion biopsies holds promise as a solution to this challenge. This can be achieved through the integration of deep learning algorithms into the biopsy process. In recent years, there has been rapid development in artificial intelligence (AI) and machine learning due to the implementation of deep learning [3]. It is important to clarify that while ML and DL are related, they are not the same (Figure 1). Machine learning uses input datasets and algorithms to uncover patterns and make predictions. The two primary approaches in machine learning are supervised and unsupervised learning. The key difference lies in the type of data used to train the model. In supervised learning computer is trained on dataset that are similar to the problem at hand.

Once the model learns the relationship between the input and the output, it can classify new unknown datasets and make predictions or decisions based on them. On the other hand, unsupervised learning using unannotated data. Model learns from input data without expected values, and the available dataset does not provide answers to the given task. Thus, the main goal of supervised learning is to predict or classify new, unseen data based on the learned patterns, while unsupervised learning aims to discover hidden patterns, structures, or relationships within the data. Due to the extensive nature of classical machine learning methods and their divergence from the topic of this review, we recommend the article by Kufel et al. [4] for those interested in a more in-depth discussion of this subject.
A comprehensive review of the literature on automatic prostate segmentation in multiparametric magnetic resonance imaging (mpMRI) images reveals a significant focus on assisting radiologists in their image interpretation tasks. While these studies demonstrate the potential of segmentation algorithms to enhance diagnostic accuracy and efficiency, they largely neglect the practical application of these tools within the workflow of urologists performing fusion biopsy procedures.
Our experience indicates that a part of urologists independently delineate prostate contours on mpMRI scans, highlighting the need for segmentation algorithms that seamlessly integrate into their workflow. To fulfill this gap, future research should prioritize the development and evaluation of segmentation tools tailored to the specific needs of urologists during fusion biopsy procedures.
We undertake assess the improvement by AI in the contouring and segmentation of the prostate in MRI used for fusion biopsy and try compare the effectiveness of different algorithms build in CCNs architecture.

The principles of fusion biopsy

The distinction between clinically significant and clinically insignificant prostate cancer does not have a sharp boundary; it is more of a balance between the characteristics of the tumor and the patient himself. CSPCa can cause morbidity or death, but insignificant not. This distinction is crucial because the treatment itself carries the risk of harmful side effects for the patient. Due to the fact that transrectal ultrasound (TRUS)-guided systematic biopsy does not detect up to 20% of clinically significant cancers, a better alternative was sought [5]. Today, the most sensitive method to detect CSPCa is fusion biopsy (Figure 2) [6–8]. Currently, there are three types of Fusion biopsies: visual estimation TRUS-guided biopsy (known also as "cognitive"), in-bore MRI-guided biopsy and software-based co-registration guided biopsy with MRI to ultrasound fusion. It is based on the analysis of mpMRI in search of lesions suspicious of neoplastic features (regions of interest – ROI) and obtaining a biopsy from these lesions. It has been more than 10 years since targeted mpMRI-GB was introduced into the diagnostic pathway for detecting early prostate cancers [9] European Association of Urology (EAU) in its guidelines has approved the higher sensitivity of mpMRI compared to ultrasound-guided biopsy to detect prostate cancer for International Society of Urological Pathology (ISUP) grade ≥2 [10, 11]. Studies indicate that for the ISUP 1 group, systematic biopsy is more sensitive than mpMRI-GB; however, this often leads to overdiagnosis and possible overtreatment [12]. mpMRI consists of T2 high-resolution weighted imaging (T2w) that assesses the content of water in tissues and at least two functional MRI techniques. These two techniques include diffusion-weighted imaging (DWI; Figure 3), which evaluates the diffusion of water molecules between different tissues (from DWI, the apparent diffusion coefficient [ADC], is calculated) and dynamic contrast-enhanced imaging (DCE). DCE assesses the spread of contrast agent in the prostate gland, which, in the case of present tumor tissues, fills them more quickly (due to tumor angiogenesis) and also washes them out more rapidly [13]. T2W images are especially significant as enable the differentiation of the zonal anatomy of the prostate gland – the peripheral zone exhibits high signal intensity, the central zone shows decreased intensity, and the transition zones have heterogeneous intensity. These images also facilitate the evaluation and identification of cancer foci, which most commonly manifest as low intensity within the peripheral zone. DWI and DCE are utilized for further assessment of the

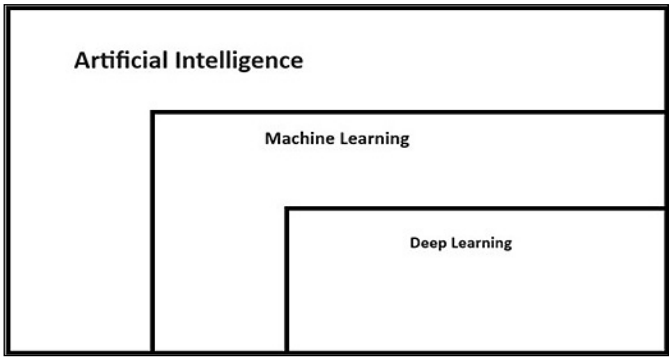

Figure 1. *Interdependence between artificial intelligence, machine learning and deep learning.*

prostate anatomy and ROI. Integral analysis of these imaging modalities significantly increases precision and sensitivity in the detection of neoplastic lesions within the prostate gland [6]. To optimize and unify the evaluation of mpMRI, the American College of Radiology, European Society of Urogenital Radiology (ESUR), and the AdMeTech Foundation developed a standardized method for assessing mpMRI images, commonly known as PI-RADS (Prostate Imaging-Reporting and Data System) [14]. PI-RADS employs a stratification system that assigns values ranging from 1 to 5. It is advised that for lesions categorized as grade 3, a biopsy should be contemplated, whereas for lesions classified with values of 4 and 5, the execution of a biopsy is emphatically recommended [15]. Over the years, the authors achieved the intended effect and enhanced the quality of prostate cancer detection due to PI-RADS [16]. PI-RADS has also been incorporated into representative clinical guidelines and has been used in clinical research as a tool for risk stratification and determining the biopsy pathway [15, 17]. Research assessing the effectiveness of PI-RADS criteria via targeted biopsy has demonstrated significant predictive power in determining the likelihood of prostate cancer, alongside a notable correlation with the Gleason score. The current version in use is PI-RADS 2v1.

The mentioned fusion biopsy techniques mainly differ in the way the needle is targeted in the ROI (Figure 4). In the cognitive method, the operator analyzes prostate gland map and, based on their own experience, collects samples from the prostate. This is a low cost method, but the learning curve is high. In the in-bore biopsy method, the biopsy is performed while the patient lies inside the MRI scanner. This method's advantage lies in its minimal image distortion detection, while its drawbacks include the high cost associated with prolonged MRI usage and the limited availability of this testing form. Prince and his research group in their study demonstrated a higher sensitivity to detect CSPCa through in-bore compared to fusion MRI-targeted biopsy [18]. The final method is software-assisted fusion biopsy, which involves manually or automatically, delineating the entire prostate on mpMRI and identifying ROIs. This phase, if manually, is not infrequently laborious, tedious,

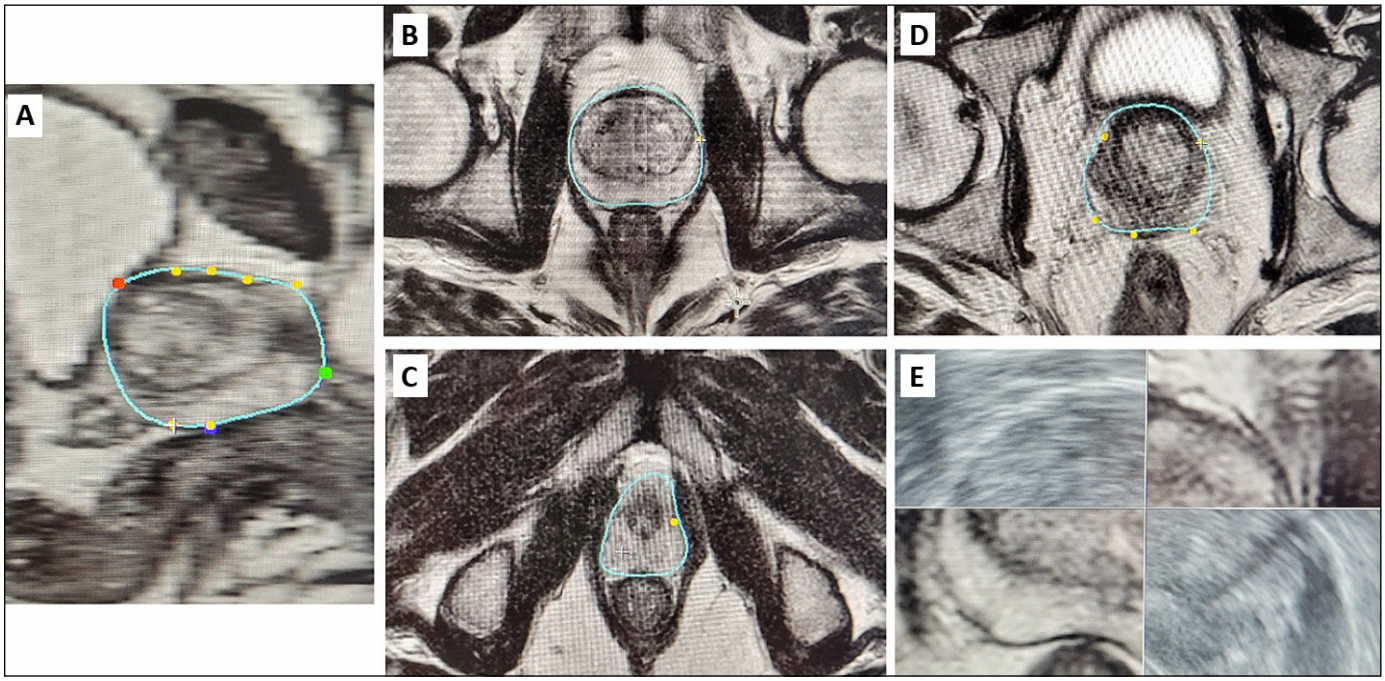

Figure 2. *Fusion performed on Urostation (Koelis). Contouring:* **A)** *The first step is to mark 3 points that generate the original outline: green – the top of the prostate gland, red – the base above the entrance to the urethra, and blue – the back wall of the gland. The software then generates the primary outline which we already contour by marking yellow points and adjusting it to the outline of the gland:* **B)** *mid,* **C)** *apex,* **D)** *base. On the finished outline we mark changes using T2 and ADC or DWI sequences, for more discrete lesions we use contrast sequences. Trinity software allows overlapping of images. The next step is to repeat these steps, but this time we work on the ultrasound image from the endorectal transducer generated live.* **E)** *After creating two contours, the apparatus performs a fusion of the images, which we check and confirm, and after confirmation we receive the superimposed lesions on the ultrasound image and can proceed to the actual part of the biopsy.*

and time-consuming, highly depending on clinician experience and skills [19].
Concurrently, TRUS is performer in real-time, and with the aid of software, the mpMRI images are merged. This co-registration is crucial step in the Fusion process, where the three-dimensionally (3D) segmented area of the prostate on MRI images is „combined" or aligned with the 3D captured area of the prostate on real-time US images. Following the completion of the co-registration, the process advances to the biopsy phase of the prostate gland. Two methods of image registration between mpMRI and real-time TRUS are available on the market: static, which directly overlays images without considering changes in the prostate visualization caused by compression from the US probe or the patient's positioning, and elastic, where the software accommodates differences in the gland's chape between MRI scans and TRUS.
The biopsy fusion stations available on the market are presented in Table 1.

The principles of deep learning

Deep learning is powered by neural networks, which mimic the information-transmitting behavior of human neurons. Similar to our brains, deep learning begins with the introduction of information, such as an image or sound. This information is then passed through the network, analyzed by successive layers until an output is generated. Each layer comprises numerous neurons that process the input data.

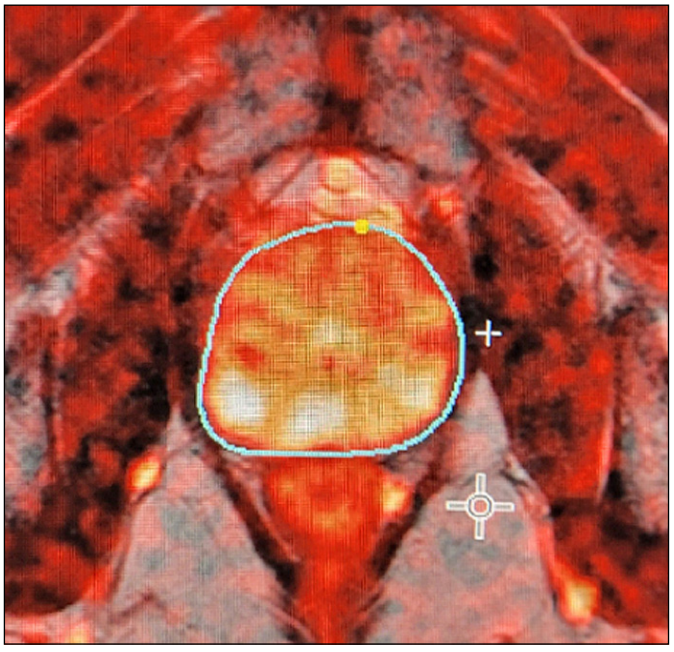

Figure 3. *Diffusion-weighted imaging.*

The number of hidden layers distinguishes between artificial neural networks (ANNs), which have one hidden layer, and deep neural networks (DNNs), which have multiple hidden layers (Figure 5).
Regardless of the training method employed, machine learning algorithms improve their performance on new data as they are exposed to more training examples. The primary distinction between ANNs and DNNs lies in their data requirements. DNNs demand significantly more input data, as they must learn to classify data independently. In contrast, ANNs rely on pre-processed and labeled data. One of the examples of DNN are CNNs [4].
Currently, the most widespread architecture in the medical industry is CNNs [21], which are primarily used for the analysis of advanced imaging, including MRI scans. CNNs are inspired by the functioning of the animal visual cortex, which attempts to emulate hierarchical, layered information processing [22]. A CNN, in contrast to traditional techniques, allows unsupervised learning and selects its own feature maps automatically while training. The basic unit of the neural network consists of: an input

Table 1. *The biopsy fusion stations available on the market*

Biopsy fusion stations	Producer
UroNav	Philips
BiopSee	MedCom
BioJet	DK Technologies
Urostation	Koelis
Semirobotic Artemis	Eigen
Virtual Navigator	Esaote

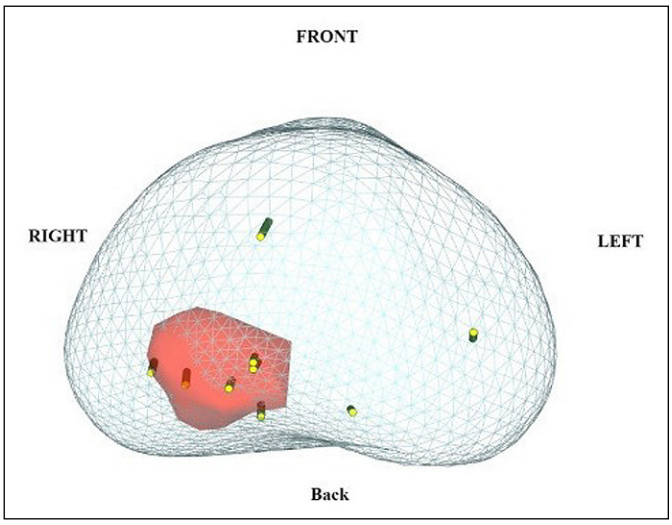

Figure 4. *Example of fusion.*

layer, connected "nodes" (equivalent of neurons) called hidden layers, and an output layer. Within the scope of hidden layers are convolutional layers (conv), pooling layers, flatten layer, and fully connected (FC) layers. Convolutional layers are made up of filters/kernels and, similar to neuronal cells, aim to extract features from the image that help in understanding the image. CNNs learn these filters, which convert the given image to extract its features like edges, colors or textures. Then, the output of the conv layer goes to an activation function layer where the ultimate goal is to map the representation in the input to a different output as per the requirements of the task. The activation function is nonlinear because without this, a neural network, no matter how many layers it has, would behave like a single layer perceptron, capable of learning only linear data. Then the image size is reduced in the pooling layer. This layer may realize the reduction using max or average pooling by converting a square (typically two by two pixels) into one pixel. In this way, overfitting is avoided, which is the phenomenon of the model being too closely fitted to the training data, critically important for maintaining the model's ability to generalize to previously unseen data. Such condensed data then go to a layer where neurons receive input from all the neurons of the previous layer. This is the FC layer, which can be likened to bridge between the features extracted by the previous layers and the final outcome/prediction, such as identifying the contours of the prostate in the mpMRI case [23]. The performance of CNNs can be influenced by various factors, with the most crucial ones being the selection of activation functions and the number of hidden layers. Networks trained on extensive datasets encompassing phenotypic and pathophysiologic variations will inherently be more robust compared to networks trained on limited datasets lacking such variety.

The ORSI Academy presents in an understandable manner the application of CNNs in creating software that assists operators during robotic surgeries as well as for training purposes [24]. If anyone is interested in more comprehensive explanation of deep learning, we highly recommend review article created by Alzubaidi et al. [21]

Analysing the experiments conducted by various researchers, we noticed that most of algorithms to a greater or lesser extent drew from the achievements of Ronneberger, Fischer, and Brox, i.e., CNNs named U-Net [25]. U-Net is a powerful tool for identifying and separating different parts or unusual areas in medical images (Figure 6). It works by analyzing images at various levels of detail. This architecture consists of an encoder-decoder structure with skip connections. The encoder part of the network gradually reduces spatial dimensions while increasing the number of feature channels through successive convolutional and pooling layers. This process captures hierarchical feature representations at multiple scales. The decoder part, on the other hand, performs upsampling and convolution operations to progressively reconstruct the segmented output. Skip connections are established between corresponding encoder and decoder layers to enable the integration of both low-level and high-level features, aiding in the preservation of fine details during the segmentation process.

One of the limitations of using these algorithms is their requirement for a vast database for training. Another limitation is the significant computational power of computer hardware that must be provided for CNNs to operate. Nowadays, researchers are trying to overcome these limitations by data augmentation, transfer learning, and creating more efficient network architectures [26–28].

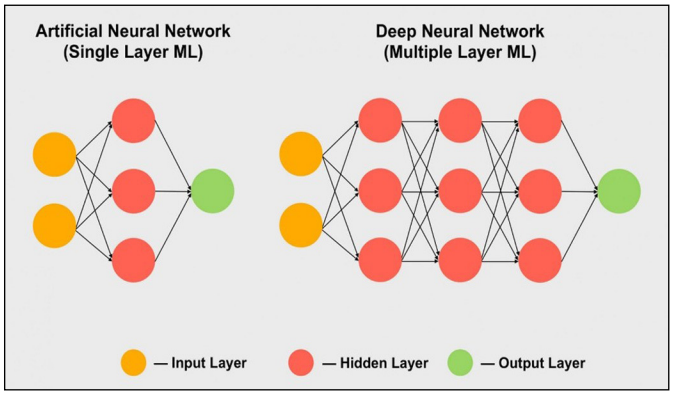

Figure 5. *A simplified example of artificial neural network and deep neural network [20].*

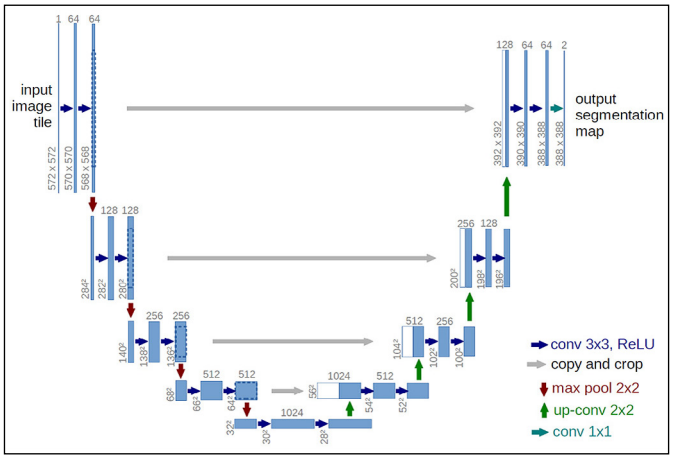

Figure 6. *U-Net architecture (example for 32 × 32 pixels in the lowest resolution) [25].*

Consumer platforms

It is important to highlight that various software platforms utilizing deep learning algorithms for the automatic contouring of the prostate gland are available on the market. However, the majority of these platforms are designed for evaluating mpMRI based on the PIRADS v 2.1 scale by radiologists, rather than as integral components of fusion biopsy workstations (Table 2).

MIM Symphony Dx™ utilizes AI to automatically segment the prostate gland and identify ROIs. Its automatic segmentation is based on multi-atlas segmentation, wherein a collection of MRI scans with manually segmented prostates by experts serves as the foundation. The atlas subjects are registered to the test case using a normalized intensity-based free-form deformable algorithm. Deformable image registration (DIR) is a technique used in medical imaging to align two or more images of the same anatomy acquired from different perspectives or at different times. The volumes of interest (VOIs) are then transformed to the test case using this deformable registration and combined using Simultaneous Truth and Performance Level Estimation (STAPLE) methods. STAPLE considers the original contours and computes a probabilistic estimate of the true representation of their combination. Atlas performance declined when tested with images of differing contrast and MRI vendors. A study published in 2018 evaluated an automatic multi-atlas-based segmentation method for generating prostate contours. The similarity coefficients between the selections of one and two experts served as benchmarks for assessing the quality of the atlas (expert radiation oncologists with 10 and 26 years of experience). The segmentation results were DSC (mean $\pm\sigma$) 0.81 $\pm$0.15 and Hausdorff distance (mm) (mean $\pm\sigma$) 2.7 $\pm$1.9. Segmentation time averaged less than 90 seconds per patient [29].

Philips DynaCAD automates segmentation for clinical use. However, its performance remains unclear due to the proprietary nature of the software and the lack of performance metrics such as the Dice score. According to the official website, UroNav does not include an algorithm for automatic segmentation but instead imports segmented images from the DynaCAD system. A significant limitation is that using this functionality requires the purchase of both products.

AI-Rad Companion also provides automated segmentation of the prostate, but no scientific reports on segmentation speed or accuracy have been found.

It is crucial to mention that the aforementioned software primarily serves to contour the prostate on desktop computers or laptops and not on fusion biopsy workstations. The literature includes review papers on AI-based software for automatic prostate segmentation, but these are predominantly intended for radiologists. We have selected software's directly associated with companies producing fusion biopsy platforms as these are directly related to the work of urologists.

ProMap Contour™ is an added software option to the Koelis Trinity® system. There are no articles assessing the time required for automatic segmentation, its accuracy, or validation. The advantage of this product lies in its integration into a platform used for performing fusion biopsies, enhancing the workflow for urologists.

ProFuse CAD Semirobotic Artemis (Eigen). This software is part of the Siemens Healthineers fusion biopsy platform and offers automated prostate gland contouring and segmentation. It utilizes deep learning algorithms to generate accurate contours on T2-weighted MRI scans. We were unable to locate any studies that validate its accuracy and speed in segmentation

In the reviewed literature, CNN-based algorithms achieved comparable accuracy in prostate segmentation tasks compared to MIM Symphony Dx™. However, CNN-based algorithms demonstrated significantly faster segmentation times in the four studies that directly assessed this metric. While MIM Symphony Dx™ achieves competitive accuracy, its segmentation speed is slower than CNN-based approaches. The segmentation speed of MIM Symphony Dx™ is reported to be under 90 seconds per patient, whereas CNN-based algorithms achieve segmentation times in the range of seconds. It is important to note that the studies referenced here have a relatively small sample size, and further research with larger cohorts is warranted to solidify these findings.

MIM Symphony Dx™ relies on a multi-atlas segmentation technique, which may be less generalizable to MRI scans with significant variations in contrast or acquired from different vendors compared to CNNs.

Table 2. *Software along with their companies*

MIM Symphony Dx™	MIM Software Inc.
Philips DynaCAD	Philips
AI-Rad Companion	Siemens Healthineers
ProMap Contour™	Koelis Trinity®
ProFuse CAD	Semirobotic Artemis (Eigen)

LITERATURE REVIEW

Search strategy

To conduct a comprehensive review, we search literature across PubMed and IEEE Xplore. These sources were selected because of their extensive publications of research in this area of study. Search included observational, randomized and non-randomized studies. It was limited to articles in English language with an abstract and published in peer-reviewed journals during the last 5 years in open access. Search was performed by title or abstract, utilizing keywords, as follows: for PubMed: (imaging-guided biopsy OR fusion biopsy) AND (mpMRI OR T2W) AND (deep learning OR CNN) AND (prostate segmentation OR prostate OR prostate contour), for IEEE Xplore ("All Metadata":fusion biopsy) AND ("All Metadata":prostate contour) OR ("All Metadata":prostate segmentation) AND ("All Metadata":convolutional neural network) Filters Applied: 2019–2024. The last search was conducted on 20.05.2024. The search was supplemented by checking published reviews, and their references. Exclusion criteria were reviews, letters, non-peer reviewed articles, conference abstracts and proceedings. Our method for identifying and evaluating data complied with the Preferred Reporting Items for Systematic Reviews and Meta-analyses (PRISMA) 2020 statement and checklist.

Data extraction

The full texts of the qualified papers chosen for review were acquired, and the reviewers independently collected all study data, resolving disagreements via consensus. The references, year of publication, study setting, ML approach, improvement of segmentation time, performance measures used and accuracy attained were all extracted for every included paper, and comparative analyses were conducted on the extracted dataset. Two independent authors (MZ, PC) screened and extracted the studies. A third reviewer (AK) was consulted in the event of discordance resulting in agreement in all instances.

Risk of bias

Our study assessment aims to evaluate the methodological quality and potential sources of bias that could influence the reported findings. For instance, studies that rely solely on single-center datasets or imbalanced class distributions may introduce biases that affect the model generalizability. Additionally, the lack of clear documentation of preprocessing steps, considerations for model-fitting problems and hyperparameter tuning could hinder reproducibility.

Comparative analysis

Database searches provides 44 results. After title and abstract screening, the full texts of 31 reported studies were analyzed, but only 12 were found eligible for inclusion. The excluded articles are outlined in Supplementary Table 1. A flowchart based on PRISMA 2020 statement is shown in Figure 7.
The results section is divided into three parts: segmentation accuracy, validation, and improvement of segmentation time.

Segmentation accuracy of prostate

Results in the segmentation accuracy of prostate category are shown in Table 3.
The Dice similarity coefficient (DSC) is a diagnostic tool that assesses the degree of similarity between two sets of data. The DSC score ranges between 0 and 1, where 0 indicates no similarity, and 1 represents perfect overlap. The Hausdorff distance to evaluate the results of the algorithm developed. The Hausdorff distance is a measure used to quantify

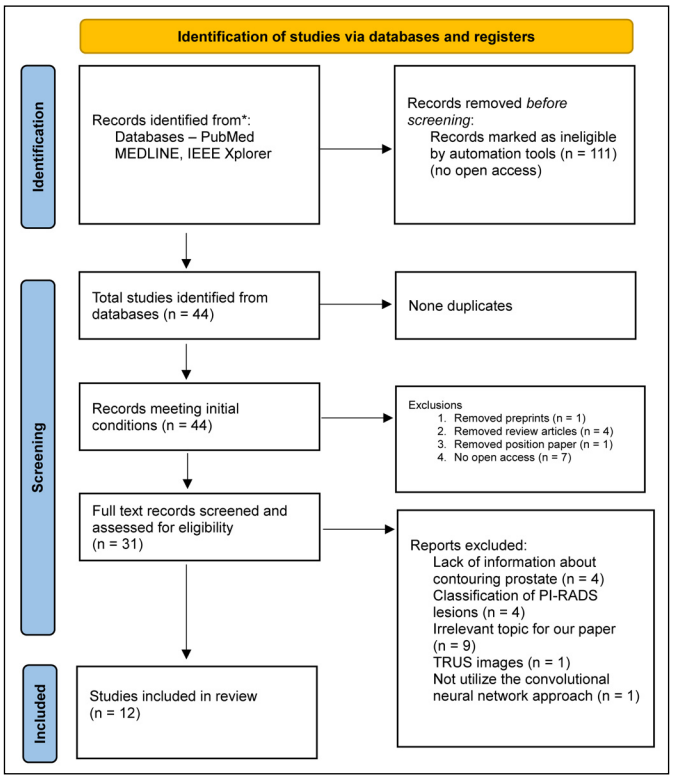

Figure 7. *PRISMA numerical flow guideline for systematic review employed in this study.*

the difference between two sets of points. The Pearson correlation coefficient values range from –1 to 1, with 1 and –1 denoting a strong linear relationship between two variables, while a value proximate to 0 indicates an absence of linear correlation between the variables.

DSC ranged from 0.74 to 0.94, indicating good to excellent agreement between CNN segmentation and expert annotations.

While DSC appears as the predominant metric for evaluating prostate segmentation algorithms in the reviewed studies, a closer examination reveals a lack of uniformity in the utilization of other validation metrics. Within the twelve studies reviewed, only two employed the Hausdorff distance, and two others utilized the Pearson correlation coefficient.

Among studies reviewed, only one compared the accuracy and time efficiency between the algorithm and human performance in segmenting the prostate [31], while another compared the consistency of humans and AI in delineating the prostate [40].

Soerensen et al. [31] created an algorithm demonstrates a narrow range in the DSC test <0.90, indicating consistency in the algorithm's accuracy in segmentation in various cases. Besides testing the algorithms on an internal database of T2-MRI scans, for further evaluation of the code's generalization capabilities, the tested its efficacy on two publicly available datasets: The results demonstrated a performance of 0.87 ±0.05 on the PROMISE12 dataset and 0.89 ±0.05 on the NCI-ISBI dataset. Researchers confirmed a high level of precision of automated segmentation obtained 2.8 mm Hausdorff distance. The culmination of the experiment was the application of ProGNet in practice, during work in the clinic. ProGNet (average DSC = 0.93 ±0.03) significantly outperformed radiology technicians (average DSC = 0.90 ±0.03, p <0.0001) in an 11-case set of prospective fusion biopsy tests.

Liu et al. [40] developed novel CNN for automatic segmentation of the prostatic transition zone (TZ) and peripheral zone. DSC was used to evaluate the segmentation performance. DSCs for peripheral

Table 3. *Segmentation accuracy of prostate*

Investigators	Mean DSC	Human experts (mean DSC)	Mean HD	Pearson correlation coefficient
Bardis et al. [30]	0.940	None	Not used	0.981 (95% CI: 0.966–0.989)
Soerensen et al. [31]	0.92 ±0.02 (100) (retrospective internal test) 0.93 ±0.03 (prospective 11 patients)	DSC = 0.89 (retrospective internal test) 0.90 ±0.03 (prospective 11 patients)	Algorithm reduced the mean HD by 2.8 mm compared to the radiology technicians	
Ushinsky et al. [32]	0.898	None	Not used	0.974
Palladino et al. [33]	0.7773 for internal dataset 0.7709 for external dataset	None	Not used	
Hassanzadeh et al. [34]	0.873	None	Not used	
Ren and Ren [35]	0.9394	none	Not used	
Huang et al. [36]	0.8782	None	10.9443	
Qian et al. [37]	0.908 (for PROMISE12) 0.892 (for ProstateX)	None	9.87 (for PROMISE12) 10.45 (for ProstateX)	
Su et al. [38]	0.9071	None	Not used	
Qian et al. [39]	0.8912 (for ProstateX)	None	Not used	
Liu et al. [40]	PZ 0.74 ±0.08 internal testing dataset TZ 0.86 ±0.07 internal testing dataset PZ external data 0.74 ±0.07 TZ external data 0.79 ±0.12	Expert 1 vs expert 2 PZ 0.71 ±0.13 p <0.05 TZ 0.75 ±0.14 p <0.051 when taking expert 1's annotations as the ground truth	Not used	
Comelli et al. [41]	ENet showed a mean DSC of 0.9089 ±0.0387, U-Net of 0.9014 ±0.0469, and ERFNet of 0.8718 ±0.0644	None	Not used	

[1]Authors used Wilcoxon Signed-Rank Test

DSC – Dice similarity coefficient; ENet – efficient neural network; ERFNet – efficient residual factorized convNet; HD – Hausdorff distance; PZ – peripheral zone; TZ – transition zone

zone (PZ) and prostatic transition zone (TZ) were 0.74 ±0.08 and 0.86 ±0.07 in the internal testing dataset (ITD) respectively. In the external testing dataset (ETD), DSCs for PZ and TZ were 0.74 ±0.07 and 0.79 ±0.12, respectively. The inter-reader consistency (Expert 2 vs Expert 1) were 0.71 ±0.13 (PZ) and 0.75 ±0.14 (TZ)

Validation

Results in the validation category are shown in Table 4.

The most commonly used technique for training and validation was k-fold cross-validation. In each iteration of this procedure, the dataset is divided into k subsets, with k-1 subsets used for training and the remaining subset used for validation. This process is repeated k times, ensuring that each subset is used exactly once for validation. This approach aims to optimize the utilization of the available dataset for robust model evaluation.

Number of epochs ranged widely, from 10 to 500.

The studies employed a diverse range of databases, encompassing both in-house image collections and publicly accessible datasets such as PROMISE12 and ProstateX:

- In-house database 6 studies,
- PROMISE12 6 studies,
- ProstateX 3 studies,
- Other datasets 2 studies.

PROMISE12 data set contained prostate MR images with well-curated prostate organ labels.

The definition of "ground truth" (gold standard) varies across studies. Certain investigations utilize radiologists, whereas others rely on urologists.

Improvement of segmentation time

Results in the improvement of segmentation time category are shown in Table 5.

Soerensen et al. [31] describe a promising result in their experiment: after a 20-hour training session, the ProGNet algorithm segmented a single case in roughly 35 seconds, resulting in the completion of a database of 100 clinical cases in about 1 hour. For comparison, radiologists took an average of 10 minutes per case. Completing the entire database took about 17 hours. ProGNet can save up to 17 times more time according to this trial. A limitation of this result may be the comparison of the algorithm with radiology technicians. In many facilities around the world, the aforementioned segmentation is performed by physicians with specialties in urology or radiology.

In another study, Ushinksy et al. modified traditional 2D-2D U-Net technique creating hybrid 3D-2D U-Net to assess its clinical utility in identifying and segmenting the entire prostate gland in mpMRI images [32]. (The algorithm is similar with developed by another researcher team Michelle Bardis et al. However, Michelle Bardis adapted their network to segment not only the entire prostate but also PZ and TZ by producing 3 separate, collaborative CNNs). Algorithm was verified by a board-certified urologist. On each axial T2WI included in the training database, two specialist radiologists contoured the prostate gland to create ground truth for assessing the segmentation quality by the algorithm. Research team from United States implemented for the quantitative evaluation of the segmentation overlap of the prostate image post manual and automatic segmentation, the authors employed the DSC. Additionally, the Pearson correlation coefficient was utilized to assess the neural network in predicting prostate volume. Findings are documented in Table 5. The authors noted that manual segmentation of the prostate requires approximately 5–10 minutes per patient. Accordingly, the neural network was able to segment the prostate in 9.4 seconds per patient.

Comelli et al. [41] presents three deep-learning approaches, namely U-Net, efficient neural network (ENet), and efficient residual factorized convNet (ERFNet), whose aim is to tackle the fully-automated, real-time, and 3D delineation process of the prostate gland on T2-weighted MRI. They found that ENet and U-Net are more accurate than ERFNet, with ENet much faster than U-Net. Specifically, ENet obtains a segmentation time of about 6 seconds using central processing unit (CPU) hardware to simulate real clinical conditions where graphics processing unit (GPU) is not always available.

Despite the absence of automatic segmentation speed assessment in the remaining eight studies, they provide significant insights into the accuracy of these algorithms, highlighting the potential for integrating CNNs into clinical practice.

DISCUSSION

Based on the studies and comparisons we collected, we have reached several conclusions, summarized below.

In comparative experiments involving ANNs and human experts, the algorithms demonstrated comparable, and in some cases even superior, performance in prostate segmentation (Soerensen et al. [31] and Liu et al. [40]). In studies where algorithms were solely compared to ground truth annotations made by radiologists or urologists, the DSC did not fall below 74%. It is important to note, however, that a significant limitation of these experiments is

Table 4. *Validation*

Investigators	Ground truth	Number of epoches	Type of used database	Evaluation	Data augmentation
Bardis et al. [30]	A board-certified subspecialty-trained abdominal radiologist with more than 10 years of experience	U-NetA, U-NetB, and U-NetC were trained for 50,000, 18,000, and 3,800 iterations U-NetA trained for approximately 7 hours, while U-NetB and U-NetC each trained for 5 hours[1]	Own database 242 T2-weighted images (6,292 axial images)	Included datasets were split into 60% training, 20% validation, and 20% test sets for model development	Not explicitly stated
Soerensen et al. [31]	Urologic oncology expert with 7 years of experience	150	Own database: 905 T2-MRI and 26 T2-MRI (PROMISE12) 30 T2-MRI (NCI-ISBI)	A deep learning model, ProGNet, was trained on 805 cases. ProGNet was retrospectively tested on 100 independent internal and 56 external cases. Algorithm was prospectively implemented as part of the fusion biopsy procedure for 11 patients	Not explicitly stated
Ushinsky et al. [32]	Two specialist radiologists images who were verified by a board-certified urologist	Not provided	Own database: 299 MRI (7,774 images)	Five-fold cross-validation	Not explicitly stated
Palladino et al. [33]	Ground truth was created using a semi-automatic procedure	Not provided (less than 2 hours)	ProstateX as training set (internal) and own dataset: MRI Local Hospital – 6 patients (external)	20% of the images were used for testing and the remaining images were split with a ratio of 0.8 in training set and 0.2 in validation set	Not explicitly stated
Hassanzadeh et al. [34]	Experienced readers at each center used a contouring tool then A second expert (C.H.) who has read more than 1,000 prostate MRIs, to make sure they were consistent	25 epochs	PROMISE12 [] 50 MRI (1377 image slices) volumes for training, 30 MRI volumes for testing (without grand truth)	Ten-fold cross-validation	Random rotation within a 10-degree range, horizontal flip, vertical flip, zoom, horizontal and vertical translation, and elastic transformation (result = 150,000 slices)
Ren and Ren [35]	Three clinicians with 5 years of experience spent 3 months annotating the segmented region. The other three specialists examined and corrected the annotated regions	400–500 epoch	Own database: 180 patients (122 healthy and 58 prostate cancer patients) scanned on the GE 3.0T 750 MR	Five cross-validation approach	Rotation, random merging, zooming in and out
Huang et al. [36]	Experienced readers at each center used a contouring tool then A second expert (C.H.) who has read more than 1,000 prostate MRIs, to make sure they were consistent. I2CVB – An experienced radiologist	200 epoch	PROMISE12 50 MRI (1,377 image slices) volumes for training, 30 MRI volumes for testing and I2CVB	Not explicitly stated	Rotation, zooming in and out, random horizontal or vertical flip, random movement along the X-axis and Y-axis
Qian [37]	Experienced readers at each center used a contouring tool then A second expert (C.H.) who has read more than 1,000 prostate MRIs, to make sure they were consistent (PROMISE12) In order to verify the generalization performance of the prostate segmentation algorithm, prostate masks were marked on the MR images of 40 randomly selected patients from the ProstateX dataset by a professional radiologist	10	PROMISE12 dataset and ProstateX dataset	Five-fold cross-validation	Not explicitly stated

Table 4. *Continued*

Investigators	Ground truth	Number of epoches	Type of used database	Evaluation	Data augmentation
Su et al. [38]	Experienced readers at each center used a contouring tool then A second expert (C.H.) who has read more than 1,000 prostate MRIs, to make sure they were consistent (PROMISE12)	Not explicitly stated	PROMISE12	Not explicitly stated	Elastic deformation, rotation with 90, 180, 270, and flip
Qian et al. [39]	Randomly selected 35 patients' MR images to label their prostate contours	60	ProstateX and PROMISE12	Five-fold cross-validation	Geometric transformations,local disturbance and combined disturbance Not explicitly stated
Liu et al. [40]	PROSTATEX – two MRI research fellows, where the contours were later cross-checked by both genitourinary (GU) radiologists (10–15 years of post-fellowship experience interpreting over 1,000 prostate mpMRI) and clinical research fellows WMHP – two clinical genitourinary (GU) radiologists research fellows, supervised by expert GU radiologists	100	PROSTATEX (internal testing) and WMHP (external testing)	Five-fold cross validation	Flipped horizontally, rotated randomly between [–5°, 5°], elastic transformations
Comelli et al. [41]	A set of trained clinical experts (FV, MP, GC, and GS authors) hand segmented the prostate region. The simultaneous ground truth estimation STAPLE tool (Warfield, Zou i Wells, 2004) was used to combine the different segmentations from the clinical experts in a consolidated reference	100	Own data set: 85 axial T2W	Five-fold cross-validation	Six different modalities – not explicitly stated

[1]An epoch refers to one complete pass through the entire training dataset. Iterations, on the other hand, can represent individual training steps within an epoch. The number of iterations per epoch can vary depending on the batch size (number of images processed at once).

Table 5. *Improvement of segmentation time*

Author, reference	Time
Bardis et al. [30]	The three U-Nets completed their tasks of bounding box creation, prostate segmentation, and prostate zone classification in 0.196 second, 0.226 second, and 0.219 second
Soerensen et al. [31]	35 seconds to segment each case
Ushinsky et al. [32]	9.4 seconds per patient
Palladino et al. [33]	Not tested
Hassanzadeh [34]	Not tested
Ren and Ren [35]	Not tested
Huang et al. [36]	Not tested
Qian [37]	Not tested
Su et al. [38]	Not tested
Qian et al. [39]	Not tested
Liu et al. [40]	Not tested
Comelli et al. [41]	ENet – 6.17 seconds ERFNet – 8.59 seconds U-Net – 42.02 seconds

ENet – efficient neural network; ERFNet – efficient residual factorized convNet

the lack of a human segmentation accuracy benchmark on the datasets used to evaluate the algorithms. Integration of CNN-based segmentation into clinical practice requires validation in larger cohorts. Of the studies available to us, four assessed the speed of prostate segmentation from T2-weighted images. In each case, segmentation of a single instance took less than one minute, with the fastest algorithms segmenting the prostate in approximately 0.3 seconds. In comparison, manual segmentation is reported by authors to take 5–10 minutes per patient [32], 10 minutes per patient [31]. From our experience, manual segmentation takes about 4–10 minutes per patient, depending on individual conditions and the quality of mpMRI. Based on this information, it can be estimated that AI-based CNNs can segment the prostate 800 to 2,000 times faster than humans. It is also important to remember that the speed of the algorithm is primarily dependent on the computational power.

Challenges and limitations

In the course of our investigation and analytical examination of deep learning algorithms applied

to prostate delineation and automated segmentation in mpMRI, we identified a notable lack of uniformity in the methodologies employed for comparing results. The considerable heterogeneity in the assessment protocols for the efficacy of neural networks significantly impedes the qualitative comparison of convolutional neural networks (CNNs). Studies utilized different datasets and evaluation metrics, making direct comparisons challenging. This diversity often leads to the inability to compare studies directly, including statistical data, thus impeding meta-analysis. As of now, no guidelines or standardization have been universally accepted. However, some studies have designed experiments specifically for network comparison [44].

We observed a significant lack of studies implementing deep learning algorithms for automatic prostate contouring in the practice of urologists performing fusion biopsies. Despite numerous studies on mpMRI contouring, these are predominantly intended as tools for radiologists, not for enhancing the workflow of urologists. In our review, we found only two studies that described the integration of deep learning algorithms into fusion biopsy stations, assessing their actual impact and accuracy in prostate contouring [31, 33].

Evaluating automated prostate delineation for fusion biopsy include significant inter-institutional variability in clinical workflows. Established protocols often entrust the delineation of prostate boundaries on T2-weighted MRI (T2W MRI) to radiologists or radiology technicians. However, at our institution, this task is handled by the urologists performing the biopsy. While the literature extensively explores deep learning algorithms for prostate delineation by radiologists, there is little research on the use of these algorithms by urologists. The final decision on the suitability of the contour for mpMRI-TRUS fusion biopsy rests with the urologist. Incorporating AI at this stage with sufficient accuracy and stability would significantly improve the urologist's workflow.

Another constraint pertains to the inherent complexity of this domain. The development and implementation of deep learning algorithms for MRI-US fusion require collaborative efforts among specialists from various scientific disciplines. This interdisciplinary team should encompass software developers, physicians specializing in urology and/or radiology, as well as professionals in computer vision, biomedical engineering, or other relevant fields such as mechatronics.

A limitation of our review is the relatively small sample size [12] which may limit generalizability to a broader population and preclude meta-analysis. To mitigate these limitations, we employed a rigorous search strategy and carefully considered the inclusion and exclusion criteria for studies. We also acknowledge that further research with larger sample sizes is needed to confirm our findings.

The last notable limitation of this review is the lack of open access to a significant number of articles. By restricting access to knowledge and expertise, it hinders comprehensive reviews, slows scientific progress, and creates an uneven playing field.

Future directions for research and clinical practice

As proven above, there is a significant gap in research on the implementation of CNNs for prostate segmentation during MRI-targeted TRUS biopsies and their integration into clinical practice. That is why the authors of this review highly recommend more experiments in this field. Benefits to clinical practice would include speeding up the biopsy process. Implementing automatic prostate segmentation to optimize the process would allow time for one more patient within the same timeframe as manual segmentation. The number may not seem staggering, but multiplying it by the number of facilities performing this examination would result in a satisfactory outcome in expanding the bottleneck. It should be noted that the rate of "machine" evaluation is predominantly determined by the computational capacity of the computer utilized. Hence, the greater the computing power dedicated to prostate segmentation, the quicker the automatic segmentation process can occur, potentially reaching to receive results even in 1 second or less as we could see in results.

Maris [45] has published a case study in "Medical Robotics" highlighting the PROST robot as a significant advancement in integrating AI into prostate biopsy procedures. The robot utilizes a prostate segmentation model known as PROST-Net, initially described by Palladino et al. [33]. In validation on ultrasound test data, PROST-Net achieved a Dice coefficient of 0.78 for prostate segmentation. Following the inclusion of additional data from a second cohort, the model's accuracy improved, exceeding a Dice coefficient of 0.80. The accuracy of prostate segmentation in MRI images was assessed using in-house MRIs, yielding a Dice coefficient greater than 0.95. Moreover, following rigid fusion, the Dice coefficient between MRI and ultrasound (US) segmentations was determined to be 0.75. Post-fusion, the distances between each lesion identified in MRI and the corresponding lesion in US were measured. The authors observed that the application of AI-driven image processing facilitates the automation of image fusion, as well as the identification and localization of prostate lesions, thereby enhancing

the procedure's efficiency and reliability. The robot is currently undergoing pre-clinical testing.
Another argument in favor would be the reduction of the risk of human errors. The human factor is prone to mistakes due to various external factors such as fatigue, low quality of images, distractions etc. [46]. Liu et al. [40] in their experiment, demonstrated that the algorithm was more consistent with the ground truth than the second expert. The directions this technological trend and its application might take include the integration of CNNs into clinical practice on a larger scale for software-co-registered MRI-targeted TRUS biopsy. Moving forward, automating the fusion biopsies could involve the development of technologies for automatic lesion delineation within the prostate glands. A significant advancement has recently been made in this field. An article published in "The Lancet Oncology", an internationally trusted source of clinical research with an Impact Factor of 41.6, investigates the performance of AI systems in detecting CSPCa on MRI compared to radiologists using the prostate imaging – reporting and Data System version 2.1 (PI-RADS 2.1). The authors demonstrate that AI was, on average, superior to radiologists using PI-RADS 2.1 in detecting CSPCa. The study compared 62 radiologists against AI in a test group comprising 400 cases [47].

CONCLUSIONS

Our review of the literature demonstrates that various CNN architectures have shown substantial potential in improving the accuracy and efficiency of prostate segmentation in mpMRI images. Tătaru et al. [48] analyzed the application of machine learning in the diagnosis of prostate cancer and highlighted that studies have reported AUC values as high as 0.91 using CNNs. This suggests that CNNs offer superior sensitivity and specificity compared to traditional radiological methods. Additionally, algorithms such as random forest classifiers and k-nearest neighbors have shown high predictive accuracy, particularly when used in conjunction with mpMRI. These techniques provide a robust set of tools for clinicians in identifying CSPCa. The integration of CNNs into the segmentation of prostate MRI images during fusion biopsy holds significant promise for improving the detection and diagnosis of CSPCa. Despite the advancements, there is a notable gap in the practical application of these tools within clinical workflows. Future research should focus on creating user-friendly, efficient segmentation tools that can be seamlessly integrated into the fusion biopsy process. Future research should focus on the development and refinement of these algorithms to ensure their robustness and applicability in clinical settings, as well as exploring methods to overcome current limitations such as the need for large training datasets and high computational power. Ultimately, the successful implementation of these advanced segmentation tools in clinical practice could lead to more accurate and efficient prostate cancer diagnoses, facilitating early detection and appropriate therapeutic decisions. The ongoing evolution of AI in medical imaging heralds a promising future for more precise and personalized prostate cancer diagnostics and treatment.

CONFLICTS OF INTEREST
The authors declare no conflict of interest.

FUNDING
This research received no external funding.

ETHICS APPROVAL STATEMENT
The ethical approval was not required.

Supplementary Table 1. *Ineligible studies for review*

van Sloun et al. [I]	TRUS images
Tollens et al. [II]	General review
Bonekamp et al. [III]	General review
Suarez-Ibarrola et al. [IV]	General review
Yilmaz et al. [V]	Based on the patient after radiotherapy
Lin et al. [VI]	No open access
Penzkofer et al. [VII]	Position paper
Lin et al. [VIII]	No open access
Hosseinzadeh et al. [IX]	Lack of information about contouring prostate
Soni et al. [X]	Segmentation of the prostate cancer lesion region. Lack of information about contouring prostate
Khosravi et al. [XI]	Lack of prostate segmentation description
Schelb et al. [XII]	Classification of PI-RADS lesions
Winkel et al. [XIII]	Classification of PI-RADS lesions
Kaneko et al. [XIV]	No open access
Jimenez-Pastor et al. [XV]	No open access
Guo et al. [XVI]	Irrelevant topic for our paper
Zhang et al. [XVII]	No open access
Labus et al. [XVIII]	No open access
Zheng et al. [XIX]	CSPCa lesion detection only
Al-Bourini et al. [XX]	No open access
Khan et al. [XXI]	General review
Saunders et al. [XXII]	Compares how the strategies of transfer learning and aggregated training
Alzate-Grisales et al. [XXIII]	Segmenting csPCa regions from MRI images. Lack of information about conturing prostate
Akhoondi and Baghshah [XXIV]	irrevelant topic for our paper – histopatological images
Elmahdy et al. [XXV]	Irrelevant topic for our paper – automatic re-contouring of follow-up scans for adaptive radiotherapy
Lee and Nishikwa [XXVI]	Mammograms segmentation/transferability of a traditionally transfer-learned CNN
Huang et al. [XXVII]	No statistical results about whole prostate contouring
Ren et al. [XXVIII]	The algorithm does not utilize the convolutional neural network approach
Shao et al. [XXIX]	Irrelevant topic for our paper – predict the Gleason Grade Group (GG-RP) of prostate cancer using bpMRI

CNN – convolutional neural networks; CSPCa – clinically significant prostate cancer; MRI – magnetic resonance imaging; PI-RADS – Prostate Imaging-Reporting and Data System; TRUS – transrectal ultrasound

I. van Sloun RJG, Wildeboer RR, Mannaerts CK, et al. Deep Learning for Real-time, Automatic, and Scanner-adapted Prostate (Zone) Segmentation of Transrectal Ultrasound, for Example, Magnetic Resonance Imaging-transrectal Ultrasound Fusion Prostate Biopsy. Eur Urol Focus. 2021; 7: 78-85.

II. Tollens F, Westhoff N, von Hardenberg J, et al. MRT-gestützte minimal-invasive Therapie des Prostatakarzinoms [MRI-guided minimally invasive treatment of prostate cancer]. Radiologe. 2021; 61: 829-838. German.

III. Bonekamp D, Schlemmer HP. Maschinelles Lernen und multiparametrische MRT in der Früherkennung des Prostatakarzinoms [Machine learning and multiparametric MRI for early diagnosis of prostate cancer]. Urologe A. 2021; 60: 576-591. German.

IV. Suarez-Ibarrola R, Sigle A, Eklund M, et al. Artificial Intelligence in Magnetic Resonance Imaging-based Prostate Cancer Diagnosis: Where Do We Stand in 2021? Eur Urol Focus. 2022; 8: 409-417.

V. Yilmaz EC, Harmon SA, Belue MJ, et al. Evaluation of a Deep Learning-based Algorithm for Post-Radiotherapy Prostate Cancer Local Recurrence Detection Using Biparametric MRI. Eur J Radiol. 2023; 168: 111095.

VI. Lin Y, Yilmaz EC, Belue MJ, et al. Evaluation of a Cascaded Deep Learning-based Algorithm for Prostate Lesion Detection at Biparametric MRI. Radiology. 2024; 311: e230750.

VII. Penzkofer T, Padhani AR, Turkbey B, et al. ESUR/ESUI position paper: developing artificial intelligence for precision diagnosis of prostate cancer using magnetic resonance imaging. Eur Radiol. 2021; 31: 9567-9578.

VIII. Lin Y, Belue MJ, Yilmaz EC, Harmon SA, et al. Deep Learning-Based T2-Weighted MR Image Quality Assessment and Its Impact on Prostate Cancer Detection Rates. J Magn Reson Imaging. 2024; 59: 2215-2223.

IX. Hosseinzadeh M, Saha A, Brand P, Slootweg I, de Rooij M, Huisman H. Deep learning-assisted prostate cancer detection

on bi-parametric MRI: minimum training data size requirements and effect of prior knowledge. Eur Radiol. 2022; 32: 2224-2234.

X. Soni M, Khan IR, Babu KS, Nasrullah S, Madduri A, Rahin SA. Light Weighted Healthcare CNN Model to Detect Prostate Cancer on Multiparametric MRI. Comput Intell Neurosci. 2022; 2022: 5497120.

XI. Khosravi P, Lysandrou M, Eljalby M, et al. A Deep Learning Approach to Diagnostic Classification of Prostate Cancer Using Pathology-Radiology Fusion. J Magn Reson Imaging. 2021; 54: 462-471.

XII. Schelb P, Kohl S, Radtke JP, et al. Classification of Cancer at Prostate MRI: Deep Learning versus Clinical PI-RADS Assessment. Radiology. 2019; 293: 607-617.

XIII. Winkel DJ, Wetterauer C, Matthias MO, et al. Autonomous Detection and Classification of PI-RADS Lesions in an MRI Screening Population Incorporating Multicenter-Labeled Deep Learning and Biparametric Imaging: Proof of Concept. Diagnostics (Basel). 2020; 10: 951.

XIV. Kaneko M, Fukuda N, Nagano H, et al. Artificial intelligence trained with integration of multiparametric MR-US imaging data and fusion biopsy trajectory-proven pathology data for 3D prediction of prostate cancer: A proof-of-concept study. Prostate. 2022; 82: 793-803.

XV. Jimenez-Pastor A, Lopez-Gonzalez R, Fos-Guarinos B, et al. Automated prostate multi-regional segmentation in magnetic resonance using fully convolutional neural networks. Eur Radiol. 2023; 33: 5087-5096.

XVI. Guo H, Kruger M, Xu S, Wood BJ, Yan P. Deep adaptive registration of multi-modal prostate images. Comput Med Imaging Graph. 2020; 84: 101769.

XVII. Zhang KS, Schelb P, Netzer N, et al. Pseudoprospective Paraclinical Interaction of Radiology Residents With a Deep Learning System for Prostate Cancer Detection: Experience, Performance, and Identification of the Need for Intermittent Recalibration. Invest Radiol. 2022; 57: 601-612.

XVIII. Labus S, Altmann MM, Huisman H, et al. A concurrent, deep learning-based computer-aided detection system for prostate multiparametric MRI: a performance study involving experienced and less-experienced radiologists. Eur Radiol. 2023; 33: 64-76.

XIX. Zheng H, Hung ALY, Miao Q, et al. AtPCa-Net: anatomical-aware prostate cancer detection network on multi-parametric MRI. Sci Rep. 2024; 14: 5740.

XX. Al-Bourini O, Seif Amir Hosseini A, Giganti F, et al. T1 Mapping of the Prostate Using Single-Shot T1FLASH: A Clinical Feasibility Study to Optimize Prostate Cancer Assessment. Invest Radiol. 2023; 58: 380-387.

XXI. Khan Z, Yahya N, Alsaih K, Al-Hiyali MI, Meriaudeau F, Recent Automatic Segmentation Algorithms of MRI Prostate Regions: A Review. IEEE Access. 2021; 9: 97878-97905.

XXII. Saunders SL, Leng E, Spilseth B, Wasserman N, Metzger GJ, Bolan PJ, Training Convolutional Networks for Prostate Segmentation With Limited Data. IEEE Access. 2021; 9: 109214-109223.

XXIII. Alzate-Grisales JA, Mora-Rubio A, García-García F, Tabares-Soto R, De La Iglesia-Vayá M, SAM-UNETR: Clinically Significant Prostate Cancer Segmentation Using Transfer Learning From Large Model. IEEE Access. 2023; 11: 118217-118228.

XXIV. Akhoondi PE, Baghshah MS. Semantic Segmentation With Multiple Contradictory Annotations Using a Dynamic Score Function. IEEE Access. 2023; 11: 64544-64558.

XXV. Elmahdy MS, Beljaards L, Yousefi S, et al. Joint Registration and Segmentation via Multi-Task Learning for Adaptive Radiotherapy of Prostate Cancer. IEEE Access. 2021; 9, 95551-95568.

XXVI. Lee J, Nishikawa RM. Cross-Organ, Cross-Modality Transfer Learning: Feasibility Study for Segmentation and Classification. IEEE Access. 2020; 8: 210194-210205.

XXVII. Huang H, Zhang b, Zhang X, et al. Application of U-Net Based Multiparameter Magnetic Resonance Image Fusion in the Diagnosis of Prostate Cancer. IEEE Access. 2021; 9: 33756-33768.

XXVIII Ren C, Guo Z, Ren H, Jeong D, Kim DK, Zhang S. Prostate Segmentation in MRI Using Transformer Encoder and Decoder Framework. IEEE Access. 2023; 11: 101630-101643.

XXIX. Shao L, Liu Z, Yan Y, et al. Patient-Level Prediction of Multi-Classification Task at Prostate MRI Based on End-to-End Framework Learning From Diagnostic Logic of Radiologists. IEEE Trans Biomed Eng. 2021; 68: 3690-3700.

References

1. WHO. www.gco.iarc.fr. 2022 [cited 2024 02 08. Available at: https://gco.iarc.fr/today/en/dataviz/pie?mode=cancer&group_populations=1&sexes=1&group_cancers=1&multiple_cancers=1.

2. Wojciechowska U, Barańska K, Miklewska M, Didkowska J. Cancer incidence and mortality in Poland in 2020. Nowotwory. Journal of Oncology. 2023; 73: 129-145.

3. Kaluarachchi T, Reis A, Nanayakkara S. A Review of Recent Deep Learning Approaches in Human-Centered. Sensors. 2021; 21: 2514.

4. Kufel J, Bargieł-Łączek K, Kocot S, Koźlik M, Bartnikowska W, Janik M, et al. What Is Machine Learning, Artificial Neural Networks and Deep Learning? – Examples of Practical Applications in Medicine. Diagnostics (Basel). 2023; 13: 2582.

5. Schouten M, van der Leest M, Pokorny M, et al. Why and Where do We Miss Significant Prostate Cancer with Multi-parametric Magnetic Resonance Imaging followed by Magnetic Resonance-guided and Transrectal Ultrasound-guided Biopsy in Biopsy-naïve Men? Eur Urol. 2017; 71: 896-903.

6. Bjurlin M, Mendhiratta N, Wysock J, Taneja S. Multiparametric MRI and targeted prostate biopsy: Improvements in cancer detection, localization, and risk assessment. Cent European J Urol. 2016; 69: 9-18.

7. Schoots IG, Roobol MJ, Nieboer D, Bangma C, Steyerberg E, Hunink M.

Magnetic resonance imaging-targeted biopsy may enhance the diagnostic accuracy of significant prostate cancer detection compared to standard transrectal ultrasound-guided biopsy: a systematic review and meta-analysis. Eur Urol. 2015; 68: 438-450.

8. Brock M, Bodman Cv, Palisaar J, Becker W, Martin-Seidel P, Noldus J. Detecting Prostate Cancer. Dtsch Arztebl Int. 2015; 112: 605-611.

9. Siddiqui M, Rais-Bahrami S, Turkbey B, et al. Comparison of MR/ultrasound fusion-guided biopsy with ultrasound-guided biopsy for the diagnosis of prostate cancer. JAMA. 2015; 313: 390-397.

10. Drost F, Osses D, Nieboer D, et al. Prostate MRI, with or without MRI-targeted biopsy, and systematic biopsy for detecting prostate cancer. Cochrane Database Syst Rev. 2019; 4: CD012663.

11. Exterkate L, Wegelin O, Barentsz JO, et al. Is There Still a Need for Repeated Systematic Biopsies in Patients with Previous Negative Biopsies in the Era of Magnetic Resonance Imaging-targeted Biopsies of the Prostate? Eur Urol Oncol. 2020; 3: 216-223.

12. Rouvière O, Puech P, Renard-Penna R, et al. se of prostate systematic and targeted biopsy on the basis of multiparametric MRI in biopsy-naive patients (MRI-FIRST): a prospective, multicentre, paired diagnostic study. Lancet Oncol. 2019; 20: 100-109.

13. Verma S, Turkbey B, Muradyan N, et al. Overview of dynamic contrast-enhanced MRI in prostate cancer diagnosis and management. AJR Am J Roentgenol. 2012; 198: 1277-1288.

14. Barentsz J, Richenberg J, Clements R, et al. European Society of Urogenital Radiology. ESUR prostate MR guidelines 2012. Eur Radiol. 2012; 22: 746-757.

15. Cornford P, Tilki D, Briers E, et al. EAU Guidelines on Prostate Cancer. In Edn. presented at the EAU Annual Congress; Paris 2024.

16. Woo S, Suh C, Kim S, Cho J, Kim S. Diagnostic Performance of Prostate Imaging Reporting and Data System Version 2 for Detection of Prostate Cancer: A Systematic Review and Diagnostic Meta-analysis. Eur Urol. 2017; 72: 177-188.

17. Padhani A, Barentsz J, Villeirs G, Rosenkrantz A, Margolis D, Turkbey B, et al. PI-RADS Steering Committee: The PI-RADS Multiparametric MRI and MRI-directed Biopsy Pathway. Radiology. 2019; 292: 464-474.

18. Prince M, Foster B, Kaempf A, et al. n-Bore Versus Fusion MRI-Targeted Biopsy of PI-RADS Category 4 and 5 Lesions: A Retrospective Comparative Analysis Using Propensity Score Weighting. AJR Am J Roentgenol. 2021; 217: 1123-1130.

19. Kongnyuy M, George A, Rastinehad A, Pinto P. Magnetic Resonance Imaging-Ultrasound Fusion-Guided Prostate Biopsy: Review of Technology, Techniques, and Outcomes. Curr Urol Rep. 2016; 17: 32.

20. Jeffrey C. Explainer: What is Machine Learning? TechSpot. 2020. Available at: https://www.techspot.com/article/2048-machine-learning-explained/ (accessed on 3 May 2023).

21. Alzubaidi L, Zhang J, Humaidi A, et al. Review of deep learning: concepts, CNN architectures, challenges, applications, future directions. J Big Data. 2021; 8: 53.

22. Hubel D, Wiesel T. Receptive fields of single neurones in the cat's striate cortex. J Physiol. 1959; 148: 574-591.

23. Sarvamangala D, Kulkarni R. Convolutional neural networks in medical image understanding: a survey. Evol Intell. 2022; 15: 1-22.

24. Backer D. UROwebinar: Artificial intelligence and the current applications in the field of urology 2023. Available at: https://youtu.be/0-0yD_L2j_Y?t=90.

25. Ronneberger O, Fischer P, Brox T. U-Net: Convolutional Networks for Biomedical Image Segmentation. In Medical Image Computing and Computer-Assisted Intervention – MICCAI 2015; Springer, Cham, Munich 2015.

26. Shorten C, Khoshgoftaar TM. A survey on Image Data Augmentation for Deep Learning. J Big Data. 2019; 6: 60.

27. Wang F, Wang H, Wang H, Li G, Situ G. Learning from simulation: An end-to-end deep-learning approach for computational ghost imaging. Opt Express. 2019; 27: 25560-25572.

28. Yosinski J, Clune J, Bengio Y, Lipson H. How transferable are features in deep neural networks? Advances in Neural Information Processing Systems. 2014; 27: 3320-3328.

29. Padgett K, Swallen A, Pirozzi S, et al. Towards a universal MRI atlas of the prostate and prostate zones: Comparison of MRI vendor and image acquisition parameters. Strahlenther Onkol. 2019; 195: 121-130.

30. Bardis M, Houshyar R, Chantaduly C, et al. Segmentation of the Prostate Transition Zone and Peripheral Zone on MR Images with Deep Learning. Radiol Imaging Cancer. 2021; 3: e200024.

31. Soerensen S, Fan R, Seetharaman A, et al. Deep Learning Improves Speed and Accuracy of Prostate Gland Segmentations on Magnetic Resonance Imaging for Targeted Biopsy. J Urol. 2021; 206: 604-612.

32. Ushinsky A, Bardis M, Glavis-Bloom J, et al. A 3D-2D Hybrid U-Net Convolutional Neural Network Approach to Prostate Organ Segmentation of Multiparametric MRI. AJR Am J Roentgenol. 2021; 216: 111-116.

33. Palladino L, Maris B, Antonelli A, Fiorini P. PROST-Net: A Deep Learning Approach to Support Real-Time Fusion in Prostate Biopsy. IEEE Transactions on Medical Robotics and Bionics. 2022; 4: 323-326.

34. Hassanzadeh T, Hamey LGC, Ho-Shon K. Convolutional Neural Networks for Prostate Magnetic Resonance Image Segmentation. IEEE Access. 2019; 7: 36748-36760.

35. Ren C, Ren H. Prostate Segmentation on Magnetic Resonance Imaging. IEEE Access. 2023; 11: 145944-145953.

36. Huang X, Pang B, Zhang T, Jia G, Wang Y, Li Y. Improved Prostate Biparameter Magnetic Resonance Image Segmentation Based on Def-UNet. IEEE Access. 2023; 11: 43089-43100.

37. Qian Y. ProSegNet: A New Network of Prostate Segmentation Based on MR Images. IEEE Access. 2021; 9: 106293-106302.

38. Su C, Huang R, Liu C, Yin T, Du B. Prostate MR Image Segmentation With Self-Attention Adversarial Training Based on Wasserstein Distance. IEEE Access. 2019; 7: 184276-184284.

39. Qian Y, Zhang Z, Wang B. ProCDet: A New Method for Prostate Cancer Detection Based on MR Images. IEEE Access. 2021; 9: 143495-143505.

40. Liu Y, Yang G, Mirak SA, Hosseiny M, Azadikhah A, Zhong X. Automatic Prostate Zonal Segmentation Using Fully Convolutional Network With Feature Pyramid Attention. IEEE Access. 2019; 7: 163626-163632.

41. Comelli A, Dahiya N, Stefano A, et al. Deep Learning-Based Methods for Prostate Segmentation in Magnetic Resonance Imaging. Appl Sci (Basel). 2021; 11: 782.

42. Litjens G, Toth R, van de Ven W, Hoeks C, et al. Evaluation of prostate segmentation algorithms for MRI: the PROMISE12 challenge. Med Image Anal. 2014; 18: 359-373.

43. Warfield S, Zou K, Wells W. Simultaneous truth and performance level estimation (STAPLE): an algorithm for the validation of image segmentation. IEEE Trans Med Imaging. 2004; 23: 903-921.

44. Ghavami N, Hu Y, Gibson E, et al. Automatic segmentation of prostate MRI using convolutional neural networks: Investigating the impact of network architecture on the accuracy of volume measurement and MRI-ultrasound registration. Med Image Anal. 2019; 58: 101558.

45. Maris B. Advancing robotic prostate biopsy through artificial intelligence. Med Robot. 2024; 2: 1-7.

46. Ruben DM, Grace JG, Xin L, Wang G. Comparison of deep learning and human observer performance for detection and characterization of simulated lesions. J Med Imag. 2019; 6: 025503.

47. Saha A, Bosma J, Twilt J, et al. PI-CAI consortium. Artificial intelligence and radiologists in prostate cancer detection on MRI (PI-CAI): an international, paired, non-inferiority, confirmatory study. Lancet Oncol. 2024; 25: 879-887.

48. Tătaru OS, Vartolomei MD, Rassweiler JJ, et al. Artificial Intelligence and Machine Learning in Prostate Cancer Patient Management – Current Trends and Future Perspectives. Diagnostics. 2021; 11: 354.

Central European Journal of Urology

REVIEW PAPER

UROLOGICAL ONCOLOGY

Cancer stem cells and their role in metastasis

Michał C. Czarnogórski[1], Aleksandra Czernicka[1], Krzysztof Koper[2], Piotr Petrasz[3], Marta Pokrywczyńska[4], Kajetan Juszczak[1], Filip Kowalski[1], Tomasz Drewa[1], Jan Adamowicz[1]

[1]*Department and Chair of Urology and Andrology, Ludwik Rydygier's Collegium Medicum in Bydgoszcz, Nicolaus Copernicus University in Torun, Poland*
[2]*Department of Oncology, Ludwik Rydygier's Collegium Medicum in Bydgoszcz, Nicolaus Copernicus University in Torun, Poland*
[3]*Department of Urology and Urological Oncology, Multidisciplinary Regional Hospital in Gorzow Wielkopolski, Poland*
[4]*Department of Regenerative Medicine, Chair of Urology, Ludwik Rydygier's Collegium Medicum in Bydgoszcz, Nicolaus Copernicus University in Torun, Poland*

Citation: Czarnogórski MC, Czernicka A, Koper K, et al. Cancer stem cells and their role in metastasis. Cent European J Urol. 2025; 78: 40-51.

Article history
Submitted: Jul. 23, 2024
Accepted: Oct. 30, 2024
Published online: Nov. 28, 2024

Corresponding author
Michał C. Czarnogórski
Department and Chair of Urology and Andrology, 9 Skłodowskiej-Curie St. 85-094 Bydgoszcz, Poland
mcczarnogorski@gumed.edu.pl

Introduction Cancer, next to cardiovascular diseases, remains the primary concern of modern medicine in developed countries. Despite the unprecedented progress in targeted therapies and personalised medicine, including immunotherapy and gene therapy, we are still unable to efficiently treat many malignancies. One of the major obstacles to treating cancer is its ability to metastasise. Hence, a better understanding of cancer biology with emphasis on the metastasis formation may hold the key to further ameliorating cancer treatment. Nowadays, there is a growing body of evidence for the common denominator of neoplasia, which seems to be universal – cancer stem cells which are being found in a growing number of cancers.

Material and methods We conducted a Web of Science and Medline database search using the terms "cancer stem cells", "carcinogenesis", and "stem cells" in conjunction with "metastasis", without setting time limits.

Results The existence of cancer stem cells was proven both in animal models and in humans. We know beyond doubt that cancer stem cells may be found in bladder cancer, breast cancer, and colon cancer, among others. The cancer stem cells in the aforementioned cancers may initiate tumour formation *ex vivo* and thus theoretically lead to tumour recurrence. Their role in the formation of metastases, however, is still under investigation.

Conclusions Although their exact role is yet to be identified, it is now obvious that cancer stem cells give rise to primary mass in solid tumours and differentiated cancer cells in leukaemias. However, the role of cancer stem cells in metastasis is still obscure.

Key Words: cancer stem cells ‹› carcinogenesis ‹› bladder cancer ‹› metastasis

INTRODUCTION

In the modern world the widespread of cancer remains a major health issue in industrialised and developing countries. In 2023, in the United States alone, over 600,000 cancer-related deaths are projected to occur [1]. Ongoing studies in the field of cancer biology are conducted to ameliorate our understanding of oncogenesis and develop novel therapeutic options for cancer patients. Over the last few decades, we achieved immense progress in the field of cancer biology thanks to discovering novel cellular biomarkers that allow precise characterisation of specific cancer cell subpopulations, which further allows the development of advanced therapeutic options, specifically targeting those cells [2]. The aforementioned advances in the molecular biology and discoveries of cellular biomarkers or clusters of differentiation, on the cellular surface as well as intracellularly, have led to the observation that the tumour mass contains a variety of cellular subpopulations including cells with stem cell-like phenotype and properties [3]. Those cells have been named cancer stem cells (CSCs) or tumour-initiating cells (TICs) and presently are thought to play a pivotal role in the cancer growth, spread, and relapse [4].

Surprisingly, the first notion of the existence of the cells that originate the tumour development comes from the mid 19th century and Julius Cohnheim's concept of "embryonic rests", i.e. embryonic cells that were not utilised during ontogenesis, as an origin of all tumours [5]. Many decades later, further research on germinal tumours has led to the discovery of embryonic stem (ES) cells in mice [6] by Stevens and Little, and as a consequence to the development of cancer stem cells theory by Kleinsmith and Pierce in 1964 [7], based on the observation that ES cells produce various differentiated tissues as well as embryonal carcinoma when transplanted in mice. That concept was confirmed by Bonnet and Dick in 1997, who observed that only a small population of acute myeloid leukaemia cells is able to initiate the acute myeloid leukemia and has vast self-renewal capacity [8]. Further studies have shown that CSCs are also encountered in solid tumours – colon and breast cancers among others [9]. The progeny of CSCs transplanted into a new host consist of cells with stem-like properties and differentiated cells without tumourigenic potential. This observation is of utmost importance because it signifies that tumours, much like healthy tissues, are hierarchically organised and there is a fraction of cells that is responsible for tumour initiation, formation, and growth – namely CSCs.

A malignant tumour's cellular architecture is highly heterogeneous. Among the tumour cells, there is a subgroup with the ability to self-renew despite cytotoxic treatment [10]. Those cells are called cancer stem cells (CSC), a subpopulation of tumour cells characterised by low, although sustained potential for unlimited proliferation [11]. In addition to the ability to divide and increase the pool of their stem cells, CSCs are able to differentiate into non-tumourigenic cancer target types, which most likely constitute the majority of cells in the tumour mass [12]. It appears that the presence of just one CSC is sufficient to stimulate tumour growth. CSCs prefer hypoxic niches with low pH and limited availability of nutrients, making them highly resistant to challenging environmental conditions [13].

However, they are not autonomous entities but rather components of a larger ecosystem, actively influencing the tumour's microenvironment by restructuring it and receiving information from the niches they inhabit [14]. The existence of CSCs should be understood not through the prism of the hierarchy of development of normal tissues in a binary approach based on stem and non-stem elements, but based on the stem theory, understood as a series of interactions with the microenvironment, cancer cells, and other types of cells [15].

Considering the origin of CSCs, 3 crucial and well-established processes should be taken into account: spontaneous reprogramming of somatic cells, epigenetic and genetic changes such as methylation, rearrangement, demethylation in the pool of stem, progenitor and differentiated cells, and activation of the tumour microenvironment (TME) [16].

CSCs are in general characterised by 4 features: hierarchical cell organisation, hierarchy arising from the presence of self-renewing cells and those exhibiting transient proliferation, the consistent identity of CSC within the tumour structure, and the resistance of CSC to classical chemotherapy and radiotherapy [17].

RESULTS

Signal transduction pathways involved in cancer stem cell regulation

In order for CSCs to multiply and self-renew, they exploit dysfunction in stemness signalling pathways [18]. The signalling pathways that determine the specific features of CSCs mainly include the following: JAK/STAT, Wnt/β-catenin, PI3K/Akt, PTEN36, hedgehog, Notch, NF-κB, and Bcl-2 [19].

The JAK/STAT is an intracellular signalling pathway involved in cellular proliferation, differentiation, and the signal transduction [20]. This signalling pathway also mediates the process of haematopoiesis, maintaining proper immune function, tissue repair, and apoptosis [21].

In breast cancer, it was noted that constant activation of STAT3 enables CSC survival and maintenance of stemness, and interleukin-6 (IL-6) enables the transition of non-stem cancer cells into the cancer pathway, which was discovered as one of the mechanisms behind the self-renewal of glioma stem-like cells [22].

Wnt signalling pathway is involved in the processes of cell differentiation, survival, proliferation, and apoptosis [23]. The Wnt pathway consists of 3 subpathways: the non-canonical planar cell polarity (PCP) pathway, non-canonical Wnt/calcium pathway, and canonical pathway [24].

Both canonical and non-canonical pathways have a significant effect on CSCs. The canonical pathway affects the proliferation of those cells, while the non-canonical pathways enable the induction of CSC's dormancy. The Wnt/β-catenin pathway stimulates the reactivation of dormant CSCs, which promotes tumour recurrence [25].

The Notch signalling pathway performs a crucial function in the process of organ formation and tissue repair, and its disturbances broadly contribute to the development of cancer. This pathway interacts

with 4 NOTCH receptors [26]. The family of those receptors mediates the transmission of information in the cell over a short distance, and acts as a transcription factor activated by a family of ligands: Delta, Lag-2, and Serrate [27].
Increased activity of the Notch pathway is observed in CSCs, and some even claim that this signalling allows the tumour to achieve its native cancer phenotype. Consequently, this pathway causes these cells to show a lower level of proliferation, which allows them to survive in a dormant state and trigger tumour recurrence. This translates into resistance to anticancer therapy [28].
The Hedgehog pathway is a ligand-dependent signalling pathway in which the ligand can be Desert hedgehog, Sonic hedgehog, and Indian hedgehog. It plays an important role in the process of cell differentiation, proliferation, tissue polarity, cell survival, and stem cell formation [29].
There are indications that this pathway regulates CSCs in pancreatic adenocarcinoma, glioblastoma multiforme, and chronic myeloid leukaemia (CML) [30].
The significant impact of the Hedgehog pathway on CSCs has been demonstrated in a study of plasmocytic myeloma (PCM), which consists of a population of stem cells resembling memory B cells and a population of malignantly differentiated plasma cells, which constitute the majority. It turned out that maintaining the signalling of this pathway keeps PCM stem cells in an undifferentiated state, capable of proliferation [31].
Specific markers are probably expressed on the surface of CSCs. Those include the following: CD44, CD24, CD29, CD90, CD133, epithelial-specific antigen (ESA), and aldehyde dehydrogenase-1 (ALDH1) [32].
Other key markers of CSCs are transcription factors like OCT-4 and SOX-2, and drug-efflux pumps like ATP-binding cassette (ABC) drug transporters [33].
Of those, the surface marker CD133 has been observed in the CSC population in variety of neoplasms, among others: breast cancer, brain tumours, lung cancer, pancreatic cancer, prostate cancer, and ovarian cancer [34].
Interestingly, CSCs undergo both the epithelial-to-mesenchymal transition (EMT) and the mesenchymal-to-epithelial transition (MET), both of which promote tumour progression and metastasis [35].
Our review aims to determine the CSC's supposed role in tumour metastasis.

Stem cells and cancer stem cells – similarities and differences

Generating mutations in cellular DNA using carcinogens, i.e. causative agents, contributes to the development of cancer. These substances can include ionising radiation and various types of chemicals such as components of cigarette smoke, alcohol, formaldehyde, oncogenic viruses, and many others [36].
It has been estimated that the number of single-strand breaks and spontaneous base loss in nuclear DNA is approximately 10,000 changes per cell per day [37]. However, overcoming the carcinogenesis barrier, countered by the DNA repair process and apoptosis, requires a cell to accumulate between 3 and 7 mutations [38]. Somatic mutations can undergo clonal amplification, the number of which increases with age in human tissues [39]. Damaged tissues can be repaired through the impact of stem cells, which possess the ability to self-renew and divide throughout their lifespan [40]. The accumulation of genetic disorders at the level of epigenetic regulators may cause the transformation of normal stem-cells into CSCs, which is crucial in carcinogenesis [41].
Stem cells remain undifferentiated both in embryonic and adult stem cells. During the stem cell differentiation process, the stem cell program is silenced, but in the process of developing cancer, epigenetic reactivation of the stem cells leads to tumour multiplication and progression [42]. It may result in the transformation of a normal stem cell (NSC) into a CSC. Therefore, normal haematopoietic stem cells and cancer stem cells should present with similar features [43]. Firstly, both stem cells and CSCs are capable of self-renewal and division [44]. However, the potential for self-renewal is internally limited and reaches the division limit depending on the activity of p53 [45].
CSCs, on the other hand, can unlimited self-renewal and unlimited division, without the risk of differentiation, aging or cellular death [46]. Some differences and similarities also occur in the type of cell division. Stem cells usually divide asymmetrically. As a result of this division, a SC gives rise to another stem cell and a progenitor cell [45].
CSCs divide mainly by symmetric divisions, although it is worth noting that both CSCs and SCs have the capacity for both types of divisions. However, the symmetric division favoured by CSCs promotes tumour growth and is accompanied by a loss of the protective effect of p53 [47].
Another common feature is that they have common surface markers. CD34 is present both on the surface of haematopoietic stem/progenitor cells (HSPCs) and, judging by numerous reports, on the surface of CSCs [48]. An important common feature of both normal stem cells and CSCs is that both types of cells inhabit niches, i.e. specialised microenvironments, which consist of fibroblasts, immune cells,

endothelial cells, perivascular cells, extracellular matrix (ECM) components, cytokines, and growth factors [49].

Therefore, there are reasons to believe that cells in the niche, activated by the tumour, support not only normal stem cells but also CSCs in the development of its characteristic features [50].

It is worth mentioning that mesenchymal stem cells (MSCs) interact with both adult stem cells and CSCs in the microenvironments of both those cell types and mobilise them to secrete cytokines such as IL-10 and TGF-β. These actions are aimed at stimulating CD4+ T-cells to their anti-inflammatory phenotype [51].

Both stem cells and CSCs are characterised by a similar transcriptional profile. Even signalling pathways such as Wnt and Notch are active among both stem cells and CSCs, which increases their ability to progress [52].

Thirdly, normal cells capable of proliferation such as immune cells and stem cells can reprogram their metabolism similarly to cancer cells [53]. Cancer cells show a preference for a metabolism focused on glycolysis in terms of obtaining energy, even in the presence of oxygen [54].

Although this process is less efficient than oxidative phosphorylation in the context of obtaining ATP molecules, cancer cells compensate for this by increasing the rate of glycolysis and thus increasing the rate of obtaining ATP [55]. In addition to ATP, cancer cells require intermediate products and precursors that are important for the biosynthesis of macromolecules necessary to increase tumour mass, with reduced demand for nutrients [56].

A similar metabolic plasticity is demonstrated by haematopoietic stem progenitor cells (HSPCs), which are able to obtain ATP through mitochondrial respiration and glycolysis. Due to their small mitochondrial mass, their metabolism is maintained mainly by glycolysis [57].

Metastatic niche and the role of cancer stem cells in metastasis formation

Cancer cells may spread to distant organs from the primary tumour, leading to cancer dissemination, and consequently to the patient's death. This phenomenon is called metastasis [58]. Metastasis is associated with detachment of the cells from the primary tumour mass. This is followed by local infiltration and angiogenesis. In the next stage, cancer cells move to blood and lymphatic vessels, and from there they begin to invade distant organs [59].

At each stage, the process of cancer metastasis and progression is supported by suppressing the host's immune system. This is possible by stimulating immunosuppressive cells and inhibiting immune effector cells [60].

There are several hypotheses regarding the metastasis process, including: EMT, altered integrin expression, a macrophage facilitation process, and a macrophage origin involving either transformation or fusion hybridisation with neoplastic cells and microRNAs (miRNAs) [61–63]. There are also mutations in genes encoding proteins that determine the invasive potential of the tumour, such as mutation of p53 (TP53), cyclin-dependent kinase inhibitor 2A (CDKN2A), phosphatase and tensin homologue (PTEN), and phosphatidylinositol-4,5-bisphosphate 3-kinase catalytic subunit α (PIK3CA) [64].

Among many models of metastasis, there is also one based on the premise that the metastasis process can be initiated by CSCs [65]. CSCs show increased EMT activity. EMT also contributes to the development of a CSC-like phenotype in cells other than CSCs [66]. EMT also contributes to the loss of epithelial adhesion receptors, such as E-cadherin, occludin, α-catenin, and claudin, and consequently the loss of cell polarity. The consequence of this process is an increase in the invasiveness of cancer cells [67]. Through numerous transcription factors, EMT also influences the maintenance of the proper structure of the cytoskeleton and extracellular matrix degradation [68]. The intensified process of destruction of the normal matrix favours its replacement by the cancer matrix. Additionally, this process may lead to the destruction of the basement membrane, which further enhances the metastatic process [69].

When analysing the metastasis formation process, it is worth taking a closer look at microRNA It is a short sequence RNA, the main purpose of which is post-transcriptional silencing of selected genes [70]. miRNA is involved in cancer progression and metastasis, and it enables contact between cancer cells and the TME [71].

According to the latest research, miRNAs can influence CSC properties such as tumourigenesis, self-renewal, and resistance to cytotoxic treatment, thereby enhancing cancer progression [72]. Increased resistance to chemotherapy and radiotherapy in CSCs is also explained by increased expression of anti-apoptotic proteins and increased levels of ATP-binding cassette transporters [73]. It is currently believed that ATP-binding cassette transporters may be involved at every stage of tumourigenesis, including metastasis [74].

As seen above, the metastasis process is a complex process that consists of many factors and mechanisms. However, the metastasis formation is not only limited to changes that occur in tumour cells, but

it additionally requires interaction with stromal cells at both the local and systemic levels [75]. It is therefore worth looking at the TME, which plays a decisive role in cancer progression. The relationship between cancer cells and the TME is inseparable. This is primarily observed in the context of reprogramming of the TME by tumour-derived factors by which the microenvironment enables its survival [76].

There are reasons to believe that the environment has a special impact on cancer cells, thanks to which they acquire the features of "stemness" [77]. It is even believed that the tumour microenvironment induces a change in the phenotype from differentiated cancer cells to CSCs, and this plasticity particularly influences resistance to therapy [78].

It is well known that CSCs live in a special microenvironment, which can be called the "stem-cell niche", and their survival is conditioned by various factors from the niche, which act directly or in a paracrine manner [79]. The entire tumour microenvironment consists of fibroblasts, endothelial cells, immune cells, and extracellular factors such as hormones, growth factors, cytokines, extracellular matrix, etc. The role of the TME is particularly important in the process of metastasising, and it influences the resistance to anti-cancer therapy [80]. Cancer cells activate stromal cells in the microenvironment, i.e. fibroblasts, smooth cells, adipocytes, mesenchymal, progenitor, and inflammatory cells. They, in turn, stimulate the secretion of growth factors and proteases, creating something like a chain reaction in the carcinogenesis process [81].

Fibroblasts are the key component of the TME. Cancer-associated fibroblasts (CAFs) belong to the stromal cells. They secrete the extracellular matrix components, creating a dense tumour network, and contribute largely to tumour progression [82]. Cancer cells can move along collagen fibres and spread further. Additionally, CAFs and cancer cells support the release of matrix metalloproteinases (MMPs), which degrade of the basement membrane, supporting cancer spread [83]. According to some studies, especially concerning breast cancer and hepatocellular cancer, it was observed that CAFs can produce mechanisms of resistance to chemotherapy and induction of CSCs [84]. This most likely occurs through the interaction of hepatocyte growth factor (HGF), IL-6, TGF-β, chemokines, and factors activating Wnt signalling provided by CAFs [85].

One of those factors is periostin, which is secreted, among others, by CAFs. It can activate the PI3K/Akt and/or Wnt/β-catenin oncogenic pathways. Therefore, because those pathways are pathologically dysregulated in CSCs, it may be speculated that periostin, and thus CAFs, enhance the activation of CSCs [86]. The tumour microenvironment is, as we know, a place rich in factors promoting tumour proliferation and metastasis. Uncontrolled growth is a natural consequence of tumorigenesis, but it is also associated with an increased demand for oxygen and generates problems in its supply. It therefore appears to be a natural phenomenon that the tumour environment is in a state of chronic hypoxia [87]. To counteract hypoxia and acidification, TME stimulates angiogenesis, a process that allows the tumour to create vessels supplying the tumour with oxygen and nutrients, while removing unnecessary and harmful metabolic products [88].

Because this phenomenon is crucial in tumour progression, it has become the subject of many studies. It was hypothesised that even if angiogenesis inhibitors were used and oxygen-poor conditions were created, the tumour mass would continue to grow due to CSCs and the associated activation of the Akt/β catenin pathway. Later studies drew attention to the fact that cancer stem cells produce vascular endothelial growth factor (VEGF) at much higher levels under various environmental conditions compared to SCs [89]. It promotes angiogenesis and has mitogenic and anti-apoptotic effects. Additionally, it increases vascular permeability and promotes cell migration [90].

However, the functions of VEGF go beyond the ability to perform angiogenesis. It exhibits paracrine and autocrine signalling because it can modulate the host response to cancer by influencing immune cells in the microenvironment, and VEGF receptors modulate the function of fibroblasts in the tumour stroma. This is believed to be one of the mechanisms for maintaining the capacity of CSCs [91]. There is a correlation between the number of CSCs in tumour tissue and the number of immune cells that infiltrate the tumour. It is suspected that CSCs impair the process of antigen presentation to T lymphocytes using MHC-I. This leads to the development of resistance to the cytotoxic effects of CD8+ T lymphocytes [92].

Dendritic cells (DCs) are the main elements of the adaptive immune response and have the ability to activate T lymphocytes, which is a defence mechanism against cancer. Of course, cancer can affect DC functions by preventing their maturation or through molecules originating from the microenvironment, inhibiting their activation [93].

Moreover, cancer-altered DCs may even promote tumourigenesis. Recent studies based on renal cancer draw attention to the role of CSCs in this process. Renal cancer cells that expressed the surface marker CD105 blocked the maturation of monocyte-derived DCs *in vitro* at a higher rate than tumour cells

negative for this marker. This is important because CD105 is also a surrogate marker for CSCs [94].
We can also distinguish tumour-associated macrophages (TAMs) among the immune cells in the TME. They can enhance immunosuppression, the process of vascular formation, and the proliferation of cancer cells, and thus may increase the tumour mass and the probability of metastasising [95]. TAMs have protective functions towards CSCs against chemotherapy, thus driving therapy resistance. Additionally, TAMs increase the ability of CSCs to initiate tumourigenesis [96].
The state of the CSC is regulated by many different signals from the niche. One of them is transforming growth factor β (TGF-β), a cytokine that gives CSCs drug resistance [97]. TGF-β determines the low immunogenicity of CSCs compared to non-CSCs. The same effect is exerted by the other cytokines like IL-4 and IL-10, which also have immunosuppressive effects, and high expression of which is observed in CSCs [98]. One of its many functions is to stimulate the production of T-reg cells, the function of which is to suppress the immune response against the tumour [99].

Bladder cancer

In 2018, bladder cancer was the 10th most common cancer in the world, with a predominance among men. In this sex, bladder cancer was the sixth most common cancer [100]. In the case of non-muscle invasive bladder cancer (NMIBC), the first-line treatment is bladder-sparing therapy. If the muscle layer becomes infiltrated, as in the case of muscle-invasive bladder cancer (MIBC), cystectomy is performed along with lymph node dissection (LND). The inclusion of neoadjuvant chemotherapy further improves the prognosis. Although the combination of these 2 methods is a standard approach in the case of MIBC, it remains controversial [101].
If metastases occur, cytotoxic chemotherapy based on cisplatin is initiated. Despite that, some patients experience relapses and develop resistance to therapy. The utilisation of chemotherapy itself is associated with many side effects, most importantly with renal toxicity [102].
Therefore, it seems extremely important to search for novel, targeted methods of treatment of bladder cancer, based on better understanding its biology. It is crucial to look at its development and progression, including metastatic pathways.
The presence of CSCs was also discovered in bladder cancer, where they showed typical CSC surface markers such as CD44, CD133, ALDH1, SOX2, and SOX4, and a set of characteristic features such as self-renewal or the ability to initiate cancer, and an increased expression of genes involved in EMT [103].
In superficial papillary carcinomas, the origin is sought among intermediate cells. But even their morphological structure resembles a normal epithelium with a basal layer. This involves questioning the theory that the intermediate cell is a universal cell in the context of cancer formation. Believing in the existence of a universal cell and trying to explain the existence of a basal-like target in NMIBC, it should be noted that in the basal layer of papillary carcinoma regeneration occurs through a process of dedifferentiation, and the microenvironment most likely contributes to this process [104].

Colon cancer

In the United States, colorectal cancer is the third most frequently diagnosed cancer and the third leading cause of cancer death among men and women [105]. It is expected that by 2035 in the world there will be up to 2.5 million new cases of this type of cancer, which makes it a significant global problem that should be a focus of attention of researchers in the context of searching for new therapeutic methods [106]. Therefore, it seems important to understand the structure of cancer and the mechanisms that contribute to its development.
It is highly probable that CSCs are present in colorectal cancer, and further, they have been identified as one of the causative factors capable of developing the tumour [107]. It is even believed that CSCs are mainly responsible for cancer progression, including the ability to metastasise and their resistance to therapy [108].
Under normal conditions, stem cells present at the bottom of the colon crypts divide and give rise to daughter cells. These cells migrate upwards, differentiate, and replace old epithelial layer cells. Sometimes, however, this process may be disturbed. It is suspected that CSCs are formed under the influence of the microenvironment, leading to abnormal divisions and thus tumourigenesis [109].
When considering CSCs and their role in the development of colorectal cancer, it is worth taking a closer look at leucine-rich-repeat-containing G-protein-coupled receptor 5 (Lgr5), which is a protein that is expressed in columnar cells in intestinal crypts. Crypt base columnar cells with positive Lgr5 show features of stem cells, and they were identified as a potential stem marker in cancer [110]. Moreover, in the progression of colorectal cancer and its metastases, a hierarchical structure characteristic of CSCs was noticed, while functional CSCs themselves showed expression of Lgr5 [111].

Based on the research, it was also discovered that Lgr5-negative tumours sometimes progress, but even then, those cells, just like Lgr5-positive cells, have increased rDNA transcription and protein synthesis at a level similar to that of stem cells. This is related to microenvironmental signalling and the induction of a certain plasticity of tumour cells [112].
It is worth mentioning that Lgr5 stimulates canonical Wnt/β-catenin signalling [113], which has a proven impact on the formation of CSCs.
Baker et al. noticed that the introduction of the APC (adenomatous polyposis coli) mutation into Lgr5-positive cells in mouse bodies resulted in the formation of adenomas in the small and large intestine. Thanks to this, the process was better understood, and it was demonstrated that mutated CSCs with a positive Lgr marker may be cancerous [114].
The existence of the 22-kDa transmembrane-4-L-six-family member-1 (TM4SF1) protein, which consists of 4 transmembrane domains, may also be crucial in explaining this process. The protein itself is often called tumour-associated antigen L6, and its increased expression is observed in many cancers, including colon cancer [115]. TM4SF1 is associated with many tumour characteristics, such as growth, invasiveness, and metastatic ability [116].
A study was conducted to look for the function of TM4SF1 in the process of chemotherapy resistance with the help of fluorouracil. Silencing TM4SF1 resulted in reduced expression of surface markers CD133, CD44, SOX2, and ALDHA1. When this intermembrane protein was overexpressed, CD133 and SOX2 were increased [117].
The aforementioned markers are characteristic of CSCs. The ability of TM4SF1 to interfere with the expression of these surface molecules demonstrates that it has an impact on maintaining tumour stemness and is important for CSCs-dependent CRC progression.
Further research using RNA-Seq to identify the differentially expressed genes (DEGs) attempted to discover the connection between TM4SF1, EMT, and cell stemness. It turned out, based on gene set enrichment analysis (GSEA), that CRC with suppressed TM4SF1 showed significant disruptions in the Wnt pathway and a reduction in β-catenin levels, but stimulation of the Wnt/β-catenin pathway could reverse the effects of TM4SF1-deficiency [117]. Therefore, both this signalling pathway and the protein seem to be closely related.
The Wnt/β-catenin pathway is one of the main pathways involved in the development of colorectal cancer. This pathway also regulates CSCs and is an important factor for maintaining the self-renewal capacity of CSCs. It influences the production of CSCs from normal stem cells or non-CSCs cell populations, contributing to their resistance to anticancer therapy [118].
Moreover, myofibroblasts present in the niche are able to stimulate the Wnt pathway, thereby restoring the CSCs phenotype in more differentiated tumour cells by secreting HGF [119].

Breast cancer

Breast cancer is the most frequently diagnosed cancer in the world and is currently the leading cause of cancer-related death among women [120]. According to statistics from 2017 approximately 1.7 million new cases of breast cancer are diagnosed worldwide each year [121].
Its treatment depends on the stage. There are many treatment methods, such as radical surgery, radiotherapy, hormone therapy depending on the receptor status, immunotherapy, chemotherapy, or a combination of several methods [122].
Randomised, controlled trials show that widespread screening with and introduction of novel, targeted therapies have led to a reduction in breast cancer mortality [123].
However, this does not change the fact that breast cancer is a significant social problem, and every effort should be made to ameliorate our understanding of the mechanisms of cancer formation and metastasis in order to further develop novel therapeutic methods.
Despite all the abovementioned, resistance to therapy is still observed. In the course of diagnostics on the specificity of this cancer, a small group of cancer stem cells was identified in the breast tumour – breast cancer stem cells (BCSC). It is suspected that those cells are the cause of resistance and recurrence of cancer [124].
In BCSCs, we are able to observe the functioning of signalling pathways such as Notch, Hedgehog, Wnt, etc. [125]. Those pathways are important and recognised modulators of CSCs function. Thanks to them, BSCSs are able to maintain their unique characteristics.
Moreover, BCSCs interact with immune system cells and host cells, creating a picture of the tumour microenvironment. This complex signalling between microenvironmental cells and BCSCs leads to tumour initiation and progression [126].
Cancer cells are surrounded by normal tissue and CAFs, endothelial cells, and ECM, which together with immune cells create the abovementioned evolving environment. Breast tumours show a certain phenotypic plasticity, which is achieved

thanks to numerous signals from the tumour microenvironment that influence their adaptation to the ecological niche of the tumour [127].

Long non-coding RNA (lncRNA) represents the largest class among non-coding RNA subtypes. It plays an important role in the regulation of transcription and post-transcriptional mechanisms. Its participation is observed in processes such as proliferation, apoptosis, and cellular differentiation [128].

IncRNAs are hypothesised to be involved in "stemness" maintenance. Their dysregulation is observed in CSCs. Although they are found in low quantities, there are reports describing lncRNAs that are specific to BCSCs. When analysing IncRNA, one may come across IncROPM (a regulator of phospholipid metabolism), related to PLA2G16 and thus to phospholipid metabolism. Some studies suggest that lncROPM may up-regulate the expression of PLA2G16 by stabilising PLA2G16 mRNA. This causes a change in phospholipid metabolism and the production of free fatty acids, in particular arachidonic acid, which is able to activate PI3K/AKT, Wnt/β-catenin, and Hippo/YAP signalling pathways [129]. These pathways are, of course, closely related to CSCs, determining their specific features.

The group of researchers also noted that luminal or basal-like breast tumour may arise from mutations of phosphatidylinositol-4,5-bisphosphate 3-kinase catalytic subunit α (PIK3CA) in mammary luminal stem cells. Moreover, it is believed that basal-like cancer with a BRCA1 mutation could arise from basal stem cells, and the loss of BRCA1 leads to uncontrolled division of stem cells, and the population of cells with this mutation gives a chance to develop cancer [130].

When analysing the process of breast cancer development, it is crucial to mention the EGFR-HER2 module. HER2 is an epidermal growth factor whose overexpression is observed in 20% of breast cancers. It can form heterodimers with EGFR, HER3, or HER4. The heterodimerisation process is believed to be one of the mechanisms of resistance to anticancer therapy in cancers with HER2 overexpression [131].

This module is an important marker of clonal expression of transit-amplifying cells (TACs) and their interaction with stem cells. The active EGFR–HER2 complex of TACs modulates the functioning of progenitor cells and promotes their dedifferentiation into stem cells. TAC itself is an intermediary in the transition between stem cells and differentiated cells, and therefore participates in the process of tumour formation [132].

There are reports that under the influence of fractional irradiation, the level of reactive oxygen species decreased in cancer stem cells in breast cancer compared to the level in differentiated cancer cells, which suggests a certain mechanism of resistance to radiotherapy. However, treatment with multidrug CT, in addition to promoting CSCs markers, led to an increase in the number of CSCs of non-stem origin. This process was probably dependent on the influence of CSCs [133].

CONCLUSIONS

The sole existence of cancer stem cells has been proven beyond reasonable doubt. In a variety of cancers CSCs have been identified and phenotypically characterised. It is evident that they are an important part of the complex interplay between signal transduction pathways, cytokine and chemokine interactions, and epithelial-mesenchymal transition. However, their exact role in the carcinogenesis remains unclear. Similarly, they evidently play part in the metastasis formation process; however, data are scarce and more speculative than conclusive. The question of whether CSCs play a key role in carcinogenesis and metastasis requires further extensive research.

CONFLICT OF INTERESTS

The authors declare no conflict of interest.

FUNDING

The review article required no funding.

ETHICS APPROVAL STATEMENT

The ethical approval was not required.

References

1. Siegel RL, Miller KD, Wagle NS, Jemal A. Cancer statistics, 2023. CA Cancer J Clin. 2023; 73: 17-48.
2. Walcher L, Kistenmacher AK, Suo H, et al. Cancer Stem Cells – Origins and Biomarkers: Perspectives for Targeted Personalized Therapies. Front Immunol. 2020; 11: 1280.
3. Yu Z, Pestell TG, Lisanti MP, Pestell RG. Cancer stem cells. Int J Biochem Cell Biol. 2012; 44: 2144-2151.
4. Reya T, Morrison SJ, Clarke MF, Weissman IL. Stem cells, cancer, and cancer stem cells. Nature. 2001; 414: 105-111.
5. Capp JP. Cancer Stem Cells: From Historical Roots to a New Perspective. J Oncol. 2019; 2019: 5189232.
6. Stevens LC, Little CC. Spontaneous Testicular Teratomas in an Inbred Strain of Mice. Proc Natl Acad Sci U S A. 1954; 40: 1080-1087.

7. Kleinsmith LJ, Pierce GB Jr. Multipotentiality of single embryonal carcinoma cells. Cancer Res. 1964; 24: 1544-1551.

8. Bonnet D, Dick JE. Human acute myeloid leukemia is organized as a hierarchy that originates from a primitive hematopoietic cell. Nat Med. 1997; 3: 730-737.

9. Hermann PC, Bhaskar S, Cioffi M, Heeschen C. Cancer stem cells in solid tumors. Semin Cancer Biol. 2010; 20: 77-84.

10. Skvortsova I. Cancer Stem Cells: What Do We Know about Them? Cells. 2021; 10: 1528.

11. Biserova K, Jakovlevs A, Uljanovs R, Strumfa I. Cancer Stem Cells: Significance in Origin, Pathogenesis and Treatment of Glioblastoma. Cells. 2021; 10: 621.

12. Clarke MF, Dick JE, Dirks PB, et al. Cancer Stem Cells-Perspectives on Current Status and Future Directions: AACR Workshop on Cancer Stem Cells. Available at: www.aacrjournals.org.

13. Najafi M, Mortezaee K, Majidpoor J. Cancer stem cell (CSC) resistance drivers. Life Sci. 2019; 234.

14. Lathia JD, Mack SC, Mulkearns-Hubert EE, Valentim CLL, Rich JN. Cancer stem cells in glioblastoma. Genes Dev. 2015; 29: 1203.

15. Prager BC, Xie Q, Bao S, Rich JN. Cancer Stem Cells: The Architects of the Tumor Ecosystem. Cell Stem Cell. 2019; 24: 41-53.

16. Dianat-Moghadam H, Heydarifard M, Jahanban-Esfahlan R, et al. Cancer stem cells-emanated therapy resistance: Implications for liposomal drug delivery systems. J Control Release. 2018; 288: 62-83.

17. Batlle E, Clevers H. Cancer stem cells revisited. Nat Med. 2017; 23: 1124-1134.

18. Ajani JA, Song S, Hochster HS, Steinberg IB. Cancer stem cells: the promise and the potential. Semin Oncol. 2015; 42 Suppl 1: S3-S17.

19. Chen K, Huang YH, Chen JL. Understanding and targeting cancer stem cells: therapeutic implications and challenges. Acta Pharmacol Sin. 2013; 34: 732-740.

20. Xin P, Xu X, Deng C, et al. The role of JAK/STAT signaling pathway and its inhibitors in diseases. Int Immunopharmacol. 2020; 80: 106210.

21. Hu X, Li J, Fu M, Zhao X, Wang W. The JAK/STAT signaling pathway: from bench to clinic. Signal Transduct Target Ther. 2021; 6: 1-33.

22. Yang L, Shi P, Zhao G, et al. Targeting cancer stem cell pathways for cancer therapy. Signal Transduct Target Ther. 2020; 5: 8.

23. Willert K, Jones KA. Wnt signaling: is the party in the nucleus? Genes Dev. 2006; 20: 1394-1404.

24. Duchartre Y, Kim YM, Kahn M. The Wnt signaling pathway in cancer. Crit Rev Oncol Hematol. 2016; 99: 141-149.

25. Katoh M, Katoh M. WNT signaling and cancer stemness. Essays Biochem. 2022; 66: 319-331.

26. Zhou B, Lin W, Long Y, et al. Notch signaling pathway: architecture, disease, and therapeutics. Signal Transduct Target Ther. 2022; 7: 95.

27. Ehebauer M, Hayward P, Martinez-Arias A. Notch signaling pathway. Sci STKE. 2006; 2006: cm7.

28. Janghorban M, Xin L, Rosen JM, Zhang XHF. Notch Signaling as a Regulator of the Tumor Immune Response: To Target or Not To Target? Front Immunol. 2018; 9: 1649.

29. Banaszek N, Kurpiewska D, Kozak K, Rutkowski P, Sobczuk P. Hedgehog pathway in sarcoma: from preclinical mechanism to clinical application. J Cancer Res Clin Oncol. 2023; 149: 17635.

30. Merchant AA, Matsui W. Targeting Hedgehog – A cancer stem cell pathway. Clin Cancer Res. 2010; 16: 3130-3140.

31. Peacock CD, Wang Q, Gesell GS, et al. Hedgehog signaling maintains a tumor stem cell compartment in multiple myeloma. Proc Natl Acad Sci U S A. 2007; 104: 4048-4053.

32. Yu Z, Pestell TG, Lisanti MP, Pestell RG. Cancer stem cells. Int J Biochem Cell Biol. 2012; 44: 2144-2151.

33. Murar M, Vaidya A. Cancer stem cell markers: premises and prospects. Biomark Med. 2015; 9: 1331-1342.

34. Kim WT, Ryu CJ. Cancer stem cell surface markers on normal stem cells. BMB Rep. 2017; 50: 285-298.

35. Han J, Won M, Kim JH, et al. Cancer stem cell-targeted bio-imaging and chemotherapeutic perspective. Chem Soc Rev. 2020; 49: 7856-7878.

36. Huang M, Xia Y, Li K, et al. Carcinogen exposure enhances cancer immunogenicity by blocking the development of an immunosuppressive tumor microenvironment. J Clin Invest. 2023; 133: e166494.

37. Hoeijmakers JHJ. DNA damage, aging, and cancer. N Engl J Med. 2009; 361: 1475-1485.

38. Yin W, Wang J, Jiang L, James Kang Y. Cancer and stem cells. Exp Biol Med (Maywood). 2021; 246: 1791-1801.

39. Vijg J, Schumacher B, Abakir A, et al. Mitigating age-related somatic mutation burden. Trends Mol Med. 2023; 29: 530-540.

40. Clarke MF. Clinical and Therapeutic Implications of Cancer Stem Cells. N Engl J Med. 2019; 380: 2237-2245.

41. Kreso A, Dick JE. Evolution of the cancer stem cell model. Cell Stem Cell. 2014; 14: 275-291.

42. Lytle NK, Barber AG, Reya T. Stem cell fate in cancer growth, progression and therapy resistance. Nat Rev Cancer. 2018; 18: 669-680.

43. Vlaski-Lafarge M, Labat V, Brandy A, et al. Normal Hematopoetic Stem and Progenitor Cells Can Exhibit Metabolic Flexibility Similar to Cancer Cells. Front Oncol. 2020; 10: 713.

44. Das D, Fletcher RB, Ngai J. Cellular mechanisms of epithelial stem cell self-renewal and differentiation during homeostasis and repair. Wiley Interdiscip Rev Dev Biol. 2020; 9: e361.

45. Verga Falzacappa MV, Ronchini C, Reavie LB, Pelicci PG. Regulation of self-renewal in normal and cancer stem cells. FEBS J. 2012; 279: 3559-3572.

46. Chen HY, Cheng AJ, Chen HY, Cheng AJ. Potential to Eradicate Cancer Stemness by Targeting Cell Surface GRP78. Biomolecules. 2022; 12: 941.

47. Cicalese A, Bonizzi G, Pasi CE, et al. The tumor suppressor p53 regulates polarity of self-renewing divisions in mammary stem cells. Cell. 2009; 138: 1083-1095.

48. Kapoor S, Shenoy SP, Bose B. CD34 cells in somatic, regenerative and cancer stem cells: Developmental biology, cell therapy, and omics big data perspective. J Cell Biochem. 2020; 121: 3058-3069.

49. Plaks V, Kong N, Werb Z. The Cancer Stem Cell Niche: How Essential is the Niche in Regulating Stemness of Tumor Cells? Cell Stem Cell. 2015; 16: 225.

50. Hanahan D, Coussens LM. Accessories to the crime: functions of cells recruited to the tumor microenvironment. Cancer Cell. 2012; 21: 309-322.

51. Aponte PM, Caicedo A. Stemness in Cancer: Stem Cells, Cancer Stem Cells, and Their Microenvironment. Stem Cells Int. 2017; 2017: 5619472.

52. Luo Q, Liu P, Yu P, Qin T. Cancer Stem Cells are Actually Stem Cells with Disordered Differentiation: the Monophyletic Origin of Cancer. Stem Cell Rev Rep. 2023; 19: 827-838.

53. De Berardinis RJ, Chandel NS. Fundamentals of cancer metabolism. Sci Adv. 2016; 2: e1600200.

54. Zhang Y, Yang JM. Altered energy metabolism in cancer: a unique opportunity for therapeutic intervention. Cancer Biol Ther. 2013; 14: 81-89.

55. Lunt SY, Vander Heiden MG. Aerobic glycolysis: meeting the metabolic requirements of cell proliferation. Annu Rev Cell Dev Biol. 2011; 27: 441-464.

56. Ganapathy-Kanniappan S, Geschwind JFH. Tumor glycolysis as a target for cancer therapy: progress and prospects. Mol Cancer. 2013; 12: 152.

57. Scapin G, Goulard MC, Dharampuriya PR, Cillis JL, Shah DI. Analysis of Hematopoietic Stem Progenitor Cell Metabolism. J Vis Exp. 2019; 9: 10.3791/60234.

58. Suhail Y, Cain MP, Vanaja K, et al. Systems Biology of Cancer Metastasis. Cell Syst. 2019; 9: 109-127.

59. Duffy MJ, McGowan PM, Gallagher WM. Cancer invasion and metastasis: changing views. J Pathol. 2008; 214: 283-293.

60. Quail DF, Joyce JA. Microenvironmental regulation of tumor progression and metastasis. Nat Med. 2013; 19: 1423-1437.

61. Seyfried TN, Huysentruyt LC. On the origin of cancer metastasis. Crit Rev Oncog. 2013; 18: 43-73.

62. Hamidi H, Ivaska J. Every step of the way: integrins in cancer progression and metastasis. Nat Rev Cancer. 2018; 18: 533-548.

63. Bouyssou JMC, Manier S, Huynh D, Issa S, Roccaro AM, Ghobrial IM. Regulation of microRNAs in Cancer Metastasis. Biochim Biophys Act. 2014; 1845: 255.

64. Fares J, Fares MY, Khachfe HH, Salhab HA, Fares Y. Molecular principles of metastasis: a hallmark of cancer revisited. Signal Transduct Target Ther. 2020; 5: 28.

65. Tang KD, Holzapfel BM, Liu J, et al. Tie-2 regulates the stemness and metastatic properties of prostate cancer cells. Oncotarget. 2015; 7: 2572-2784.

66. Najafi M, Farhood B, Mortezaee K. Cancer stem cells (CSCs) in cancer progression and therapy. J Cell Physiol. 2019; 234: 8381-8395.

67. Chen C, Zhao S, Karnad A, Freeman JW. The biology and role of CD44 in cancer progression: therapeutic implications. J Hematol Oncol. 2018; 11: 1-23.

68. Puisieux A, Brabletz T, Caramel J. Oncogenic roles of EMT-inducing transcription factors. Nat Cell Biol. 2014; 16: 488-494.

69. Cox TR. The matrix in cancer. Nat Rev Cancer. 2021; 21: 217-238.

70. Lu TX, Rothenberg ME. MicroRNA. J Allergy Clin Immunol. 2018; 141: 1202-1207.

71. Solé C, Lawrie CH. MicroRNAs in Metastasis and the Tumour Microenvironment. Int J Mol Sci. 2021; 22: 4859.

72. Takahashi R u., Miyazaki H, Ochiya T. The role of microRNAs in the regulation of cancer stem cells. Front Genet. 2013; 4: 72858.

73. Zhang J, Li Q, Chang AE. Immunologic Targeting of Cancer Stem Cells. Surg Oncol Clin N Am. 2019; 28: 431-445.

74. Nobili S, Lapucci A, Landini I, Coronnello M, Roviello G, Mini E. Role of ATP-binding cassette transporters in cancer initiation and progression. Semin Cancer Biol. 2020; 60: 72-95.

75. El-Kenawi A, Hänggi K, Ruffell B. The Immune Microenvironment and Cancer Metastasis. Cold Spring Harb Perspect Med. 2020; 10: a037424.

76. Liu W, Powell CA, Wang Q. Tumor microenvironment in lung cancer-derived brain metastasis. Chin Med J (Engl). 2022; 135: 1781.

77. Sun HR, Wang S, Yan SC, et al. Therapeutic Strategies Targeting Cancer Stem Cells and Their Microenvironment. Front Oncol. 2019; 9: 1104.

78. Clara JA, Monge C, Yang Y, Takebe N. Targeting signalling pathways and the immune microenvironment of cancer stem cells – a clinical update. Nat Rev Clin Oncol. 2020; 17: 204-232.

79. Duan H, Liu Y, Gao Z, Huang W. Recent advances in drug delivery systems for targeting cancer stem cells. Acta Pharm Sin B. 2021; 11: 55-70.

80. Wu T, Dai Y. Tumor microenvironment and therapeutic response. Cancer Lett. 2017; 387: 61-68.

81. van der Pluijm G. Epithelial plasticity, cancer stem cells and bone metastasis formation. Bone 2011; 48: 37-43.

82. Foster DS, Januszyk M, Delitto D, et al. Multiomic analysis reveals conservation of cancer-associated fibroblast phenotypes across species and tissue of origin. Cancer Cell. 2022; 40: 1392-1406.e7.

83. Piersma B, Hayward MK, Weaver VM. Fibrosis and cancer: A strained relationship. Biochim Biophys Acta Rev Cancer. 2020; 1873: 188356.

84. Nallasamy P, Nimmakayala RK, Karmakar S, et al. Pancreatic Tumor Microenvironment Factor Promotes Cancer Stemness via SPP1-CD44 Axis. Gastroenterology. 2021; 161: 1998-2013.e7.

85. Weiland A, Roswall P, Hatzihristidis TC, Pietras K, Ostman A, Strell C. Fibroblast-dependent regulation of the stem cell

properties of cancer cells. Neoplasma. 2012; 59: 719-727.

86. Xu X, Chang W, Yuan J, et al. Periostin expression in intra-tumoral stromal cells is prognostic and predictive for colorectal carcinoma via creating a cancer-supportive niche. Oncotarget. 2016; 7: 798-813.

87. Jing X, Yang F, Shao C, et al. Role of hypoxia in cancer therapy by regulating the tumor microenvironment. Mol Cancer. 2019; 18: 1-15.

88. Anderson NM, Simon MC. The tumor microenvironment. Curr Biol. 2020; 30: R921-R925.

89. Markowska A, Sajdak S, Markowska J, Huczyński A. Angiogenesis and cancer stem cells: New perspectives on therapy of ovarian cancer. Eur J Med Chem. 2017; 142: 87-94.

90. Stanca Melincovici C, Boşca AB, Şuşman S, et al. Vascular endothelial growth factor (VEGF)-key factor in normal and pathological angiogenesis. Rom J Morphol Embryol. 2018; 59: 455-467.

91. Mercurio AM. VEGF/Neuropilin Signaling in Cancer Stem Cells. Int J Mol Sci. 2019; 20: 490.

92. Tsuchiya H, Shiota G. Immune evasion by cancer stem cells. Regen Ther. 2021; 17: 20-33.

93. Gardner A, Ruffell B. Dendritic Cells and Cancer Immunity. Trends Immunol. 2016; 37: 855-865.

94. Bayik D, Lathia JD. Cancer stem cell-immune cell crosstalk in tumour progression. Nat Rev Cancer. 2021; 21: 526-536.

95. Ngambenjawong C, Gustafson HH, Pun SH. Progress in tumor-associated macrophage (TAM)-targeted therapeutics. Adv Drug Deliv Rev. 2017; 114: 206-221.

96. Jinushi M, Chiba S, Yoshiyama H, et al. Tumor-associated macrophages regulate tumorigenicity and anticancer drug responses of cancer stem/initiating cells. Proc Natl Acad Sci U S A. 2011; 108: 12425-12430.

97. Oshimori N. Cancer stem cells and their niche in the progression of squamous cell carcinoma. Cancer Sci. 2020; 111: 3985-3992.

98. Miyata H, Hirohashi Y, Yamada S, et al. GRIK2 is a target for bladder cancer stem-like cell-targeting immunotherapy. Cancer Immunol Immunother. 2022; 71: 795-806.

99. MaruYama T, Chen W, Shibata H. TGF-β and Cancer Immunotherapy. Biol Pharm Bull. 2022; 45: 155-161.

100. Jubber I, Ong S, Bukavina L, et al. Epidemiology of Bladder Cancer in 2023: A Systematic Review of Risk Factors. Eur Urol. 2023; 84: 176-190.

101. Hamad J, McCloskey H, Milowsky MI, Royce T, Smith A. Bladder preservation in muscle-invasive bladder cancer: a comprehensive review. Int Braz J Urol. 2020; 46: 169-184.

102. Xu Y, Luo C, Wang J, et al. Application of nanotechnology in the diagnosis and treatment of bladder cancer. J Nanobiotechnology. 2021; 19: 1-18.

103. Wang H, Mei Y, Luo C, et al. Single-Cell Analyses Reveal Mechanisms of Cancer Stem Cell Maintenance and Epithelial-Mesenchymal Transition in Recurrent Bladder Cancer. Clin Cancer Res. 2021; 27: 6265-6278.

104. Kripnerova M, Parmar HS, Pesta M, et al. Urothelial Cancer Stem Cell Heterogeneity. Adv Exp Med Biol. 2019; 1139: 127-151.

105. Siegel RL, Wagle NS, Cercek A, Smith RA, Jemal A. Colorectal cancer statistics, 2023. CA Cancer J Clin. 2023; 73: 233-254.

106. Dekker E, Tanis PJ, Vleugels JLA, Kasi PM, Wallace MB. Colorectal cancer. The Lancet. 2019; 394: 1467-1480.

107. Pang R, Law WL, Chu ACY, et al. A subpopulation of CD26+ cancer stem cells with metastatic capacity in human colorectal cancer. Cell Stem Cell. 2010; 6: 603-615.

108. Zheng H, Liu H, Li H, et al. Characterization of stem cell landscape and identification of stemness-relevant prognostic gene signature to aid immunotherapy in colorectal cancer. Stem Cell Res Ther. 2022; 13: 1-20.

109. Gupta R, Bhatt LK, Johnston TP, Prabhavalkar KS. Colon cancer stem cells: Potential target for the treatment of colorectal cancer. Cancer Biol Ther. 2019; 20: 1068-1082.

110. Barker N, Van Es JH, Kuipers J, et al. Identification of stem cells in small intestine and colon by marker gene Lgr5. Nature. 2007; 449: 1003-1007.

111. Fumagalli A, Oost KC, Kester L, et al. Plasticity of Lgr5-Negative Cancer Cells Drives Metastasis in Colorectal Cancer. Cell Stem Cell. 2020; 26: 569-578.e7.

112. Vasquez EG, Nasreddin N, Valbuena GN, et al. Dynamic and adaptive cancer stem cell population admixture in colorectal neoplasia. Cell Stem Cell. 2022; 29: 1213-1228.e8.

113. Morgan RG, Mortensson E, Williams AC. Targeting LGR5 in Colorectal Cancer: therapeutic gold or too plastic? Br J Cancer. 2018; 118: 1410-1418.

114. Lei X, He Q, Li Z, et al. Cancer stem cells in colorectal cancer and the association with chemotherapy resistance. Med Oncol. 2021; 38: 43.

115. Peng XC, Zeng Z, Huang YN, Deng YC, Fu GH. Clinical significance of TM4SF1 as a tumor suppressor gene in gastric cancer. Cancer Med. 2018; 7: 2592.

116. Park YR, Lee ST, Kim SL, et al. MicroRNA-9 suppresses cell migration and invasion through downregulation of TM4SF1 in colorectal cancer. Int J Oncol. 2016; 48: 2135-2143.

117. Tang Q, Chen J, Di Z, et al. TM4SF1 promotes EMT and cancer stemness via the Wnt/β-catenin/SOX2 pathway in colorectal cancer. J Exp Clin Cancer Res. 2020; 39: 232.

118. Zhao H, Ming T, Tang S, et al. Wnt signaling in colorectal cancer: pathogenic role and therapeutic target. Mol Cancer. 2022; 21: 144.

119. Du L, Cheng Q, Zheng H, Liu J, Liu L, Chen Q. Targeting stemness of cancer stem cells to fight colorectal cancers. Semin Cancer Biol. 2022; 82: 150-161.

120. Wilkinson L, Gathani T. Understanding breast cancer as a global health concern. Br J Radiol. 2022; 95: 20211033.

121. da Costa Vieira RA, Biller G, Uemura G, et al. Breast cancer screening in developing countries. Clinics (Sao Paulo). 2017; 72: 244-253.

122. Waks AG, Winer EP. Breast Cancer Treatment: A Review. JAMA 2019; 321: 288-300.

123. Coleman C. Early Detection and Screening for Breast Cancer. Semin Oncol Nurs. 2017; 33: 141-155.

124. Palomeras S, Ruiz-Martínez S, Puig T. Targeting Breast Cancer Stem Cells to Overcome Treatment Resistance. Molecules. 2018; 23: 2193.

125. Dandawate PR, Subramaniam D, Jensen RA, Anant S. Targeting cancer stem cells and signaling pathways by phytochemicals: Novel approach for breast cancer therapy. Semin Cancer Biol. 2014; 40-41: 192-208.

126. Guha A, Goswami KK, Sultana J, et al. Cancer stem cell-immune cell crosstalk in breast tumor microenvironment: a determinant of therapeutic facet. Front Immunol. 2023; 14: 1245421.

127. Fico F, Santamaria-Martínez A. The Tumor Microenvironment as a Driving Force of Breast Cancer Stem Cell Plasticity. Cancers (Basel). 2020; 12: 1-28.

128. Akhade VS, Pal D, Kanduri C. Long Noncoding RNA: Genome organization and mechanism of action. Adv Exp Med Biol. 2017; 1008: 47-74.

129. Liu S, Sun Y, Hou Y, et al. A novel lncRNA ROPM-mediated lipid metabolism governs breast cancer stem cell properties. J Hematol Oncol. 2021; 14: 178.

130. Zhang L, Chen W, Liu S, Chen C. Targeting Breast Cancer Stem Cells. Int J Biol Sci. 2023; 19: 552-570.

131. Weinberg F, Peckys DB, de Jonge N. EGFR Expression in HER2-Driven Breast Cancer Cells. Int J Mol Sci. 2020; 21: 1-19.

132. Yang F, Xu J, Tang L, Guan X. Breast cancer stem cell: the roles and therapeutic implications. Cell Mol Life Sci. 2017; 74: 951-966.

133. Bai X, Ni J, Beretov J, Graham P, Li Y. Cancer stem cell in breast cancer therapeutic resistance. Cancer Treat Rev. 2018; 69: 152-163. ■

REVIEW PAPER

UROLOGICAL ONCOLOGY

The potential of gallium-68 prostate-specific membrane antigen positron emission tomography/computed tomography as a main diagnostic tool in prostate cancer staging

Oleksii Pisotskyi[1*], Piotr Petrasz[1*], Piotr Zorga[5], Marcin Gałęski[1], Paweł Szponar[1], Krzysztof Koper[3], Katarzyna Brzeźniakiewicz-Janus[4], Tomasz Drewa[5], Krzysztof Kaczmarek[1], Michał Cezary Czarnogórski[5], Jan Adamowicz[5]

[1]*Urology and Urological Oncology Department, Multidisciplinary Regional Hospital, Gorzow Wielkopolski, Poland*
[2]*Nuclear Medicine Clinical Department, University of Zielona Gora, Multidisciplinary Regional Hospital, Gorzow Wielkopolski, Poland*
[3]*Clinical Oncology and Nursing Department, Collegium Medicum, Nicolaus Copernicus University, Bydgoszcz, Poland*
[4]*Haematology, Oncology, and Radiotherapy Department and Clinic, University of Zielona Gora, Multidisciplinary Regional Hospital, Gorzow Wielkopolski, Poland*
[5]*Department and Chair of Urology and Andrology, University Hospital No. 1 in Bydgoszcz, Ludwik Rydygier's Collegium Medicum in Bydgoszcz, Nicolaus Copernicus University in Torun, Poland*
** These authors contributed equally.*

Citation: Pisotskyi O, Petrasz P, Zorga P, et al. The potential of gallium-68 prostate-specific membrane antigen positron emission tomography/computed tomography as a main diagnostic tool in prostate cancer staging. Cent European J Urol. 2025; 78: 52-60.

Article history
Submitted: Jan. 17, 2025
Accepted: Feb. 9, 2025
Published online: Mar. 14, 2025

Corresponding authors
Oleksii Pisotskyi,
Piotr Petrasz
Multidisciplinary Regional Hospital,
1 Dekerta St.,
66-400 Gorzów Wielkopolski,
Poland
alexkiev96@gmail.com
piotr.petrasz@szpital.gorzow.pl

Introduction Prostate cancer (PC) remains a significant global health burden, necessitating accurate staging for optimal treatment planning. Conventional imaging methods, including multiparametric magnetic resonance imaging (mpMRI), computed tomography (CT), and bone scintigraphy (BS), exhibit limitations in sensitivity and specificity. Gallium-68 prostate-specific membrane antigen positron emission tomography/computed tomography (^{68}Ga PSMA-PET/CT) has emerged as a promising alternative, with potential advantages in staging accuracy.

Material and methods A comprehensive review of current literature was conducted to assess the role of ^{68}Ga PSMA-PET/CT in primary PC staging. The diagnostic performance of PSMA-PET/CT was compared with conventional imaging techniques in detecting locoregional and distant metastases. Studies evaluating sensitivity, specificity, and clinical utility in treatment decision-making were analyzed.

Results ^{68}Ga PSMA-PET/CT demonstrated superior sensitivity and specificity in detecting lymph node and distant metastases compared to conventional imaging. It enables earlier and more precise disease staging, potentially reducing the need for multiple imaging modalities. Emerging evidence suggests its role in guiding therapeutic strategies, particularly in high-risk and recurrent PC cases. Despite its advantages, limitations such as accessibility, cost, and occasional false-negative findings must be considered.

Conclusions ^{68}Ga PSMA-PET/CT represents a transformative diagnostic tool for PC staging, offering enhanced accuracy compared to traditional imaging. Its integration into clinical practice could streamline diagnostic pathways, improve treatment selection, and potentially optimize patient outcomes. Further research and cost-effectiveness analyses are needed to establish its widespread implementation.

Key Words: prostate cancer ‹› ^{68}Ga PSMA-PET/CT ‹› staging accuracy ‹› imagin comparison

INTRODUCTION

Prostate cancer (PC) is the second-most-prevalent malignancy globally and the fifth leading cause of cancer-related deaths among males [1]. The American Cancer Society predicted approximately 288,300 new cases of PC and 34,700 deaths attributed to the disease in 2023 [2].

For accurate local tumour staging, seminal vesicle (SV) invasion (SVI) and extracapsular extension (ECE) are critical parameters, and prostate magnetic resonance imaging (MRI) is the worldwide standard imaging technique [3]. Traditional methods for evaluating locoregional lymph node metastases (LNMs) and remote metastatic spread typically involve computed tomography (CT) and bone scintigraphy (BS). However, the sensitivities of those modalities remain modest at approximately 42% for CT and 79% for BS [4, 5]. Consequently, patients often require multiple imaging procedures before treatment, to precisely evaluate the disease stage.

From a public health perspective, the rising number of new PC cases and, in turn, patients waiting for rapid radiological imaging, demand optimised staging protocols. Therefore, this study aimed to assess the feasibility of single-stage examination of primary PCa with the utilisation of single, novel diagnostic tool. Investigating gallium-68 prostate-specific membrane antigen positron emission tomography/CT (^{68}Ga PSMA-PET/CT) presents an encouraging avenue for addressing this question. Leveraging the advanced imaging capabilities of this diagnostic technique potentially offers a feasible solution for conducting a single-stage examination to diagnose primary PC. This cutting-edge technology holds the potential to streamline the diagnostic process, providing valuable insights into the feasibility of a more efficient and comprehensive approach to PCa staging.

The aim of this review is to evaluate the potential of ^{68}Ga PSMA-PET/CT as a primary diagnostic tool in prostate cancer staging. Specifically, we aim to compare its diagnostic accuracy with conventional imaging techniques, assess its clinical applications in different stages of prostate cancer, and explore its role in guiding treatment decisions. Additionally, we discuss the limitations and economic implications of integrating PSMA-PET/CT into routine clinical practice.

IMAGING TECHNOLOGIES IN PRIMARY STAGING

T-staging (magnetic resonance imaging)

T2-weighted MRI is the preferred method for local staging, renowned and commonly accepted in international guidelines with standardised protocol. A meta-analysis by Caglic et al. [6] showed that the sensitivity and specificity for extraprostatic extension (EPE) were 0.57 (95% confidence interval [CI]: 0.49–0.64) and 0.91 (95% CI: 0.88–0.93), respectively. For SVI, the sensitivity was 0.58 (95% CI: 0.47–0.68), and the specificity was 0.96 (95% CI: 0.95–0.97) [6].

N-staging (magnetic resonance imaging and computed tomography)

MRI (T1-T2-weighted) and abdominal CT indirectly evaluate nodal invasion by examining the lymph node (LN) size. Typically, LNs with short axes measuring >8 mm in the pelvic region and >10 mm outside the pelvis are indicative of malignancy. Reducing these threshold values increases the sensitivity but decreases the specificity, making the optimal size threshold uncertain [7, 8]. The sensitivities of CT and MRI for detecting LN involvement are <40% [9, 10]. Significantly, the sensitivity of identifying microscopic LN invasion through CT scans is <1% in patients with International Society of Urological Pathology (ISUP) grade <4, prostate-specific antigen (PSA) level <20 ng/ml, or localised disease [11–13]. In summary, such methods show limited sensitivity and specificity for N-staging and might not be an optimal option for identifying lymph nodes involvement.

M-staging (bone scintigraphy)

The ^{99m}Tc bone scan (BS) is a widely used conventional imaging technique that exhibits high sensitivity in assessing the pattern of active bone formation across the entire skeleton, aiding in the detection of both malignant and benign diseases. In a meta-analysis assessing its effectiveness, BS demonstrated a sensitivity and specificity of 79% and 82%, respectively [14]. Notably, the diagnostic output of BS is significantly affected by factors such as the clinical stage, PSA level, and ISUP grade of the tumour [15]. A retrospective study of 703 patients with newly diagnosed PC who were referred for BS showed the association between age, PSA level, and Gleason score (GS). The findings revealed a substantial increase in the incidence of bone metastases with higher PSA levels and GS [16]. These factors play crucial roles in determining the likelihood of detecting bone metastasis through BS.

PROSTATE-SPECIFIC MEMBRANE ANTIGEN POSITRON EMISSION TOMOGRAPHY/COMPUTED TOMOGRAPHY

Biological principles and clinical applications

PSMA-PET/CT is an advanced imaging modality designed to identify PC cells. This technique utilises a radioactive substance that specifically targets PSMA, a protein expressed by PC cells. The PSMA PET precision surpasses that of other imaging modalities com-

monly employed for PC detection. While PSMA expression is evident in both normal prostate epithelium and PC cells, it is also detected in other tissues such as the kidneys, small intestine, and salivary glands. Notably, PSMA expression in PC cells is approximately 1000-fold higher than that in normal tissues [17].

Elevated PSMA expression has been observed in PCa cells, not only in primary focus but also in lymph nodes, soft tissues, and bone metastases [18]. Additionally, PSMA is expressed during the neovascularisation of various tumours and their metastases [19, 20]. While PSMA expression has been noted in benign granulomatous and inflammatory diseases, the precise mechanisms governing PSMA uptake have not been fully elucidated. However, tracer accumulation in neovascular processes, reduced vascular permeability, heightened blood flow during inflammation, and other nonspecific elements may be contributing factors. PSMA expression has also been observed in diverse bone-related illnesses and conditions [21–23]. The positive correlation between increased PSMA expression, higher GS, and the development of metastatic disease further underscores the significance of PSMA as a valuable target in PC imaging [24–26]. In contemporary PCa treatment, urologists are increasingly integrating PSMA-PET/CT as a standard imaging tool. The evolving body of evidence, encompassing its performance across diverse PCa stages, along with the incorporation of insights from new tracers, has fuelled a collective effort among urologists to optimise the application of this technology. While this tool is regularly utilised in metastatic scenarios, where it might outperform traditional imaging methods and potentially guide treatment decisions, interest in extending its utility to localised PC has increased, particularly in high-risk cases [27].

Prostate cancer recurrence detection

Biochemical recurrence (BCR) in PC, i.e. signalling recurrence following curative-intent treatments such as prostatectomy or radiation therapy, is characterised by elevated PSA levels. BCR affects approximately 4 in every 10 patients with PC, with approximately a quarter experiencing clinical recurrence after 7–8 years [28]. Despite advancements in MRI technology, pinpointing specific BCR sites through imaging has proven challenging. The clinical significance of disease detection lies in directing effective treatment planning and minimising the unnecessary treatment and its associated side effects [29].

Conventional imaging methods, such as BS and CT, exhibit limited accuracy in identifying metastases to lymph nodes and bones, particularly among patients with low PSA levels. In this scenario, MRI has emerged as the preferred approach for detecting local recurrence, boasting a sensitivity of approximately 75%. However, even though MRI outperforms conventional imaging, its primary utility lies in identifying local recurrence. For patients with low PSA levels, experiencing BCR, radiation therapy of the prostate bed is the first-line salvage treatment, making the identification of local recurrence a critical but not the sole determinant for treatment adjustments.

In the last 5 years, ^{68}Ga PSMA-PET/CT has become a revolutionary imaging technique for detecting PC relapse. Numerous studies have consistently illustrated that PSMA exhibits superior sensitivity and specificity compared to traditional approaches or choline PET, particularly in identifying tumour recurrence, especially in patients with low PSA levels (<1.0 ng/ml) [30]. While promising results suggest a significant clinical impact in altering approaches based on PSMA PET evaluations of BCR, demonstrating improvements in long-term outcomes is crucial to validate the clinical utility of this transformative molecular imaging technique [31].

While PSMA-PET/CT enhances the detection of metastases in biochemically recurrent prostate cancer, its impact is further underscored by the recognition of metastasis-free survival (MFS) as a validated intermediate endpoint in localised prostate cancer. Recent guidelines highlight MFS as a crucial marker for evaluating the effectiveness of treatment strategies in patients without detectable metastases on conventional imaging but with biochemical recurrence. Incorporating PSMA-PET/CT findings into this framework may refine risk stratification and treatment selection, as discussed in Miszczyk et al. [32].

Detection of lymph node involvement

In a study by Van Leeuwen et al. [33], the main objective was to scrutinise the precision of ^{68}Ga PSMA-PET/CT for LN staging in patients diagnosed with intermediate- and high-risk PC. Their findings indicate that ^{68}Ga PSMA-PET/CT is a promising alternative to current imaging techniques for LN staging in patients with PC undergoing radical prostatectomy (RP) [33].

Cytawa et al. [34] used ^{68}Ga PSMA-PET/CT for staging in 82 men with PC. They found PSMA-positive disease in 83% of patients, and 80.5% of primary tumours were visualised. PSMA-avid lymph nodes were present in 20.7% of patients, and distant disease was identified in 17.1% of patients. The maxi-

mum standardised uptake value (SUV_{max}) of primary tumours was weakly correlated with PSA levels and GS. LN metastasis detection had a 35.0% sensitivity, 98.4% specificity, 63.6% positive predictive value (PPV), 95.0% negative predictive value (NPV), and 93.0% accuracy [34].

In another study, patients diagnosed with PC were compared based on whether they underwent ^{68}Ga PSMA-PET/CT or conventional imaging alone. The analysis focused on predicting clinical regional node-positive disease, metastatic disease, and the treatment received. Of 6,139 patients, 14% received a staging PET scan, 40% had conventional imaging without a PET scan, and 45% had no recorded PET or conventional imaging. Over time, the proportion of patients undergoing staging PET increased, especially in the high-risk group. After adjusting for the grade, patients who underwent PET had a higher proportion of cN1 disease, but not cM1 disease, compared to those who had conventional imaging alone [35]. The results suggest an increasing use of PET imaging, particularly for patients with high-risk PC, and hints at its potential contribution to improved nodal disease detection, possibly optimising patient selection for definitive PC treatment.

In summary, ^{68}Ga PSMA-PET/CT has emerged as a valuable staging tool for individuals initially diagnosed with intermediate- to high-risk PC. It demonstrates effectiveness in detecting nodal and distant metastases. Nevertheless, PSMA-PET/CT is constrained in low-risk diseases due to the relatively low occurrence of extraprostatic extension.

COULD PROSTATE-SPECIFIC MEMBRANE ANTIGEN POSITRON EMISSION TOMOGRAPHY/COMPUTED TOMOGRAPHY GUIDE THE TREATMENT OF PROSTATE CANCER?

Accurate staging is a critical factor through which PSMA-PET/CT can influence treatment strategies. Traditional imaging modalities, such as BS and CT scans, may sometimes miss small metastatic lesions. In contrast, PSMA-PET/CT has shown superior sensitivity, particularly for detecting LN metastases and distant organ involvement. This enhanced sensitivity can lead to a more precise determination of the extent of the disease, influencing decisions regarding the treatment intensity and modality.

Lima et al. [36] focused on PSMA-PET/CT for the initial assessment of intermediate- and high-risk PC. Patients were categorised based on whether additional imaging modalities were used alongside PSMA-PET/CT. The results of 57 patients were gathered, with 77.2% (n = 44) having a CT scan or bone scan (BS) prior to PSMA-PET/CT. Prostate cancer management strategy was changed in 61.4% (n = 27), when PSMA-PET/CT was performed following CT and BS. BS and CT results were consistent with PSMA-PET/CT in 43.2% and 44.8%, respectively. In 30 cases, a curative strategy was used based on PSMA-PET/CT findings. PSMA-PET/CT revealed a negative predictive value of 95.2% in 23 patients submitted to radical prostatectomy with bilateral pelvic lymphadenectomy. Prostate SUV values on preoperative PSMA-PET/CT correlated with initial PSA, ISUP grade, PC risk staging, and presence of extraprostatic lesions [36].

The superior sensitivity of PSMA-PET/CT in detecting subclinical metastases has notable implications for prostate cancer treatment strategies. This imaging modality often identifies oligometastatic lesions that remain undetected by conventional imaging techniques, leading to a phenomenon known as stage migration. Patients initially considered to have localised disease may be reclassified as oligometastatic, prompting reconsideration of treatment approaches.

The detection of oligometastatic disease has opened new avenues for personalised therapies. Local therapies have shown efficacy in treating oligometastatic lesions, offering potential benefits in delaying disease progression and improving survival outcomes [37, 38]. Furthermore, metastasis-directed therapy (MDT) is increasingly being employed in patients with low-volume metastatic prostate cancer, demonstrating promise in prolonging progression-free survival and delaying the need for systemic treatments. Recent evidence also suggests that MDT can improve clinical outcomes in carefully selected patients with oligometastatic disease, emphasising the role of targeted interventions in this population [39].

By facilitating the identification of patients with limited metastatic burden, PSMA-PET/CT enhances the ability to apply these personalised treatment strategies. The precise detection of metastases allows clinicians to tailor therapeutic interventions more accurately, integrating local and metastasis-directed therapies into the management plans of patients who may have previously been managed with systemic therapy alone. This integration underscores the evolving role of PSMA-PET/CT not only as a diagnostic tool but also as a pivotal component in guiding contemporary prostate cancer treatment.

Taking the abovementioned data into consideration, it may be speculated that indeed PSMA-PET/

CT might in fact guide the therapeutic decisions in PC treatment. However, due to the lack of long-term follow-up of the patients treated based on the PSMA-PET/CT findings, it is still too early for the introduction of this diagnostic modality into the diagnostic algorithms and guidelines.

PROSTATE-SPECIFIC MEMBRANE ANTIGEN POSITRON EMISSION TOMOGRAPHY/COMPUTED TOMOGRAPHY AS A SINGLE DIAGNOSTIC TOOL FOR PROSTATE CANCER STAGING

Prostate-specific membrane antigen positron emission tomography/computed tomography for T-staging

Precisely evaluating T-staging is vital to determine the most suitable treatment course, thereby enhancing the likelihood of achieving the longest progression-free survival. Comprehension of the spatial correlation among the suspected lesion and nearby critical structures is crucial for effective surgical and intensity-modulated radiotherapy planning. MRI has been the traditional approach [40]. However, detecting subtle signs depends on the subjective evaluation of neurovascular symmetry and focal low-signal intensity in the SV or periprostatic fat.

CT plays a restricted role in primary PC diagnosis and is primarily employed for distant staging in patients with PC or for assessing LNM and bone metastases in metastatic PC cases. Despite its common usage in PC management, CT imaging lacks adequate soft tissue contrast and targeted molecular information [41].

Prostate MRI was initially used for staging in males with known PC before treatment. In this setting, prostate MRI provides information on the presence or absence of ECE or the involvement of the neurovascular bundles and SV, thus helping to differentiate stage T2 disease from locally advanced disease.

Studies have compared PSMA-PET/CT and MRI. Berger et al. [42] compared both techniques with histopathological analysis of prostatectomy specimens. Their findings revealed that PSMA-PET/CT exhibits supreme sensitivity in PCa lesions detection compared to MRI. All 50 histopathologically confirmed index lesions were identified by PSMA-PET/CT, achieving a detection rate of 100%, while MRI detected 47 (94%) lesions. Moreover, PSMA-PET/CT demonstrated superior sensitivity for localising index lesions compared to MRI (81.1% vs 64.8%) [42].

Another study comparing both modalities in patients with intermediate- and high-risk PC found that ^{68}Ga PSMA-PET/CT, MRI, and a combination of both had similar cancer detection rates. However, MRI outperformed ^{68}Ga PSMA-PET/CT in detecting EPE and SVI. In the evaluation of T staging, MRI was the reference imaging modality. In summary, those studies indicate that both modalities have similar accuracies in detecting and localising PC foci. ^{68}Ga PSMA-PET/CT shows better sensitivity and detection rates, whereas MRI performs better at identifying EPE and SVI. Therefore, MRI is still the reference imaging modality for T-staging evaluation [43].

Li et al. [44] conducted a study involving a consecutive cohort of 115 patients who underwent both tools. They showed that ^{68}Ga PSMA-PET/CT exhibits superior diagnostic performance, especially in terms of specificity, compared to MRI in individuals suspected of having PC, with PSA levels of 4–20 ng/ml. Additionally, the uptake values of ^{68}Ga PSMA-PET/CT (SUV max or SUV ratio) were positively correlated with the GS, suggesting the potential use of this imaging modality as a noninvasive tool for predicting PC risk and determining malignancy severity. The findings reveal that ^{68}Ga PSMA-PET/CT exhibits a superior sensitivity for detecting ECE in comparison to MRI, while there is no significant difference in detecting SVI [44].

While BS plays an essential role in the overall staging of PC, particularly in identifying bone metastases (M-staging), its direct contribution to T-staging is limited. T-staging is typically performed using other imaging modalities, such as MRI [45].

Prostate-specific membrane antigen positron emission tomography/computed tomography for N-staging

The N staging of PC involves the assessment of LN involvement. Determining whether PC has spread to nearby LN plays a crucial role in cancer staging that influences treatment decisions and prognosis.

In a randomised controlled trial comparing ^{68}Ga PSMA--PET/CT with conventional CT and BS, G^{68}Ga PSMA--PET/CT was superior to other tools in LNM detection, both in sensitivity and specificity. Additionally, CT and BS identified more equivocal lesions compared to ^{68}Ga PSMA-PET/CT, and CT and BS resulted in superior radiation exposure than ^{68}Ga PSMA-PET/CT [46].

In a recent meta-analysis that evaluated LNM identification using MRI and 68Ga PSMA-PET/CT, the PSMA-PET/CT exhibited superior sensitivity and comparable specificity. Moreover, 68Ga PSMA-PET/CT has more positive outcomes in detecting smaller LN than MRI [47].

Summarising, there is a growing body of evidence justifying the sole use of PSMA-PET/CT in N-staging of prostate cancer.

Prostate-specific membrane antigen positron emission tomography/tomography for M-staging

Conventional imaging techniques are valuable for detection of distant metastases, and CT can identify sclerotic bone lesions and metastases in internal organs. Nonetheless, CT has produced positive results in only 14% of cases [48].

Accurately diagnosing bone metastasis in PC is becoming increasingly important for guiding both local and systemic treatments. Globally, both tools are utilised for assessing bone metastases in PC. In a meta-analysis of a high-volume series conducted by Liu et al. [49], the effectiveness of ^{68}Ga PSMA--PET/CT with various radioligands was compared to that of MRI with different parameters. This comprehensive review and network meta-analysis of diagnostic tests, involving 45 studies with 2,843 patients and 4,263 lesions, recommended the use of ^{68}Ga PSMA-PET/CT for diagnosing bone metastasis in patients with PC.

^{68}Ga PSMA-PET/CT surpasses planar BS in detecting affected bone regions and assessing the overall involvement of the bones in patients with PC.

In a comparative study by Pyka et al. [50], bone metastasis was diagnosed in 60% of patients. ^{68}Ga PSMA-PET/CT demonstrated sensitivities and specificities ranging from 98.7% to 100% and 88.2% to 100%, respectively, for overall bone involvement. In contrast, for BS, the values were 86.7–89.3% for sensitivity and 60.8–96.1% for specificity ($p < 0.001$), considering "optimistic" or "pessimistic" classifications of equivocal lesions. A region-based analysis of 1,115 bone regions with 410 metastases showed a PSMA-PET/CT sensitivity and specificity of 98.8–99.0% and 98.9–100%, respectively, while BS demonstrated a sensitivity of 82.4–86.6% and specificity of 91.6–97.9%. ^{68}Ga PSMA PET/CT exhibited superior performance in all subgroups, except for the patient-based analysis of mCRPC [50].

Prostate-specific membrane antigen positron emission tomography/computed tomography and other diagnostic modalities in high-risk prostate cancer

Hirmas et al. [26] compared the diagnostic efficacy of ^{68}Ga PSMA-PET/CT with that of CT, MRI, and BS for the primary staging of 21 patients with high-risk PC. ^{68}Ga PSMA-PET/CT demonstrated a markedly increased concordance rate with BS, MRI, and CT (90%, 75%, and 73%, respectively). It exhibited similar precision to that of MRI in identifying prostate lesions but superior accuracy in detecting suspicious pelvic LNs. It outperformed CT in detecting suspicious pelvic LNs and extra-pelvic LNs, and outperformed BS in detecting bone lesions. Utilisation of ^{68}Ga PSMA--PET/CT resulted in management changes for 11 patients. Those findings suggest potential advantages of using ^{68}Ga PSMA-PET/CT over other modalities in PC diagnosis and staging, particularly in terms of specificity, accuracy in detecting LNs, and impact on patient management. However, further research and larger populations are needed for confirmation.

ECONOMIC ASPECTS

Several studies have explored the cost implications of utilising PSMA-PET/CT in different healthcare settings. Holzgreve et al. [51] found that in Europe and the US, PSMA-PET/CT is generally associated with increased costs. Notably, the scan duration plays a significant role in determining the cost-effectiveness. Despite the higher upfront costs, the expenses related to achieving an accurate diagnosis through ^{68}Ga PSMA-PET/CT appear to be reasonable when compared to the potential downstream costs associated with inaccurate diagnosis [51].

LIMITATIONS OF PROSTATE-SPECIFIC MEMBRANE ANTIGEN POSITRON EMISSION TOMOGRAPHY/COMPUTED TOMOGRAPHY

Although it is a rapid and noninvasive imaging modality, it has limitations and potential side effects. The efficacy of ^{68}Ga PSMA-PET/CT can be influenced by various factors, such as dual-time-point acquisition, androgen deprivation therapy, forced diuresis, and hydration. Although patients undergoing ^{68}Ga PSMA-PET/CT are subjected to radiation, the dose is relatively low [52]. Notably, the risk of cancer mortality due to serial radiation exposure through CT, estimated at approximately 2% over 30 consecutive years of annual exposure, is considered negligible for most patients who undergo several ^{68}Ga PSMA-PET/CT scans during their lifetime [53].

Difficulties in interpreting ^{68}Ga PSMA-PET/CT images may occur for patients who have trouble remaining still during the scan, possibly necessitating repeat imaging or sedation to improve the image quality. Additionally, variations in the timing of tracer administration and SUV measurements can introduce interdepartmental and international differences [54, 55].

Clinically, the effectiveness of ^{68}Ga PSMA-PET/CT for detecting PC has been extensively documented, with positive scans observed in most patients with suspected cancer (approximately 83%), demonstrating high specificity.

Despite its high accuracy compared to that of cross-sectional imaging, ^{68}Ga PSMA-PET/CT has limitations, such as occurrence of false-negative results, especially in detecting small nodal metastases below the spatial resolution of PET [55]. Mannweiler et al. [56] found that 5% of primary PC and 15% of PC metastases show negativity for PSMA on immunohistochemistry. Moreover, the concept of stage migration, impacted by the precision of ^{68}Ga PSMA-PET/CT, has become a topic of interest. Patients who experience upstaging may now represent a more favourable disease state than others in the updated stage classification. While survival rates have improved, no impact on individual patient outcomes is evident – a phenomenon commonly referred to as the "Will Rogers phenomenon".

Despite its diagnostic superiority, PSMA-PET/CT faces several practical limitations. Accessibility remains a major challenge because this technology is not uniformly available across healthcare systems, particularly in low-resource settings. Additionally, the high costs associated with PSMA ligands and PET imaging infrastructure can limit widespread adoption. Economic analyses, such as the research by Holzgreve et al. [51], highlight that although PSMA-PET/CT may reduce downstream costs by improving diagnostic accuracy, the upfront expenses are significantly higher compared to conventional imaging modalities. These factors necessitate a balanced consideration of cost-effectiveness and resource allocation when integrating PSMA-PET/CT into routine clinical practice.

CONCLUSIONS

The advent of PSMA-PET/CT imaging for the primary staging of PC presents transformative potential for refining diagnostic accuracy and treatment planning. Traditional methods, including MRI, CT, and BS, have sensitivity limitations, which leads to the necessity of multiple imaging procedures to comprehensively assess the disease stage, therefore prolonging the time-to-treat, which potentially exacerbates oncological outcomes. Integrating PSMA-PET/CT, with its high specificity for prostate-specific membrane antigens, with traditional methods holds promise for a more efficient and precise staging examination.

The question posed regarding the feasibility of a single-stage examination for primary PC before RP determines the potential of PET/PSMA imaging. This technology offers a comprehensive and efficient approach for T-, N-, and M-staging, potentially streamlining the diagnostic pathway. However, ongoing research and economic evaluations are essential to determine the feasibility of its widespread clinical application and optimal integration of PSMA-PET/CT into the evolving landscape of PC staging protocols.

Economic evaluations underline the possible cost-effectiveness of ^{68}Ga PSMA-PET/CT, especially when considering its impact on treatment outcomes and avoidance of futile approaches. The demonstrated accuracy of PSMA-PET/CT in guiding treatment decisions, as reflected in its superior sensitivity and specificity compared to those of traditional methods, supports its role in optimising patient selection for definitive treatment.

Retrospective studies offer compelling evidence that integrating ^{68}Ga PSMA-PET/CT into the diagnostic pathway potentially leads to changes in tactics for managing patients diagnosed with PC. The ability to identify lesions that may be missed by other imaging modalities, coupled with their impact on treatment decisions, positions PSMA-PET/CT as a transformative tool in the clinical landscape of PC.

In essence, PSMA has emerged not only as a diagnostic powerhouse but also as a driver of change in treatment strategies. As research continues to validate its long-term impact on patient outcomes, PSMA-PET/CT remains a pivotal player in the pursuit of precision medicine for PC management. Whilst PSMA-PET/CT has significant advantages in detecting PC, its limitations include technical challenges, radiation exposure, and potential clinical implications, such as false-negative results and stage migration. The overall effects of those limitations on patient outcomes and survival rates require careful consideration.

CONFLICTS OF INTEREST

The authors declare no conflict of interest.

FUNDING

This research received no external funding.

ETHICS APPROVAL STATEMENT

The ethical approval was not required.

References

1. Rawla P. Epidemiology of Prostate Cancer. World J Oncol. 2019; 10: 63-89.
2. Siegel RL, Miller KD, Wagle NS, Jemal A. Cancer statistics, 2023. CA Cancer J Clin. 2023; 73: 17-48.
3. Brizmohun Appayya M, Adshead J, Ahmed HU, et al. National implementation of multi-parametric magnetic resonance imaging for prostate cancer detection – recommendations from a UK consensus meeting. BJU Int. 2018; 122: 13-25.
4. Turpin A, Girard E, Baillet C, Pasquier D, Olivier J, Villers A, et al. Imaging for Metastasis in Prostate Cancer: A Review of the Literature. Front Oncol. 2020; 10: 55.
5. Oesterling JE, Martin SK, Bergstralh EJ, Lowe FC. The Use of Prostate-Specific Antigen in Staging Patients With Newly Diagnosed Prostate Cancer. JAMA. 1993; 269: 57-60.
6. Caglic I, Kovac V, Barrett T. Multiparametric MRI – Local staging of prostate cancer and beyond. Radiol Oncol. 2019; 53: 159-170.
7. Abuzallouf S, Dayes I, Lukka H. Baseline staging of newly diagnosed prostate cancer: A summary of the literature. J Urol. 2004; 171: 2122-2127.
8. Kiss B, Thoeny HC, Studer UE. Current Status of Lymph Node Imaging in Bladder and Prostate Cancer. Vol. 96, Urology. 2016; 96: 1-7.
9. Harisinghani MG, Barentsz J, Hahn PF, et al. Noninvasive Detection of Clinically Occult Lymph-Node Metastases in Prostate Cancer. N Engl J Med. 2003; 348: 2491-2499.
10. Hövels AM, Heesakkers RAM, Adang EM, et al. The diagnostic accuracy of CT and MRI in the staging of pelvic lymph nodes in patients with prostate cancer: a meta-analysis. Clin Radiol. 2008; 63: 387-395.
11. Flanigan RC, McKay TC, Olson M, Shankey TV, Pyle J, Waters WB. Limited efficacy of preoperative computed tomographic scanning for the evaluation of lymph node metastasis in patients before radical prostatectomy. Urology. 1996; 48: 428-432.
12. Tiguert R, Gheiler EL, Tefilli MV, et al. Lymph node size does not correlate with the presence of prostate cancer metastasis. Urology. 1999; 53: 367-371.
13. Spevack L, Killion LT, West JC, Rooker GM, Brewer EA, Cuddy PG. Predicting the patient at low risk for lymph node metastasis with localized prostate cancer: An analysis of four statistical models. Int J Radiat Oncol Biol Phys. 1996; 34: 543-547.
14. Shen G, Deng H, Hu S, Jia Z. Comparison of choline-PET/CT, MRI, SPECT, and bone scintigraphy in the diagnosis of bone metastases in patients with prostate cancer: a meta-analysis. Skeletal Radiol. 2014; 43: 1503-1513.
15. Briganti A, Passoni N, Ferrari M, et al. When to Perform Bone Scan in Patients with Newly Diagnosed Prostate Cancer: External Validation of the Currently Available Guidelines and Proposal of a Novel Risk Stratification Tool. Eur Urol. 2010; 57: 551-558.
16. Lin Y, Mao Q, Chen B, et al. When to perform bone scintigraphy in patients with newly diagnosed prostate cancer? A retrospective study. BMC Urol 2017; 17: 41.
17. Kwon DH, Velazquez AI, De Kouchkovsky I. PSMA PET Scan. JAMA Oncol. 2022; 8: 1860.
18. Lauri C, Chiurchioni L, Russo VM, Zannini L, Signore A. PSMA Expression in Solid Tumors beyond the Prostate Gland: Ready for Theranostic Applications? J Clin Med. 2022; 11: 6590.
19. Heitkötter B, Steinestel K, Trautmann M, et al. Neovascular PSMA expression is a common feature in malignant neoplasms of the thyroid. Oncotarget. 2018; 9: 9867-9874.
20. Jiao D, Li Y, Yang F, et al. Expression of prostate-specific membrane antigen in tumor-associated vasculature predicts poor prognosis in hepatocellular carcinoma. Clin Transl Gastroenterol. 2019; 10: 1-7.
21. Bilgin R, Ergül N, Çermik TF. Incidental meningioma mimicking metastasis of prostate adenocarcinoma in 68Ga-labeled PSMA ligand PET/CT. Clin Nucl Med. 2016; 41: 956-958.
22. Zacho HD, Nielsen JB, Dettmann K, Hjulskov SH, Petersen LJ. 68Ga-PSMA PET/CT uptake in intramuscular myxoma imitates prostate cancer metastasis. Clin Nucl Med. 2017; 42: 487-488.
23. Malik D, Basher RK, Sood A, Devana SK, Bhattacharya A, Mittal BR. Herniated thoracic spleen mimicking lung metastasis on 68Ga-labeled prostate-specific membrane antigen pet/ct in a patient with prostate cancer. Clin Nucl Med. 2017; 42: 485-486.
24. Wu SY, Boreta L, Shinohara K, et al. Impact of Staging 68 Ga-PSMA-11 PET Scans on Radiation Treatment Plansin Patients With Prostate Cancer. Urology. 2019; 125: 154-162.
25. Fuccio C, Castellucci P, Schiavina R, et al. Role of 11C-choline PET/CT in the restaging of prostate cancer patients showing a single lesion on bone scintigraphy. Ann Nucl Med. 2010; 24: 485-492.
26. Hirmas N, Al-Ibraheem A, Herrmann K, et al. [68Ga]PSMA PET/CT Improves Initial Staging and Management Plan of Patients with High-Risk Prostate Cancer. Mol Imaging Biol. 2019; 21: 574-581.
27. Hoffman A, Amiel GE. The Impact of PSMA PET/CT on Modern Prostate Cancer Management and Decision Making – The Urological Perspective. Cancers (Basel) 2023; 15: 3402.
28. Kotb AF, Elabbady AA. Prognostic Factors for the Development of Biochemical Recurrence after Radical Prostatectomy. Prostate Cancer. 2011; 2011: 485189.
29. Heidenreich A, Bastian PJ, Bellmunt J, et al. EAU guidelines on prostate cancer. Part II: Treatment of advanced, relapsing, and castration-resistant prostate cancer. Eur Urol. 2014; 65: 467-479.
30. Caroli P, Sandler I, Matteucci F, et al. 68 Ga-PSMA PET/CT in patients with recurrent prostate cancer after radical treatment: prospective results in 314 patients. Eur J Nucl Med Mol Imaging. 2018; 45: 2035-2044.
31. Houshmand S, Lawhn-Heath C, Behr S. PSMA PET imaging in the diagnosis and management of prostate cancer. Abdom Radiol (NY). 2023; 48: 3610-3623.
32. Miszczyk M, Rajwa P, Fazekas T, et al. The State of Intermediate Clinical Endpoints as Surrogates for Overall Survival in Prostate Cancer in 2024. Eur Urol Oncol. 2024; 7: 1195-1198.
33. van Leeuwen PJ, Emmett L, Ho B, et al. Prospective evaluation of 68Gallium-prostate-specific membrane antigen positron emission tomography/computed tomography for preoperative lymph node

staging in prostate cancer. BJU Int. 2017; 119: 209-215.

34. Cytawa W, Seitz AK, Kircher S, et al. 68Ga-PSMA I&T PET/CT for primary staging of prostate cancer. Eur J Nucl Med Mol Imaging. 2020; 47: 47: 168-177.

35. Papa N, Perera M, Murphy DG, et al. Patterns of primary staging for newly diagnosed prostate cancer in the era of prostate specific membrane antigen positron emission tomography: A population-based analysis. J Med Imaging Radiat Oncol. 2021; 65: 649-654.

36. Lima JP, Carvalho J, Quaresma V, et al. The role of Ga-68-PSMA PET/CT in the initial staging of prostate cancer – a single center 4 year experience. Res Rep Urol. 2021;13: 479-485.

37. Burdett S, Boevé LM, Ingleby FC, et al. Prostate Radiotherapy for Metastatic Hormone-sensitive Prostate Cancer: A STOPCAP Systematic Review and Meta-analysis. Eur Urol. 2019; 76: 115-124.

38. Fizazi K, Foulon S, Carles J, et al. Abiraterone plus prednisone added to androgen deprivation therapy and docetaxel in de novo metastatic castration-sensitive prostate cancer (PEACE-1): a multicentre, open-label, randomised, phase 3 study with a 2×2 factorial design. Lancet. 2022; 399: 1695-1707.

39. Miszczyk M, Rajwa P, Yanagisawa T, et al. The Efficacy and Safety of Metastasis-directed Therapy in Patients with Prostate Cancer: A Systematic Review and Meta-analysis of Prospective Studies. Eur Urol. 2024; 85: 125-138.

40. Barentsz JO, Richenberg J, Clements R, et al. ESUR prostate MR guidelines 2012. Eur Radiol. 2012; 22: 746-757.

41. Daryanani A, Turkbey B. Recent Advancements in CT and MR Imaging of Prostate Cancer. Semin Nucl Med. 2022; 52: 365-373.

42. Berger I, Annabattula C, Lewis J, et al. 68Ga-PSMA PET/CT vs. mpMRI for locoregional prostate cancer staging: Correlation with final histopathology. Prostate Cancer Prostatic Dis. 2018; 21: 204-211.

43. Sonni I, Felker ER, Lenis AT, et al. Head-to-head comparison of 68Ga-PSMA-11 PET/CT and mpMRI with histopathology gold-standard in the detection, intra-prostatic localization and local extension of primary prostate cancer: results from a prospective single-center imaging trial. J Nucl Med. 2022; 63: 847-854.

44. Li Y, Han D, Wu P, Ren J, Ma S, Zhang J, et al. Comparison of 68Ga-PSMA-617 PET/CT with mpMRI for the detection of PCa in patients with a PSA level of 4–20 ng/ml before the initial biopsy. Sci Rep. 2020; 10: 10963.

45. Oprea-Lager DE, Cysouw MCF, Boellaard R, et al. Bone Metastases Are Measurable: The Role of Whole-Body MRI and Positron Emission Tomography. Front Oncol. 2021; 11: 772530.

46. Hofman MS, Lawrentschuk N, Francis RJ, et al. Prostate-specific membrane antigen PET-CT in patients with high-risk prostate cancer before curative-intent surgery or radiotherapy (proPSMA): a prospective, randomised, multicentre study. Lancet. 2020; 395: 1208-1216.

47. Wang X, Wen Q, Zhang H, Ji B. Head-to-Head Comparison of 68Ga-PSMA-11 PET/CT and Multiparametric MRI for Pelvic Lymph Node Staging Prior to Radical Prostatectomy in Patients With Intermediate to High-Risk Prostate Cancer: A Meta-Analysis. Front Oncol. 2021; 11: 737989.

48. Kane CJ, Amling CL, Johnstone PAS, et al. Limited value of bone scintigraphy and computed tomography in assessing biochemical failure after radical prostatectomy. Urology. 2003; 61: 607-611.

49. Liu F, Dong J, Shen Y, et al. Comparison of PET/CT and MRI in the Diagnosis of Bone Metastasis in Prostate Cancer Patients: A Network Analysis of Diagnostic Studies. Front Oncol. 2021; 11: 736654.

50. Pyka T, Okamoto S, Dahlbender M, et al. Comparison of bone scintigraphy and 68Ga-PSMA PET for skeletal staging in prostate cancer. Eur J Nucl Med Mol Imaging. 2016; 43: 2114-2121.

51. Holzgreve A, Unterrainer M, Calais J, et al. Is PSMA PET/CT cost-effective for the primary staging in prostate cancer? First results for European countries and the USA based on the proPSMA trial. Eur J Nucl Med Mol Imaging. 2023; 50: 3750-3754.

52. Fendler WP, Eiber M, Beheshti M, et al. 68Ga-PSMA PET/CT: Joint EANM and SNMMI procedure guideline for prostate cancer imaging: version 1.0. Eur J Nucl Med Mol Imaging. 2017; 44: 1014-1024.

53. Brenner DJ, Elliston CD. Estimated radiation on risks potentially associated with full-body CT screening. Radiology. 2004; 232: 735-738.

54. Kapoor M, Kasi A. PET Scanning. StatPearls [Internet]. 2022 Oct 3. Available at: https://www.ncbi.nlm.nih.gov/books/NBK559089/.

55. Afshar-Oromieh A, Malcher A, Eder M, et al. Pet imaging with a [68ga]gallium-labelled psma ligand for the diagnosis of prostate cancer: Biodistribution in humans and first evaluation of tumour lesions. Eur J Nucl Med Mol Imaging. 2013; 40: 486-495.

56. Mannweiler S, Amersdorfer P, Trajanoski S, Terrett JA, King D, Mehes G. Heterogeneity of prostate-specific membrane antigen (PSMA) expression in prostate carcinoma with distant metastasis. Pathol Oncol Res. 2009; 15: 167-172. ■

REVIEW PAPER

FUNCTIONAL UROLOGY

Role of gabapentin in the management of neurogenic overactive bladders: A systematic review

Roshan Chanchlani[1], Ketan Mehra[2], Pramod K. Sharma[1], Sudarsan Agarwal[3], Amit Gupta[1], Reyaz Ahmad[1], Rakesh Mishra[4], Amit Agarwal[4], Suresh Kumar Thanneeru[1]

[1]*Department of Pediatric Surgery, All India Institute of Medical Sciences, Bhopal, India*
[2]*Department of Urology, All India Institute of Medical Sciences, Bhopal, India*
[3]*Department of Neurosurgery, SVRRGGH Tirupati, India*
[4]*Department of Neurosurgery, All India Institute of Medical Sciences, Bhopal, India*

Citation: Chanchlani R, Mehra K, Sharma PK, et al. Role of gabapentin in the management of neurogenic overactive bladders: A systematic review. Cent European J Urol. 2025; 78: 61-69.

Article history
Submitted: May 30, 2024
Accepted: Sep. 24, 2024
Published online: Mar. 21, 2025

Corresponding author
Suresh Kumar Thanneeru
Department of Pediatric Surgery,
All India Institute of Medical Sciences,
2nd-floor Hospital Building,
Academic block,
AIIMS, Bhopal,
Madhya Pradesh, India
tanirsuresh@yahoo.in

Introduction Neurogenic lower urinary tract dysfunction is typically managed through a step-up approach, beginning with anticholinergic medications, progressing to Botulinum toxin injections, and surgical interventions. Gabapentin offers a less invasive option, either as an adjunct to anticholinergics or as a standalone therapy. This systematic review examines gabapentin's efficacy and safety in treating neurogenic overactive bladders (NOAB) in both paediatric and adult populations.
To determine gabapentin's effect on reducing bladder pressure, increasing bladder capacity, and alleviating incontinence symptoms in NOAB patients.

Material and methods A systematic search was conducted on PubMed, Scopus, ScienceDirect, and Cochrane to identify studies on gabapentin for NOAB. Articles were sorted according to PRISMA guidelines, and the risk of bias was assessed using the JBI clinical appraisal tool. Data from the selected articles were synthesized qualitatively.

Results Of the 116 identified articles, 6 were selected. Two focused on paediatric patients with neural tube defects, while four studies involved adults with conditions like spinal trauma, Parkinson's disease, and multiple sclerosis. Urodynamic parameters improved in four studies, whether gabapentin was used alone or as an adjunct. All 6 studies reported significant improvements and minimal side effects.

Conclusions While limitations in dosages and study durations hinder a definitive endorsement of gabapentin, the overall positive response across studies suggests its potential efficacy in managing NOAB. Further high-quality randomized controlled trials comparing gabapentin with other treatments and exploring factors related to non-responsiveness are warranted for conclusive insights.

Key Words: gabapentin ‹› anticholinergics ‹› neurogenic overactive bladder

INTRODUCTION

Neurogenic bladder overactivity is prevalent among both pediatric and adult patients with Neurogenic lower urinary tract dysfunction. Management typically progresses from oral medication, with or without clean intermittent catheterization (CIC), to interventions such as Botulinum toxin injections and, in some cases, surgical procedures [1]. Anticholinergics represent a common pharmacological approach, yet their efficacy is variable, with many patients experiencing significant side effects that impact tolerability [2]. In response, alternative treatments have been explored, including gabapentin, which operates via a distinct mechanism from anticholinergics. Although gabapentin has been investigated in limited studies as either an adjunct or standalone therapy for this indication, the overall evidence remains fragmented. This systematic review aims to synthesize and evaluate existing findings to elucidate

the current understanding of gabapentin's efficacy and safety profile in the treatment of neurogenic overactive bladder (NOAB).

PICO Question

In patients with neurogenic overactive bladder (P), does the use of gabapentin (I) reduce bladder pressure, increase bladder capacity, and alleviate symptoms of incontinence (O)?

MATERIAL AND METHODS

We used the Preferred Reporting Items for Systematic Reviews and Meta-Analyses (PRISMA) guidelines for conducting the present review [3].

Search strategy

A systematic literature search was conducted on PubMed, SCOPUS, the Cochrane Library, and ScienceDirect databases using the search terms outlined in Table 1. Additionally, the reference lists of included studies were reviewed for potentially relevant articles. Four investigators (SKT, AA, SA, and RC) independently screened abstracts, with selected articles undergoing full-text evaluation. Conflicts were resolved through consensus, resulting in a final list of studies.

Inclusion criteria

Studies assessing the efficacy of gabapentin, either alone or in combination with other drugs, for managing patients with NOAB were considered. This includes randomized controlled trials, non-randomized studies, prospective and retrospective observational studies, and case series published in English.

Exclusion criteria

Studies not using gabapentin or studies using gabapentin but not for NOAB, postmortem studies, case reports, letters to the editor, abstracts from congresses, conferences, symposiums, reports published in meeting booklets, and literature not in English were excluded.

Data extraction

Four investigators (SKT, AA, SA, and RC) independently assessed studies and extracted data using a pre-designed proforma based on the inclusion criteria. The study selection process is illustrated in Figure 1 using the PRISMA flowchart. Details

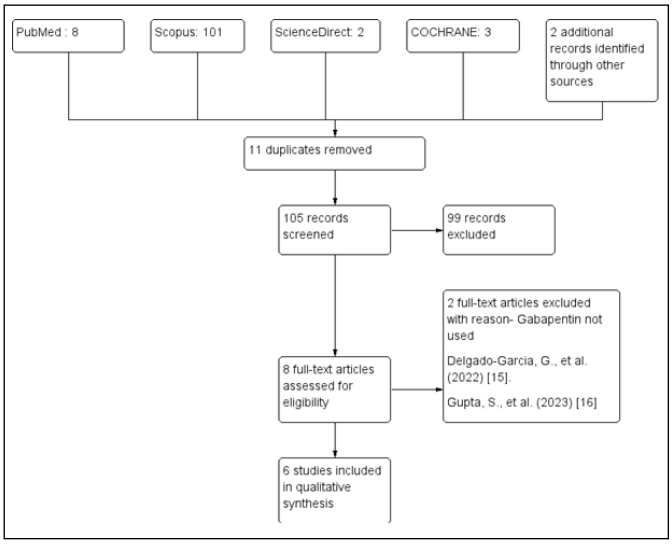

Figure 1. *PRISMA Flow Chart.*

extracted included Study ID, Journal, Country of Publication, Study Design, Number of Participants, Patient Characteristics, Objectives, Results, Key Conclusions, and Outcomes. Specific information collected encompassed urodynamic parameters such as bladder capacity and volume, as well as data related to bladder diary entries, including incontinence episodes, total voided volume, and other symptomatology scores.

Missing data

Authors were contacted for missing data, and any discrepancies were resolved through consensus.

Risk of bias and quality assessment

We utilized the revised JBI (Joanna Briggs Institute in Royal Adelaide Hospital in Melbourne) critical appraisal tool to assess the risk of bias in accordance with the methodologies of the included studies [4], encompassing randomized controlled trials [5], Qausi experimental studies [6], cohort studies, case series [7], and observational analytical studies.

RESULTS

Study selection

Our search strategy yielded 114 studies, with 11 identified as duplicates. After excluding 99 records based on title search, 6 full-text articles were selected for review. Additionally, 2 articles were added based on citations from the selected articles, while 2 were excluded with reasons. In total, 6 arti-

cles were included for qualitative synthesis. Details of the study selection process are illustrated in Figure 1 using the PRISMA chart.

Study characteristics

Of the 6 articles included in our review, two focused on pediatric patients, while the remaining four studied adults. Combined, these articles involved a total of 243 patients. Both pediatric studies were conducted in India, while the adult studies spanned Turkey, Italy, the USA, and the Philippines. In the pediatric studies, neural tube defects were the primary pathology, while spinal cord injury was the focus of one adult study, and various spinal and supraspinal pathologies were examined in the other three. Three studies utilized gabapentin as an adjunct therapy, while three employed it as a standalone treatment. Outcomes assessed included maximum bladder capacity and detrusor pressure through urodynamic studies in four of the included studies, while symptom improvement was evaluated in all six studies. The detailed study characteristics are mentioned in Table 2.

The dosage of gabapentin used across all the studies

For paediatric patients, Ansari et al. [8] utilized gabapentin at 10-20 mg/kg/day in three divided doses for a mean duration of 14.5 ±7.5 months, while Dash et al. [2] administered gabapentin at a dosage of 20 mg/kg/day for 6 months to 1 year.
In studies involving adult patients, Cakici et al. [9] initiated gabapentin with incremental doses ranging from 100 mg/day to 3600 mg/day. Carbone et al. [10] administered gabapentin at a dosage of 300 mg once daily, which was increased to 900 mg/day over 1 month. Kim et al. [11] prescribed gabapentin at 100 to 300 mg at bedtime, gradually titrating up to 3,000 mg based on symptoms, with follow-up ranging from 12 weeks to 12 months. Chua et al. [12] utilized gabapentin at a dosage of 100 mg OD, up to a maximum of 900 mg OD.

Table 1. *Details of search strategy*

Database	Search details
COCHRANE	3 trials matching gabapentin neurogenic bladder in Title Abstract Keyword
PubMed	(“gabapentin” [MeSH Terms] OR “gabapentin” [All Fields] OR “gabapentine” [All Fields] OR “gabapentin s” [All Fields]) AND (“urinary bladder, neurogenic” [MeSH Terms] OR (“urinary” [All Fields] AND “bladder” [All Fields] AND “neurogenic” [All Fields]) OR “neurogenic urinary bladder” [All Fields] OR (“neurogenic” [All Fields] AND “bladder” [All Fields]) OR “neurogenic bladder” [All Fields])) AND (1000/1/1:2024/4/24[pdat])
ScienceDirect	Title, abstract, keywords: gabapentin neurogenic bladder
SCOPUS	TITLE-ABS-KEY (gabapentin AND neurogenic AND bladder)

Results with respect to urodynamic study indicators

Four studies reported outcomes regarding urodynamic parameters, namely Ansari, M. S., et al. (2013) [8], Cakici, O. U., et al. (2021) [9], Carbone, A., et al. (2006) [10], Dash, V., et al. (2016) [2]. Across these four studies, there was a significant trend of improvement in urodynamic parameters following gabapentin usage. There were significant reductions in maximal detrusor pressure from the baseline reported across all the studies. Similarly, the bladder capacity was reported to have significantly enhanced. Detailed results are presented in Table 3.

Results with respect to symptomatic improvement

Six studies reported outcomes related to patient-reported outcome measures, including Ansari, et al. [8], Cakici et al. [9], Carbone et al. [10], Dash et al. [2], Kim et al. [11], Chua et al. [12]. All these studies demonstrated a significant improvement in symptomatic outcomes following gabapentin usage. The symptomatic outcomes were mainly a reduction in incontinence episodes, improvement in patient/parent perception of bladder contraction (PPBC), voiding volumes, decrease in frequency, and nocturia. Detailed results are presented in Table 3.

Risk of bias and quality assessment

Of the six articles included in our review, two were randomized controlled trials (RCTs), one was a quasi-non-randomized trial, one was a retrospective cohort study, one was a cross-sectional analytical study, and one was a case series. We utilized the JBI tool to assess the risk of bias and the quality of the methodology. Detailed assessments are provided in Table 4.
Chua et al. [12], conducted an RCT with a lower risk of bias. Dash et al. [2], conducted an RCT with a moderate risk of bias. Ansari et al. (2013) [8], conducted a Quasi-Non-Randomized study with a moderate risk of bias. Cakici et al. [9], conducted a retrospective cohort study with moderate risk of bias. Kim et al. [11], conducted an analytical cross-sectional study with moderate risk of bias. Carbone et al. [10], conducted a case series with a lower risk of bias. Additional details are provided in Table 3.

Table 2. *Characteristics of included studies*

Study authors (year)	Country	Type of study	Participants	Sample size	Mean age (years)	Inclusion criteria	Exclusion criteria	Dosage and follow-up	Outcomes/Results	Adverse effects	Conclusion
Ansari et al. 2013 [8]	India	Quasi Randomised trial	Paediatric spina bifida (84.61%) Tethered cord (11.54%) Sacral agenesis (3.85%)	NB – 26, NNB – 5	8.5 ±5.3	Children with LUTS with urodynamically proven Detrusor overactivity ± low compliance; not responding to anticholinergics for 6 months	UTI and bladder stones	GP 10–20 mg/kg/ day in three divided doses. The mean duration of treatment was 14.5±7.5 months	**UDS:** Max bladder capacity: p <0.02; Max Detrusor contraction: p <0.05 **PPBC scale:** p <0.05 **Symptoms:** Voided volume: p <0.03 Urge incontinence/ day: p <0.05 PVR >10%: NS	46.7% did not respond to GP. Concentration problems, mood swings, hyperactivity, somnolence, anxiety. 1 patient had drowsiness, dizziness, and headache – stopped GP	GP has given moderate results in OAB refractory to conventional anticholinergics with fewer adverse effects
Cakici et al. 2021 [9]	Turkey	Retrospective cohort study	Adults with spinal cord injury above the sacral level	27	32.03 ± 6.7	Spinal cord injury patients with UDS showing OAB despite anticholinergic and mirabegron	Not clear	GP incremental doses starting with 100 mg/day to 3,600 mg per day	**Symptoms:** Visual Analogue Scale: p <0.001 Daily incontinence episodes: p< 0.001 **UDS:** Max detrusor pressure: p <0.01 Max bladder volume: p <0.01	Response is seen in only 11 (40.17%), unresponsive in 16 (but they have an improvement in pain). No side effects were mentioned	GP can be considered for 3rd or further option before Botulinum toxin injection for OAB-NB who are not responding
Carbone et al. 2006 [10]	Italy	Case series	Multiple infarctions, Parkinson's, multiple sclerosis, post-infectious myelitis, frontal syndrome	16	61.69 ±10.72	Patients with detrusor overactivity due to neurogenic origin	Not clear	GP 300 mg once daily and increased to 900 mg/day; 1 month follow-up	**Symptoms:** IPSS score: p <0.023; **UDS:** Medium amplitude of involuntary detrusor contractions: NS Bladder capacity: p = 0.05 P Det/Qmax: p = 0.05	2 patients (12.5%) minor adverse reactions- dizziness and somnolence	GP can be a novel treatment for the treatment of overactive bladder
Chua et al. 2018 [12]	Philippines	RCT	Adults with overactive bladder symptoms	GP – 31 Solifenacin – 31 Placebo – 32	GP – 55.2 Solifenacin – 57.2 Placebo –53.9	Ambulatory patients with OAB symptoms for > 3 months based on OAB-Q scores	Contraindi-cation for drugs GP and solifenacin; UTI, stones, mixed incontinence, outlet obstruction	GP 100 mg OD to max of 900 mg OD; solifenacin 5 mg OD to 10 mg OD for 3 months	**Symptoms:** Mean change in urge incontinence episodes/ day; nocturia; mean volume per void were significant in GP and solifenacin groups **The health-related quality of life domain assessment is significant, and sleeping is significantly improved with GP**	5 patients (16%) in placebo, 5 (16%) in GP, and 11 (35%) in solifenacin group have adverse effects but not significant	Study was able to evaluate the efficacy of GP by showing the improvement in OAB symptoms

Table 2. *Continued*

Study authors (year)	Country	Type of study	Participants	Sample size	Mean age (years)	Inclusion criteria	Exclusion criteria	Dosage and follow-up	Outcomes/Results	Adverse effects	Conclusion
Dash et al. 2016 [2]	India	RCT	Children operated for lumbo-sacral menin-gomyelocele	Oxybutynin group – 14 GP – 17 Both drugs group – 13	6.1	At least 3 years old, not on anticholinergics, and had detrusor instability	VUR, bladder areflexia, already on medication, post-surgery for neurogenic bladder	GP 20 mg/kg/ day; oxybutynin 5 mg twice a day, follow up for 6 months and 1 year, drugs were stopped 3 weeks before UDS	**Symptoms:** DVSS improvement (1 year): p 0.076 Mean incontinence grade: p 0.774; **UDS:** Mean compliance: p = 0.322; Peak detrusor pressure: p = 0.04 Bladder capacity: p = 0.008	2 patients (30%) had severe headaches and were taken off the study	GP is a good alternative to oxybutynin for overactive bladders, both as mono and add-on therapy
Kim et al. 2004 [11]	USA	Analytical cross-sectional study	OAB/Nocturia due to Multiple sclerosis, mixed urge, and stress incontinence, transurethral resection of the prostate, 3 microwave of prostate	31	51	Patients with OAB and nocturia not responding to anticholinergic therapy (at least for 8 weeks)	Not clear? Bladder outlet obstruction, dyssynergia	GP – 100 mg to 300 mg at bedtime and slowly titrated to 3,000 mg based on symptomatology. Followed up for 12 weeks to 12 months	14 of the 31 patients responded Symptoms: Frequency at 12 weeks-improved with p = 0.01 Nocturia – improved with p = 0.03	6 patients had adverse effects of drowsiness and lethargy	GP well tolerated and can be considered in selective patients with failed anticholinergic therapy

GP – gabapentin; IPSS – International Prostate Symptom Score; LUTS – lower urinary tract symptoms; NB – neurogenic bladder; NNB – non-neurogenic-neurogenic bladder; PPBS scale – Patient/Parent perception of bladder condition; PVR – post-void residue; UDS – urodynamic studies; UTI – urinary tract infection

Table 3. *Results of the included studies*

Author	Urodynamic parameters		Symptomatic parameters	
	Detrusor pressure	Bladder capacity	Continence	Others
Ansari et al. 2013 [8]	Decreased pressures from 75 ±35 to 25 ±15 cm H_2O (p < 0.02)	Increased bladder capacity from 210 ±94 to 360 ±110 ml (p < 0.02).	Improved continence in 53% of patients, with an increase in voiding volume from 170 ±90 to 320 ±110 ml (p < 0.03)	Reported significant improve-ment in PPBC scale (p < 0.05)
Cakici et al. 2021 [9]	Decreased pressures from 38.81 ±15.17 to 21.72 ±8.62 cm of H_2O (p = 0.01)	Improved bladder volume from 239.63 ±58.19 to 262.81 ±48.01 ml (p = 0.01)	Improvement in daily incontinence episodes in the responsive group (p < 0.001), from 6.54 episodes before treatment to 2.27 episodes after treatment	NA
Carbone et al. 2006 [10]	Decreased medium amplitude of involuntary detrusor contraction pressures from 49 ±16 cm H_2O to 42.4 ±17 cm of H_2O (p = not significant)	Increased bladder capacity from 342 ±99 ml to 430 ±98 ml (p = 0.05)	Observed a decrease in incontinence episodes per day from 3 (2) to 1 (0.3)	Significant improvement in the IPSS (p < 0.023). 14.8 before tre-atment to 8.8 after treatment
Chua et al. 2018 [12]	NA	NA	Significant changes in mean urge incontinence episodes/ day: 0.68 (0.14) with a p-value of <0.001	Nocturia: 1.39 (0.15) with a p-value of <0.001 The volume of void urine im-proved from a baseline of 44.39 (1.72) ml with a p-value of <0.001
Dash et al. 2016 [2]	Maximum detrusor pressure from 69.40 ±16.36 to 44.73 ±17.40 cm of H_2O (p = 0.04)	Improvement in bladder capacity from 10.24% to 16.72% (p = 0.008)	Mean incontinence grade (p = 0.774).	Improvement in DVSS (p = 0.076)
Kim et al. 2004 [11]	NA	NA	Improvement in frequency (p = 0.01)	Improvement in nocturia (p = 0.03)

DVSS – Dysfunctional Voiding Symptom Score; IPSS – International Prostate Symptom Score; NA – not applicable; PPBC – Patient/Parent perception of bladder condition

Table 4. *JBI critical appraisal tool for RCTs*

Study ID	P1	P2	P3	P4	P5	P6	P7	P8	P9	P10	P11	P12	P13
Chua et al. 2018 [12]	Yes	Yes	Yes	Yes	Yes	Yes	Yes	Yes	Yes	Yes	Yes	Yes	Yes
Dash et al. 2016 [2]	Yes	Unclear	Yes	Unclear	Unclear	Yes	Unclear	Yes	Yes	Yes	Yes	Yes	Yes
JBI critical appraisal tool for analytical cross-sectional studies													
Kim et al. 2004 [11]	Unclear	Yes	Yes	No	Unclear	Unclear	Yes	Yes					
JBI critical appraisal tool for qasi experimental studies													
Ansari et al. 2013 [8]	Yes	No	Unclear	Unclear	Yes	Yes	Yes	Yes	Yes				
JBI critical appraisal tool for cohort studies													
Cakici et al. 2021 [9]	Yes	Yes	Yes	Unclear	Unclear	Yes	Yes	Yes	Unclear	Unclear	Yes		
JBI critical appraisal tool for case series													
Carbone et al. 2006 [10]	Yes	Yes	Yes	Unclear	Yes	Yes	Yes	Yes	Unclear	Yes			

JBI – Joanna Briggs Institute in Royal Adelaide Hospital in Melbourne

DISCUSSION

NOAB can affect individuals across the lifespan, from children with neural tube defects to the elderly. The pathophysiology of NOAB involves neurogenic origins, including reduced inhibitory neural impulses and increased afferent impulses from the bladder, a sensitive detrusor muscle exhibiting increased spontaneous activity, and an autonomous bladder with muscarinic stimulation. This can affect the upper tracts with increased pressures generated in the bladder, leading to renal damage. Moreover, NOAB significantly impacts daily activities such as work, travel, physical exercise, sleep, and sexual function. Early recognition and management of NOAB and reduction of the pressures generated in the bladder can help prevent renal damage due to back pressure changes and improve the quality of life in these patients [1].

Anticholinergics are commonly employed as first-line management for NOAB, exerting their effect by relaxing bladder smooth muscle via action on muscarinic receptors. However, these medications are associated with side effects such as dry mouth, fever, constipation, blurred vision, and somnolence. Studies have shown that only 50% of patients remain compliant with anticholinergic medication due to these adverse effects [1]. Consequently, newer anticholinergics have been introduced to mitigate these side effects. Patients who are refractory to pharmacotherapy may undergo botulinum injection and, if unsuccessful, may require surgical intervention.

Gabapentin, a gamma-aminobutyric acid analogue, is FDA-approved for epilepsy and neuropathic pain but has been utilized off-label for various conditions, including bipolar disorder, complex regional pain syndrome, attention deficit disorder, restless leg syndrome, sleep disorders, and alcohol withdrawal [13]. Although gabapentin shares structural similarities with GABA, it does not act directly on GABA receptors. The exact mechanism of action of gabapentin on neurogenic lower urinary tract symptoms (LUTS) is not known. Gabapentin and pregabalin, which is the S-enantiomer of 3-isobutyl GABA, are known as gabapentinoids. The excitation of afferent C fiber activity might be a possible cause of lower urinary tract symptoms in neurogenic bladder dysfunction. These gabapentinoids act on the $\alpha 2\delta$ subunits of voltage-gated calcium channels. By binding to these subunits, they inhibit calcium currents, thereby decreasing calcium influx. This results in a decreased release of neurotransmitters such as glutamate, noradrenaline, and substance P in the presynaptic area. The reduction in these signals can help the bladder relax and improve symptoms like urinary frequency [13, 14]. Gabapentin was first employed in urology for the treatment of interstitial cystitis [8]. However, its use and safety profile in children, particularly those under five years old, are not well-established despite its established use in epilepsy [16]. Given its distinct mechanism of action compared to anticholinergics, gabapentin may have an additive effect in managing NOAB. This review aims to assess the efficacy of gabapentin and elucidate its safety profile, particularly in children

Of the included studies, two are from the pediatric population. Ansari et al. [8] conducted a quasi-experimental study involving pediatric patients with neural tube defects and a mean age of 8.5 ±5.3 years. they focused on patients who did not respond to anticholinergics, using gabapentin in combination with anticholinergics for a minimum follow-up period of 6 months. Dash et al. [2] conducted a randomized controlled trial (RCT) on children with a mean age of 6.1 years diagnosed with lumbosacral myelomeningocele (MMC). These children had undergone surgery before the age of three and exhib-

ited detrusor instability. This study included three groups: anticholinergic therapy alone, gabapentin alone, and a combination of both. Unlike Ansari et al. [8], they included patients irrespective of their response to anticholinergics.

Both studies reported significant improvements in maximum detrusor pressure and bladder capacity with gabapentin. Dash et al. highlighted that combination therapy showed the most significant improvement compared to monotherapies, and gabapentin was better tolerated than oxybutynin. Ansari et al. [8] reported 46% non-responders to gabapentin, while Dash et al. did not report any non-responders to gabapentin.

Ansari et al. [8] used the patient/parent perception of bladder condition (PPBC) scale ($p < 0.05$), bladder dairy for continence, and voided volume, which was improved significantly. However, Dash et al. [2] used the Dysfunctional Voiding Symptom Score (DVSS) ($p = 0.076$) and mean incontinence grade ($p = 0.774$), which showed improvement but were not statistically significant.

Both studies showed substantial improvement in urodynamic parameters and Patient-Reported Outcome Measures (PROM) with gabapentin. However, the differences in the statistical significance of PROM improvements and non-responders to gabapentin may be attributed to sample size, which was small from both the studies and patient inclusion criteria where Ansari et al. [8] specifically included patients who were non-responders to anticholinergics, potentially indicating a more refractory patient population. In contrast, Dash et al. included all patients with detrusor instability, providing a broader patient base.

The remaining four studies are from the adult population. Cakici et al. [9], conducted a retrospective cohort study involving adults with spinal cord injuries above the sacral level who had refractory overactive detrusor that did not respond to anticholinergics and mirabegron and had neuropathic pain. The mean age of participants in their study was 32.03 ±6.7 years. Carbone et al. [10], presented a case series involving 16 patients with supraspinal pathologies such as multiple infarctions, Parkinson's disease, and multiple sclerosis. The mean age of their patients was 61.69 ±10.72 years. Kim et al. [11], conducted an analytical cross-sectional study on adult patients with various causes of overactive bladder (OAB), including multiple sclerosis, mixed urge and stress incontinence, and post-prostate resection, among others. The mean age of the patients was 51. They specifically included patients who had not responded to anticholinergic therapy and gabapentin was used as an add on therapy. Chua et al. [12], conducted a randomized controlled trial (RCT) in adults presenting with OAB symptoms, with a mean age of 55 years. They compared gabapentin with solifenacin and placebo.

With respect to the urodynamic profiles, two studies by Cakici et al. [9] and Carbone et al. [10] published their results. Both showed improvement in urodynamic parameters like maximum detrusor pressure, medium amplitude of involuntary detrusor contraction, and maximum bladder volume. However, Cakici et al. [9] reported that only 40% of the patients were responsive to gabapentin add-on therapy. The difference might be due to the use of gabapentin in patients already non-responsive to anticholinergics and mirabegron. Carbone et al. [10] did not report on maximum detrusor pressure per se but reported on the medium amplitude of involuntary detrusor contractions, which was decreased but not significant. This might be due to the very small number of included patients and the methodology being a case series. However, they reported that Pdet/Qmax in the pressure flow study showed a significant improvement with $p = 0.05$.

All four studies reported the results of the PROMs. Cakici et al. [9] reported a significant decrease in daily incontinence episodes in the responsive group from 6.54 (2.7) episodes before gabapentin to 2.27 (1.54) episodes after the treatment with a $p < 0.001$. Even though the incontinence episodes decreased in the unresponsive group also, the values were not significant. Carbone et al. [10] reported significant improvement in IPSS score, from 14.8 before treatment to 8.8 after treatment, with a p-value of 0.023. Chua et al. [12] reported improvement in urge incontinence episodes per day, nocturia, and volume per void with a p-value of <0.001. However, the results were not significant in comparison with solifenacin except for nocturia. Kim et al. [11] reported response in 14 out of 31 patients included. As mentioned before, gabapentin was used in refractory cases as an add-on therapy. Frequency has been improved in responders from 14.1 ±2.2 episodes before therapy to 10.0 ±2.1 episodes after therapy with a p-value of 0.01. Nocturia improved in responders from 4.0 ±1.3 to 1.0 ±0.3 with a p-value of 0.03.

Ansari et al. [8] reported serious adverse effects like drowsiness, dizziness, and headache in only one patient (3.3%), which required stoppage of gabapentin. 80% of the patients experienced mild adverse effects like concentration problems, mood swings, and hyperactivity. Dash et al. [2] reported severe headaches in two of their patients with gabapentin that required discontinuation of therapy, and 70% of the patients did not report any adverse reactions.

They also mentioned that only 43% of the patients were able to tolerate oxybutynin without any adverse effects, making a better comparison profile between gabapentin and oxybutynin. Cakici et al. [9] highlighted the abusive potential of gabapentin; however, they did not report any such side effects in their study population. Carbone et al. [10] reported no severe adverse reactions or discontinuation of gabapentin in their study. However, minor adverse reactions like dizziness and somnolence were reported in 12.5% of the patients. Chua et al. [12] reported minor adverse reactions with gabapentin, which were similar to the placebo group (16%). However, the solifenacin group reported side effects in 35% of patients even though they were not statistically significant. All the side effects of gabapentin were reported to improve spontaneously. Kim et al. [11] reported no discontinuation of therapy, and all the side effects were transient.

The side effect profile of gabapentin across these studies is minimal, with few patients requiring discontinuation. However, long-term follow-up, especially in children, is needed to document the safety profile of gabapentin.

The limitations of our review include a limited number of RCTs, with the majority of studies exhibiting a moderate risk of bias. Additionally, we were unable to conduct a meta-analysis due to variations in methodology, dosage of gabapentin, and follow-up protocols across the included studies.

Even though the usage of gabapentin for overactive bladder has been explored since 2004, there are not many studies defining the criteria for usage, dosage recommendations, or estimating the proportion of patients who may be non-responsive. However, combined results from studies, whether gabapentin is used alone or in conjunction with anticholinergics, have consistently shown significant improvement in symptoms and changes in urodynamic parameters. It's important to note that there is a subset of patients who may not respond to gabapentin, similar to other medications, and may require second-line management options such as botulinum toxin injection. Our review will definitely shed light on future studies with RCTs, promoting uniformity in reporting findings and addressing the need for standardized criteria for gabapentin usage, optimal dosage recommendations, and strategies for identifying non-responsive patients.

CONCLUSIONS

Although a definitive conclusion supporting gabapentin may not be drawn due to differences in dosages and treatment duration across studies, along with the limited number of high-quality studies, the majority of the included studies demonstrated a positive response to gabapentin, whether used alone or in combination with other drugs. High-quality randomized controlled trials comparing gabapentin with other medications and investigating factors related to non-responsiveness would be valuable for future endeavours.

CONFLICTS OF INTEREST

The authors declare no conflict of interest.

FUNDING

This research received no external funding.

ETHICS APPROVAL STATEMENT

The ethical approval was not required.

REGISTRATION AND PROTOCOL

Prospero CRD42024540949.

References

1. Leron E, Weintraub AY, Mastrolia SA, Schwarzman P. Overactive Bladder Syndrome: Evaluation and Management. Curr Urol. 2018; 11: 117-125.
2. Dash V, Bawa M, Mahajan JK, Kanojia RP, Samujh R, Rao KL. Role of gabapentin and anticholinergics in management of neurogenic bladder after repair of spina bifida- a randomized controlled study. J Pediatr Surg. 2016; 51: 2025-2029.
3. Page MJ, McKenzie JE, Bossuyt PM, et al. The PRISMA 2020 statement: An updated guideline for reporting systematic reviews. Int J Surg. 2021; 88: 105906.
4. Barker TH, Stone JC, Sears K, et al. Revising the JBI quantitative critical appraisal tools to improve their applicability: an overview of methods and the development process. JBI Evid Synth. 2023; 21: 478-493.
5. Barker TH, Stone JC, Sears K, et al. The revised JBI critical appraisal tool for the assessment of risk of bias for randomized controlled trials. JBI Evid Synth. 2023; 21: 494-506.
6. Barker TH, Habibi N, Aromataris E, et al. The revised JBI critical appraisal tool for the assessment of risk of bias for quasi-experimental studies. JBI Evid Synth. 2024; 22: 378-388.
7. Munn Z, Barker TH, Moola S, et al. Methodological quality of case series studies: an introduction to the JBI critical appraisal tool. JBI Evid Synth. 2020; 18: 2127-2133.
8. Ansari MS, Bharti A, Kumar R, Ranjan P, Srivastava A, Kapoor R. Gabapentin: A novel drug as add-on therapy in cases of refractory overactive bladder in children. J Pediatr Urol. 2013; 9: 17-22.
9. Cakici OU, Kaya C, Sanci A, Gencler OS, Mammadkhanli O, Cindas A. Gabapentin add-on therapy for patients

with spinal cord injury associated neurogenic overactive detrusors that are unresponsive to combined anticholinergic and beta-3 adrenergic therapy. Cent European J Urol. 2021; 74: 547-551.

10. Carbone A, Palleschi G, Conte A, Bova G, Iacovelli E, Bettolo CM, et al. Gabapentin treatment of neurogenic overactive bladder. Clin Neuropharmacol. 2006; 29: 206-214.

11. Kim YT, Kwon DD, Kim J, Kim DK, Lee JY, Chancellor MB. Gabapentin for overactive bladder and nocturia after anticholinergic failure. Int Braz J Urol. 2004; 30: 275-278.

12. Chua ME, See MC, Esmeña EB, Balingit JC, Morales ML. Efficacy and Safety of Gabapentin in Comparison to Solifenacin Succinate in Adult Overactive Bladder Treatment. Low Urin Tract Symptoms. 2018; 10: 135-142.

13. Chincholkar M. Gabapentinoids: pharmacokinetics, pharmacodynamics and considerations for clinical practice. Br J Pain. 2020; 14: 104-114.

14. Loutochin O, Afraa TA, Campeau L, Mahfouz W, Elzayat E, Corcos J. Effect of the anticonvulsant medications Pregabalin and Lamotrigine on urodynamic parameters in an animal model of neurogenic detrusor overactivity. Neurourol Urodyn. 2012; 31: 1197-1202.

15. Ziganshina LE, Abakumova T, Hoyle CHV. Gabapentin monotherapy for epilepsy: A review. Int J of Risk Saf Med. 2023; 34: 243-286.

16. Delgado-Garcia G, Lapidus S, Talero R, Levy M. The patient journey with NMOSD: From initial diagnosis to chronic condition. Front Neurol. 2022; 13: 966428.

17. Gupta S, McColl MA, Smith K, McColl A. Prescribing patterns for treating common complications of spinal cord injury. J Spinal Cord Med. 2023; 46: 237-245.

Central European Journal of Urology

ORIGINAL PAPER

UROLITHIASIS

Renal and ureteral temperatures changes during ureteroscopic pulsed thulium: YAG laser lithotripsy: an *in vitro* analysis

Felipe Urrea[1], José M. Villena[1], Matias Larrañaga[2], José Antonio Salvadó[3]

[1]*Urology Resident, Faculty of Medicine, Finis Terrae University, Santiago, Chile*
[2]*Urology Intern, Faculty of Medicine, Finis Terrae University, Santiago, Chile*
[3]*Department of Urology, Santa María Clinic, Santiago, Chile*

Citation: Citation: Urrea F, Villena JM, Larrañaga M, Salvadó JA. Renal and ureteral temperatures changes during ureteroscopic pulsed thulium: YAG laser lithotripsy: an *in vitro* analysis. Cent European J Urol. 2025; 78: 70-76.

Article history
Submitted: Aug. 19, 2024
Accepted: Nov. 11, 2024
Published online: Feb. 28, 2025

Corresponding author
José Antonio Salvadó
Department of Urology,
Clínica Santa María,
Avenida Santa María,
0500 Providencia, Santiago,
7550000 Región
Metropolitana,
Chile
jasalvadob@gmail.com

Introduction Promising studies have shown a high stone-free rate achieved with the pulsed solid-state thulium YAG laser. However, studies on its safety concerning temperature effects during activation remain limited. The aim of this study was to characterize temperature variations during laser activation.

Material and methods This *in vitro* experimental study utilized a high-fidelity uretero-renal simulation model to assess temperature changes during intracorporeal laser lithotripsy. Temperatures reached after laser activation at 15, 20, and 30 seconds were recorded. The flow rates used were 10 ml/min and 20 ml/min. The maximum allowed temperature was set at 43°C, given its association with thermal tissue damage. A linear logistic regression model was used to analyze variations and project temperature behavior over time.

Results In the renal model, temperature increases were correlated with the applied energy. With a 10 ml/min flow rate, no laser configuration exceeded 43°C at 15 seconds; at 20 seconds, only the 30 W (2.5 J/20 Hz) configuration exceeded this temperature. By 30 seconds, all 30 W configurations exceeded 43°C, except for 0.4 J/75 Hz. With a 20 ml/min flow rate, no laser configuration exceeded 43°C. The 20 ml/min flow rate decreased renal temperature by 1.96°C ($p = 0.01$). In the ureteral model, the temperature increase was not proportional to the applied energy, but in no scenario the temperatures reach the 43°C.

Conclusions The temperature variations observed in this study with the use of the pulsed solid-state thulium YAG laser should be considered to avoid potential renal and ureteral thermal damage.

Key Words: radical cystectomy ‹› emergency department ‹› readmission ‹› bladder cancer

INTRODUCTION

The increasing case volume of ureteroscopy (URS), particularly flexible ureteroscopy (f-URS), over shock wave lithotripsy (SWL) globally [1] may be attributed to the widespread adoption of the Holmium:YAG (Ho:YAG) laser since its introduction for endoscopic lithotripsy in 1992 [2]. Urologists currently face fierce competition in developing superior lasers, prompting manufacturers to produce high-power devices, often without fully assessing associated risks. In recent years, newer platforms such as the Ho:YAG with pulse modulation and the thulium fiber laser (TFL) have been compared mainly based on their stone-free rates [3, 4]. However, increased power carries potential risks, including elevated temperatures during laser activation, which could impact renal and urinary tract tissues [5–7]. Recently, the new pulsed solid-state thulium YAG (p-Tm:YAG) laser has been

added to the lasers already mentioned above. This laser has already shown reliable results in both *in vitro* and *in vivo* studies, proving to be effective even on hard stones [8, 9] which is likely determined by an adjustable power peak (1000–2000 W, PP) that is higher than that of the TFL (≤ 500 W). In terms of initial clinical experience with this new device, stone-free rates close to 80% have been demonstrated, placing it in a very good position compared to its competitors [10], even more it has been rated as "a safe and effective compromise between Ho:YAG laser and TFL for endoscopic lithotripsy" [11]. However, studies on its safety regarding temperature effects during its activation remain limited. In 2023, our group studied the temperature effects on the areas surrounding the activation site of the Ho:YAG laser Moses 2.0, detecting that several combinations of parameters commonly used could exceed the temperature deemed risky for generating thermal damage [12]. This study aimed to evaluate temperature variations generated by the p-Tm:YAG laser in the sectors surrounding the laser fiber tip using different parameters combinations while a flexible ureteroscopy is performed in a simulated bench model

MATERIAL AND METHODS

The experimental setup replicated our prior high-fidelity simulation bench model [12]. For this study, we employed the same equipment: a flexible disposable ureteroscope (Lithovue, Boston Scientific, Marlborough, MA, USA) passed through a 36 cm, 11/13 Fr access sheath (Navigator HD, Boston Scientific). We utilized irrigation with 3 l saline bags at 23°C, suspended by gravity to achieve inflow rates of 10 ml/min and 20 ml/min. The p-Tm:YAG laser (Tm:YAG, Dornier MedTech Laser GmbH, Wessling, Germany) was employed in the experiment, utilizing a new laser fiber of 270 μm. For intrarenal temperature measurement, a thermocouple (Leaton R Digital Thermometer) was positioned 5 mm proximal to the stone phantom (T-IR). For ureteral temperature measurement a second thermocouple recorded 5 mm distal to the stone (T-UR) (Figure 1). Before each measurement, the distal transparent part of the laser fiber tip was removed using standard scissors. Laser parameters were set according to the pre-setting recommendation (pulse modulation). For the "Dusting" pre-setting, the following parameters were selected: 0.3 J/25 Hz, 0.5 J/50 Hz, and 0.4 J/75 Hz. For the "Flex Long Pulse" pre-setting, the evaluation included: 0.3 J/100 Hz, 1 J/15 Hz, 1.5 J/20 Hz, and 2 J/15 Hz. The selection of the parameters was based on those commonly used in clinical practice with this laser.

Both thermocouples recorded temperatures at 15, 20, and 30 seconds after laser activation, and only the maximum temperature reached in each test (in Celsius degrees) was recorded. The temperature for each power and irrigation combination was recorded three times. A rest period of 30 seconds was allowed to equilibrate the temperature for each new irrigation pressure before each run. To determine the influence of the flow rate of physiological solution, measurements were conducted with 10 and 20 ml/min. For all trials, we considered 43°C as the threshold temperature because it is associated with

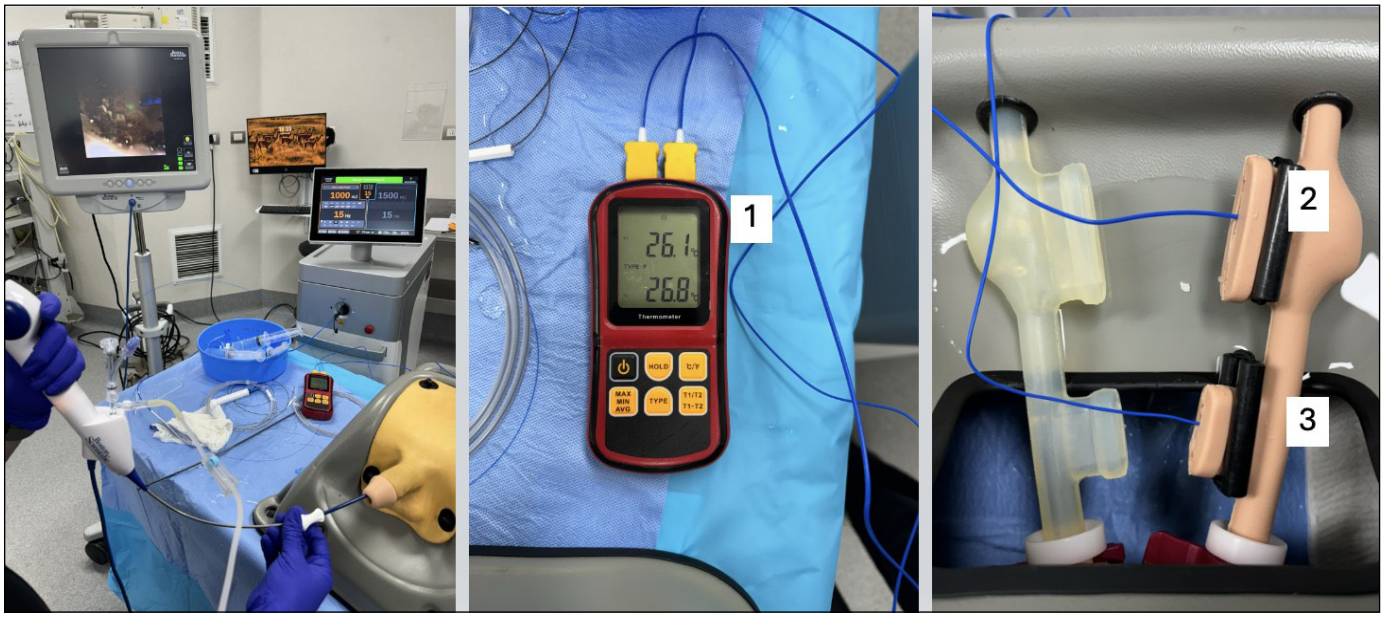

Figure 1. *Experimental setup: 1 – thermometer, 2 – thermocouple at renal pelvis, 3 – thermocouple at proximal ureter.*

denaturation of proteins [13]. Statistical analyses and graphics were performed using RStudio software version 2023.03.0+386. A linear logistic regression model was performed to compare the variation of renal and ureteral temperature according to laser configuration. The level of statistical significance was set at $p < 0.05$.

RESULTS

In the renal model test (T-IR), temperature increases correlated with energy applied. In the subgroup using 30 W, the setting of 0.3 J/100 Hz (Flex Long Pulse) reached the highest temperatures: 46.3°C at a flow rate of 10 ml/min and 41.4°C at a flow rate of 20 ml/min, both within 30 seconds. At a flow rate of 10 ml/min, no laser configuration exceeded 43°C at 15 seconds; at 20 seconds, only the 30 W configuration (2.5 J/20 Hz) exceeded 43°C, recording 44.8°C. By 30 seconds, all 30W configurations exceeded 43°C, except for 0.4 J/75 Hz. At a flow rate of 20 ml/min, no laser configuration exceeded 43°C. Table 1 presents the results obtained. Using a linear logistic regression model, the temperature behavior was projected up to 60 seconds (Table 2). It was observed that the 7.5 W and 15 W configurations would not exceed 43°C at a flow rate of 10 ml/min (Figure 2). At a flow rate of 20 ml/min, only the 30 W configurations would exceed 43°C (Figure 3). Compared with the 15 W configuration, it was observed that at a flow rate of 10 ml/min, the 30W configuration (0.4 J/75 Hz) showed the highest temperature rise per second ($p < 0.01$). At a flow rate of 20 ml/min, the 30 W configuration (0.3 J/100 Hz) exhibited the highest temperature rise per second ($p < 0.01$). The 20 ml/min flow rate resulted in a decrease in renal temperature of 1.96°C ($p = 0.01$) (Table 2). In the tests of the ureteral model (T-UR), it was observed that the temperature increase was not

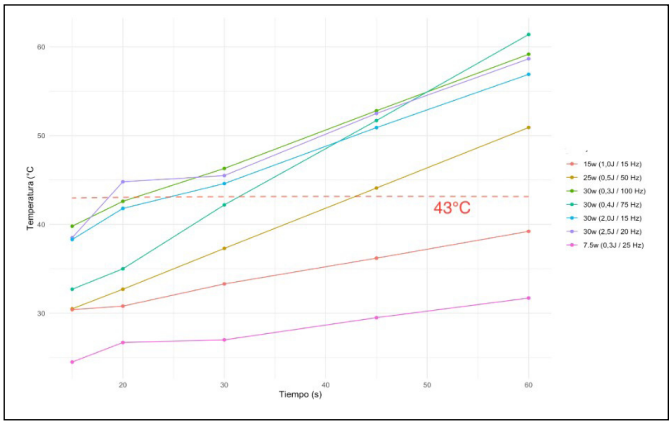

Figure 2. *Projected renal temperature with laser activation over 60 seconds at a flow rate of 10 ml/min.*

Table 1. *Renal and ureteral temperature*

Power	Renal temperatures						
	Flow rates	10 ml/min			20 ml/min		
	Firing times	15 s	20 s	30 s	15 s	20 s	30 s
7.5 W (0.3 J/25 Hz)		24.5	26.7	27	25.5	25.8	26.5
25 W (0.5 J/50 Hz)		30.5	32.7	37.3	34.3	34.4	35.5
30 W (0.4 J/75 Hz)		32.7	35	42.2	33.5	37	41.1
30 W (0.3 J/100 Hz)		39.8	42.6	46.3	33.7	37.2	41.4
15 W (1.0 J/15 Hz)		30.4	30.8	33.3	29.6	30.4	31.9
30 W (1.5 J/20 Hz)		38.5	44.8	45.5	35.6	37	39.4
30 W (2.0 J/15 Hz)		38.3	41.8	44.6	35.5	38.5	40.3
Power	Ureteral temperatures						
	Flow rates	10 ml/min			20 ml/min		
	Firing times	15 s	20 s	30 s	15 s	20 s	30 s
7.5 W (0.3 J/25 Hz)		22.6	22.6	22.8	24.5	25	25
25 W (0.5 J/50 Hz)		23.5	23.6	25.4	24.5	26	26
30 W (0.4 J/75 Hz)		23.2	24.8	25.6	25	26	27.5
30 W (0.3 J/100 Hz)		23.2	25.2	26	25.4	26	27.5
15 W (1.0 J/15 Hz)		25.4	25.2	25.4	26.4	25.5	26.1
30 W (1.5 J/20 Hz)		26.5	25.6	26.2	28.8	33.8	36.3
30 W (2.0 J/15 Hz)		24.6	25	26	29	27.5	30.6

proportional to the applied energy. The configuration of 2.5 J/20 Hz recorded the highest temperatures: 26.5°C with a flow rate of 10 ml/min at 15 seconds and 36.3°C with a flow rate of 20 ml/min at 30 seconds. Regardless of the laser settings, physiological saline flow rate, and laser activation time, temperatures above 43°C were never recorded. Table 1 summarizes the results obtained. Using a linear logistic regression model, the temperature behavior was projected up to 120 seconds. It was observed that only the 30 W configuration (0.3 J/100 Hz) would reach 43°C at a flow rate of 10 ml/min (Figure 4).

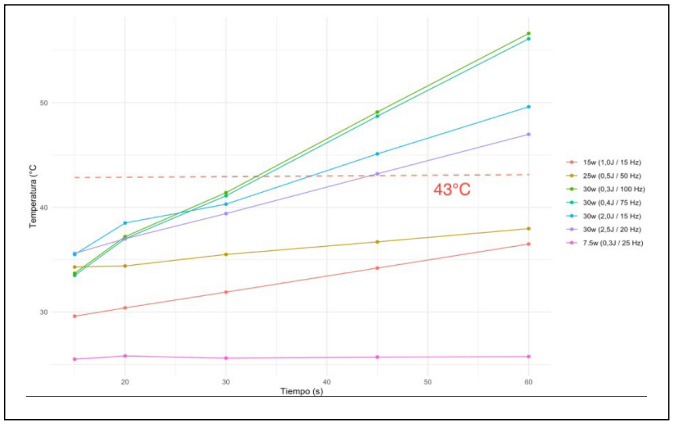

Figure 3. *Projected renal temperature with laser activation over 60 seconds at a flow rate of 20 ml/min.*

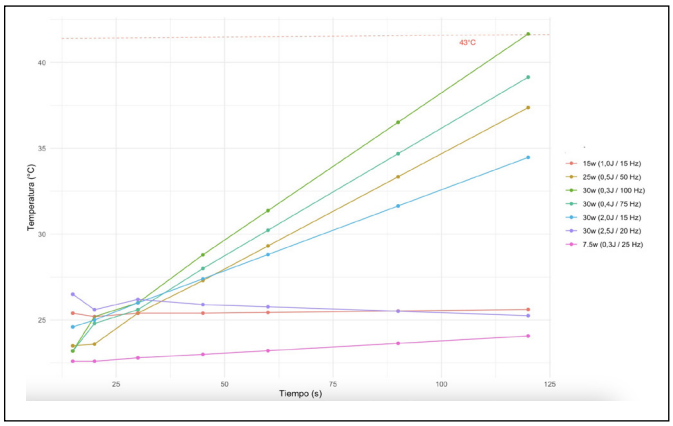

Figure 4. *Projected ureteral temperature with laser activation over 120 seconds at a flow rate of 10 ml/min.*

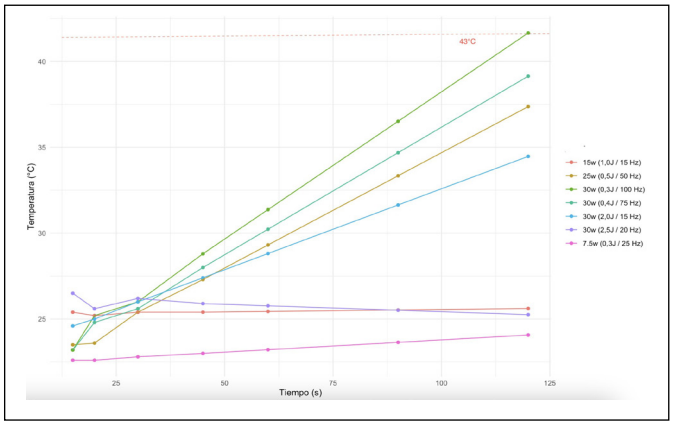

Figure 5. *Projected ureteral temperature with laser activation over 120 seconds at a flow rate of 20 ml/min.*

Table 2. *Logistic regression model for renal temperatures*

Laser setting	Coefficient	p-value
Renal temperature with flow rate of 10 ml/min		
7.5 W (0.3 J/25 Hz)	–0.054	0.09
30 W (2.0 J/15 Hz)	0.198	<0.01
30 W (2.5 J/20 Hz)	0.208	<0.01
30 W (0.3 J/100 Hz)	0.222	<0.01
25 W (0.5 J/50 Hz)	0.252	<0.01
30 W (0.4 J/75 Hz)	0.444	<0.01
Renal temperature with flow rate of 20 ml/min		
7.5 W (0.3 J/25 Hz)	–0.015	<0.01
25 W (0.5 J/50 Hz)	–0.006	<0.01
30 W (2.5 J/20 Hz)	0.098	<0.01
30 W (2.0 J/15 Hz)	0.147	<0.01
30 W (0.4 J/75 Hz)	0.34	<0.01
30 W (0.3 J/100 Hz)	0.347	<0.01
Temperature delta according to flow rate		
20 ml/min	–1.96	0.01

Table 3. *Logistic regression model for ureteral temperatures*

Laser setting	Coefficient	p-value
Ureteral temperature with flow rate of 10 ml/min		
30 w (2.5 J/20 Hz)	–0.011	<0.01
7.5 w (0.3 J/25 Hz)	0.011	<0.01
30 w (2.0 J/15 Hz)	0.091	<0.01
25 w (0.5 J/50 Hz)	0.131	<0.01
30 w (0.4 J/75 Hz)	0.145	<0.01
30 w (0.3 J/100 Hz)	0.168	<0.01
Ureteral temperature with flow rate of 20 ml/min		
7.5 w (0.3 J/25 Hz)	0.037	<0.01
30 w (0.3 J/100 Hz)	0.037	<0.01
25 w (0.5 J/50 Hz)	0.09	<0.01
30 w (0.4 J/75 Hz)	0.15	<0.01
30 w (2.0 J/15 Hz)	0.172	<0.01
30 w (2.5 J/20 Hz)	0.472	<0.01
Temperature delta according to flow rate		
20 ml/min	2.5	<0.01

At a flow rate of 20 ml/min, only the 30W configuration (2.5 J/20 Hz) would exceed 43°C (Figure 5). When comparing with the 15 W configuration, it was observed that at a flow rate of 10 ml/min, the 30 W configuration (0.3 J/100 Hz) showed the highest temperature increase per second ($p < 0.01$). At a flow rate of 20 ml/min, the 30 W configuration (2.5 J/20 Hz) exhibited the highest temperature increase per second ($p < 0.01$). However, it is noted that the 20 ml/min flow rate resulted in an increase in ureteral temperature of 2.5°C ($p < 0.01$) (Table 3).

DISCUSSION

The potential thermal damage generated by laser during endoscopic urinary stone lithotripsy had been intensely evaluated in the last time [14–17]. There is increasing awareness about this issue and there is consensus that exceeding 43°C implies a risk [13, 14]. Theoretically a few seconds of activation of the Ho:YAG laser of lithotripsy can produce ureteral injury even without direct contact due to its photothermal mechanism. In a laboratory study using a simulated model, it was observed that in the absence of irrigation flow, temperatures can reach between 44 to 100 degrees Celsius even with laser powers starting from 5 watts. However, most of the heat effect dissipates when irrigation flow exceeds 15 ml/min [18]. In our study, a similar observation was made, where an increase of 10 mL/min (from 10 to 20 ml/min) in irrigation flow prevents any combination of laser settings from exceeding 43°C, even when reaching a total power of 30 watts. The effect of irrigation on temperature reduction becomes even more evident when using a semi-rigid ureteroscope, which has a larger working channel diameter than traditionally flexible ureteroscopes and a shorter distance for irrigation outflow. In a study published in 2019 using a simulation model to evaluate the temperature effect when using Ho:YAG laser, measurements were taken every second during activation for a total of 15 seconds. Temperature increases of more than 6°C above baseline were chosen as the threshold for potential ureteral damage risk, given the average body temperature of 37°C, which would reach 43°C with such an increase. When using a semirigid ureteroscope with irrigation pressures of 200 mmHg with saline solution, the temperature increases never exceeded the 6°C threshold. In contrast, with flexible ureteroscopes, the threshold was surpassed within 15 seconds of activation, even with power settings as low as 10 W [19]. Regarding the thermal effect of TFL, it has also been *in vivo* predominantly evaluated *in vitro* studies comparing it simultaneously with Ho:YAG laser. In an setting, Okhunob et al. [20] conducted temperature measurements in a porcine model, continuously recording temperatures in the upper, middle, and lower calyxes, as well as using an additional probe to measure temperatures near the tip of the ureteroscope. One of the most striking findings of this study was that temperatures recorded at the tip of the ureteroscope were between 4°C to 22°C lower than those recorded in the renal calyces [20]. In our study, temperature increases at the level of the proximal ureter consistently remained lower than those recorded in the renal pelvis, regardless of the laser settings employed and irrigation flow used. This phenomenon could theoretically be explained by a rapid decrease in temperature once the peak is reached and as the irrigating fluid flows back towards the bladder. In the same vein, a factor rarely evaluated relates to the total volume of fluid present at the laser activation site. In the only study published so far, conducted in real patients, it was demonstrated that a renal pelvis anteroposterior diameter greater than 20 mm is an independent protective factor against temperature increases exceeding 43°C [21]. Regarding our study, the p-Tm:YAG laser appears to exhibit quite stable and safe behavior, at least in this simulated scenario and with preset laser parameters not exceeding 30 W of total energy. The temperature only exceeded the 43°C threshold when a relatively slow irrigation flow was used, coupled with total energies above 25 W. One of the most striking findings of our study is the effect of pulse modulation on temperature. When comparing various combinations to achieve 30 W, the "Flex Long Pulse" modulation consistently resulted in higher temperatures compared to "dusting" modulation, across each measured time interval and regardless of the combination of Hertz and Joules used. In a previous study published by Petzold et al. [22], the effect of temperature generated by p-Tm:YAG laser was evaluated and compared with that generated by Ho:YAG laser. In this study, laser activation was continuous for 120 seconds, with energies ranging from 2 to 30 W and an irrigation flow of 50 ml/min. The temperature increases were found to be very similar and comparable between both lasers, posing a higher risk when reaching 30 W in either case. In 2023, our group published the results of a study similar to the one presented this time, where the experimental setup was the same, but we evaluated the Ho:YAG laser with the Moses 2.0 effect [12]. In that study, the 43°C limit was exceeded on several occasions, even during activation periods as short as 15 seconds and with energies starting from 25 W,

although the effect of increased irrigation led to a decrease in temperature, it was not as pronounced as that achieved with the p-Tm:YAG laser. A potential explanation for this phenomenon could be attributed to the shape of the bubble generated by each laser, which could impact the distribution and dissipation of the heat generated during lithotripsy. The Ho:YAG laser tends to produce more spherical bubbles, whereas the p-Tm:YAG laser generates more elongated bubbles [23]. The p-Tm:YAG laser has recently shown clinical effectiveness. In a publication detailing the first 25 patients treated with this technology, stone-free rates of 95% and zero-fragment rates of 55% were achieved, which is comparable to traditionally reported outcomes with TFL or Ho:YAG lasers [10]. In any case, it should be noted that in that initial experience, "Captive Fragmenting" pulse modulation was used in all cases, mode that was not evaluated in our study. The efficacy in terms of ablation has also been evaluated, demonstrating that this laser achieves good results regardless of the chemical composition of the stone. Thus, the total energy consumption (J/mg) per treated stone did not show a statistically significant difference when comparing calcium oxalate monohydrate stones with uric acid stones [8]. To our knowledge, this is the first study evaluating the effect of p-Tm:YAG laser with different pulse modulation alternatives on temperature. However, there are several limitations to consider. Firstly, the study was conducted using a high-fidelity simulation model, which may not necessarily reflect clinical reality. Additionally, we only selected two pulse modulation alternatives from those available, based arbitrarily on our experience with this laser in real patients. A third limitation relates to its application in daily practice, as we defined activation times and irrigation flows based on our practice, which may not be standard elsewhere in the world.

CONCLUSIONS

The p-Tm:YAG laser is one of the tools available in the attempt to achieve better stone free rates, and like its competitors in this pursuit, there is a real risk of generating thermal damage. We believe that this study can contribute to the ongoing search for safer treatments for patients, always mindful of the potential harmful thermal effects, especially in this new era of so-called "high-power lasers".

CONFLICTS OF INTEREST

The authors declare no conflict of interest.

FUNDING

This research received no external funding.

ETHICS APPROVAL STATEMENT

The ethical approval was not required.

References

1. Geraghty RM, Jones P, Somani BK. Worldwide trends of urinary stone disease treatment over the last two decades: asystematic review. J Endourol. 2017; 31: 547-556.
2. Johnson DE, Cromeens DM, Price RE. Use of the holmium:YAG laser in urology. Lasers Surg. Med. 1992; 12: 353-363.
3. Traxer O, Pearle M. Thulium Fiber Laser Versus Holmium:Yttrium Aluminum Garnet for Lithotripsy: Which Is the Winner? Eur Urol. 2024; 85: 541-542.
4. Tang X, Wu S, Li Z, et al. Comparison of Thulium Fiber Laser versus Holmium laser in ureteroscopic lithotripsy: a Meta-analysis and systematic review. BMC Urol. 2024; 24: 44.
5. Belle JD, Chen R, Srikureja N, Amasyali AS, Keheila M, Baldwin DD. Does the Novel Thulium Fiber Laser Have a Higher Risk of Urothelial Thermal Injury than the Conventional Holmium Laser in an In Vitro Study? J Endourol. 2022; 36: 1249-1254.
6. Rice P, Somani BK, Nagele U, Herrmann TRW, Tokas T. Generated temperatures and thermal laser damage during upper tract endourological procedures using the holmium: yttrium-aluminum-garnet (Ho:YAG) laser: a systematic review of experimental studies. World J Urol. 2022; 40: 1981-1992.
7. Peteinaris A, Pagonis K, Vagionis A, et al. What is the impact of pulse modulation technology, laser settings and intraoperative irrigation conditions on the irrigation fluid temperature during flexible ureteroscopy? An in vivo experiment using artificial stones. World J Urol. 2022; 40:1853-1858.
8. Kwok JL, Ventimiglia E, De Coninck V, et al. Pulsed Thulium:YAG laser – What is the lithotripsy ablation efficiency for stone dust from human urinary stones? Results from an in vitro PEARLS study. World J Urol. 2023; 41: 3723-3730.
9. Kwok JL, Ventimiglia E, De Coninck V, et al. Pulsed thulium:YAG laser-ready to dust all urinary stone composition types? Results from a PEARLS analysis. World J Urol. 2023; 41: 2823-2831.
10. Panthier F, Solano C, Chicaud M, et al. Initial clinical experience with the pulsed solid-state thulium YAG laser from Dornier during RIRS: first 25 cases. World J Urol. 2023; 41: 2119-2125.
11. Chicaud M, Corrales M, Kutchukian S, et al. Thulium:YAG laser: a good compromise between holmium:YAG and thulium fiber laser for endoscopic lithotripsy? A narrative review. World J Urol. 2023; 41: 3437-3447.
12. Villena JM, Elorrieta V, Salvadó JA. Temperature effect of Moses™ 2.0

during flexible ureteroscopy: an in vitro assessment. Cent European J Urol. 2023; 76: 331-335.

13. Sapareto SA, Dewey WC. Thermal dose determination in cancer therapy. Int J Radiat Oncol Biol Phys. 1984; 10: 787-800.

14. Pauchard F, Ventimiglia E, Corrales M, Traxer O. A Practical Guide for Intra-Renal Temperature and Pressure Management during Rirs: What Is the Evidence Telling Us. J Clin Med. 2022; 11: 3429.

15. Tonyali S, von Bargen MF, Ozkan A, Gratzke C, Miernik A. The heat is on: the impact of excessive temperature increments on complications of laser treatment for ureteral and renal stones. World J Urol. 2023; 41: 3853-3865.

16. Æsøy MS, Juliebø-Jones P, Beisland C, Ulvik Ø. Temperature Measurements During Flexible Ureteroscopic Laser Lithotripsy: A Prospective Clinical Trial. J Endourol. 2024; 38: 308-315.

17. Aldoukhi AH, Dau JJ, Majdalany SE, et al. Patterns of Laser Activation During Ureteroscopic Lithotripsy: Effects on Caliceal Fluid Temperature and Thermal Dose. J Endourol. 2021; 35: 1217-1222

18. Maxwell AD, MacConaghy B, Harper JD, Aldoukhi AH, Hall TL, Roberts WW. Simulation of Laser Lithotripsy-Induced Heating in the Urinary Tract. J Endourol. 2019; 33: 113-119.

19. Winship B, Wollin D, Carlos E, et al. The Rise and Fall of High Temperatures During Ureteroscopic Holmium Laser Lithotripsy. J Endourol. 2019; 33: 794-799.

20. Okhunov Z, Jiang P, Afyouni AS, et al. Caveat Emptor: The Heat Is "ON"- An In Vivo Evaluation of the Thulium Fiber Laser and Temperature Changes in the Porcine Kidney During Dusting and Fragmentation Modes. J Endourol. 2021; 35: 1716-1722.

21. Æsøy MS, Juliebø-Jones P, Beisland C, Ulvik Ø. Temperature Measurements During Flexible Ureteroscopic Laser Lithotripsy: A Prospective Clinical Trial. J Endourol. 2024; 38: 308-315.

22. Petzold R, Suarez-Ibarrola R, Miernik A. Temperature Assessment of a Novel Pulsed Thulium Solid-State Laser Compared with a Holmium:Yttrium-Aluminum-Garnet Laser. J Endourol. 2021; 35: 853-859.

23. Petzold R, Suarez-Ibarrola R, Miernik A. Gas Bubble Anatomy During Laser Lithotripsy: An Experimental In Vitro Study of a Pulsed Solid-State Tm:YAG and Ho:YAG Device. J Endourol. 2021; 35: 1051-1057.

Central European Journal of Urology

ORIGINAL PAPER

UROLITHIASIS

A prospective comparative study between retrograde intrarenal surgery vs supine mini percutaneous nephrolithotomy for single upper ureteric stones >10 mm

Nitesh Kumar[1], Bhaskar K. Somani[2]

[1]Consultant Urologist, Ford Hospital, Patna, India
[2]Consultant Urological Surgeon, University Hospital Southampton, United Kingdom

Citation: Kumar N, Somani BK. A prospective comparative study between retrograde intrarenal surgery vs supine mini percutaneous nephrolithotomy for single upper ureteric stones >10 mm. Cent European J Urol. 2025; 78: 77-84.

Article history
Submitted: Sep. 20, 2024
Accepted: Nov. 11, 2024
Published online: Jan. 22, 2025

Corresponding author
Bhaskar K. Somani
University Hospital Southampton NHS Trust
Tremona Road,
Southampton,
Hampshire SO16 6YD,
United Kingdom
b.k.somani@soton.ac.uk

Introduction To compare retrograde intrarenal surgery (RIRS) and supine mini percutaneous nephrolithotomy (smPCNL) in the management of upper ureteric stones larger than 10 mm.

Material and methods Patients with upper ureteric stones (above L4 vertebra transverse process) larger than 10 mm at Ford Hospital and Research Centre between January 2023 and June 2024 were included in the study and were operated with either RIRS (group A) or smPCNL (group B) based on the informed consent and patients' decision. Patient demographics, stone parameters, intraoperative variables, postoperative outcomes, stone-free rates (SFR) and complications were recorded, and the two groups were compared.

Results Over 18 months, 140 patients (70 in each group) were available for comparison. Both the groups were comparable in terms of patient's demographics and the stone parameters. For RIRS and smPCNL, the mean stone size was 13.87 ±3.69 and 14.21 ±3.47 mm (p = 0.329), mean operative duration was 42.52 ±28.37 and 30.69 ±18.55 minutes (p = 0.0001), mean drop in haemoglobin at 24 hours was 0.44 ±0.96 and 0.69 ±0.92 g/dl (p = 0.364) and postoperative hospital stay was 0.92 ±0.68 and 1.13 ±0.76 days, respectively.

The SFR (at 3 months post-surgery) were 94.2% for RIRS and 98.57% for smPCNL (p = 0.084) and complications rate (Clavien-Dindo ≥II) was 2.88% for both groups. Primary access was not possible in 30% of patients in RIRS leading to staged intervention.

Conclusions RIRS and smPCNL are safe and effective surgical alternatives for managing upper ureteric stones larger than 10 mm. smPCNL offers a single stage solution and equivalent results with RIRS for the large upper ureteric stones.

Key Words: supine PCNL ‹› ureteroscopy ‹› retrograde intrarenal surgery ‹› ureter ‹› kidney calculi

INTRODUCTION

Urinary tract stones have become a common cause of morbidity worldwide, with a lifetime risk for stone development estimated to be around 5.0–10.0% and recurrences in up to 50.0% of patients [1]. Impacted upper ureteric stone is a urological emergency and it poses a serious risk for kidney damage if left untreated [2]. There are various management options for treating the upper ureteric stones, such as extracorporeal shockwave lithotripsy (ESWL), retrograde rigid ureteroscopy (RURS), retrograde intrarenal surgery (RIRS), antegrade percutaneous lithotomy (PCNL), laparoscopy, open surgery and pushback PCNL (pbPCNL) which is a combination of RURS followed by antegrade PCNL [2, 3]. RIRS and PCNL form the mainstay of treatment of upper ureteric stones in the current era, still there

is dilemma regarding the best approach to manage this set of patients [3, 4].
While both techniques aim to provide effective stone removal, their comparative efficacy, safety profiles, and patient-related outcomes necessitate thorough investigation to determine optimal treatment strategies for patients presenting with single upper ureteric stones larger than 10 mm [5]. Recent studies have indicated that both procedures yield favourable outcomes, but there remains a lack of comprehensive data directly comparing the two techniques in a prospective manner. There is need for specialized research in this domain to better guide clinical decision-making and optimize patient care.
In the current study, we aim to compare the clinical outcomes, safety profiles, and patient-reported satisfaction between RIRS and supine mini PCNL (smPCNL). As per our knowledge, there is no study at present which compares smPCNL with RIRS for management of upper ureteric stones larges than 10 mm.

MATERIAL AND METHODS

A prospective comparative study consisting of patients who underwent surgical treatment for upper ureteric stones larger than 10 mm was conducted at Ford Hospital and Research Centre from January 2023 and April 2024. All patients aged over 14 years old, presenting with upper ureteric stones [above the L4 vertebra transverse process and below the ureteropelvic (UPJ)], measuring more than 10 mm, were included in the study. Patients with associated renal stones, obstruction distal to stone, pregnancy, renal anomalies, non-functioning renal units, associated pyelonephritis/urosepsis, uncorrected coagulopathy and with incomplete data or follow-up were excluded.
Patients were informed about both procedures and their associated cost, complications, advantages and disadvantages. After thorough understanding of the procedure and its related issues, patients were asked to select between RIRS or smPCNL for removal of their stone. We could not randomise the participants because of the cost difference between both the procedures. Baseline demographic data and following parameters were recorded: age, sex, body mass index (BMI), comorbidities, side, size, stone location, impaction, Hounsfield unit (HU), renal anomalies, previous surgery and type of anaesthesia.

RIRS group (A)

Spinal anaesthesia (SA) was administered to all the patients except for a few who demanded general anaesthesia (GA), and they were placed in the lithotomy position. Rigid ureteroscopy was performed with a 6 Fr ureteroscope and ureteral compliance was noted. A 10/12 Fr ureteral access sheath (UAS) was placed over a Terumo 0.035 in guidewire under fluoroscopic guidance. If the ureter was too narrow and it was difficult to pass the UAS or the ureteroscope, a double J (DJ) stent was placed, and the procedure was staged. A 7.5 Fr flexible ureterorenoscope (Seeshen Medicals, China) was used to access the stone and Holmium 60 W laser (Cyber Ho Quanta) was used for lithotripsy of the stone.
A setting of 0.6 J and 10 Hz (6 W) fragmentation mode was used initially to break and dislodge the stone proximally (either in the more proximal ureter or in the kidney) from its impacted position. The scope and UAS was then advanced and the stone was dusted using 0.8 J and 12 Hz (9.6 W, vapour tunnel mode) or further fragmentation into small pieces using 1 J and 10 Hz (10 W, fragmentation mode). For the latter, a flexible navigable access sheath (FANS) was used to remove the fragments. If the stone was densely impacted and could not be pushed up, a channel was created, a wire was passed across and a stent was placed for a staged procedure. At end of the surgery a 5 Fr 26 cm DJ stent was placed in all cases and 14 Fr urethral catheter was placed (Figure 1).

smPCNL group (B)

Spinal anaesthesia (SA) was administered to all patients except for a few who demanded general anaesthesia. A 25 gauge spinal needle was used and 3 ml of bupivacaine was instilled, 1 ml (50 μg) of fentanyl was used as an adjuvant in cases with larger stone burden.
After achieving the necessary anaesthesia effect, patients were positioned in modified supine position. The contralateral leg was kept in lithotomy position and ipsilateral leg was kept either straight or flexed at the knee. The contralateral arm was kept on an arm rest, abducted less than 90 degrees, and the patient was asked to hold the contralateral shoulder with the ipsilateral arm. The patient was brought to the edge of the table and two small bolsters were placed, one below the scapula and the other below the buttocks (Figure 2). Tilt of the trunk was kept to a minimum to avoid overlap between the pelvicalyceal system (PCS), stones and bony spinal structures.
The operation theatre and instruments were set up in a very particular way to help the surgeon perform the procedure with minimal assistance. The camera trolley was placed near the patient's head, the c-arm

machine in the center, and the screen of the c-arm near the patient's feet (all three on the contralateral side of the stone). The c-arm foot switch was kept on the floor (head end), the lithotripsy/laser foot pedal was kept near the feet of the patient and the laser was also located near the feet (Figure 2). Assistance from operating theatre (OT) floor staff was limited to changing saline and water pressure regulation.

A 5 Fr ureteric catheter was placed, and retrograde pyelogram (RGP) was performed. Middle calyx was preferably punctured, then the tract was dilated to 16.5 Fr (Storz mini dilator) and a sheath was placed under c-arm guidance. Supine monoplanar technique (c-arm in 0 degrees) was used in all cases and biplanar technique was used only after 3 failed initial attempts (Figure 2).

Holmium 60 W laser (Cyber Ho Quanta) was used for lithotripsy of the stone with settings of 1 J and 10 Hz and a combination of vapour tunnel dusting and fragmentation modes. The fragments were removed mostly by gravity and with forceps when required. After clearing the stone, a 5 Fr 26 cm DJ stent was placed and cystoscopy was performed to confirm the bladder end coil of the DJ stent. Tubeless exit was done in all cases and a single staple applied to the puncture site.

In the RIRS group, primary/secondary, ureteric access sheath (UAS) placement, use of suction, were recorded. In the smPCNL group, number, size, location of tracts and exit strategy were recorded.

The lithotripsy modality, duration of surgery, stone clearance, haemoglobin (Hb) drop, transfusion rate, hospital stay, and complications were recorded for both the groups. Primary outcomes were stone-free rates (SFR) and incidence of postoperative complications (graded by the Clavien-Dindo classification), while secondary outcomes included duration of surgery, postoperative pain scores, hospital stay, and time to resume normal activities. Patient satisfaction scores were noted using the Freiburg Index of Patient Satisfaction (FIPS) questionnaire.

Imaging was performed on the morning of the next day to check for any residual stones. Patients were discharged on the first or second postoperative day

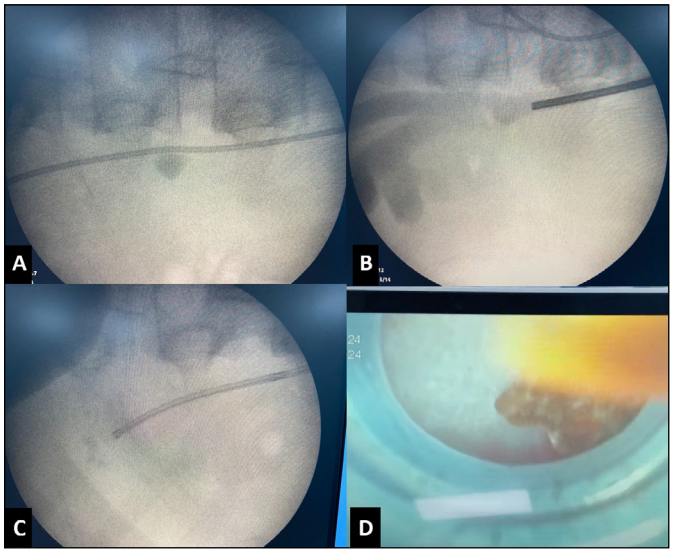

Figure 1. A) *Upper ureteric calculus in pre-stented patient.* **B)** *Initial assessment with semirigid ureteroscope.* **C)** *RIRS in progress, stone pushed in upper calyx.* **D)** *FNAS sheath.*

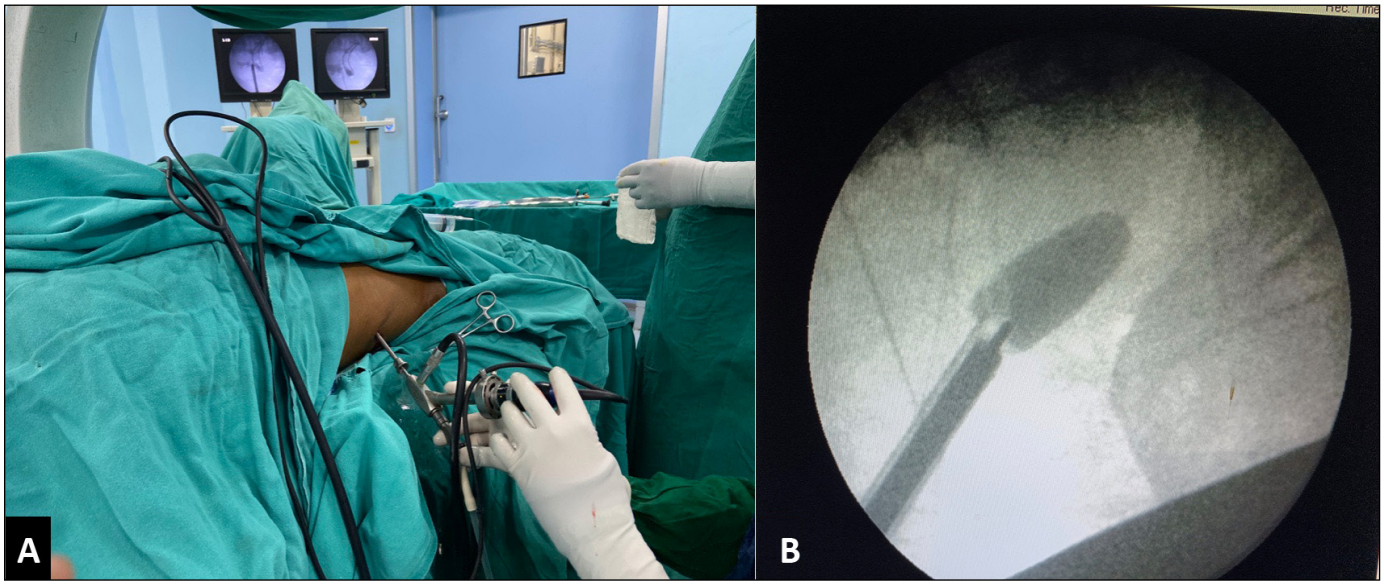

Figure 2. A) *Position and smPCNL for a 12 mm upper ureteric stone, middle calyx access.* **B)** *smPCNL for a large 4 cm upper ureteric stone.*

after removing the Foley catheter, depending on the clinical condition. All patients were reviewed after a month with non-contrast CT scan (NCCT) bone window, to document and assess stone clearance and the DJ stent was removed. Relook RIRS was done at the time of stent removal in cases with residual stones based on patient counselling and shared decision making. A repeat follow-up was performed at 3 months with abdominal ultrasound (US) and patient satisfaction scores were recorded. SFR was defined as complete clearance of stone endoscopically or presence of fragments <2 mm on the follow-up imaging. Complications were graded according to the Clavien-Dindo classification system.

Statistical analysis

Data analysis was done with XlStat2021 software. Continuous variables were expressed as mean ±standard deviation and compared using the Student's t-test. Categorical variables were analysed using the χ^2 test. A p-value of <0.05 was considered statistically significant.

Bioethical standards

Ethical approval was obtained by Ford Hospital Research Centre Institutional Ethics Committee in January 2023 (FHRC/IEC/JAN-2023/002).

RESULTS

One hundred forty-eight patients were ultimately enrolled in the study, out of which 140 were available for final analysis (70 patients in the RIRS group and 70 patients in the smPCNL group). Eight patients were excluded (4 from each group) due to incomplete follow-up not meeting our protocol.

Patient demographics and stone characteristics are shown in Table 1. Mean age was 41.64 ±13.87 and 42.42 ±13.43 years, male to female ratio was 1.26 : 1.33, stone laterality (right : left) ratio was 1.33 and 1.25, one or more comorbidities were present in 45.8% and 47.2% patients in the RIRS and smPCNL groups, respectively.

Mean stone size was 13.87 ±3.69 and 14.21 ±3.47 mm, mean HU of stone was 1068 ±218.63 and 1052 ±227.73 in the RIRS and smPCNL groups, respectively. Stone impaction was noted in 35.71% and 37.14%, with a prior history of upper ureteric or renal stone surgery in 14.3% and 11.5% in the RIRS and smPCNL groups, respectively.

The procedure details, outcome and complications of both the groups are recorded in Table 2. A total of 94.2% of RIRS and 97.1% of PCNL cases were performed under spinal anaesthesia. The smPCNL access was mid-pole in 50 (70.1%), lower pole in 11 (15.7%) and upper pole in 9 (12.8%) patients. A 16.5 Fr Storz mini tract was used in 57 (81.4%) and a 22 Fr tract was used in 13 (18.5%) cases in the smPCNL group. Primary RIRS was possible in 50 (71.4%) cases, where a 10/12 Fr UAS was used in 53 (75.7%) cases and 9/11 Fr was used in 17 (24.2%) cases. Of these, a flexible navigable access sheath (FNAS) was used in 40 (57.1%) cases. DJ stent was placed in all the cases in both the groups as the exit strategy, and no percutaneous nephrostomy (PCN tube) was placed in any case in the smPCNL group.

The duration of surgery was 42.52 ±28.37 and 30.69 ±18.55 minutes, respectively in groups A and B (p = 0.001). Haemoglobin drop at 24 hours was 0.44 ±0.96 and 0.69 ±0.92 g/dl, and it was slightly higher in smPCNL patients but this was statistically insignificant (p = 0.364). None of the patients in either group required blood transfusion. The SFR was 98.57% and 94.2% (p = 0.137), with a mean duration of hospital stay of 1.13 ±0.76 and 0.92 ±0.68 (p = 0.084) for smPCNL and RIRS, respectively.

High-grade (Clavien-Dindo ≥II) complications were noted in 2 patients each group (2.8%). In the RIRS group this included a case of sepsis and ureteric colic each, while in the smPCNL group it was prolonged haematuria needing hospitalisation. Postoperative

Table 1. *Patient demographics and stone characteristics*

Variables	Group A: RIRS (n = 70)	Group B: smPCNL (n = 70)	p-value
Mean age ±SD (range)	41.64 ±13.87	42.42 ±13.43	
Sex (male : female)	1.26	1.33	
BMI	24.5 ±3.56	24.3 ±3.81	0.451
Comorbidities (0 : 1 : 2 : >2) [%]	54.2 : 22.8 : 15.7 : 7.1	52.8 : 24.2 : 14.2 : 8.5	
Stone side (right : left)	1.33	1.25	
Mean stone size ±SD (range) [mm]	13.87 ±3.69	14.21 ±3.47	0.329
Mean HU ±SD (range)	1,068 ±218.63 (315–1,478)	1,052 ±227.73 (321–1,503)	0.274
Impacted stone [%]	35.71	37.14	
Previous surgery [n (%)]			
Nil	60 (85.7)	62 (88.5)	
PCNL	6 (8.5)	5 (7.1)	
RIRS	3 (4.3)	1 (1.4)	
Open surgery	1 (1.4)	2 (2.8)	

BMI – body mass index; HU – Hounsfield Unit; PCNL – percutaneous nephrolithotomy; RIRS – retrograde intrarenal surgery

haematuria was noted in 4.3% and 7.1% with fever noted in 7.1% and 1.6% for RIRS and smPCNL groups, respectively.

The patient reported outcomes are summarised in Table 3. Postoperative pain was comparatively less in the RIRS group both at 1 and 24 hours after the surgery, being 2.59 ±0.87 and 0.43 ±0.54 vs 3.72 ±1.15 and 1.24 ±0.89 and the difference was significant (p = 0.013 and 0.017, respectively). Time to resume normal activities (in days) was significantly shorter (p = 0.002) in the RIRS group 3.58 ±3.63 when compared to the smPCNL group 6.16 ±4.24. Patient satisfaction at the end of surgery was almost equal in both groups (p = 0.721).

Table 2. *Procedure details, outcomes and complications*

Variables	Group A: RIRS (n = 70)	Group B: smPCNL (n = 70)	p-value
Anaesthesia	SA – 66, GA – 4	SA – 68, GA – 2	
Tract location (U : M : L)	NA	9 (12.8%) : 50 (70.1%) : 11 (15.7%)	
Tract size (A – 22, B –16.5)	NA	A – 13 (18.5%), B – 57 (81.4%)	
Primary : secondary	50 (71.4%) : 20 (28.5%)	NA	
UAS size (A – 10/12, B – 9/11)	A – 53 (75.7%), B – 17 (24.2%)	NA	
FANS	40 (57.1%)	NA	
Exit strategy	DJ – 70 (100.0%)	DJ – 70 (100.0%)	
Duration of surgery [min]	42.52 ±28.37	30.69 ±18.55	0.001
Haemoglobin drop [g/dl]	0.44 ±0.96	0.69 ±0.92	0.364
Transfusion rate	0 (0%)	0 (0%)	0.000
Mean hospital stay [days]	0.92 ±0.68	1.13 ±0.76	0.084
Stone-free rates	94.2%	98.57%	0.137
Complications (Calvien-Dindo ≥II)	2 (2.8%)	2 (2.8%)	0.275
Complications (Calvien-Dindo I) – fever	5 (7.1%)	1 (1.6%)	0.026
Complications (Calvien-Dindo I) – haematuria	3 (4.3%)	5 (7.1%)	0.059

DJ – Double J stent; FNAS – flexible navigable access sheath; GA – general anaesthesia; smPCNL – supine mini percutaneous nephrolithotomy; SA – spinal anaesthesia; RIRS – retrograde intrarenal surgery; UAS – ureteral access sheath

Table 3. *Patient reported outcomes*

Variables	RIRS (n = 70)	smPCNL (n = 70)	p-value
Postoperative pain (VAS) (1 hour : 24 hours)	2.59 ±0.87 : 0.43 ±0.54	3.72 ±1.15 : 1.24 ±0.89	0.013 : 0.017
Time to resume normal activities	3.58 ±3.63	6.16 ±4.24	0.002
Patient satisfaction	1.71 ±0.92	1.75 ±0.88	0.721

RIRS – retrograde intrarenal surgery; smPCNL – supine mini percutaneous nephrolithotomy; VAS – Visual Analogue Scale

DISCUSSION

There are a few papers comparing RIRS and prone mini PCNL for large upper ureteric stone, but studies comparing supine mini PCNL with RIRS are limited. Upper ureteric stones are a commonly encountered problem in everyday practise and they pose a serious threat to the function of the kidney because of the effect of impaction and obstruction [2, 6].

These stones need timely treatment to prevent irreversible damage to the kidney. Multiple modalities of treatment of these stones are available, but still uncertainty exists over which is best [3, 7]. Out of all available options, ESWL, RURS, RIRS, antegrade PCNL, laparoscopy, open surgery and pushback PCNL, we choose the 2 modalities which are probably more commonly used to treat the upper ureteric stone in this era, RIRS and smPCNL.

Efficacy of ESWL in upper ureteric stones measuring more than 10 mm is only 42.0%, and it does not provide complete relief of obstruction [8]. Patients often have to suffer from repeated colic episodes, flank pain and a substantial proportion require repeated treatment [4, 8]. The biggest disadvantage of RURS is stone retropulsion (28.0–60.0%) and poor stone clearance rates (68.0–76.0%), poor vision, with inflammatory and oedematous mucosa increasing the chances of injury and subsequent stricture [9].

The practice of prone PCNL for upper ureteric stones is common in India, which enables urologists to access the stone easily and avoid the supracostal, upper pole punctures. But this technique is associated with multiple fragments which can migrate into different calyces, requiring multiple punctures, leading to incomplete clearance [5, 10].

RIRS for stone surgery is recommended for renal and upper ureteric stones up to 2 cm and recently there has been a sharp rise in this modality due to availability of digital smaller flexible ureteroscopes and thulium fibre laser (TFL) [11].

RIRS has the advantage of being less invasive as it uses the natural passage, easier access to stone, less fluoroscopy exposure and shorter hospital stay. However, there are a few issues related to this procedure especially for the upper ureteric stones. There is associated ureteral mucosal edema distal to the stone limiting the working space, making lithotrip-

sy difficult. In less experienced hands this may lead to ureteric mucosal injury and subsequent stricture, urosepsis and procedural staging may be required in larger stones [6, 12]. We avoided in situ dusting of the stone in the upper ureter, these were disimpacted and relocated preferably to the upper calyx for dusting/fragmentation.

Antegrade approach to upper ureteric stones by PCNL is a safe and effective treatment, associated with high SFR. It provides access to stone from a dilated upper ureter, better visualisation, resulting in better and safe lithotripsy [5, 6, 13]. In smPCNL, there is no need to push the stone and less chances of stone migration, with a majority of these cases done with middle calyx puncture, and if the stone needs to be pushed, this can be done after the sheath is placed in the upper ureter [10].

There are a few disadvantages of PCNL such as its higher invasiveness due to puncture of the kidney, associated higher risk of bleeding, rare need for angioembolization, increased radiation exposure and slightly prolonged hospital stay [14]. Although most of these limitations are overcome by mini PCNL.

The mean age in our study population was 41.64 ±3.87 years, similar to Elgebaly et al. [6] and Gu et al. [8]. In our study, the mean stone size was 13.87 ±3.69 and 14.21 ±3.47 mm which was similar to the study by Zhang et al. [10] (15.6 ±2.5 and 14.9 ±2.3 mm) and Elgebaly et al. [6] (13.5 mm and 13.2 mm) but less than Gu et al. [8] (17.27 mm and 16.23 mm). The mean HU of stone was slightly more in our study (1,068 ±218.63 and 1,052 ±227.73) when compared to Elgebaly et al. [6] (979.4 and 871.4) and Mohey et al. [1] (980.9 and 989.5).

Few studies by Gu et al. [8], Mohey et al. [1] and Elgebaly et al. [6] included only impacted upper ureteric stones in their study, while Zhang et al. [10] included all upper ureteric stones. In our study 35.7% and 37.1% stones were impacted in the 2 groups. Most of our procedures were performed under spinal anaesthesia and patients were satisfied with the procedure, especially that they were able to see the stone on the monitor during the procedure. General anaesthesia was administered only for patients who demanded GA.

There is paucity of data regarding the tract location for accessing the upper ureteric stones, and we preferred the mid pole for access in most of our cases (70.1%) and avoided the polar calyces. Upper pole in supine position does not give similar access to the ureter as in the prone position because the accessed calyx is the upper lateral one. Lower pole approach creates slightly higher torque for accessing the upper ureter. We were able to perform primary RIRS in 71.4% patients, while Mahajan et al. [15] reported primary access in 94.5% patients and Yuk et al. [16] in 85.3% patients. We went for elective and informed staged RIRS in impacted stones to minimise infective complications.

Haemoglobin drop at 24 hours was slightly higher in smPCNL (0.44 vs 0.69 g/dl), but it was insignificant, similar to Moufid et al. [17] (0.23 vs 0.36). It signifies that both the procedures are safe in terms of blood loss. Though the duration of hospital stay was slightly lower in the RIRS group (0.92 vs 1.13 days), it was insignificant. Much higher stay was reported in several studies for PCNL, with Moufid et al. [17] (1.67 vs 2.27 days), Zhang et al. [10] (1.8 vs 4.2 days), and Güler et al. [18] (2.0 vs 4.1 days). Most of our patients were discharged within 24 hours in both the groups, with supine PCNL and mini tract size making the hospital stay shorter.

SFR were better for smPCNL group (98.5% vs 94.2%) but the difference was insignificant. Higher SFR of PCNL was consistently reported across various studies by Elgebaly et al. [6] (83.3% vs 60.0%), Mohey et al. [1] (90.3% vs 70.0%), Zhang et al. [10] (93.7% vs 84.1%), Moufid et al. [17] (95.5% vs 66.7%), Güler et al. [18] (97.4% vs 83.7%), and Gu et al. [8] (100.0% vs 89.7%). The SFR of RIRS group was better in our study probably due to use of FNAS and on table clearance.

Both the groups had very low rates of high-grade (Calvin-Dindo ≥II) complications at 2 each (2.8%), and overall complications were 14.2% vs 11.4%. Other studies have reported lower overall complications rates in RIRS, Moufid et al. [17] (13.3% vs 22.7%), Güler et al. [18] (20.9% vs 24.0%), Zhang et al. [10] (6.8% vs 12.5%), and Mohey et al. [1] (19.4% vs 23.4%). Fever was reportedly significantly higher in the RIRS group (6.0% vs 1.66%) in our study, but other studies have reported lower rates of fever in the RIRS group, with Moufid et al. [17] (3.3% vs 9.0%), and Güler et al. [18] (2.1% vs 5.3%). It is worth noting that sepsis and other complications were lesser in studies where supine mini PCNL was performed.

RIRS was superior in terms of postoperative pain (Visual Analogue Scale – VAS) both at 1 and 24 hours after the surgery, being (2.59 vs 3.72) and (0.43 vs 1.24), and it was a similarly reported in studies of Moufid et al. [17] (3.1 vs 4.7) and Güler et al. [18] (3.6% vs 4.8%). Patients in the RIRS group returned to their normal activities earlier than smPCNL (3.58 vs 6.16 days) in our study, similar to Sun et al. [19] (2.7 vs 7.8 days) and Yavuz et al. [20] (3.9 vs 9.3 days). Patients were overall satisfied with the procedure they underwent for the removal of their stones and if necessary they would select the same procedure again.

While this study shows an important aspect of management of upper ureteric stones, there are certain limitations. The study is not randomised and therefore there is inherent bias to the outcomes. Future studies should focus on multicentric, ideally randomised, studies with more patient numbers to evaluate and compare the outcomes between smPCNL and RIRS. These studies should also take into consideration the cost and quality of life using patient reported outcome measures, and the role guidelines play in this [21–23].

CONCLUSIONS

Both RIRS and smPCNL are safe and effective surgical alternatives for managing upper ureteric stones larger than 10 mm. RIRS is less invasive, associated with less postoperative pain, lesser bleeding and earlier patient recovery. On the other hand, smPCNL offers a single stage and a quicker solution for large upper ureteric stones with less febrile complications.

CONFLICTS OF INTEREST

The authors declare no conflict of interest.

FUNDING

This research received no external funding.

ETHICS APPROVAL STATEMENT

The study was approved by Ford Hospital Research Centre Institutional Ethics Committee in January 2023 (FHRC/IEC.JAN-2023/002).

References

1. Mohey A, Abdelfattah AA, Mohammed AE, Marzouk A, El-Dakhakhny AS. Comparative study between antegrade flexible ureteroscopy and reterograde intrarenal surgery in the management of impacted upper ureteric stones 1.5 cm or larger. World J Urol. 2023; 41: 3731-3736.
2. Feng F, Xu Z. A new perspective on the treatment of upper ureteric stones. World J Urol. 2024; 42: 66.
3. De S, Gupta S, Singh M, Chugh R, Bell H, Gupta M. The impacted ureteral stone: Factors predicting for successful outcome with endoscopic management. J Urol. 2017; 197: e683.
4. Jiang H, Yu Z, Chen L, et al. Minimally invasive percutaneous nephrolithotomy versus retrograde intrarenal surgery for upper urinary stones: a systematic review and meta-analysis. Biomed Res Int. 2017; 2017: 2035851.
5. Jayaprakash SP, Thangarasu M, Jain N, Bafna S, Paul R. In situ management of large upper ureteric calculus by mini-percutaneous nephrolithotomy in the era of retrograde intrarenal surgery. Res Rep Urol. 2020; 12: 633-638.
6. Elgebaly O, Abdeldayem H, Idris F, Elrifai A, Fahmy A. Antegrade mini-percutaneous flexible ureteroscopy versus retrograde ureteroscopy for treating impacted proximal ureteric stones of 1–2 cm: a prospective randomised study. Arab J Urol. 2020; 18: 176-180.
7. Long Q, Guo J, Xu Z, et al. Experience of mini-percutaneous nephrolithotomy in the treatment of large impacted proximal ureteral stones. Urolo Int. 2013; 90: 384-388.
8. Gu XJ, Lu JL, Xu Y. Treatment of large impacted proximal ureteral stones: randomized comparison of minimally invasive percutaneous antegrade ureterolithotripsy versus retrograde ureterolithotripsy. World J Urol. 2013; 31: 1605-1610.
9. Park H, Park M, Park T. Two-year experience with ureteral stones: extracorporeal shockwave lithotripsy v ureteroscopic manipulation. J Endourol. 1998; 12: 501-504.
10. Zhang Y, Yu CF, Jin SH, Zhu H, Na YQ. A prospective comparative study between minimally invasive percutaneous nephrolithotomy in supine position and flexible ureteroscopy in the management of single large stone in the proximal ureter. Urology. 2014; 83: 999-1002.
11. Jiao B, Lai S, Xu X, Zhang M, Diao T, Zhang G. The efficacy of flexible ureteroscopy lithotripsy and miniaturized percutaneous nephrolithotomy for the treatment of renal and proximal ureteral calculi of ≤2 cm: A retrospective study. Medicine (Baltimore). 2019; 98: e14535.
12. Chen Y, Wen Y, Yu Q, Duan X, Wu W, Zeng G. Percutaneous nephrolithotomy versus flexible ureteroscopic lithotripsy in the treatment of upper urinary tract stones: a meta-analysis comparing clinical efficacy and safety. BMC Urol. 2020; 20: 109.
13. Winter M, Lynch C, Appu S, Kourambas J. Surgery illustrated – focus on details: Access sheath-aided percutaneous antegrade ureteroscopy; a novel approach to the ureter. BJU Int. 2011; 108: 620-622.
14. Liu Y, Zhou Z, Xia A, Dai H, Guo L, Zheng J. Clinical observation of different minimally invasive surgeries for the treatment of impacted upper ureteral calculi. Pak J Med Sci. 2013; 29:1358-1362.
15. Mahajan PM, Padhye AS, Bhave AA, Sovani YB, Kshirsagar YB, Bapat SS. Is stenting required before retrograde intrarenal surgery with access sheath. Indian J Urol. 2009; 25: 326-328.
16. Yuk HD, Park J, Cho SY, Sung LH, Jeong CW. The effect of preoperative ureteral stenting in retrograde Intrarenal surgery: a multicenter, propensity score-matched study. BMC Urol. 2020; 20: 147.
17. Moufid K, Abbaka N, Touiti D, Adermouch L, Amine M, Lezrek M. Large impacted upper ureteral calculi: A comparative study between retrograde ureterolithotripsy and percutaneous antegrade ureterolithotripsy in the modified lateral position. Urol Ann. 2013; 5: 140-146.
18. Güler Y, Erbin A. Comparative evaluation of retrograde intrarenal surgery, antegrade ureterorenoscopy and laparoscopic ureterolithotomy in the treatment of impacted proximal ureteral stones larger than 1.5 cm. Cent European J Urol. 2021; 74: 57-63.
19. Sun X, Xia S, Lu J, Liu H, Han B, Li W. Treatment of large impacted proximal

ureteral stones: randomized comparison of percutaneous antegrade ureterolithotripsy versus retrograde ureterolithotripsy. J Endourol. 2008; 22: 913-917.

20. Yavuz A, Kilinc MF, Bayar G. Outcomes of different minimally invasive techniques in lower calyceal stones of 1 to 2 centimeters: A prospective, randomized study. Arch Esp Urol. 2020; 73: 307-315 [Article in Spanish].

21. Chapman RA, Somani BK, Robertson R, Healy S, Kata SG. Decreasing the cost of flexible ureterorenoscopy: single-use laser fiber cost analysis. Urology. 2014; 83: 1003-1005.

22. Hughes T, Ho HC, Pietropaolo A, Somani BK. Guideline of guidelines for kidney and bladder stones. Turk J Urol. 2020; 46 (Suppl 1): S104-S112.

23. Mehmi A, Jones P, Somani BK. Current status and role of patient-reported outcome measures (PROMs) in endourology. Urology. 2021; 148: 26-31.

ORIGINAL PAPER

UROLITHIASIS

Influence of pre-stenting on flexible and navigable suction (FANS) access sheath outcomes. Results of a prospective multicentre study by the EAU Section of Endourology and the global FANS collaborative group

Victoria Jahrreiss[1,2,3], Vineet Gauhar[4], Olivier Traxer[5], Khi Yung Fong[6], Saeed Bin Hamri[7], Karl Tan[8], Vigen Malkhasyan[9], Satyendra Persaud[10], Mohamed Elshazly[11], Wissam Kamal[12], Steffi Yuen[13], Vikram Sridharan[14], Daniele Castellani[15], Mehmet Ilker Gökce[16], Nariman Gadzhiev[17], Deepak Ragoori[18], Boyke Soebhali[19], Chu Ann Chai[20], Azimdjon N. Tursunkulov[21], Yiloren Tanidir[22], Tzevat Tefik[23], Anil Shrestha[24], Marek Zawadzki[25], Mohamed Amine lakmichi[26], Christian Seitz[1], Bhaskar K. Somani[2]

[1]*Department of Urology, Medical University of Vienna, Austria*
[2]*Department of Urology, University Hospital Southampton, United Kingdom*
[3]*YAU Working Group Endourology & Urolithiasis*
[4]*Department of Urology, Ng Teng Fong General Hospital, Singapore*
[5]*Department of Urology, Hospital Tenon, AP-HP, Sorbonne University, Paris, France*
[6]*Yong Loo Lin School of Medicine National University of Singapore, Faculty of Medicine, Singapore*
[7]*King Abdullah International Medical Research Centre, Department of Surgery, Riyadh, Saudi Arabia*
[8]*Department of Surgery, Section of Urology, Veterans Memorial Medical Centre, Quezon City, Philippines*
[9]*Urology Unit, A.I. Evdokimov Moscow State University of Medicine and Dentistry, Moscow, Russian Federation*
[10]*Division of Clinical Surgical Sciences, University of the West Indies, St Augustine, Trinidad and Tobago*
[11]*Urology Unit, Menoufla University, Shibin el Kom, Egypt*
[12]*Department of Urology, King Fahad Hospital, Jeddah, Saudi Arabia*
[13]*Department of Surgery, S.H. Ho Urology Centre, The Chinese University of Hong Kong, Shatin, Hong Kong SAR, China*
[14]*Department of Urology, Sree Paduka Speciality Hospital, Thillai Nagar, India*
[15]*Department of Urology, IRCCS INRCA, Ancona, Italy*
[16]*Department of Urology, Ankara University School of Medicine, Ankara, Turkey*
[17]*Department of Urology, Saint-Petersburg State University Hospital, Saint-Petersburg, Russia*
[18]*Department Urology, Asian Institute of Nephrology and Urology, Hyderabad, India*
[19]*Department of Urology, Abdul Wahab Sjahranie Hospital Medical Faculty, Muliawarman University, Samarinda, Indonesia*
[20]*Department of Surgery Urology Unit, University Malaya, Kuala Lumpur, Malaysia*
[21]*Department of Urology, AkfaMedline Hospital, Tashkent, Uzbekistan*
[22]*Department of Urology, Marmara University School of Medicine, Istanbul, Turkey*
[23]*Department of Urology, Istanbul Faculty of Medicine, Istanbul University, Istanbul, Turkey*
[24]*Department of Urology, National Academy of Medical Sciences, Bir Hospital, Kanti Path, Kathmandu, Nepal*
[25]*Urology Unit, St. Anna Hospital, Piaseczno, Poland*
[26]*Department of Urology, Federal University of Paraná, School of Medicine, Department of Urology, Hospital das Clínicas, Curitiba, Brazil*

Citation: Jahrreiss V, Gauhar V, Traxer O, et al. Influence of pre-stenting on flexible and navigable suction (FANS) access sheath outcomes. Results of a prospective multicentre study by the EAU Section of Endourology and the global FANS collaborative group. Cent European J Urol. 2025; 78: 85-93.

Article history
Submitted: Sep. 8, 2024
Accepted: Oct. 16, 2024
Published online: Nov. 28, 2024

Introduction Pre-stenting remains a subject of debate, and its influence on FANS assisted ureteroscopy is unclear. The global FANS collaborative group aims to address the influence of pre-stenting on FANS-assisted ureterorenoscopy (URS).

Material and methods This prospective multicentre study assesses the outcomes of 394 patients undergoing FANS-assisted ureteroscopy for renal stones. Patients were stratified into a non-pre-stented (group 1, n = 163) and pre-stented group (group 2, n = 231). Data on demographics, stone characteristics, operative parameters, and postoperative 30-day outcomes were analysed. Statistical analyses, including multivariate regression, were performed for stone-free rates (SFR) and complications. SFR was defined by bone window on non-contrast computed tomography (CT).

Corresponding author
Victoria Jahrreiss
Department of Urology,
Medical University
of Vienna,
Währinger Gärtel 18-10
1090 Vienna, Austria
Victoria.jahrreiss@
meduniwien.ac.at

Results Pre-stented patients had a higher prevalence of positive urine culture treated with preoperative antibiotics (23.8% vs 12.3%, p = 0.006). Larger stone volumes were noted (1,306 mm^3 vs 1,200 mm^3, p = 0.027) in group 1. Postoperative complications were minor. Sepsis was not reported in either group. Group 1 had a higher incidence of low-grade Traxer grade 1 ureteric injuries (4.3% vs 0.4%, p = 0.021). FANS resulted in high overall SFRs of 97.5% and 97.0% in groups 1 and group 2. Multivariate analysis showed no statistical difference in SFR between the groups (63.2% vs 53.2%, p = 0.063). Only thulium fibre laser (TFL) and stone volume were significant predictors of residual fragments (RF).
Conclusions Pre-stenting for FANS is not mandatory irrespective of stone location and volume. The use of TFL and stone volume significantly influenced SFR, while FANS itself proved highly effective in achieving high SFR.

Key Words: FANS ‹› suction ‹› access sheaths ‹› ureteroscopy ‹› ureterorenoscopy ‹› RIR

INTRODUCTION

Pre-stenting before retrograde intra-renal surgery (RIRS) remains controversial, with studies [1] and guidelines [2, 3] differing in recommendations. It does improve the ability to insert a ureteric access sheath (UAS) in different populations [4] but does not necessarily translate into better stone-free rates (SFR).
Flexible and navigable sheaths (FANS) are effective tools to improve flexible ureteroscopy safety. As FANS crosses the pelviureteric junction (PUJ) and, like a flexible scope, uses active and passive deflection, it must be manoeuvred within the pelvicalyceal system to maximise efficacy [5].
The global FANS collaborative group initiative was established primarily to assess if FANS can be used safely in non-stented patients and if it can achieve a zero residual fragment status, renderi (FURS) outcomes [5]. With miniaturisation, different sheath sizes are available, and further studies need to ascertain if pre-stenting does indeed improve the utility without compromising patients 100% stone-free in a real-world setting, both with and without pre-stenting.

MATERIAL AND METHODS

Twenty-five centres worldwide prospectively contributed data on 394 adult patients undergoing FURS using FANS. A 100 watt pulse-modulated, high-power holmium laser (HpHL) from Lumenis with and without MOSES technology or a 60 watt thulium fibre laser (TFL) from IPG Photonics or Quanta fibre dust or SOLTIVE laser was used for renal stones of any size/number and location in kidneys with a normal pelvicalyceal system (PCS) between 1 April 2023 and 10 January 2024.
All patients had a preoperative and at least one postoperative non-contrast CT scan (NCCT) to assess stone(s) features and residual fragments (RF) within 30 days of the index procedure. Children and patients who had abnormal renal anatomy, ureteral stones, or insufficient data records were excluded. Because most surgeons were new users or had limited exposure to FANS, prior to case enrolment all surgeons were asked to see the step-by-step video on FANS use (9) and perform a trial of at least 2 cases.
The choice of energy source for RIRS, sheath size and brand, perioperative decisions, and postoperative exit strategy was at the respective surgeon's discretion. Data on the reason for pre-stenting (symptomatic relief/obstruction/failure to primary access/staged RIRS or preferred choice) was collected. Only patients in whom FANS was successfully deployed with and without pre-stenting were eligible. The primary outcome was to assess for SFR and complications. RF were classified using the bone window in a NCCT within 30 days of RIRS. Patients were categorised as follows:

- grade A: 100% stone-free, indicating zero RF, no fragments or dust visible on the CT scan,
- grade B: single RF not more than 2 mm,
- grade C: single RF 2.1–4 mm,
- grade D: single RF >4 mm or multiple RF of any size.

Patients with grade A were classified as having zero RF, while grade A and B were considered stone-free with no further imaging or follow-up needed. Grade C and D were considered as non-stone-free. These patients, if planned for intervention by a second RIRS, would need a CT scan to reassess the need for the same.
Details about laser type, preferred technique, and lasing mode for laser lithotripsy were recorded. The evaluation was compared between the non-pre-stented (group 1) and pre-stented patients (group 2). Other outcomes of interest included postoperative complications within 24 hours and any readmission within 30 days or future planned re-intervention.

Statistical analysis

Statistical analyses were performed using R Statistical language, version 4.3.0 (R Foundation for Statistical Computing, Vienna, Austria) with $p < 0.05$ indicating statistical significance. Continuous variables were described using median and interquartile range, while categorical variables were described using absolute numbers and percentages. The Shapiro-Wilk test was used to assess for normality. To visualise the similarities and differences between both study arms, patient demographics, peri-operative parameters, and 30-day outcomes were compared between the HpHL and TFL groups using the χ^2 test or Fisher exact test for categorical parameters and the Mann-Whitney U test for continuous variables.

Bioethical standards

Patient consent was obtained to contribute to the IRB-approved anonymised global FANS registry (#AINU 12/2022) maintained by the principal site (Asian Institute of Nephro-Urology, Hyderabad, India).

RESULTS

Baseline characteristics

Of 394 patients, 163 were in group 1 and 231 in group 2. The median age was 50 years (IQR: 36–60) in group 1 and 49 years (IQR: 36–61) in group 2. Both groups had comparable distributions of gender, BMI, and presentation symptoms. A higher percentage of patients in group 2 had positive urine cultures treated with preoperative antibiotics (23.8% vs 12.3%, $p = 0.006$) and received prophylactic preoperative antibiotics more frequently (76.6% vs 92.0%, $p < 0.001$). Stone diameter distribution differed significantly between the groups ($p = 0.044$), with a higher proportion of stones larger than 1 cm in group 1. Stone volume also showed a significant difference ($p = 0.007$), with a higher prevalence of larger stone volumes in group 1 (Table 1).

Operative characteristics

No significant differences were observed in the rates of spinal anaesthesia between the 2 groups.

Table 1. *Baseline characteristics*

	Entire cohort		
	Not pre-stented (n = 163)	Pre-stented (n = 231)	p-value
Age	50 [36, 60]	49 [36, 61]	0.498
Male gender	94 (57.7)	139 (60.2)	0.694
Body mass index (BMI) [kg/m^2]	26 [24, 29]	26 [24, 29]	0.96
Presentation			
Haematuria	15 (9.2)	19 (8.2)	0.874
Pain	133 (81.6)	185 (80.1)	0.807
Fever	3 (1.8)	8 (3.5)	0.514
Incidental	17 (10.4)	22 (9.5)	0.9
Urine culture positive (preoperative treated with antibiotics)	20 (12.3)	55 (23.8)	**0.006**
Preoperative antibiotics (prophylactic)	150 (92.0)	177 (76.6)	**<0.001**
Hounsfield units	1,070 [895, 1,213]	1,100 [888, 1,241]	0.923
Right-sided stone	71 (43.6)	95 (41.1)	0.705
Stone diameter			
<1 cm	29 (17.8)	66 (28.6)	**0.044**
1–2 cm	105 (64.4)	126 (54.5)	
>2 cm	29 (17.8)	39 (16.9)	
Stone volume [mm^3] (continuous variable)	1,306 [793, 1,943]	1,200 [636, 1,600]	**0.027**
Stone volume [mm^3] (categorical variable)			
≤1,500	94 (57.7)	159 (68.8)	**0.007**
1,501–3,000	49 (30.1)	49 (21.2)	
>3,000	20 (12.3)	23 (10.0)	
Stone location			
Multiple locations	12 (7.4)	13 (5.6)	
Upper pole only	32 (19.6)	63 (27.3)	0.177
Middle pole only	59 (36.2)	89 (38.5)	
Lower pole only	60 (36.8)	66 (28.6)	

Differences were noted in sheath size, ureteroscopy time, and total operation time. The distribution of sheath sizes was similar, although more patients in group 2 had larger sheath sizes. Group 1 had longer median ureteroscopy time (39 minutes [IQR: 29–60] vs 32 minutes [IQR: 24–49], p = 0.004) and total operation time (54 minutes [IQR: 39.5–75] vs 45 minutes [IQR: 36–63.5], p = 0.008). Stone fragmentation techniques and laser parameters were similar, although the use of TFL was more common in group 1 (53.4% vs 40.7%, p = 0.017) (Table 2).

Postoperative outcomes

The incidence of mild bleeding due to scope/sheath movement was higher in group 2 (7.8% vs 3.7%, p = 0.142), but this difference was not statistically significant. Ureteric injury was more common in group 1 (4.3% vs 0.4%, p = 0.021). Other complications, including postoperative transfusion, fluid extravasation, perinephric stranding, fever, and sepsis, did not differ significantly between the groups. Loin pain scores on the first postoperative day were similar between the groups (p = 0.093) (Table 3).

Stone-free rates

Stone-free parameters, including intraoperative 100% SFR (zero R, grade A) and 30-day outcomes, were comparable between both groups. Intraoperative 100% stone-free rates were 50.3% in group 1 and 51.9% in group 2 (p = 0.203). At the 30-day follow-up, the rates of achieving 100% stone-free status (zero RF) were 63.2% and 53.2% in group 1 and 2, respectively

Table 2. *Operative characteristics*

	Not pre-stented (n = 163)	Pre-stented (n = 231)	p-value
Spinal anaesthesia	29 (17.8)	41 (17.7)	>0.99
Sheath size (Fr)			
12–14	32 (19.6)	51 (22.1)	0.75
11–13	64 (39.3)	83 (35.9)	
10–12	67 (41.1)	97 (42.0)	
Sheath			
Clearpetra	103 (63.2)	141 (61.0)	
Innovex	5 (3.1)	20 (8.7)	0.058
Elephant	45 (27.6)	49 (21.2)	
Others	10 (6.1)	21 (9.1)	
Disposable scope	144 (88.3)	208 (90.0)	0.709
Scope size ≥8 (Fr)	69 (42.3)	104 (45.0)	0.669
Laser time [min]	19 [12, 28.5]	17. [11, 27]	0.177
Ureteroscopy time [min] (actual usage of Flexible scope)	39 [29, 60]	32 [24, 49]	**0.004**
Total operation time [min] (from cystoscopy to exit)	54 [39.5, 75]	45 [36, 63.5]	**0.008**
Stone fragmentation technique			
Dusting with aspiration only	68 (41.7)	87 (37.7)	
Popcorning with aspiration only	7 (4.3)	9 (3.9)	0.848
Fragmentation and basketing only	3 (1.8)	4 (1.7)	
Fragmentation and aspiration only	85 (52.1)	131 (56.7)	
TFL	87 (53.4)	94 (40.7)	**0.017**
Laser parameters			
Dusting energy [J]	0.5 [0.4, 0.8]	0.50 [0.4, 0.8]	0.688
Dusting frequency [Hz]	25 [20, 45]	25 [12, 40]	**0.01**
Popcorning/fragmentation energy [J]	1.0 [0.6, 1.0]	1.0 [0.8, 1.2]	**<0.001**
Popcorning/fragmentation frequency [Hz]	18 [10, 35]	15 [10, 33]	**0.002**
Stone basketing (for relocation and extraction)	26 (16.0)	26 (11.3)	0.228
Sheath able to access all parts of kidney	147 (90.2)	195 (84.4)	0.13
Postoperative strategy (exit strategy)			
DJ stent	135 (82.8)	176 (76.2)	0.282
Overnight ureteric catheter	19 (11.7)	37 (16.0)	
No stent or ureteric catheter	9 (5.5)	18 (7.8)	
Likert scale rating for UAS performance			
Ease of suction	2 [1, 2]	2 [1, 2]	0.229
Manipulation	2 [1.5, 2]	2 [1, 3]	0.384
Visibility	1 [1, 2.5]	1 [1, 3]	0.186

DJ stent – double J stent; TFL – thulium fibre laser; UAS – ureteric access sheath

(p = 0.063). Single-stage SFR (grade A + B) was 97.5% in group 1 and 97.0% in group 2 (p = 0.975).

Multivariate analysis

Table 4 presents the multivariate analysis (MVA) of 100% SFR in the matched cohort. The analysis revealed no significant effect of presenting on SFR (OR 0.819, 95% CI: 0.430–1.550, p = 0.539). TFL usage was associated with higher SFR compared to HpHL (OR 1.93, 95% CI: 1.044–3.625, p = 0.038). Additionally, larger stone volume (>1,500 mm^3) was associated with lower SFR (OR 0.274, 95% CI: 0.116–0.619, p = 0.002).

Table 3. *Postoperative outcomes*

	Not pre-stented (n = 163)	Pre-stented (n = 231)	p-value
Mild bleeding due to scope/sheath movement not affecting intraoperative surgery	6 (3.7)	18 (7.8)	0.142
Postoperative transfusion (CD1)	0	1 (0.4)	>0.99
Ureteric injury (all cause managed by stenting)	7 (4.3)	1 (0.4)	**0.021**
Level of injury: PUJ/proximal/mid/distal	1/2/2/2	1/0/0/0	
PCS injury (due to scope/sheath or laser managed by stenting only)	3 (1.8)	2 (0.9)	0.693
Fluid extravasation not needing intervention	5 (3.1)	2 (0.9)	0.214
Perinephric stranding reported on first NCCT	14 (8.6)	14 (6.1)	0.446
Fever within 24 hours	7 (4.4)	5 (2.4)	0.458
Sepsis	0	0	NA
Persistent haematuria needing intervention	0	0	NA
Loin pain score (1st postoperative day)	1 [1, 2]	1 [1, 2]	0.093
Stone freedom parameters			
Intraoperative 100% SFR	82 (50.3)	120 (51.9)	0.203
30-day outcomes			
100% SFR (zero residual fragment)	103 (63.2)	123 (53.2)	0.063
Single-stage stone free (grade A + B)	159 (97.5)	224 (97.0)	0.975
Single-stage non-stone free (grade C + D)	4 (2.5)	7 (3.0)	
Reintervention planned after 1st CT: RIRS/ESWL	4 (2.5)/0	7 (3.0)/0	

CT – computed tomography; ESWL – extracorporeal shock-wave lithotripsy; NCCT – postoperative non-contrast CT scan; PCS – pelvicalyceal system; PUJ – pelviureteric junction; RIRS – retrograde intra-renal surgery; SFR – stone-free rates

Table 4. *Multivariate analysis of 100% stone-free rates in the matched cohort*

	Odds ratio (OR)	95% CI	p-value
Pre-stenting	0.819	0.430–1.550	0.539
Laser type (TFL vs HL)	1.93	1.044–3.625	**0.038**
Stone location (vs multiple locations)			
Upper pole	2.328	0.579–9.743	0.236
Middle pole	1.146	0.319–4.231	0.834
Lower pole	1.438	0.389–5.420	0.584
Stone volume (categorical variable, vs ≤1,500)			
1,501–3,000	0.274	0.116–0.619	**0.002**
>3,000	0.696	0.218–2.255	0.538
Hounsfield units	1.001	0.999–1.002	0.436
Laser time	1.01	0.953–1.071	0.725
URS time	0.967	0.928–1.003	0.088
Total operation time	1.007	0.959–1.058	0.786

HL – holmium laser; TFL – thulium fibre laser; URS – ureterorenoscopy

DISCUSSION

Traditionally, UAS was preferably used in pre-stented patients because it allowed for better drainage of irrigation and facilitated multiple scope passages if inserted atraumatically [6]. However, larger sheaths increased ureteric injury risk, leading to a perception that pre-stenting was necessary to prevent ureteric injury and achieve safe RIRS [7]. FANS has emerged as a promising tool in FURS, offering benefits such as improved intraoperative visualisation, enhanced SFR, and reduced intrarenal pressure, temperature, and postoperative complications [5, 8–10]. One notable advantage is its flexible and navigable proximal 10-cm tip, which allows for active and passive deflection, which is particularly beneficial in cases of a dilated system, facilitating navigation into the desired calyx. With the advent of novel FANS designs that can be inserted beyond the PUJ, the role of pre-stenting in these scenarios requires further investigation.

In this study, pre-stenting was conducted for symptomatic relief, obstruction, failure to achieve primary access, or for staged RIRS. The number of patients with asymptomatic incidental renal stones (AIRS) [11] was nearly equal in both groups (10.4% vs 9.5%). Despite FANS being a newer accessory involving sheath movement within the kidney, surgeons did not consider size, volume, and non-pre-stenting as deterrents to perform FANS. In fact, non-pre-stented patients had larger stones compared to pre-stented patients with stone volumes of 1,306 mm^3 (IQR: 793–1,943) and 1,200 mm^3 (IQR 636–1,600), respectively, $p = 0.027$.

Although the stone fragmentation techniques were similar between the groups ($p = 0.848$), TFL was more commonly utilised in group 1 (53.4% vs 40.7%, $p = 0.017$). This could be due to personal preference bias of surgeons or the availability only of TFL at certain centres. Interestingly, group 1 exhibited lower mean laser energy settings, suggesting a more conservative approach to laser energy delivery. This might explain why lasing time, ureteroscopy time, and total operation time were significantly higher in group 1, in addition to larger stone volumes requiring longer total ablation time. This is also reported in traditional RIRS by Chai et al. [1], whereby in the FLEXOR studies the mean operative time for non-pre-stented patients was significantly longer (68.17 min vs 58.92 min, $p < 0.001$).

For our study the ureteroscopy time was recorded specifically representing the surgeon's time spent navigating FANS into different calyces for inspection/lasering and/or aspiration of dust and fragments. One would expect this to prolong operative times, but notably the operative times using FANS are shorter or comparable to most other series (non-pre-stented vs pre-stented: 54 min [39.5, 75] vs 45 min [36, 63.5], respectively, $p < 0.008$) [1, 4]. Noting that dusting or fragmentation with immediate suction was the preferred technique, it might have been more efficacious.

Dusting or fragmentation with suction will depend on the surgeon's preferred choice, but as seen in our study, these methods lead to a lesser need for popcorning or basket extraction of fragments. This might allow surgeons to spend less overall time in the PCS. The trifecta mechanism that enables this is the vacuum effect, which prevents stone debris from migration into other calyces, dust aspiration allowing for clear vision, and active fragment removal via sheath by whirlpool effect of high irrigation flow rates.

Using suction, and lowering lasering time and overall operative times contribute to the well-established benefit of preventing the damage that high intrarenal temperature and pressure may cause during RIRS [12].

Smaller diameter sheaths and scopes have been suggested as preferred choices in multiple studies [5, 13]. In our study, there was a trend towards the utilisation of smaller scopes and sheaths in both groups. Overall, there was no significant difference in sheath sizes between the 2 groups ($p = 0.75$). Interestingly, the sheath reached all parts of the kidney more successfully in group 1 than in group 2, i.e. 90.2% and 84.4%, respectively ($p = 0.13$). This raises questions about potential factors contributing to this difference, such as surgeon skill, sheath design, or the use of smaller scopes in group 1.

Intraoperative bleeding due to scope or sheath movement was slightly higher in group 2 (7.8% vs 3.7%, $p = 0.142$). The larger diameter scopes and sheaths used in pre-stented cases might also have contributed to increased inadvertent mucosal rubbing, leading to mild oozing. This could also be induced by the stones or pre-stenting-induced mucosal inflammation. However, due to effective suction management this did not affect intraoperative surgery significantly. While the incidence of ureteric injuries was low and mostly minor – primarily Traxer grade 1 [7] – they occurred more frequently in group 1 (4.3% vs 0.4%, respectively, $p = 0.021$). Importantly, these injuries predominantly occurred not at the site of the PUJ but rather in the ureter.

This finding is noteworthy, particularly in light of existing concerns regarding the deployment of access sheaths beyond the PUJ. These findings reaffirm that urologists should be mindful while inserting any UAS, especially in non-pre-stented cases, and

more so if a larger diameter is preferred. However, the use of FANS itself is not a reason for PUJ or calyceal injury, unless carelessly inserted.

Group 2 had a higher proportion of patients with positive urine cultures requiring preoperative antibiotic treatment, aligning with the known association between indwelling ureteric stents and increased susceptibility to urinary tract infections, even in patients with initially negative urine cultures [14]. Patients with longer durations of pre-procedural indwelling ureteric stents face a higher risk of postoperative urinary tract infection and sepsis [15]. Despite these considerations, no cases of sepsis were reported in either group, and the incidence of postoperative fever was low, at 4.4% and 2.4% in group 1 vs group 2, respectively. This may be attributed to the lower intrarenal pressures associated with the use of FANS, which can help prevent pyelovenous backflow [16, 17]. This is consistent with prior studies demonstrating either no or minimal infectious complications in FANS-assisted ureteroscopy [5, 17–19].

In group 1 there was a higher rate of postoperative stent placement (82.8% vs 76.2%, respectively). Conversely, the confidence to leave only an overnight ureteric catheter was lower in group 1 (11.7% vs 16.0%, respectively). Furthermore, fewer cases in group 1 opted for neither stent nor ureteric catheter placement. The difference in postoperative strategies between the 2 groups was not statistically significant ($p = 0.282$). This does raise a paradoxical situation wherein should we therefore pre-stent to avoid postoperative stenting? Further studies are warranted to determine the optimal approach.

No statistically significant difference was seen between both groups regarding postoperative loin pain, with very low scores. This suggests a favourable outcome for patients undergoing FANS-assisted retrograde intrarenal surgery (RIRS), regardless of pre-stenting status. Probably the low IRP prevents retro- and intrarenal extravasation that contributes to lower pain [19–21].

SFR between the 2 groups were comparable. Intraoperatively, both groups exhibited similar rates of achieving 100% SFR, with 50.3% in group 1 and 51.9% in group 2 ($p = 0.203$). At the 30-day follow-up, the differences in SFR remained non-significant. The proportion of patients achieving 100% SFR (zero residual fragments) was 63.2% in group 1 and 53.2% in group 2 ($p = 0.063$). Furthermore, the single-stage SFR (grades A and B) were notably high and comparable between both groups, with 97.5% in group 1 and 97.0% in group 2 ($p = 0.975$). Reintervention rates after the first CT scan were similar between the groups, with 2.5% in group 1 and 3.0% in group 2 requiring further intervention, either by RIRS or extracorporeal shock-wave lithotripsy (ESWL). Overall, these findings suggest that pre-stenting does not significantly impact stone-free outcomes.

MVA demonstrated that pre-stenting had no significant effect on SFR. This suggests that pre-stenting does not independently contribute to higher SFR. Interestingly, only TFL usage was associated with higher SFR compared to HpHL, with an OR of 1.93 and a p-value of 0.038. Indeed, TFL has been shown to be a better ablative laser for RIRS due to its ability to produce finer dust, perhaps allowing for easier aspiration. However, the use of TFL itself is not responsible for a better SFR compared to other lasers [22]. We believe that the combination of FANS and TFL, allowing for targeted access to all parts of the calyces, may have contributed to more effective removal of finer dust. However, this warrants corroboration with studies that specifically look at ablation efficiency with FANS.

Furthermore, stone volume was a significant predictor of SFR. Stones with volumes ranging from 1,501 to 3,000 mm^3 were associated with a significantly lower likelihood of achieving 100% SFR compared to stones with volumes of 1,500 mm^3 or less, with an OR of 0.274 and a p-value of 0.002. Stones larger than 3,000 mm^3 showed lower odds of SFR, but our study had very high overall SFR at 30 days. Indeed, stone volume should be used instead of stone diameter as a predictor for RIRS efficacy.

Overall, the findings suggest that pre-stenting does not independently influence stone-free outcomes. Instead, factors such as the type of laser used and stone volume play more significant roles in determining the success of the procedure. Perhaps FANS technology itself may be the primary driver of improved SFR, rather than pre-stenting.

While this study provides valuable insights into the outcomes of FANS-assisted RIRS and the role of pre-stenting, several limitations should be considered:

- Although this study benefits from its prospective and multicentric design, it was not randomised, and its sample size may not be sufficient to draw definitive conclusions.
- The study's multicentre design with use of different UAS and instrumentation manufacturers introduces variability in surgical techniques, which may affect generalisability. However, to minimise variability in outcome reporting, a uniform methodology of NCCT in bone window and strict follow-up protocol were applied in a real-world practice.

Further prospective, randomised controlled trials with larger sample sizes and longer follow-up periods are warranted to validate the findings of this study.

CONCLUSIONS

Our findings suggest that pre-stenting for FANS procedures is not mandatory regardless of stone location and volume. However, the preference for smaller sheaths and disposable scopes to minimise incidental low-grade injuries emphasises the importance of meticulous instrumentation selection.
TFL and stone volume were critical variables influencing stone-free rates. Nonetheless, the efficacy of FANS itself in achieving a high SFR highlights its utility in RIRS as a useful accessory.
We speculate from our study findings that pre-stenting may minimise postoperative stent requirements; however, the trade-off between pre-stenting and postoperative stenting warrants further investigation to optimise patient outcomes and resource utilisation.

CONFLICTS OF INTEREST
The authors declare no conflict of interest.

FUNDING
This research received no external funding.

ETHICS APPROVAL STATEMENT
The ethical approval was not required.

References

1. Chai CA, Teoh YC, Tailly T, et al. Influence of pre-stenting on RIRS outcomes. Inferences from patients of the Global Multicentre Flexible Ureteroscopy Outcome Registry (FLEXOR). Minerva Urol Nephrol. 2023; 75: 493-500.
2. Tzelves L, Türk C, Skolarikos A. European Association of Urology Urolithiasis Guidelines: Where Are We Going? Eur Urol Focus. 2021; 7: 34-38.
3. Zeng G, Traxer O, Zhong W, et al. International Alliance of Urolithiasis guideline on retrograde intrarenal surgery. BJU Int. 2023; 131: 153-164.
4. Law YXT, Teoh JYC, Castellani D, et al. Role of pre-operative ureteral stent on outcomes of retrograde intra-renal surgery (RIRS): systematic review and meta-analysis of 3831 patients and comparison of Asian and non-Asian cohorts. World J Urol. 2022; 40: 1377-1389.
5. Gauhar V, Traxer O, Castellani D, et al. A Feasibility Study on Clinical Utility, Efficacy and Limitations of 2 Types of Flexible and Navigable Suction Ureteral Access Sheaths in Retrograde Intrarenal Surgery for Renal Stones. Urology. 2023; 178: 173-179.
6. Huang J, Zhao Z, AlSmadi JK, et al. Use of the ureteral access sheath during ureteroscopy: A systematic review and meta-analysis. PLoS One. 2018; 13: e0193600.
7. Traxer O, Thomas A. Prospective evaluation and classification of ureteral wall injuries resulting from insertion of a ureteral access sheath during retrograde intrarenal surgery. J Urol. 2013; 189: 580-584.
8. Jahrreiss V, Nedbal C, Castellani D, et al. Is suction the future of endourology? Overview from EAU Section of Urolithiasis. Ther Adv Urol. 2024; 16: 17562872241232275.
9. De Coninck V, Somani B, Sener ET, et al. Ureteral Access Sheaths and Its Use in the Future: A Comprehensive Update Based on a Literature Review. J Clin Med. 2022; 11: 5128.
10. Özman O, Akgül HM, Başataç C, et al. Multi-aspect analysis of ureteral access sheath usage in retrograde intrarenal surgery: A RIRSearch group study. Asian J Urol. 2024; 11: 81-85.
11. Ong WLK, Somani BK, Fong KY, et al. Retrograde intrarenal surgery for asymptomatic incidental renal stones: a retrospective, real-world data analysis. BJU Int. 2024; 134: 201-206.
12. Giulioni C, Castellani D, Traxer O, et al. Experimental and clinical applications and outcomes of using different forms of suction in retrograde intrarenal surgery. Results from a systematic review. Actas Urol Esp (Engl Ed). 2024; 48: 57-70.
13. Liang H, Liang L, Lin Y, et al. Application of tip-bendable ureteral access sheath in flexible ureteroscopic lithotripsy: an initial experience of 224 cases. BMC Urol. 2023; 23: 175.
14. Vallée M, Cattoir V, Malavaud S, et al. Perioperative infectious risk in urology: Management of preoperative polymicrobial urine culture. A systematic review. By the infectious disease Committee of the French Association of Urology. Prog Urol. 2019; 29: 253-262.
15. Chugh S, Pietropaolo A, Montanari E, Sarica K, Somani BK. Predictors of Urinary Infections and Urosepsis After Ureteroscopy for Stone Disease: a Systematic Review from EAU Section of Urolithiasis (EULIS). Curr Urol Rep. 2020; 21: 16.
16. Baboudjian M, Gondran-Tellier B, Abdallah R, et al. Predictive risk factors of urinary tract infection following flexible ureteroscopy despite preoperative precautions to avoid infectious complications. World J Urol. 2020; 38: 1253-1259.
17. Qian X, Liu C, Hong S, et al. Application of Suctioning Ureteral Access Sheath during Flexible Ureteroscopy for Renal Stones Decreases the Risk of Postoperative Systemic Inflammatory Response Syndrome. Int J Clin Pract. 2022; 2022: 9354714.
18. Quhal F, Zeng G, Seitz C. Current evidence for suction in endourological procedures: comprehensive review of literature. Curr Opin Urol. 2023; 33: 77-83.
19. Zhu Z, Cui Y, Zeng F, Li Y, Chen Z, Hequn C. Comparison of suctioning and traditional ureteral access sheath during flexible ureteroscopy in the treatment of renal stones. World J Urol. 2019; 37: 921-929.
20. Lai D, He Y, Li X, Chen M, Zeng X. RIRS with Vacuum-Assisted Ureteral Access Sheath versus MPCNL for the Treatment

of 2–4 cm Renal Stone. Biomed Res Int. 2020; 2020: 8052013.

21. Zhang Z, Leng S, Xie T, Yuan Y, Wang X. Flexible ureteroscopic lithotripsy with a suctioning ureteral access sheath for removing upper urinary calculi under local anesthesia. Front Surg. 2023; 10: 1242981.

22. Chua ME, Bobrowski A, Ahmad I, et al. Thulium fibre laser vs holmium: yttrium-aluminium-garnet laser lithotripsy for urolithiasis: meta-analysis of clinical studies. BJU Int. 2023; 131: 383-394.

Central European Journal of Urology

REVIEW PAPER

UROLITHIASIS

Ureteral stents with extraction strings – a review on infection risk and prevention

Patryk Osiński[1], Jakub Bartłomiej Kawecki[1], Martyna Zofia Stachoń[1], Izabela Teresa Zawadzka[1], Ewa Bres-Niewada[1,2], Bartosz Dybowski[1,2]

[1]*Faculty of Medicine, Lazarski University, Warsaw, Poland*
[2]*Department of Urology, Roefler Memorial Hospital, Pruszkow, Poland*

Citation: Osiński P, Kawecki JB, Stachoń MZ, et al. Ureteral stents with extraction strings – a review on infection risk and prevention. Cent European J Urol. 2025; 78: 94-99.

Article history
Submitted: Sep. 20, 2024
Accepted: Nov. 11, 2024
Published online: Feb. 28, 2025

Corresponding author
Patryk Osiński
Faculty of Medicine,
Lazarski University,
43 Świeradowska St.,
02-662 Warsaw, Poland
44452@lazarski.pl

Introduction This review aims to determine whether the use of ureteral stents with extraction strings in adult patients undergoing upper urinary tract endoscopic procedures results in a higher incidence of urinary tract infections (UTIs) compared to stents without strings.

Material and methods A systematic literature search was conducted using PubMed, Scopus, and Google Scholar. Studies evaluating differences in UTI rates among adult patients with ureteral stents with or without extraction strings were included. Data on UTI rates, antibiotic prophylaxis protocols, and stent dwell time were extracted.

Results The review included 11 trials published between 2015 and 2023. One multicenter retrospective study involving 4,392 patients reported a significantly higher UTI rate in patients with extraction strings (2.1% vs 1.1%, p = 0.006). In the remaining 10 studies, including four randomized controlled trials, the differences were not statistically significant. Antibiotic prophylaxis was described in five studies. In two studies, a single perioperative antibiotic dose was administered, with a total UTI rate of 6.8% (28/410). In contrast, three studies using prolonged prophylactic antibiotic regimens reported a total UTI rate of 3.2% (13/403). The impact of stent dwell time on UTI risk could not be determined. The risk of bias was high in 10 studies and moderate in one retrospective study.

Conclusions Based on low-quality evidence, the difference in UTI risk between ureteral stents with and without extraction strings appears to be minimal and statistically insignificant. Well-designed studies with standardized methodologies are needed to clarify these findings.

Key Words: ureteral ‹› ureteric ‹› string ‹› stent ‹› tethered stent ‹› urinary tract infection ‹› prophylaxis ‹› ureteroscopy

INTRODUCTION

Preventing obstruction caused by oedema after upper urinary tract endoscopic procedures is one of the most common indications for ureteral stenting, and this usually requires only a few days of stenting. To reduce costs, invasiveness, and patient discomfort, stents with extraction strings are used in many centers [1–8]. Although this is an established procedure, we decided to review the available literature to assess the effect of a string protruding from the urethra on the risk of infection.

Furthermore, we observed a wide variation in antibiotic prophylaxis approaches in the published studies. Therefore, we considered it essential to evaluate the findings on stents with extraction strings in the context of antibiotic use.

Thus, the primary objective of this study was to determine whether the use of ureteral stents with extraction strings in adult patients after upper urinary tract endoscopic procedures resulted in a higher incidence of urinary tract infections compared to stents without strings (objective aligned with the PICO methodology). The secondary objective

was to assess whether the type of antibiotic prophylaxis used in these studies could have influenced the infection rates.

MATERIAL AND METHODS

Search strategy

A comprehensive literature search was performed in PubMed, Scopus, and Google Scholar/Google from database inception to January 15th, 2025. The systematic review was conducted following the Preferred Reporting Items for Systematic Reviews and Meta-Analyses (PRISMA) checklist and Cochrane guidelines. The search strategy involved identifying the terms "stent", "string", "tethered string", "ureteral", "ureteric", "ureteroscopy", and "retrograde" within titles, abstracts, key words, and Medical Subject Headings (MeSH). Additional studies were identified through manual searches of reference lists in relevant articles.

Eligibility criteria

We selected original research articles with available full texts, written in English. Our primary focus was on trials comparing infection rates between patients with ureteral stents with and without extraction strings, while also considering the use of antibiotic prophylaxis and dwell time. Articles not mentioning antibiotic prophylaxis were also included in the descriptive analysis. Studies that discussed the use of stents post-kidney transplant surgery were excluded. It was decided that only comparative studies with clearly described randomization and antibiotic prophylaxis would be used for final conclusions.

Study selection

The titles and abstracts of the selected studies were independently reviewed by two researchers based on the inclusion and exclusion criteria outlined below. Studies that did not meet the eligibility criteria were excluded, and any disagreements were resolved through discussion during a consensus meeting. The Rayyan® application was used to facilitate the systematic review process.

Data extraction

Data were extracted using a standardized form, including the following: study design, sample size, patient demographics., stent type (with string vs cystoscopic removal), UTI incidence and diagnostic criteria, antibiotic prophylaxis protocols, and stent dwell time.

Risk of bias assessment

The Cochrane Risk of Bias Tool was used for RCTs, and the ROBIN-I was applied to non-randomised case-control studies. Studies were categorised as low, moderate, or high risk of bias. The Robvis application was used to prepare risk-of-bias plots [9].

RESULTS

This review comprised 11 trials published between 2015 and 2023. Figure 1 presents the PRISMA flowchart illustrating the literature search process. Four trials were randomized controlled trials (RCTs) [10–13]. Among the non-randomized case-control studies, one had a prospective design [14], while six were retrospective [8, 15–19].

The risk of bias assessment for the RCTs, presented in Figure 2, indicated a high risk of bias across all included studies. The characteristics of these studies are detailed in Tables 1–3. None of the RCTs defined UTI incidence comparison between groups as the primary study objective. Instead, their primary focus was on patient discomfort or quality of life, with infection rates reported as a secondary outcome. No significant differences in UTI rates were observed among the RCTs, with a total of 14 reported UTI cases among 462 patients (3%). However, a substantial variation in UTI incidence was noted across studies, ranging from 0% to 9.1%.

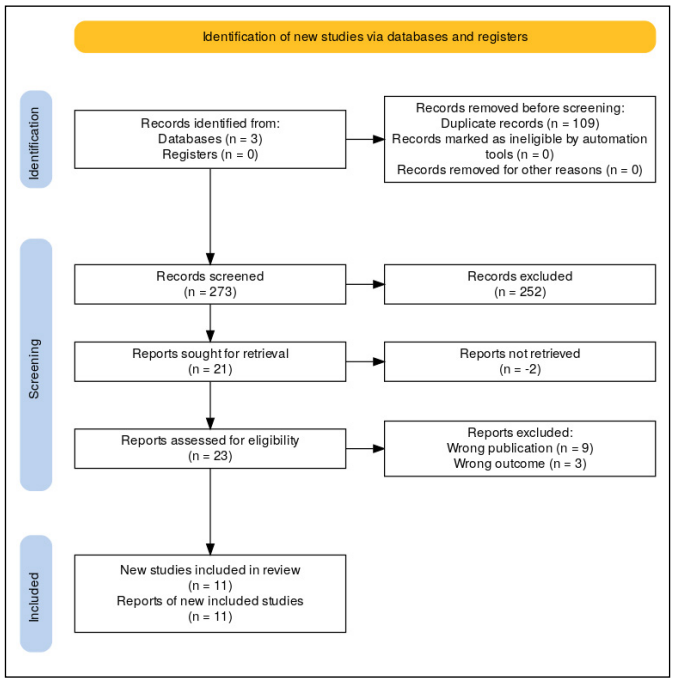

Figure 1. *Preferred Reporting Items for Systematic Reviews and Meta-Analyses (PRISMA) flow diagram of the study.*

The duration of antibiotic prophylaxis was reported in three out of four studies [10, 12, 13], while the specific antibiotic used was mentioned in only one [13]. Notably, only the study by Barnes et al. [12] adhered to European Association of Urology (EAU) guidelines by implementing perioperative prophylaxis, while two studies reported extended administration beyond one day (Table 3).

The risk of bias assessment for the non-randomized studies is presented in Figure 3, with details summarized in Tables 1–3. Among these, one study was conducted prospectively, though its primary objective was to evaluate discomfort during stent removal rather than infection rates. Only two retrospective studies [15, 16] explicitly aimed to assess the impact of extraction strings on UTI risk. However, only one study [15] provided a well-defined outcome measure and a clearly described antibiotic prophylaxis regimen adhering to current guidelines. This study, conducted on a large patient cohort, found a higher incidence of UTI in patients with extraction strings, but the difference was not statistically significant (Table 1). The only study to report a significant difference was a large multicenter retrospective study including 4,392 patients [18], which found a 1% higher UTI incidence in the string group (2.1% vs 1.1%, p = 0.006). Overall, 8 out of 11 studies reported a higher UTI rate in the extraction string group compared to the non-string group, while two studies reported identical infection rates, and one study [8]

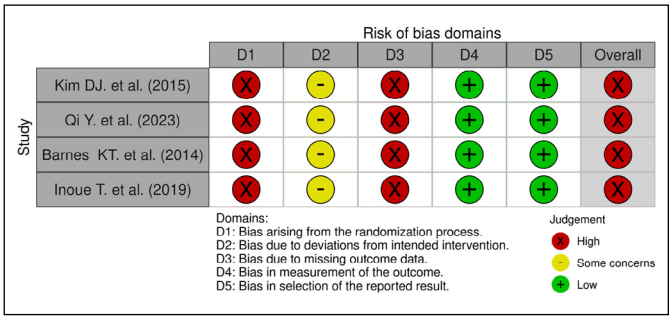

Figure 2. *Risk of bias in randomized controlled trials (ROB-2) [10–13].*

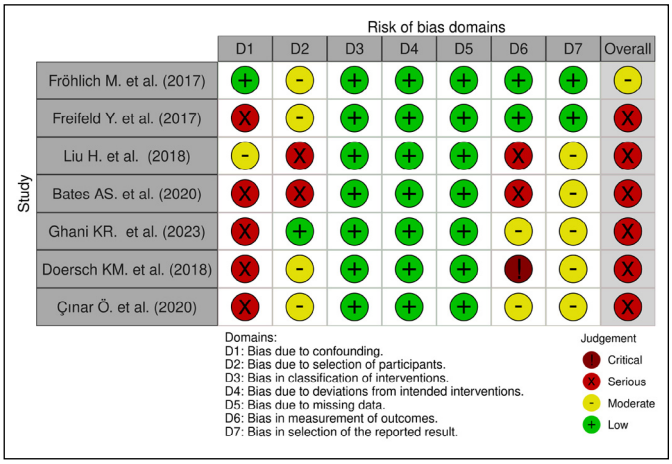

Figure 3. *Risk of bias in non-randomized controlled trials (ROBINS-I) [8, 14–19].*

Table 1. *Characteristics of the studies and reported urinary tract infection rates in stented patient groups without and with extraction strings*

Study	Research type	UTI as a primary or secondary objective of the study	Without extraction strings			With extraction strings			P for UTI	Information on antibiotic prophylaxis
			N	UTI	dwell time	N	UTI	dwell time		
Kim et al. (2015) [10]	RCT	Secondary	56	0	6.3 days	58	0	6 days	–	+
Qi et al. (2023) [11]	RCT	Secondary	66	1 (1.5%)	2.3 ±0.65 weeks	65	1 (1.5%)	2 ±0.3 weeks	0.99	–
Barnes et al. (2014) [12]	RCT	Secondary	35	3 (8.6%)	10.3 days	33	3 (9.1%)	6.3 days	0.94	+
Inoue et al. (2019) [13]	RCT	Secondary	75	2 (2.7%)	11.0 days	74	4 (5.4%)	9.7 days	0.4	+
Bates et al. (2020) [14]	Prospective	Secondary	30	2.8%	26.5 ±4.1 days	60	3.7%	10.1 ±5.3 days	>0.7	–
Fröhlich et al. (2017) [15]	Retrospective	Primary	215	12 (5.6%)	17.8 ±7.7 days	127	10 (7.9%)	7 ±2.4 days	0.4	+
Freifeld et al. (2017) [16]	Retrospective	Primary	133	4 (3%)	–	282	19 (6.7%)	–	0.12	–
Liu et al. (2018) [17]	Retrospective	Secondary	82	4 (4.9%)	11.2 ±3.2 days	58	3 (5.2%)	5.3 ±1.8 days	0.94	+
Ghani et al. (2023) [18]	Retrospective multicenter	Secondary	2,723	29 (1.1%)	9 (6.5–4) days	1,669	35 (2.1%)	5 (4–7) days	0.006	–
Doersch et al. (2018) [8]	Retrospective	Secondary	349	13 (3.7%)	–	94	2 (2.1%)	3 days	0.45	–
Çınar et al. (2020) [19]	Retrospective	Secondary	118	4 (3.4%)	12 days	59	3 (5%)	6 days	0.85	–

RCT – randomized clinical trial; UTI – urinary tract infection

found a higher UTI rate in the non-string group. Due to the substantial heterogeneity in study design, a meta-analysis could not be performed. In non-RCT studies antibiotic prophylaxis was mentioned in only two of seven studies [15, 17], and only in the Fröhlich et al. study [15] was it limited to the perioperative period, in accordance with guideline recommendations.

Overall, antibiotic prophylaxis protocols were described in five studies. In two studies, a single perioperative antibiotic dose was administered, with a total UTI rate of 6.8% (28/410). In contrast, three studies employing prolonged prophylactic antibiotic regimens reported a total UTI rate of 3.2% (13/403).

The impact of stent dwell time on UTI risk was specifically investigated in one study. Freifeld et al. [16] found that patients who had a stent with an extraction string and a dwell time exceeding 8 days had a significantly higher infection rate (20%) than those with a stent dwell time of 8 days or less (3.9%). Ghani et al. [18] also analysed effects of dwell time, however, their outcome of interest was emergency department visits rather than UTI incidence. The heterogeneity among studies precluded meaningful cross-study comparisons.

DISCUSSION

Our analysis does not provide a definitive answer regarding the impact of extraction strings on UTI incidence. However, several observations suggest a potential influence: most studies reported higher UTI rates in the extraction string group, the only study with a statistically significant difference [18] reported a higher infection rate for stents with strings, and the study with the lowest risk of bias [15] also found a numerically higher UTI incidence in the string group. Furthermore, both studies explicitly designed to compare UTI rates between groups reported higher infection rates in groups with extraction strings [15, 16]. Conversely, studies that found no difference in UTI incidence often reported exceptionally low infection rates (as low as 0%), raising concerns about the reliability of these findings.

These considerations do not constitute conclusive evidence, and the overall low quality of available studies concerning UTI incidence prevents firm conclusions about the impact of extraction strings on infection risk.

A second key aspect of this review was the evaluation of infection prevention strategies. Notably, extended antibiotic administration beyond a single perioperative dose was commonly employed in these studies. Antibiotic prophylaxis protocols were explicitly described in three RCTs and two non-RCTs. In the studies by Barnes et al. [12] and Fröhlich et al. [15], a single perioperative antibiotic dose was administered (presumably before ureteroscopy), whereas in three studies [10, 13, 17] prophylaxis was extended beyond one day.

Prolonged antibiotic administration contradicts current guidelines for ureteroscopy [20], as well as conclusions from previous research [21–25] which consistently show no significant benefit from extended antibiotic prophylaxis during stent dwell time. Studies have reported no difference between continuous

Table 2. *Definitions of urinary tract infection used in the studies included in the review*

Study	Urinary tract infection definitions
Kim et al. (2015) [10]	Febrile urinary tract infection requiring additional antibiotic treatment or a therapeutic procedure
Qi et al. (2023) [11]	Fever >38°C
Barnes et al. (2014) [12]	Symptomatic UTI
Inoue et al. (2019) [13]	Fever >38°C
Bates et al. (2020) [14]	–
Fröhlich et al. (2017) [15]	UTI within 30 days after stent placement. In patients without an extraction string UTI within 3 weeks after the procedure
Freifeld et al. (2017) [16]	Fever with a positive urinary culture or fever >38.5°C and no other infection source within 30 days after the procedure
Liu et al. (2018) [17]	Based on urinalysis within 1 month of stent placement or stent removal
Doersch et al. (2018) [8]	–
Ghani et al. (2023) [18]	Diagnosed at emergency department visit
Çınar et al. (2020) [19]	Urinary infection requiring antibiotic treatment

UTI – urinary tract infection

Table 3. *Information about antibiotic prophylaxis used in the studies. Only studies with a description of prophylaxis are listed*

Study	Description	Medication
Kim et al. [10]	Prophylactic antibiotics for several days after surgery	Not stated
Barnes et al. [12]	Perioperative prophylaxis	Not stated
Inoue et al. [13]	Antibiotic for 2 days after stent removal	Levofloxacin 500 mg/day
Fröhlich et al. [15]	Perioperative prophylaxis (half an hour prior to the procedure)	Trimethoprim/sulfamethoxazole (61.7%) Ciprofloxacin (32.2%) Other antibiotic (6.1%)
Liu et al. [17]	Prescription for prophylactic antibiotics at discharge	Not stated

low-dose antibiotic prophylaxis and a single preoperative dose. Continuous prophylaxis has been deemed unnecessary due to associated risks, including side effects and antimicrobial resistance. Although our review suggests a higher cumulative UTI rate in studies utilizing a single-dose antibiotic regimen compared to those using prolonged prophylaxis, the data originate from studies with a high risk of bias. The rationale for conducting further studies on this topic remains questionable. Analogous to findings on short-term indwelling Foley catheters, it is possible that extraction strings slightly increase infection risk (as suggested by Ghani et al. [18]), while prolonged antibiotic prophylaxis may slightly reduce this risk (as inferred from this review). However, even if this is the case, evidence from Foley catheter studies indicates that the minimal reduction in UTI risk does not justify prolonged antibiotic use due to its population-level harms, including increased antimicrobial resistance [26].

Further investigation is warranted into current clinical practices regarding antibiotic prophylaxis in patients undergoing endourological procedures with and without extraction strings. If significant variations exist, this topic should be discussed among experts in endourology and infectious diseases to promote guideline-adherent practices. The studies included in this review, which report on antibiotic prophylaxis, were conducted 6–11 years ago; therefore, an updated assessment of contemporary practices is needed.

CONCLUSIONS

Based on low-quality evidence, the difference in UTI risk between ureteral stents with and without extraction strings appears to be minimal and statistically insignificant. Variability in infection rates between studies was greater than within studies, which is probably due to heterogeneous antibiotic prophylaxis protocols and differing UTI definitions. Further investigation into current antibiotic prophylaxis practices in endourology is warranted, because variations in practice may serve as a target for future research. Future studies should incorporate well-defined outcome measures and clearly described prophylaxis protocols to provide more definitive conclusions.

CONFLICTS OF INTEREST

The authors declare no conflict of interest.

FUNDING

This research received no external funding.

ETHICS APPROVAL STATEMENT

The ethical approval was not required.

References

1. Sali GM, Joshi HB. Ureteric stents: Overview of current clinical applications and economic implications. Int J Urol. 2020; 27: 7-15.
2. Kwong J, Honey RJD, Lee JY, Ordon M. Determination of optimal stent length: a survey of urologic surgeons. Cent European J Urol. 2023; 76: 57-63.
3. Komisarenko I, Banyra O, Nikitin O, Klymenko Y, Chaplia M, Borzhievskyy A. Efficacy of combination therapy tadalafil plus tamsulosin in ureteral stents-related symptoms relief. Cent European J Urol. 2024; 77: 111-116.
4. Polat ME, Karaaslan M, Yilmaz M, Olcucuoglu E, Sirin ME. The effect of ureteral double J stent insertion on work performance in patients undergoing endoscopic stone treatment. Cent European J Urol. 2024; 77: 117-121.
5. Luo Z, Jiao B, Zhao H, Huang T, Geng L, Zhang G. The efficacy and safety of ureteric stent removal with strings versus no strings: Which is better? Biomed Res Int. 2020; 2020: 4081409.
6. Oliver R, Wells H, Traxer O, et al. Ureteric stents on extraction strings: a systematic review of literature. Urolithiasis. 2018; 46: 129-136.
7. Juliebø-Jones P, Pietropaolo A, Haugland JN, Mykoniatis I, Somani BK. Current status of ureteric stents on extraction strings and other non-cystoscopic removal methods in the paediatric setting: a systematic review on behalf of the European Association of Urology (EAU) Young Academic Urology (YAU) Urolithiasis Group. Urology. 2022; 160: 10-16.
8. Doersch KM, Elmekresh A, Machen GL, El Tayeb MM. The use of a string with a stent for self-removal following ureteroscopy: A safe practice to remain. Arab J Urol. 2018; 16: 435-440.
9. McGuinness LA, Higgins JPT. Risk-of-bias VISualization (robvis): An R package and Shiny web app for visualizing risk-of-bias assessments. Res Syn Meth. 2021; 12: 55-61.
10. Kim DJ, Son JH, Jang SH, Lee JW, Cho DS, Lim CH. Rethinking of ureteral stent removal using an extraction string; what patients feel and what is patients' preference? : a randomized controlled study. BMC Urol. 2015; 15: 121.
11. Qi Y, Kong H, Xing H, Zhang Z, Chen Y, Qi S. A randomized controlled study of ureteral stent extraction string on patient's quality of life and stent-related complications after percutaneous nephrolithotomy in the prone position. Urolithiasis. 2023; 51: 79.
12. Barnes KT, Bing MT, Tracy CR. Do ureteric stent extraction strings affect stent-related quality of life or complications after ureteroscopy for urolithiasis: a prospective randomised control trial. BJU Int. 2014; 113: 605-609.
13. Inoue T, Okada S, Hamamoto S, et al. Impact of ureteric stent removal by string on patient's quality of life

and on complications at post-ureteroscopy for urolithiasis: a controlled trial. BJU Int. 2019; 124: 314-320.

14. Bates AS, Jameson M, Nkwam NM, Khan MA. Symptom and cost evaluation of ureteric stent extraction using strings versus flexible cystoscopy at a single high-volume centre. J Clin Urol. 2020; 13: 267-272.

15. Fröhlich M, Fehr J, Sulser T, Eberli D, Mortezavi A. Extraction Strings for Ureteric Stents: Is There an Increased Risk for Urinary Tract Infections? Surg Infect (Larchmt). 2017; 18: 936-940.

16. Freifeld Y, Goldin D, Khalili L, et al. Does the use of ureteral stents with extraction strings increase urinary infection rates? Int Urol Nephrol. 2017; 49: 763-767.

17. Liu H, Pan W, Zhang N. Ureteral stent removal using an extraction string after uncomplicated ureteroscopy: a cost-benefit analysis. Urol J. 2018; 15: 329-332.

18. Ghani KR, Olumolade OO, Daignault-Newton S, et al. What is the optimal stenting duration after ureteroscopy and stone intervention? Impact of dwell time on postoperative emergency department visits. J Urol. 2023; 210: 472-480.

19. Çınar Ö, Bolat MS, Öztürk K. Should the double-J stent be removed endoscopically after a ureteroscopic stone surgery? J Urol Surg. 2020; 7: 158-165.

20. EAU Guidelines on Urolithiasis. Edn. presented at the EAU Annual Congress Paris 2024. ISBN 978-94-92671-23-3. EAU Guidelines Office, Arnhem, The Netherlands 2024.

21. Moltzahn F, Haeni K, Birkhauser FD, Roth B, Thalmann GN, Zehnder P. Peri-interventional antibiotic prophylaxis only vs continuous low-dose antibiotic treatment in patients with JJ stents: a prospective randomised trial analysing the effect on urinary tract infections and stent-related symptoms. BJU Int. 2013; 111: 289-295.

22. Madhavan K, Rustagi S, Jena R, et al. A prospective randomized study to define the role of low dose continuous prophylactic antibiotics and anti-adherence agents in altering the microbial colonization related to indwelling double-J stents. Asian J Urol. 2021; 8: 269-274.

23. Ramaswamy K, Shah O. Antibiotic prophylaxis after uncomplicated ureteroscopic stone treatment: is there a difference? J Endourol. 2012; 26: 122-125.

24. Damavand RS, Esmaeili S, Bateni BH, Tavakoli AA, Kazemnezhad E. Comparing the effect of peri-operative antibiotic prophylaxis only with continuous low-dose antibiotic treatment on the incidence of urinary tract infection and stent related-symptoms in patients undergoing Double-J (DJ) stent insertion following transurethral lithotripsy (TUL). World J Urol. 2023; 41: 3027-3032.

25. Méndez-Guerrero DM, Buitrago-Carrascal C, Puentes-Bernal AF, et al. Antibiotic prophylaxis in flexible ureterorenoscopy with negative urine culture. BJUI Compass. 2023; 4: 688-694.

26. EAU Guidelines on Urological Infections. Edn. presented at the EAU Annual Congress Paris 2024. EAU Guidelines Office, Arnhem, The Netherlands. ■

LETTER TO THE EDITOR

UROLITHIASIS

Re: Kaczmarek K, Jankowska M, Kalembkiewicz J, et al. Assessment of the incidence and risk factors of postoperative urosepsis in patients undergoing ureteroscopic lithotripsy. Cent European J Urol. 2024; 77: 122-128

Akif Erbin, Bilal Kaya, Halil Lutfi Canat

Department of Urology, Basaksehir Çam Sakura City Hospital, Istanbul, Turkey

Article history
Submitted: Dec. 1, 2024
Accepted: Dec. 2, 2024
Published online: Mar. 21, 2025

Citation: Erbin A, Kaya B, Canat HL. Re: Kaczmarek K, Jankowska M, Kalembkiewicz J, et al. Assessment of the incidence and risk factors of postoperative urosepsis in patients undergoing ureteroscopic lithotripsy. Cent European J Urol. 2024; 77: 122-128. Cent European J Urol. 2025; 78: 100-101.

Dear Editor,

we have read the study "Assessment of the incidence and risk factors of postoperative urosepsis in patients undergoing ureteroscopic lithotripsy" with great interest [1]. The authors examined data from 231 patients who underwent ureteroscopic lithotripsy (URSL), revealing that 16.8% had a confirmed positive urine culture prior to the procedure, and the incidence of urosepsis within 30 days was 4.7%. They also reported that a preoperative positive urine culture significantly correlated with the risk of urosepsis. Preoperative hydronephrosis (HN) was observed in 22.9% of the cases, and only 9.4% of the cases had preoperative DJ or percutaneous nephrostomy (PCN). In patients with impacted stones and significant HN (grade 2 and above), urine culture obtained through the urethral route may not accurately indicate infection in the obstructed kidney; it is more likely to reflect the status of the contralateral kidney. In such instances, conducting a thin PCN and acquiring a urine culture from this catheter to inform a subsequent strategy may represent a more precise approach. Furthermore, the presence of a PCN during the surgery will markedly decrease intrarenal pressure (IRP), thereby mitigating the risk of urosepsis during the procedure. In a current porcine renal model, pyelovenous backflow was observed at IRPs of 90 mmHg or greater, while pyelotubular backflow occurred at irrigation IRPs of 60 mmHg or greater [2]. Nephrostomy drainage is the most effective technique for reducing IRPs. An interesting clinical study assessed the efficacy of PCN and the antegrade irrigation method from PCN during URSL and indicated that this approach resulted in higher stone-free rates and reduced operative time compared to conventional URSL, without an increased risk of urinary tract infections [3]. We usually conduct preoperative nephrostomy for patients with obstructed ureteral or renal pelvic stones and significant HN in preparation for URSL or retrograde intrarenal surgery (RIRS) and also evaluate the preoperative nephrostomy culture. This approach not only offers a more precise antimicrobial strategy and maintains low IRPs during the surgery but also facilitates continuous fluid circulation during the procedure, thereby enhancing the clarity of the screen image.

In conclusion, for patients with substantial HN and obstructive ureteral or pelvic stones, the insertion of a nephrostomy prior to surgery while maintaining the nephrostomy during the procedure may greatly reduce the risk of urosepsis in both URSL and RIRS. If the preoperative nephrostomy rate in the presented study had been higher, the urosepsis rate might have been lower.

CONFLICTS OF INTEREST

The authors declare no conflict of interest.

FUNDING

This research received no external funding.

ETHICS APPROVAL STATEMENT

The ethical approval was not required.

References

1. Kaczmarek K, Jankowska M, Kalembkiewicz J, et al. Assessment of the incidence and risk factors of postoperative urosepsis in patients undergoing ureteroscopic lithotripsy. Cent European J Urol. 2024; 77: 122-128.
2. Hong A, du Plessis J, Browne C, Jack G, Bolton D. Mechanism of urosepsis: relationship between intrarenal pressures and pyelovenous backflow. BJU Int. 2023; 132: 512-519.
3. Jung W, Byun HJ, Lee DS. The Role of Antegrade Irrigation via Percutaneous Nephrostomy on Surgical Outcomes in Semirigid Ureteroscopy among Patients with Upper Ureteral Stones. Biomed Res Int. 2019; 2019: 8657609. ■

Correspondence
Akif Erbin
akiferbin@hotmail.com

Central European Journal of Urology

VIDEOABSTRACT

VIDEOSURGERY

Video can be found at https://www.ceju.online/journal/2024/retrocaval-ureter-2398.php

Robotic retrocaval ureter repair

Maxwell Sandberg[1], Randall Bissette[2], Ashok Hemal[1]

[1]Atrium Health Wake Forest Baptist Medical Center, Winston-Salem, North Carolina,United States
[2]Virginia Tech Carilon School of Medicine, Roanoake, Virginia, United States

Article history
Submitted: Dec. 10, 2024
Accepted: Dec. 12, 2024
Published online: Jan. 28, 2025

Citation: Sandberg M, Bissette R, Hemal A. Robotic retrocaval ureter repair. Cent European J Urol. 2025; 78: 102.

Key Words: retrocaval ureter ‹› robotics ‹› reconstruction ‹› urologic surgery

Patients with a retrocaval ureter (RU) have their ureter mispositioned posterior to the inferior vena cava (IVC). RU tends to present in the third to fourth decade of life. Patients are often symptomatic, with flank pain, abdominal pain, and recurrent urinary tract infections with imaging showing associated right-sided hydroureteronephrosis. Surgical repair is indicated for those with symptoms or worsening renal function, with various options including pyelopyelostomy and ureteroureterostomy (UU). Herein, we present robotic RU repair (RRUR) of an 80-year-old male patient with right-sided RU via UU without the need for spatulation of the ureter. Preoperatively, the patient was worked up for benign prostatic hyperplasia with lower urinary tract symptoms and flank pain. A urinalysis revealed bacteriuria so a renogram was obtained, which revealed normal kidney function and partial obstruction of the right kidney. The patient elected to undergo RRUR with the da Vinci Xi robot. He was placed in left lateral decubitus (right side up) and a foley catheter was inserted. There were 4–8 mm robotic ports and 1–5 mm air seal used. The robotic ports were placed in a row 5 cm apart from one another, with the middle port centered above the umbilicus, and the air seal port 5 cm inferior to the robotic ports. The robot was docked, and the colon was Kocherized. The dissection was carried down to the right renal pelvis to identify the ureter. Next, the inferior vena cava (IVC) was exposed, and the ureter was seen passing posterior to it. Cautery was used to mark the ureter at the point of maximal hydroureter, and it was transected. The inferior portion of the ureter was then pulled anteromedial to the IVC. The diseased ureter was trimmed proximally, and the anastomosis proceeded via UU to reattach the ureter. This was done with 5-0 running vicryl suture, without the need for spatulation. A 6 × 30 JJ stent was placed into the ureter prior to completion of the anastomosis. The anastomosis was completed with additional reinforcing 5-0 vicryl, and the case was then completed. The robot was undocked. All port sites were closed with 4-0 monocryl suture. The patient was discharged on postoperative day 1 without complication, and their catheter was removed at this time. RRUR provided excellent visualization and ease of identification of the ureter.

CONFLICTS OF INTEREST

The authors declare no conflict of interest.

FUNDING

This research received no external funding.

ETHICS APPROVAL STATEMENT

The ethical approval was not required.

Corresponding author
Maxwell Sandberg
maxwellsandberg@msn.com

@CEJUrol facebook.com/CEJUrol
www.ceju.online